Clusterin (CLU) and its interacting proteins in cell signalling and neuroblastoma

KORN-ANONG CHAIWATANASIRIKUL

A thesis submitted for the Degree of Doctor of Philosophy

Institute of Child Health

University College London

2011

DECLARATION

I, Korn-Anong Chaiwatanasirikul, confirm that the work presented in this thesis is my own. Where work has been derived from other sources, I confirm that this has been indicated in the thesis.

Sign **Date**

ACKNOWLEDGEMENTS

I am grateful to the many wonderful people in my life who have helped transform me into a better and wiser person. First and foremost, I would like to thank my supervisor, Dr. Arturo Sala for giving me the opportunity to work on this PhD project. His vision and passion for science are the essence of my inspiration. I am equally thankful to my secondary supervisor, Dr. John Anderson and to my postgraduate tutors for their kind advice throughout my project.

I would like to express my appreciation to the Hodson family and the trustees of the Olivia Hodson Cancer Fund for their financial support. Your trust and encouragement are the reasons why I wish to work hard and keep doing what I do to make a difference.

I would like to give a special thank you to Dr. Olesya Chayka, Dr. Sandy Lee and all the members of the Molecular Haematology and Cancer Biology unit at the ICH. It has been an honour to work with so many great scientists and friends. I immensely enjoyed our daily scientific discussions and appreciate all the support you gave me.

I sincerely thank Mr. Akira Thomas Matsukawa, who has remained marvellously positive throughout. Your great sense of humour and understanding are indispensable for my work. Thank you for always being there for me.

Lastly, I would like to express my deepest gratitude to my family for their unconditional love, support and advice. I owe every step of my success to my parents, who taught me the value of education and encouraged the realization of my dreams from early in life. Thank you for allowing me to pursue my passion and for inspiring me to help others. Your guidance and praise have made me become a stronger and wiser person. I wish to dedicate this thesis to my parents, grandmother and the rest of my family, who have always believed in me.

ABSTRACT

Neuroblastoma is the most common extracranial solid tumour in children, with a high mortality rate among patients with aggressive disease.

In a previous study we showed that Clusterin (CLU) inhibits the transcription factor NF-κB in a neuroblastoma cell line by stabilizing the NF-κB inhibitors (IκBs). Moreover, suppression of CLU could elicit NF-κB activation and increased the expression of markers for the epithelial-to-mesenchymal transition (EMT), a developmental process utilized by aggressive cancer cells for invasion, in a mouse neuroblastoma model. The expression of CLU is also negatively regulated by the proto-oncogene *MYCN*, which is associated with aggressive stages of neuroblastoma tumours. Thus, we hypothesised that CLU is a tumour suppressor gene, which negatively regulates NF-κB and metastasis.

In this study, we investigated the role of the different isoforms of CLU in the regulation of signalling pathways. We also aimed at identifying the precise mechanisms by which CLU regulates NF-κB.

The results show that intracellular, but not secreted CLU, inhibits NF-κB activity. Interestingly, extracellular CLU (secreted CLU) positively regulates AKT and the Phosphoinositide-3 Kinase (PI3K) pathway. Mass-spectrometry analysis and co-immunoprecipitation experiments demonstrated that a chaperone protein named Heat Shock Protein 60 (HSP60) is bound to the N-terminal region of intracellular CLU in neuroblastoma cells. Suppression of HSP60 by shRNA knock down experiments caused decreased neuroblastoma cell proliferation and increased cell death. Our results suggest that HSP60 exert its oncogenic activity by inhibiting the function of CLU and promoting NF-κB activity.

In summary, in this report we demonstrate that a direct interaction between intracellular CLU and HSP60 could play an important role in the regulation of NF-κB activity and neuroblastoma development.

TABLE OF CONTENTS

LIST OF FIGURES

LIST OF TABLES

ABBREVIATIONS

α	Alpha
ALCL	Anaplastic large cell lymphomas
ALK	Anaplastic lymphoma kinase
Å	Angstrom
ApoJ	Apolipoprotein J
AS-ODN	Antisense oligodeoxynucleotide
Asp	Aspartic acid
ATCC	American Type Culture Collection
BAD	BCL-2-associated agonist of cell death
BAFF	B-cell activating factor
BDNF	Brain-derived neurotrophic factor
β	Beta
bHLH-LZ	basic-helix-loop-helix/leucine zipper
BLAST	Basic Alignment Search Tool
BMP	Bone morphogenetic protein
bp	Base pair
BSA	Bovine serum albumin
^{o}C	Degree Celsius
CASZ1	Castor gene
CCR7	C-C chemokine receptor type 7
CHD5	Chromodomain, helicase, DNA-binding gene
ChIP	Chromatin immunoprecipitation
CIAP	Calf intestinal alkaline phosphatase
CLU	Clusterin
CypD	Cyclophillin D
Da	Dalton
DMEM	Dulbecco's Modified Eagle Medium
DMSO	Dimethyl sulfoxide

DNA	Deoxyribonucleic acid
DNA-PK	DNA-dependent protein kinase
DSB	Double-strand breaks
DTT	Dithiothreitol
ε	epsilon
EGFR	Epidermal growth factor receptor
EMT	Epithelial to mesenchymal transition
ER	Endoplasmic reticulum
ETB	Epolactaene tertiary butyl ester
FBS	Foetal bovine serum
FGF	Fibroblast growth factor
γ	Gamma
GFP	Green fluorescent protein
GST	Glutathione S-transferase
HRP	Horseradish peroxidase-conjugated
HSPs	Heat shock proteins
HSP60	Heat shock protein 60
IAP	Inhibitors of apoptosis
IER3	Immediate early response 3
IGF	Insulin-like growth factor
IGFR	Insulin-like growth factor receptor
IκBs	Inhibitors of kappa B
IKK	IκB kinase
IL	Interleukin
Inp	Input
INSS	International Neuroblastoma Staging System
IPTG	Isopropyl β-D-1-thiogalactopyranoside
IR	Ionizing radiation
IRF4	Interferon regulatory factor 4

k	Kilo
KO	Knockout
L	Litre
LB	Luria-Bertani
LC-MS/MS	Liquid Chromatography with tandem mass spectrometry
LOH	Loss of heterozygosity
LP	Leader peptide
LPS	Lipopolysaccharides
LRP2	Low-density lipoprotein receptor-related protein 2
LTb	Lymphotoxin B
mA	milliampere
MAPK	Mitogen-Activated Protein Kinase
MEFs	Mouse embryonic fibroblasts
MET	Mesenchymal-to-epithelial transition
µg	microgram
mg	milligram
MHC	Major histocompatibility complex
MIBG	meta-iodobenzylguanidine
miRNA	Micro ribonucleic acid
µm	micrometre
ml	millilitre
mm	millimetre
MRP	Multidrug resistance-associated protein
MYCN-ER	MYCN-oestrogen receptor
nCLU	Nuclear CLU
NDRG	N-Myc downstream regulated gene
NEAA	Non-essential amino acid
NEMO	NF-κB essential modulator
NF-κB	Nuclear Factor-kappa B

ng	nanogram
NGF	Nerve growth factor
NGFR	Nerve growth factor receptor
NIK	NF-κB-inducing kinase
NLSs	Nuclear localization signals
NOD	Non-obese diabetic
NS	No significance
NT	Non-transfected
NT3	Neurotrophin-3
NT4	Neurotrophin-4
OD	Optical density
ODC	Ornithine decarboxylase
PBS	Phosphate buffered saline
PCR	Polymerase chain reactions
PDGFR	Platelet-derived growth factor receptor
PDK1	Phosphoinositide-dependent kinase 1
PHOX2B	Paired-like homeobox 2B
PI	Propidium iodide
PIG	p53 induced gene
PIP2	Phosphatidylionositol-3,4 diphosphate
PIP3	Phosphatidylinositol-3,4,5 triphosphate
PI3K	Phosphatidylinositol-3 kinase
pnCLU	Precursor nuclear CLU
RE	Response element
RFP	Red fluorescent protein
RIP	Receptor interacting protein
RNaseA	Ribonuclease A
ROS	Reactive oxygen species
rpm	round per minute

RPMI	Roswell Park Memorial Institute
RTKs	Receptor tyrosine kinases
SCF	Skp1-Cullin-F-box
SCLIP	SCG10-liked protein
sCLU	Secreted CLU
SD	Standard Deviation
SDS	Sodium dodecyl sulphate
SDS-PAGE	Sodium dodecyl sulphate polyacrylamide gel electrophoresis
SGP2	Sulfated glycoprotein 2
shRNA	Short hairpin ribonucleic acid
SNS	Sympathetic nervous system
TAE	Tris-acetate-EDTA
TGFβ	Transforming growth factor beta
TLR	Toll-like receptor
TNF-α	Tumour necrosis factor alpha
TNF-R	Tumour necrosis factor-receptor
TRAF	TNF receptors associated factor
TRAIL	TNF-related apoptosis-inducing ligand
TRAP-1	Tumour necrosis-factor receptor-associated protein-1
TRPM2	Testosterone repressed prostate message 2
Trk	Neurotrophic tyrosine kinase receptor
TSA	Trichostatin A
TSG	Tumour suppressor gene
Tyr	Tyrosine
u	Unit
V	Volts
VEGF	Vascular endothelial growth factor
VHL	Von Hippel–Lindau disease

CHAPTER 1

Introduction

1.1. Neuroblastoma

Neuroblastoma is the most common extracranial solid tumour in infants and children, which accounts up to 10% of all childhood malignancies (Gurney *et al*., 1997). Approximately 90% of children with the disease are diagnosed within the first 5 years of life (Schwab *et al*., 2003). The occurrence of neuroblastoma is approximately 1 in 7,000-10,000 live births and although the disease is largely sporadic, approximately 1-2% of the patients have a family history of the disease (Shojaei-Brosseau *et al*., 2004). The hereditary predisposition to neuroblastoma is discussed in more detail in section 1.4.12.

Common signs for early detection of neuroblastoma in children include fatigue, loss of appetite/weight, fever and joint pain (Schwab *et al*., 2003). Other symptoms often depend on the primary site of tumour and metastases present. A tumour that originates in the abdomen may cause a swollen belly or constipation. A tumour in the chest may result in breathing problems. In addition, a tumour in the spinal cord may cause muscle weakness or inability to stand, crawl or walk. A tumour in the bones around the eyes may cause swelling, bruising or black-eye effect. Lastly, bone lesions in the legs or hips may cause pain and limping. However, these signs and symptoms of neuroblastoma are often unclear, making early diagnosis difficult. Thus, by the time of diagnosis, neuroblastoma often spreads to other parts of the body (Mazur, 2010). Noninvasive methods to screen for neuroblastoma such as urinary catecholamine metabolites have relatively high sensitivity and specificity for detecting the disease (Mosse *et al*., 2009). The tumour is believed to arise as a consequence of deregulated proliferations of embryonal neural crest cells, which later form the sympathetic nervous system (SNS) (see section 1.2.).

The sympathetic and parasympathetic nervous systems are part of the autonomic nervous system and are important for homeostasis. The sympathetic nervous system acts primarily on the cardiovascular system increasing heart rate, widening bronchial passages, decreasing intestinal activity in response to stress, this is also known as a *fight-or-flight* response. The parasympathetic nervous system, on the other hand, relaxes

the body function and allows the body to rest after stress by decreasing the heart rate and increasing digestion (Sherwood, 2008).

1.2. Neural crest development

In the earliest phase of neural development, neural tissue is induced in the ectodermal (outer) layer of the embryo. As a consequence of neural induction, the ectoderm becomes divided into three different regions; the neural ectoderm or neural plate, which will give rise to the central nervous system; the non-neural ectoderm, which will form the epidermis; and the cells at the border between neural and non-neural ectoderm, which for the most part will become the neural crest (Figure 1.1.). Neurulation occurs whereby the neural tissues fold inwards to form the neural tube. The neural plate border cells then bend to form the neural folds and eventually become the dorsal aspect of the neural tube. Depending on the organism and the axial level, neural crest cells initiate migration from the closing neural fold or from the dorsal neural tube (Bronner-Fraser, 2002).

Thus, neural crest cells are vertebrate-specific cells, which form during the early stages of embryonic development. They are migratory multipotent cells, which only become distinct cell type once they have migrated away from the central nervous system during embryogenesis (LeDouarin and Kalcheim, 1999). The multipsteps process of neural crest development include its initial induction, gain of the ability to respond to crest-inducing cues at the neural plate border, maintenance of multipotency in the newly induced population, control of cell cycle, epithelial to mesenchymal transition (EMT), delamination from the neuroepithelium, migration and differentiation (Sauka-Spengler and Bronner-Fraser, 2008).

Moreover, the neural plate border and neural crest cells form in response to different signalling events between newly induced neural tissue and the neighbouring non-neural ectoderm. Extracellular secreted signalling molecules (e.g. Wnt, FGF, BMP, and Notch/Delta) have been shown to be important for the initiation of neural crest induction (Stottmann and Klingensmith, 2011, Lewis *et al*., 2004, Endo *et al*., 2002, Monsoro-Burq *et al*., 2003). For example, loss of BMP type 1 receptor (BMPR1A) led to a dramatic decreased in neural crest cells in mice (Stottmann and Klingensmith, 2011).

Moreover, overexpression of FGF8 transiently induced neural crest cells in frog (Monsoro-Burq *et al*., 2003). In zebrafish, an inducible Wnt inhibitor activated during early neurulation has shown to specifically interfere with neural crest cell formation (Lewis *et al*., 2004). Lastly, Endo and coworkers (2002) demonstrated that Notch signalling is indirectly required for neural crest induction by BMP4 at the epidermis-neural plate boundary. Moreover, Notch activation in the epidermis inhibited neural crest formation in this tissue, thus, neural crest generation by BMP4 is restricted only at the border.

Afer neural crest signalling induction, the first transcription factors to appear at the neural plate border that can respond to the neural crest-specifying signals to form neural crest cells are known as neural plate border specifiers. This includes Mxs1/2, Dlx5, Pax3/7, Gbx2 and zinc finger–containing Zic proteins. For example, Dlx5 is regulated by attenuated levels of BMP (Luo *et al*., 2001). These transcription factors, in turn, regulate the neural crest specifier genes, important for cell cycle control, EMT and migration process such as Snail/Slug, AP-2, FoxD3, Twist, Id, cMyc, and Sox9/10 (Figure 1.2.).

To initiate migration, premigratory neural crest cells need to delaminate from the neuroepithelium via EMT process. Therfore, transcription factors acting on the neural crest precursors must maintain the precursors in a multipotent, proliferating state and also activate or repress effector genes involved in their EMT. Similar to FoxD3, Sox10 overexpression could induce β1 integrin expression and inhibit N-Cadherin expression whose orchestrated regulation is crucial for EMT to occur (Cheung *et al*., 2005). Moreover, Cano et al (2000) demonstrated that Snail1 was directly responsible for the negative regulation of E-cadherin (E-Cad), a cell adhesion molecule characteristic of epithelial cells.

Once the neural crest cells have migrated and reached their final destinations, expressions of most early neural crest cell specifiers, including Snail/Snail2, FoxD3, Id, and AP2α, are normally downregulated. However, SoxE transcription factor family members Sox9 and Sox10 may persist in specific subpopulations of neural crest cell derivatives such as cartilage and neuron/glial/melanocyte lineages respectively, to regulate their terminal differentiation (Kelsh 2006, Sauka-Spengler and Bronner-Fraser 2008).

Downregulation of Id has been shown to be essential for initiating neural crest cell differentiation. One possibility is that the inhibition of Id activity reduces *Sox10* expression and that low concentrations of Sox10 can sustain the multipotency of neural crest cells (Kim *et al*., 2003, Paratore *et al*., 2001).

Neural crest cells can give rise to various derivatives ranging from melanocytes, glia, and neurons to skeletal components of the head. The type of derivative depends upon the axial level from which the neural crest cells originate and the time of their emigration from the neuroepithelium. For example, early migrating cranial neural crest cells populate at the pharyngeal arches can generate bone, cartilage and connective tissue (skeletal structures). However, the later wave stays close to the central nervous system and generates the neurons and glia of the cranial ganglia (Graham *et al*., 2004).

In addition to its role in melanocyte differentiation, Sox10 also controls specification of glial and neuronal fates in neural crest derivative specification. Sox10 has been shown to participate further in the differentiation of glia, as its expression within this lineage persisted into terminal differentiation stages (Kelsh, 2006). During glial differentiation, Sox10 directly regulates the expressions of protein zero (P0), myelin basic protein (MBP), peripheral myelin protein 22 (PMP22) and the gap junction protein connexin 32 (Cx32). Thus, Sox10 has been shown to affect all major components of the myelination process (Bondurand *et al*., 2001, Peirano *et al*., 2000).

Finally, evidence concerning the direct regulatory role of Sox10 in the control of multipotency and maintenance of stem cell properties in neural crest during differentiation of neural crest–derived neurons comes from studies of sensory and autonomic lineages in the trunk. In mouse neural crest cell cultures, Sox10 regulates the expression of mouse achaete-scute homologue 1 (MASH1) and the paired homeodomain (Phox2b), transcription factors that are essential for autonomic neurogenesis. Moreover, Sox10 acts to delay differentiation of sympathetic and enteric neurons allowing the progenitors to migrate to the correct embryonic locations (Kim *et al*., 2003).

In primary sympathetic ganglia, the combined expression of the transcription factors Ascl1, Phox2a, Phox2b, Hand2 and Gata2/3 lead to the specification and differentiation of sympathetic neurons (Goridis and Rohrer, 2002, Howard, 2005, Ernsberger and

Rohrer, 1996). The Sox10+/Phox2b− subpopulation is considered as undifferentiated and pluripotent neural crest progenitors (Tsarovina *et al*., 2008).

In addition, analysis in zebrafish confirmed that a Wnt signal feeds directly to the *Sox10* regulatory element during migration and that SoxE, nuclear factor κB (NF κB), and Notch signals can potentially drive Sox10 expression in neural crest cells (Dutton *et al*., 2008). Thus, neurogenesis in sympathetic ganglia is also characterized by the Notch-mediated segregation and maintenance (Tsarovina *et al*., 2008).

.

In summary, each step of the neural crest development is crucial and alteration in any of the signalling events, for example Sox10 and its downstream target, Phox2B, may cause neural crest cells to stop migration and differentiation, which may subsequently form congenital disorders such as Hirschsprung disease (lack of ganglia in the colon) and Neuroblastoma (Kulesa *et al*., 2009).

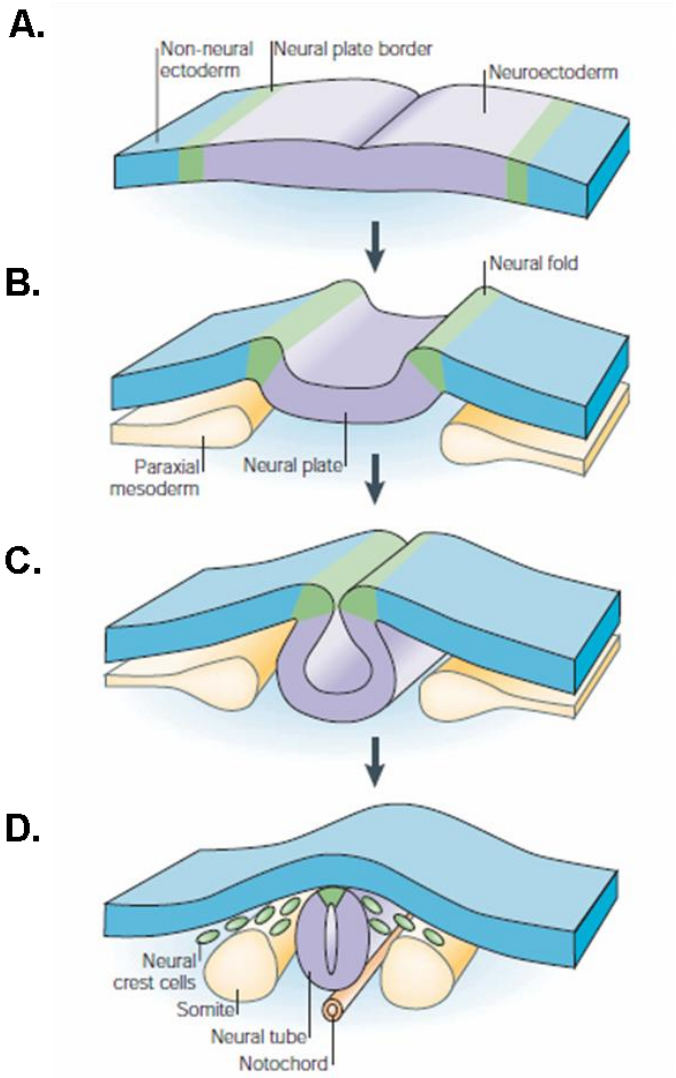

Figure 1.1. Border induction and neurulation

A) The neural plate border (green) is induced by signalling between neuroectoderm (purple) and non-neural ectoderm (blue) and from the underlying paraxial mesoderm (yellow).

B) During neurulation, the neural plate borders (neural folds) elevate.

C) This causes the neural plate to roll into a neural tube.

D) Neural crest cells (green) delaminate from the neural folds or the dorsal neural tubes (shown) depending on the species and axial level.
(Adapted from Gammill and Bronner-Fraser, 2003)

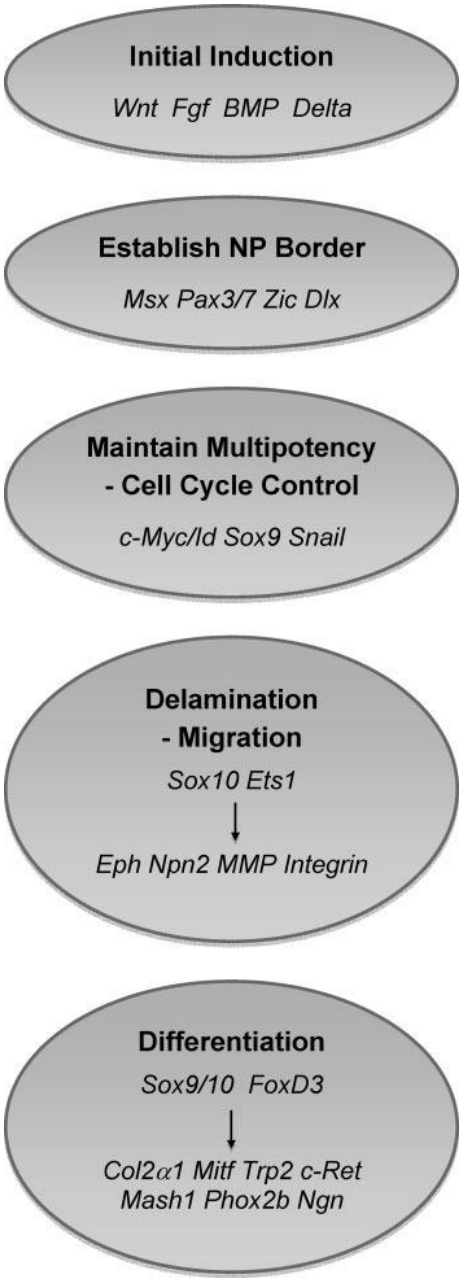

Figure 1.2. Schematic diagram illustrating the neural crest gene regulatory network and the genes involved at different times during neural crest development (Adapted from Sauka-Spengler and Bronner-Fraser, 2008b).

1.3. Classification

Neuroblastoma tumour often originates in the adrenal glands (65%). However, the tumour origin can be situated at any location of the sympathetic nervous system, which extends from the neck (5%), chest (20%) to the pelvis (5%) (Janoueix-Lerosey *et al*., 2010).

The most widely used staging system currently is the International Neuroblastoma Risk Group Staging System (INRGSS) (Table 1.1.). This is developed from the post-surgical staging system (INSS), which divided the risk groups into stages 1 (L1), 2-3 (L2), 4 (M) and 4S (Special) (MS) (Brodeur *et al*., 1993, D'Angio *et al*., 1971, Cohn *et al*., 2009). Spontaneous regression is most commonly observed in stage MS patients. However, the mechanism of tumour regression is still unknown (Brodeur, 2003, Friedman and Castleberry, 2007).

For the INRGSS, stage L1 tumours are localized tumours that do not involve vital structures as defined by the list of image-defined risk factors (IDRFs) (Table 1.1.). The tumour must be confined within one body compartment e.g. neck, chest, abdomen, or pelvis. Stage L2 tumours are locoregional tumours with one or more IDRFs. The tumour may be ipsilaterally continuous within body compartments (i.e. a leftsided abdominal tumour with left-sided chest involvement should be considered stage L2). However, a clearly left-sided abdominal tumour with right-sided chest (or vice versa) involvement is defined as metastatic disease. Stage M is defined as distant metastatic disease (i.e. not contiguous with the primary tumour) except as defined for MS. Nonregional (distant) lymph node involvement is metastatic disease. However, an upper abdominal tumour with enlarged lower mediastinal nodes or a pelvic tumour with inguinal lymph node involvement is considered locoregional disease. Ascites and a pleural effusion, even with malignant cells, do not constitute metastatic disease unless they are remote from the body compartment of the primary tumour. Stage MS is metastatic disease in patients younger than 18 months (547 days) with metastases confined to skin, liver, and/or bone marrow. Bone marrow involvement should be limited to less than 10% of total nucleated cells on smears or biopsy. MIBG scintigraphy must be negative in bone and bone marrow. Provided there is MIBG uptake in the primary tumour, bone scans are not required. The primary tumour can be

L1 or L2 and there is no restriction regarding crossing or infiltration of the midline (Monclair *et al*., 2009).

Children with neuroblastoma exhibit marked variability in outcome depending on the age, stage and biological characteristics of the disease at the time of diagnosis (DuBois *et al*., 1999). The characteristic risk group of neuroblastoma is shown in table 1.2 where INRG stage, age, histologic category, grade of tumour differentiation, *MYCN* status, presence/absence of 11q aberrations and tumour cell ploidy are considered. Moreover, the categories were divided into 16 statistically and/or clinically different pretreatment groups of patients, designated as very low (A, B, C), low (D, E, F), intermediate (G, H, I, J), or high (K, N, O, P, Q, R) pretreatment risk subsets (Cohn *et al*., 2009).

Low-risk neuroblastoma often observed in younger patients (<18 months) is associated with localized and benign tumours (ganglioneuroma or ganglioneuroblastoma) with the absence of *MYCN* amplification and/or genetic aberration in 1p, 11q and 17q. More than 10% of low-risk cases show complete spontaneous regression in the absence or minimum therapeutic intervention (Brodeur, 2003, Schwab *et al*., 2003, Cohn *et al*., 2009). Older children (>18 months) often show tumour metastases by the time of diagnosis with various genetic abnormalities (i.e. *MYCN* amplification and chromosomal alterations including loss of 1p, 11q or gain of 17q). Moreover, 11q aberration is associated with worse outcome in patients with L2 or MS tumours that lack *MYCN* amplification (Cohn *et al*., 2009). The survival probability in the high risk cases is less than 40% (Maris *et al*., 2007).

Stage	Description
L1	Localized tumour not involving vital structures as defined by the list of image-defined risk factors and confined to one body compartment
L2	Locoregional tumour with presence of one or more image-defined risk factors
M	Distant metastatic disease (except stage MS)
MS	Metastatic disease in children younger than 18 months with metastases confined to skin, liver, and/or bone marrow

Patients with multifocal primary tumours should be staged according to the greatest extent of disease as defined in the table.

Table 1.1. Internaltional Neuroblastoma Risk Group Staging System (INRGSS) (Adapted from Monclair *et al*., 2009).

INRG Stage	Age (months)	Histologic Category	Grade of Tumor Differentiation	*MYCN*	11q Aberration	Ploidy	Pretreatment Risk Group
L1/L2		GN maturing; GNB intermixed					A Very low
L1		Any, except GN maturing or GNB intermixed		NA			B Very low
				Amp			K High
L2	< 18	Any, except GN maturing or GNB intermixed		NA	No		D Low
					Yes		G Intermediate
	≥ 18	GNB nodular; neuroblastoma	Differentiating	NA	No		E Low
					Yes		H Intermediate
			Poorly differentiated or undifferentiated	NA			
				Amp			N High
M	< 18			NA		Hyperdiploid	F Low
	< 12			NA		Diploid	I Intermediate
	12 to < 18			NA		Diploid	J Intermediate
	< 18			Amp			O High
	≥ 18						P High
MS	< 18			NA	No		C Very low
					Yes		Q High
				Amp			R High

Table 1.2. International Neuroblastoma Risk Group (INRG) Consensus Pretreatment Classification schema.

GN, ganglioneuroma; GNB, ganglioneuroblastoma; Amp, amplified; NA, not amplified; L1, localized tumor confined to one body compartment and with absence of image-defined risk factors (IDRFs); L2, locoregional tumor with presence of one or more IDRFs; M, distant metastatic disease (except stage MS); MS, metastatic disease confined to skin, liver and/or bone marrow in children < 18 months of age. Letters A to R represent the 16 statistically and/or clinically different pretreatment groups of patients (Cohn *et al*., 2009).

1.4. Genetic abnormalities in neuroblastoma.

Like other cancers, the molecular biology of neuroblastoma is characterised by somatically acquired genetic events that result in the activation of oncogenes and suppression of tumour suppressor genes or alterations in gene expression. Various techniques have been used to identify potential prognostic markers, which may determine the response to therapy and clinical outcome. Tumours with *MYCN* gene amplification, chromosome 1 loss of heterozygosity (LOH) and gain of chromosome 17 are associated with aggressive neuroblastomas. Alteration in the expressions of neurotrophin and their receptors correlate with clinical behaviour and may reflect the degree of neuroblastic differentiation before malignant transformation (Maris and Matthay, 1999, Janoueix-Lerosey *et al*., 2009).

1.4.1. Ploidy

Ploidy refers to the term that describes the number of chromosomes in a cell. A normal diploid cell has 46 chromosomes with a DNA content of 1. A triploid cell (3n), on the other hand, would have 69 chromosomes with a DNA content of 1.5. The majority of neuroblastoma cell lines and advanced primary tumours have either a near-diploid (2n) or near-tetraploid (4n) DNA content. Infant neuroblastomas (<1 year old), with favourable outcome usually have hyperdiploid or near-triploid (3n) DNA index (Look *et al*., 1984, Look *et al*., 1991). The diploid/tetraploid tumours are characterised by chromosomal rearrangements including amplification, deletion and translocation (Maris and Matthay, 1999, Brodeur, 2003).

1.4.2. Gain of 17q

Gain of chromosome band 17q23 in neuroblastoma was first identified by Gilbert et al (1984) and has been shown to occur in >50% of primary tumours. This type of genetic alteration is associated with more aggressive neuroblastomas. Overexpression of survivin (inhibitor of apoptosis protein) has been proposed to occur in this region (Islam *et al*., 2000).

1.4.3. Loss of 1p

In 1977, Brodeur and coworkers first recognized that the deletion of the short arm chromosome 1 (1p) was a common karyotypic feature of neuroblastoma cell lines and tumours. LOH of chromosome 1p is observed between 19-36% of all primary tumours.

Introduction of an intact chromosome 1p to 1p-deleted neuroblastoma cell lines induce cell differentiation and/or cell death (Bader *et al*., 1991). This suggests that this region harbours tumour suppressor genes. Most 1p deletions cover almost the entire chromosomal arm, with common deletions occurring between 1p36.2-36.3 (White *et al*., 1995). One study has postulated the existence of two, or even more neuroblastoma genes in 1p (Caron *et al*., 2001). The existence of two separate 1p regions that are associated with neuroblastoma is supported by a study that identified one region at 1p36 and one at 1p22 (Mora *et al*., 2000). Moreover, Hiyama and colleagues (2001) reported three regions at 1p36.1-2, 1p36.3, and 1p32-34, each associated with different subgroups of neuroblastoma. Caron et al (1993) also found that tumours with *MYCN* amplification generally had 1p deletions extending proximal to 1p36, but single-copy *MYCN* tumours more often had small terminal deletions of 1p36 only.

There is a strong correlation between 1p LOH and high-risk features such as age >1 year at diagnosis, metastatic disease, *MYCN* amplification and 1p LOH may be used as a prognostic marker for relapse (Maris and Matthay, 1999).

Candidate tumour suppressor genes located on chromosome 1p include *TP53* homolog *TP73*; the *CDK2* homolog *CDC2L1* (p58); the transcription factors *HKR3*, *DAN*, *PAX7*, *ID3*, and *E2F2*; the transcription elongation factor *TCEB3* (Elongin A); and two members of the tumour necrosis factor receptor family, *TNFR2* and *DR3*. However, each of these genes except *HKR3* and *DR3* are located outside the current consensus region, and no mutations have been found in the non-deleted allele of any candidate (Maris and Matthay, 1999).

Two very important tumour suppressor genes often deleted (1pLOH) in neuroblastoma have recently been identified (Liu *et al*., 2011, Fujita *et al*., 2008). Firstly, human *Castor* gene (*CASZ1*) is a zinc finger transcription factor, mapped to chromosome 1p36.22, is structurally homologous to *Drosophila castor*. *CASZ1* is induced when cells of neural or mesenchymal origins undergo differentiation, suggesting its role in the differentiation program of neuroblast cell lineages. Other roles of *CASZ1* include enhancement of cell adhesion, inhibition of cell migration and suppression of tumourigenicity (Liu *et al*., 2011). There are two isoforms of human *CASZ1* (*hCasz5* and *hCasz11*) (Liu *et al*., 2006). Liu and coworkers (2011) demonstrated that both

forms of *CASZ1* function to suppress growth in neuroblastoma tumours both *in vitro* and *in vivo* and that low expressions of *CASZ1* is significantly associated with decreased survival probability of neuroblastoma patients. Treatments with retinoic acids and epigenetic modification agents (e.g. TSA) could induce neuroblastoma cell differentiation through the induction of *CASZ1* expression (Liu *et al*., 2011). *CASZ1*-expressing xenograft tumours also showed increased expressions of *NGFR* and *TrkA*, which are highly expressed in differentiated neuroblastoma tumours and markers of good prognosis, suggesting that *CASZ1* may function like a haplo-insufficient tumour-suppressor gene, where a partial loss of *CASZ1* may be sufficient to result in neuroblastoma development (Liu *et al*., 2011).

In addition, chromodomain, helicase, DNA-binding gene (*CHD5*), a chromatin remodelling gene, mapped to chromosome 1p36.31 is often deleted in human neuroblastomas (Thompson *et al*., 2003). *CHD5* is a member of the *CHD* gene family and encodes a novel class of Swi/Snf proteins that contains a Swi/Snf-like helicase ATPase domain, a DNA-binding domain and a chromodomain motif, which can directly affect chromatin structure, altering the access of the transcriptional apparatus and gene transcription (Woodage *et al*., 1997). Clonogenicity and tumour growth were abrogated in neuroblastoma cell lines overexpressing *CHD5* (Fujita *et al*., 2008). Moreover, reactivation of *CHD5* expression resulted in the induction of neuroblatoma cell differentiation (Garcia *et al*., 2010). Thompson et al (2003) demonstrated that low *CHD5* expression is correlated with 1p deletion, *MYCN* amplification, advanced stage and unfavourable neuroblastoma cases. Therefore, *CHD5* may also function like a haplo-insufficient tumour-suppressor gene, where a partial loss of *CHD5* may be sufficient to result in aggressive neuroblastoma development.

1.4.4. Loss of 11q

Chromosome 11q deletions are observed in approximately 15-20% of primary neuroblastomas. This suggests that chromosome 11q is another important site of neuroblastoma tumour suppressor genes (Mertens *et al*., 1997). The most common region for deletion is at 11q23. LOH of 11q is directly correlated with 14q deletion and poor prognosis but inversely correlated with *MYCN* amplification.

1.4.5. Loss of 14q

Deletion of the long arm of the chromosome 14 (14q) was first identified in 1989 by Suzuki and coworkers. The most common deletion region occurred within 14q23, in 23% of the 280 primary tumours studied (Thompson *et al*., 2001). This type of chromosomal alterations was highly correlated with 11q LOH and inversely correlated to *MYCN* amplification and present in all clinical risk groups, indicating that this abnormality may occur early in tumour development.

1.4.6. Deletion of other chromosomal regions/ alterations in known TSG and DNA repair genes

Other LOH and/or allelic imbalance at chromosome arms 3p, 4p, 5q, 9p and 18q have also been reported (Meltzer *et al*., 1996, Takita *et al*., 2000, Hirai *et al*., 1999). However, their molecular characteristics are less defined as these genetic alterations occur at a much lower frequency than 1p LOH.

Unlike other cancers, p53, which is located on the short arm of chromosome 17 (17p13), is only rarely inactivated (<2%) by deletion or mutation in neuroblastomas at diagnosis (Carr *et al*., 2006). p53 is a key regulator of cell cycle check point and apoptosis. Upon activation by cellular stress, particularly in DNA damage, p53 binds DNA in a sequence-specific manner to activate its downstream target genes such as *p21*, *Bax* and *PUMA* and further caused apoptosis, cell cycle arrest, differentiation or DNA repair (Michalak *et al*., 2005). MDM2 functions as an ubiquitin ligase, which targets p53 for proteasome-mediated degradation (Barak *et al*., 1993), suggesting that amplification of *MDM2* resulted in increased p53 degradation. In contrast, $p14^{ARF}$ directly binds to MDM2 and acts as a MDM2 inhibitor. Thus, $p14^{ARF}$ is a tumour suppressor protein, which sequestered MDM2 in the nucleolus, preventing its interaction with p53; subsequently p53 is released from its inhibitory state (Figure 1.2.). Goldman et al (1996) have shown that DNA damage to neuroblastoma cells caused normal translocation of wild-type p53 to the nucleus and induction of its downstream target p21, suggesting that it is unlikely that alterations in DNA repair genes play a role in neuroblastoma development.

However, Moll and coworkers (1996) reported aberrant cytoplasmic localization of p53 in neuroblastoma with dysregulated G1/S check point, suggesting that p53 could be

inactivated by cytoplasmic retention. Although genetic mutation of p53 is rare at diagnosis, aberration in the p53/MDM2/$p14^{ARF}$ pathway is commonly detected in relapsed neuroblastoma and can confer chemoresistance (Carr *et al*., 2006, Carr-Wilkinson *et al*., 2010). p53 missense mutation detected in codon 259 GAC → TAC was reported in a neuroblastoma tumour following cytotoxic treatment (Hosoi *et al*., 1994). The Universal Mutation Database showed 31 reports of this mutation, suggesting that this is a frequent mutation (www.umd.be:2072). The amino acid substitution from Asp to Tyr resulted in the change of p53 structure and, therefore, may contribute towards tumour progression (Hosoi *et al*., 1994).

Some neuroblastoma cell lines established after treatment have been found to gain alternative mechanisms of p53 inactivation such as amplification of the p53 negative regulator (*MDM2*) or suppression of the MDM2 inhibitor ($p14^{ARF}$) (Tweddle *et al*., 2003). The use of a MDM2 inhibitor (Nutlin 3a) has been shown to stabilize p53, induce p53 targets genes, sensitize cells to conventional chemotherapeutic agents in p53 wild-type neuroblastoma cells lines as well as wild-type p53 chemoresistant cell lines and xenografts (Van Maerken *et al*., 2006, Barbieri *et al*., 2006, Van Maerken *et al*., 2009). Gamble et al (2011) also demonstrated that MDM2-p53 antagonists Nutlin-3 and MI-63 were effective at inducing growth inhibition and apoptosis in *MYCN*-amplified cells compared to non-*MYCN*-amplified cells with wild-type p53.

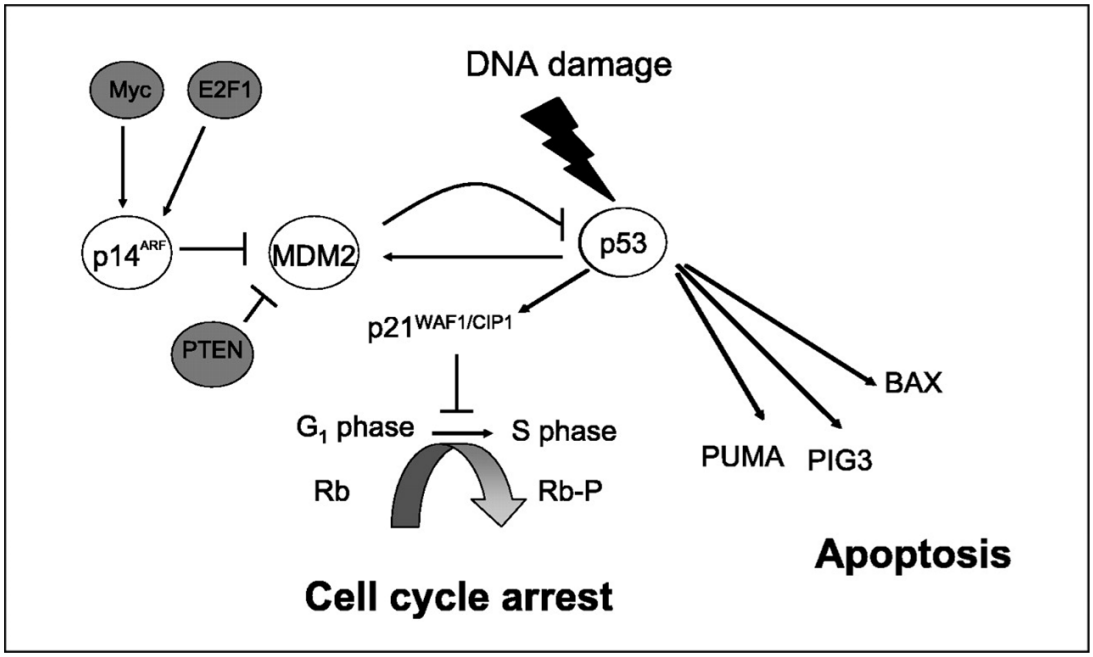

Figure 1.2. A schematic representation of the p53 pathway

p53 is activated in response to DNA damage and activates the transcription of a large number of target genes, including the CDK inhibitor $p21^{WAF1/CIP1}$, which blocks G_1 to S phase cell cycle progression or *Bax* , *p53 induced gene* (*PIG3*) and *PUMA*, which are involved in apoptosis. MDM2 is the master regulator of p53 and they form an autoregulatory feedback loop. $P14^{ARF}$ is activated in response to oncogene such as *MYC* and *E2F* and stabilizes p53 by inhibition of MDM2. In addition, PTEN negatively regulates the phosphatidylinositol-3 kinase-Akt pathway promoting the phosphorylation and movement of MDM2 into the nucleus where it downregulates p53 (Adapted from *Carr et al*., 2006).

1.4.7. *MYCN* amplification

MYCN is homologous to the *MYC* protooncogene (*MYCC*) (Kohl *et al*., 1983). The *MYCN* protooncogene encodes a 60-63 kDa protein (MycN), which is a nuclear phosphoprotein with a short half-life of 30–50 minutes. MycN is normally expressed in the developing embryo (Zimmerman *et al*., 1986). Moreover, high levels of MycN have been detected in the foetal brain, kidneys and in neuroblasts migrating from the neural crest prior to maturation. In contrast, adult tissues show relatively low expression of MycN. High levels of MycN have been observed in tumour cells of neural origin or those with neural characteristics including neuroblastoma, retinoblastoma and Wilms' tumour (Lee *et al*., 1984, Zimmerman *et al*., 1986).

The *MYCN* gene is expressed during the pre-implantation stage and is crucial for complete nervous system development. Moreover, at embryonic day 9.5, high levels of *MYCN* transcripts have been observed in mouse central nervous system (CNS), neural crest-derived tissues, lung, liver, early gut and meso-dermal derivatives where the roles of MycN include regulation of neural progenitor cell proliferation, nuclear size and differentiation (Knoepfler *et al*., 2002). Gradually, MycN is down-regulated as tissues become differentiated and growth-arrested. In addition, *MYCN* knockout mice showed normal development until embryonic day 10.5 when they became arrested in mid-gestation and further developed defects in the nervous system, heart, limbs, liver, genital ridge, lung and gut (Sawai *et al*., 1991). Wartiovaara and coworkers (2002) demonstrated that over-expression of MycN in post-mitotic sympathetic neurons could stimulate its re-entry into S-phase and survival after NGF withdrawal.

Like all myc family proteins, MycN contains an N-terminal transctivating domain (Myc box) and a C-terminal region containing a basic-helix-loop-helix/leucine zipper (bHLH-LZ) motif, which mediates DNA binding as well as binding to other bHLH-LZ proteins such as Max and Mad. MycN must first dimerize to Max and specifically bind to the canonical (5'- CACGTG) or non-canonical (5'- CA-NN-TG) E-box sequences to activate transcription. It has been suggested that histone H4-K3 methylation is a better indicator of a Myc protein binding site (Guccione *et al*., 2006). The MycN/Max transcription factor complex further recruits the chromatin remodelling complexes Swi/Snf, which altered chromatin structure and gene transcription (Lüscher, 2001).

Strong evidence providing the link between *MYCN* in neuroblastoma tumourigenesis and progression comes from the *MYCN* transgenic mouse model (Weiss *et al*., 1997). Amplification of the *MYCN* gene, located on the distal short arm of chromosome 2 (2p24) in neuroblastoma was identified by Schwab and coworkers in 1983. *MYCN* amplification results in 50-400 copies of the gene per cell. Amplification of the *MYCN* protooncogene occurs in 20-25% of neuroblastomas (Maris and Matthay, 1999). Brodeur et al (1984) were the first to show that *MYCN* amplification in neuroblastomas is correlated to poor clinical outcome.

A number of MycN targets have been identified over the years. These include the membrane ATP binding-associated multidrug resistance protein-1 (MRP1) (Haber *et al*., 1999), the cell cycle regulator, Id2 (Lasorella *et al*., 2002), cell proliferation gene such as *α-prothymosin*, teleomere maintenance enzyme (telomerase) (Mac *et al*., 2000), the DNA replication factor minichromosome maintenance protein, MCM7 (Shohet *et al*., 2002), cytokine, activin A (Breit and Schwab, 1989) and the developmental control gene, *Pax-3* (Harris *et al*., 2002). Putative MycN target genes with MycN-binding E-boxes in or near the promoter include *ornithine decarboxylase*, *regulator of chromosome condensation-1* and *IGF1R*. Morevoer, over-expression of MycN is reported to influence mRNA or protein expression of neural cell adhesion molecule, IL-6, NDRG1, MHC class I genes, and integrins (Chambery *et al*., 1999, Lutz *et al*., 1996, Mac *et al*., 2000). Therefore, increased levels of *MYCN* may confer cells to increased drug resistance, telomere length, cell cycle and proliferation (Table 1.3.).

There are several model systems developed in order to study the target genes of MycN in neuroblastoma. SHEP Tet21N cells (Tet21N) were created by Lutz et al (1996) to investigate the effect of MycN on neuroblastoma cell cycle. MycN expression can be switched off by the presence of tetracycline. In this study, MycN expression was found to shorten the time taken to progress through the cell cycle by shortening the G1 phase and direct target genes, *ornithine decarboxylase* (*ODC)*, *α-prothymosin* and *MRP-1* (Haber *et al*., 1999) were all up-regulated when MycN expression is switched on in this model.

Another regulatable MycN expression system is the p53 mutant SKNAS cell line, transfected with a *MYCN*-oestrogen receptor (*MYCN*-ER) construct. Upon stimulation with oestrogen receptor ligand (5-hydroxyl tamoxifen), the construct is translocated to the nucleus where *MYCN* is trancriptionally active (Tang *et al*., 2006). Lastly, RNAi technique is another useful method to study direct MycN target genes, MycN expression has previously been knocked down using *MYCN* anti-sense oligonucleotides, which caused neuroblastoma cell cycle arrest, differentiation and apoptosis (Bell *et al*., 2006, Kang *et al*., 2006, Woo *et al*., 2008, Nara *et al*., 2007).

From these model systems, several potential downstream target of MycN have been identified, which include genes that are important in processes like cell cycle, differentiation, apoptosis, drug resistance and angiogenesis (Table 1.3.)

Oncoprotein like MycN exerts both pro- and anti-apoptotic signals (Kaelin, 2005). In neuronal cells *MYCN* amplification causes cell death, therefore in order to survive, *MYCN* amplified neuroblastoma cells become dependent on other genes. The products of theses genes can stabilize MycN and promote further cell proliferation (Otto *et al*., 2009). Genes that become essential for cell survival when a particular gene (e.g. *MYCN*) is overexpressed is known as synthetic (dosage) lethal genes (Kroll *et al*., 1996, Measday and Hieter, 2002). Aurora kinase A expression is indirectly up-regulated by MycN and was found to inhibit MycN degradation by the ubiquitin ligase complex FBXW7 (Otto *et al*., 2009). Thus, *Aurora kinase A* is a synthetic lethal gene to *MYCN*.

CDK2 downregulation has also been found to be synthetic lethal to *MYCN*, where *CDK2* knockdown or inhibition with small molecule inhibitor induced apoptosis in *MYCN* amplified cells, but cells with a single copy of *MYCN* remained viable (Molenaar *et al*., 2009). Thus, synthetic lethal genes are key factors in *MYCN* function and are possible drug targets in *MYCN* amplified neuroblastoma.

MycN overexpression allows tumour cells to override the p21 mediated inhibition of G_1 check point after DNA damage, thus accelerating the cell cycle (Figure 1.2.) (Tweddle *et al*., 2003). Bell et al (2007) demonstrated that *MYCN* knockdown altered the expressions of several cell cycle related genes such as *SKP2* and *p53*. The same study also demonstrated that overexpression of *MYCN* caused a increased in *SKP2* and

decreased *p53*, which resulted in the reduction of *p21* and increased cell cycle of *MYCN* amplified neuroblastoma cell lines. However, in non-*MYCN* amplified neuroblastoma cell lines the expression of *MYCN* did not affect the level of *p21* or G_1 arrest in response to DNA damage, indicating that high levels of *MYCN* alone are not responsible for the failure to G_1 arrest after DNA damage. Therefore, *MYCN* may act through *p53* to reduce *p21* expression but G_1 arrest may be caused by a p53-independent pathway like the Wnt-signalling pathway. Increased in DKK3, which is a member of the Dickkopf family of secreted Wnt antagonist, levels were observed after *MYCN* knockdown and may cause a G_1 arrest through the negative regulation of β-catenin and cyclin D (Bell *et al*., 2006).

MycN and p53 are both expressed in the developing nervous system and it was suggested that MycN-driven *p53*-dependent apoptosis is important for the elimination of any rapidly proliferating neuroblasts to prevent deregulated cell proliferation and aberration during normal development (Chen *et al*., 2010). Moreover, *p53* is a direct transcriptional target of MycN and several of the p53 target genes (e.g. *p21* and *PUMA*) were also upregulated in the presence of MycN, sensitizing cells for p53-mediated apoptosis (Chen *et al*., 2010). *MYCN*-amplified cell lines may override the *p53*-dependent apoptosis by promoting the selection of cells with aberrations in the p53/MDM2 and $p14^{ARF}$ pathway. Slack et al (2005) proposed that MycN expression decreased the stability of p53 through induction of MDM2 expression and consequently inhibiting MycN-driven apoptosis and accelerating cell cycle progression.

This is not surprising since the role of p53-dependent apoptosis that acts as a safeguard mechanism to prevent cell proliferation induced by mitogenic oncogene such as *MYC* has long been established (Hermeking and Eick, 1994, Zindy *et al*., 1998, Soengas *et al*., 1999). This may explain why neuroblastomas may be initially chemosensitive.

Hermeking and Eick (1994) demonstrated that overexpression of *MYC* caused an increase in p53 mRNA and protein stability. Furthermore, the absence of Myc-induced apoptosis in $p53^{-/-}$ MEFs suggested that Myc-induced apoptosis is mediated by p53. Effectors upstream ($p14^{ARF}$ and MDM2) and downstream (Apaf-1, caspase-9 and cytochrome C release) of p53 have been shown to play a role in Myc-induced apoptosis

(Eischen *et al*., 1999, Soengas *et al*., 1999, Juin *et al*., 1999). In addition, Zindy and coworkers (1998) demonstrated that Myc activation in MEFs caused apoptosis via the induction of $p14^{ARF}$ and p53 activities. In contrast, MEFs lacking either $p14^{ARF}$ or p53 functions were resistant to Myc-induced apoptosis. In other words, MEFs, which survived Myc-induced killing, exhibited either *p53* mutation or, more rarely, biallelic $p14^{ARF}$ loss. This suggested that although Myc-induced p53 activation may protect cells from Myc-induced hyperproliferation, the absence of $p14^{ARF}$ and p53 may bypass this check point and growth promotion by Myc would predominate. Eischen et al (1999) demonstrated that induction of $p14^{ARF}$ by Myc interfered with MDM2 function in lymphoma. Similarly, Soengas and coworkers (1999) showed that MEFs deficient in Apaf-1 or caspase-9 but expressing Myc were resistant to apoptotic stimuli such TNFα. In addition, inactivation of Apaf-1 or caspase-9 could enhance the long-term survival of oncogenically transformed cells caused by Myc *in vitro* and *in vivo*. Interestingly, caspase-9 is located at chromosome 1p34-1p36.1 (Deloukas *et al*., 1998), which as mentioned previously is a hotspot for loss of heterozygosity in neuroblastomas. Therefore, disruption of the effector mechanisms of p53-dependent apoptosis may facilitate Myc transformation and tumour development

Gene	+ or - regulated by *MYCN*	Evidence of regulation by *MYCN*	Function	References
Activin-A	-	E, R	Inhibits angiogenesis (TGFβ superfamily)	Hatzi *et al*., 2000 Breit *et al*., 2000
CRABP II	+	E, C, ChIP	Regulator of retinoic acid signalling	Gupta *et al*., 2006
HMGA1	+	E, R	Proto-oncogene TF	Giannini *et al*., 2005
ID2	+	C, E, R	Inhibitor of RB	Lasorella *et al*., 2002
IL-6	-	R	Inhibits endothelial cell proliferation	Hatzi *et al*., 2002(i)
LIF	-	R	Inhibits endothelial cell proliferation	Hatzi *et al*., 2002(ii)
MCM7	+	ChIP, R	DNA replication	Shohet *et al*., 2002
MDM2	+	ChIP, R, E	Negative regulator of p53	Slack *et al*., 2005
MRP1	+	C, R	Multi-drug resistance protein	Manohar *et al*., 2004
NDRG1	-	E, G	Growth inhibitory gene	Li and Kretzner, 2003
NLRR1	+	E, C, R	Transmembrane protein	Hossain *et al*., 2008
ODC	+	E, R	Polyamine biosynthesis	Lu *et al*., 2003 Lutz *et al*., 1996
p53	+	C, ChIP, R, E	Tumour suppressor	Chen *et al*., 2010
Pax3	+	R	Developmentally regulated proto-oncogene	Harris *et al*., 2002
α-Prothymosin	+	E, ChIP	Chromatin remodelling	Lutz *et al*., 1996 Mac *et al*., 2000 Sasaki *et al*., 2001
TERT	+	ChIP	Maintenance of telomeres	Mac *et al*., 2000
TG2	-	ChIP, E	Tumour Suppressor	Liu *et al*., 2007

Table 1.3. Summary for a selection of direct MycN targets.

E = up/down regulation after ectopic *MYCN* expression, C = correlation in tumours, ChIP = chromatin immunoprecipitation, R = reporter gene assay, G= Gel-shift assay (Adapted from Bell *et al*., 2010).

1.4.8. Neurotrophin signalling pathways

Neurotrophin signalling plays a central role in normal neuronal development. Neurotrophins include nerve growth factor (NGF), brain-derived neurotrophic factor (BDNF), neurotrophin-3, and neurotrophin-4. Neurotrophin signalling is mainly mediated through the Trk family of tyrosine kinases. TrkA (also known as NTRK1) serves as the high-affinity receptor for NGF, developing neurons differentiate in response to this ligand and enter an apoptotic pathway upon NGF withdrawal. TrkB (also known as NTRK2) binds both BDNF and neurotrophin-4 (NT4) with high-affinity, and TrkC (also known as NTRK3) is the high affinity receptor for neurotrophin-3 (NT3) (Barbacid, 1995).

In normal sympathetic ganglia, most of the mature neurons at the perinatal stage express TrkA at high concentrations. It has been reported that switching expression from TrkB or TrkC to TrkA occurs in later embryonic stages (Birren *et al*., 1993). A massive physiological neuronal apoptosis occurs soon after expression of TrkA. This apoptosis is explained by the trophic theory, which states that depletion of nerve growth factor, the preferred ligand for TrkA, makes cells unable to survive. Therefore, the fate of a neuronal progenitor cell during ontogenesis is to differentiate into a highly specialised neuron or to be removed by an apoptotic process, depending on the expression of neurotrophin receptors and their ligands (Schwab *et al*., 2003).

Transfection of *TRKA* into a non–TrkA-expressing neuroblastoma cell line restores the ability to differentiate in response to NGF (Lavenius *et al*., 1995). TrkA expression is inversely correlated to disease stage and *MYCN* amplification status. Thus, high TrkA expression, usually found in patients <1 year, is a marker of favourable neuroblastomas and is correlated with an increased probability of disease survival. In contrast, full-length TrkB (there is also a truncated isoform lacking the tyrosine kinase) is expressed preferentially in advanced stage neuroblastomas with *MYCN* amplification. Many of these tumours also express BDNF, establishing an autocrine pathway promoting cell growth, enhanced angiogenesis, survival and drug resistance. TrkB is either expressed in low amounts, or as the truncated isoform, in biologically favorable tumours. Lastly, TrkC is expressed in favourable neuroblastomas, essentially all of which also express TrkA. Therefore, it seems that the expression pattern of neurotrophin receptors at the time of malignant transformation, which is related to the degree of neuroblastic

differentiation, has a critical influence on tumour behaviour (Brodeur, 2003, Maris and Matthay, 1999).

1.4.9. Overexpression of multidrug resistance genes

Acquired drug resistance is a common cause of neuroblastoma treatment failures. *MRP* encodes the multidrug resistance-associated protein, which is also an efflux pump that can render a cell resistant to drugs. In a study of 60 primary untreated neuroblastomas, Norris and coworkers (1996) showed that MRP expression was strongly correlated with MycN expression and patient survival. These data and the identification of E-box motif consensus sequences in the *MRP* promoter region suggested a potential interaction between the MycN protein and MRP expression (Zhu and Center, 1994). Norris and coworkers (1997) demonstrated that transfection of *MYCN* antisense RNA into a neuroblastoma cell line that expressed both *MRP* and *MYCN* resulted in downregulation of *MRP* messenger RNA to undetectable levels. Therefore, MycN protein overexpression may transcriptionally activate *MRP* and lead to the drug resistant phenotype, even in untreated primary tumours. However, a direct demonstration of MycN mediating increased *MRP* transcription has not yet been provided (Maris and Matthay, 1999).

1.4.10. Expression of telomerase

Telomerase is a reverse transcriptase that is important for the maintenance of chromosomal ends (telomeres). High telomerase activity has been linked to cancers. Hiyama and coworkers (1995) demonstrated that high telomerase activity is directly correlated with *MYCN* amplification and poor clinical outcome in neuroblastoma. Interestingly, in the same study, telomerase activity is absent in neuroblastoma patients with stage 4S tumours.

1.4.11. Apoptotic signalling pathway

NGF withdrawal is a major signal for apoptosis in the developing nervous system and mediates the elimination of redundant cells. Thus, lack of the neurotrophin receptors signalling can initiate the apoptotic pathway. Other cell surface proteins are involved with initiation of apoptosis in neuronal cells and neuroblastomas. Members of the tumour necrosis factor receptor family, such as p75 (binds NGF with low affinity) and *CD95*/Fas (binds Fas ligand), as well as members of the retinoic acid receptor family,

can mediate the induction of apoptosis in some neuroblastoma cell lines. In addition, increased CD95 expression seems to be an essential component of chemotherapy-induced apoptosis in neuroblastomas (Fulda *et al*., 1997).

1.4.12. Hereditary predisposition to neuroblastoma

Familial neuroblastoma is inherited in an autosomal dominant pattern (Knudson and Strong, 1972). A recent study has suggested that a very rare germline mutation of the anaplastic lymphoma kinase (*ALK*) gene may predispose individuals to the development of neuroblastoma (Mosse *et al*., 2008).

Anaplastic lymphoma kinase (ALK) is an orphan tyrosine kinase receptor first identified as part of the t(2;5) chromosomal translocation associated with most anaplastic large cell lymphomas (ALCL) and a subset of T-cell non-Hodgkins lymphomas (Morris *et al*., 1994). ALK is expressed mainly in the neonatal brain, with a postulated role in neuronal differentiation; however ALK expression falls sharply after birth (Iwahara *et al*., 1997). Many human cancers have been shown to activate ALK signalling by creating unique oncogenic fusions of the *ALK* gene at chromosomal band 2p23 with a variety of partners through chromosomal translocation events, thus resulting in the generation of oncogenic ALK fusion proteins. These oncogenic fusion proteins lead to constitutive activation of the ALK kinase domain and have been identified in various solid tumours such as non-small cell lung cancers and squamous cell carcinomas (Jazii *et al*., 2006, Soda *et al*., 2007, Rikova *et al*., 2007).

Mosse et al (2008) demonstrated that the R1275Q mutation is the most common germline mutation. The disease penetrance may be determined by mutation type as rarer mutations, such as G1128A seen in one large pedigree, was associated with very low penetrance compared with the near complete penetrance seen with the R1275Q mutation. Both mutations occur within the kinase activation loop in a region strongly associated with activating mutations seen in other oncogenic kinases. These mutated sites might offer a tractable therapeutic target. Two hot spots of ALK-activating mutations at position F1174 and R1275 have been reported in neuroblastoma sporadic tumours and cell lines and ALK expression is significantly higher in neuroblastoma cells harboring ALK mutations (Mosse *et al*., 2009, Janoueix- Lerosey *et al*., 2010).

Both F1174 and R1275 mutations resulted in constitutive phosphorylation of ALK and its downstream targets such as ERK, AKT and STAT3, depending on tissue context and cellular localization. Therefore, ALK mutations could lead to cell growth and survival (Chen *et al*., 2008, George *et al*., 2008, Janoueix-Lerosey *et al*., 2008, Mosse *et al*., 2008).

The candidate ligands of mammalian wild-type ALK receptor reported so far are pleiotropin (PTN) and midkine (MK) (Stoica *et al*., 2001, Stoica *et al*., 2002). Signalling by PTN and MK initiates the dimerization and phosphorylation of ALK, leading to activation of the PI3K/AKT pathway and cell proliferation (Powers *et al*., 2002). Moreover, binding of ALK receptor to its ligands could also cause inhibition of apoptosis and induction of neuronal cell differentiation through the MAPK pathway (Webb *et al*., 2009, Souttou *et al*., 2001).

In neuroblastoma cell lines with ALK amplification, the constitutively activated ALK has been shown to form a stable complex with hyperphosphorylated ShcC, a Src homology 2 domain-containing adaptor protein (Miyake *et al*., 2002). Subsequently, this caused deregulation of the responsiveness of the MAPK pathway to growth factors (Osajima-Hakomori *et al*., 2005). Furthermore, interference of ALK binding to ShcC significantly impaired the survival, differentiation and motility of neuroblastoma cells with activated ALK. The same study showed that MAPK and PI3K/AKT pathways were blocked and apoptosis was induced (Osajima-Hakomori *et al*., 2005). In addition, mice lacking both ShcB and ShcC displayed a significant loss of sympathetic neurons, which suggested that these adaptors are involved in sympathetic neurons development and survival. Thus, the gain-of-function ALK mutations signalled mostly through the MAPK or AKT pathways and, in some cases, STAT pathway in neuroblastoma (Chen *et al*., 2008, George *et al*., 2008, Janoueix-Lerosey *et al*., 2008, Mosse *et al*., 2008).

Currently, various therapeutic options for ALK-positive neruoblastomas have been developed. Small molecules inhibiting ALK such as crizotinib (PF-2341066) effectively caused complete and sustained regression of xenografts harboring the R1275Q mutation (Wood *et al*., 2009). Carpenter et al (2011) demonstrated that treatment of neuroblastoma cell lines with ALK-specific monoclonal antibodies induced enhanced immune cell-mediated cytotoxicity, which subsequently caused inhibition of cell proliferation and cell death.

Loss of function mutations in the *paired-like homeobox 2B* (*PHOX2B*) gene located at 4p12 have been detected in a small subset of familial neuroblastoma (Trochet *et al*., 2004). *PHOX2B* encodes a transcription factor that is essential for the regulation of neurogenesis. Germline missense or frameshift mutations in the homeodomain of *PHOX2B* identified in familial neuroblastoma are seen primarily in cases with associated anomalies of neural crest derived tissues, including Hirschsprung disease. Although *PHOX2B* was the first identified predisposition gene in neuroblastoma, mutations in this gene account for a minority of hereditary cases (Mosse *et al*., 2004).

In summary, favourable tumours with good clinical outcome are characterised by near-triploid karyotypes with whole chromosomal gain, high TrkA neurotrophin receptor expression and patients should be <1 year old. In contrast, unfavourable tumours with poor prognosis are characterised by deletions of 1p or 11q, gain of chromosome 17q and/or *MYCN* amplification. The tumours may also express TrkB neurotrophin receptor, its ligand (BDNF) and the patients are usually >1 year old with advanced stage disease.

1.5. Treatment

High-risk disease (stage 3 and 4) is difficult to cure even after intensive, multiple rounds of therapies including surgery, radiotherapy, chemotherapy and stem cell transplant (Brodeur, 2003).

Retinoic-acid derivatives have been used to induce differentiation and slow the growth of neuroblastoma cells *in vitro* (Brodeur, 2003). Treatment of high-risk neuroblastoma patients with 13-*cis* retinoic acid after bone-marrow transplantation was carried out in a randomized clinical trial, and showed a significant survival advantages with minimal extra toxicity (Matthay *et al*., 1999).

Recent new approaches for the treatment of neuroblastoma include activation of apoptosis with a novel synthetic retinoid-N-(4-hydroxyphenyl) retinamide (fenretinide) that has been used in clinical trials in neuroblastoma patients (Lovat *et al*., 2000, Ponzoni *et al*., 1995, Reynolds, 2000). Trk-specific tyrosine kinase inhibitors can reduce TrkB expression and induce apoptosis alone or in combination with chemotherapeutic agents (Evans *et al*., 1999). A phase I trial of lestaurtinib, a multi-kinase inhibitor that strongly inhibits TrkB, has recently been completed in children

with refractory neuroblastoma. This study has identified a well tolerated oral dose that results in effective TrkB inhibition, and its efficacy will be studied in future paediatric clinical trials (Minturn *et al*., 2011). Immunotherapy with antibodies raised against neuroblastoma surface antigens such as GD2 has also been developed (Yu *et al*., 1998, Cheung *et al*., 1998).

1.6. Clusterin (CLU)

CLU is a heterodimeric sulfated glycoprotein which is highly conserved among species and ubiquitously expressed in tissues and body fluids (Trougakos and Gonos, 2002, Trougakos *et al*., 2004, Pucci *et al*., 2004, Gleave and Miyake, 2005). Over the past two decades, different nomenclatures have been given to CLU due to the diversity of its function. CLU (also known as Apolipoprotein J, TRPM-2, SGP-2 and clusterin) was first discovered as a protein causing Sertoli cells, which supply nutrients to sperm, to form clusters (Fritz *et al*., 1983). CLU has been reported to be involved in various processes such as complement regulation (Jenne and Tischopp, 1989), sperm maturation (Sylvester *et al*., 1984), lipid transport (Burkey *et al*., 1992), apoptosis (Zhang *et al*., 2005) and DNA repair (Yang *et al*., 1999).

However, how CLU exerts its function has been a matter of speculation. One hypothesis is that CLU is involved in the clearance of toxic substances from extracellular spaces through its ability to bind to unfolded proteins, cell debris or immune complexes (Wilson and Easterbrook-Smith, 2000, Wyatt *et al*., 2009). CLU binds to the endocytic receptor megalin (LRP2), and the clearance effect could be achieved by internalisation of the receptor-ligand complex and lysosomal degradation of the toxic substances (Shannan *et al*., 2006, Jones and Jomary, 2002). Moreover, CLU expression is low in normal conditions but is induced by stress stimuli, suggesting that its function could also be directly or indirectly related to the stress response.

Mouse development is not affected by genetic inactivation of *CLU*. However, *CLU* null mice show increased sensitivity to autoimmune myocarditis, suggesting a role for CLU in protecting the heart tissue from post inflammatory destruction (McLaughlin *et al*., 2000). In contrast, neuronal cells are sensitized by CLU to hypoxic injury (Han *et al*., 2001). CLU has also been implicated in other diseases such as Alzheimer's disease, where excessive CLU expression is associated with accumulation of Amyloidβ plaque

and neuritic toxicity *in vivo* (Lambert *et al*., 2009, Calero *et al*., 2000), and cancer (Shannan *et al*., 2006) (see section 1.6.2.).

1.6.1. CLU synthesis and Glycosylation

CLU is encoded by a single-copy gene in humans, located on chromosome 8p21. The 449-amino acid primary peptide chain is expressed in various forms, depending on the location of the protein. CLU expression is initiated by translation of the first start codon (AUG) from the full length *CLU* mRNA (1.6kb) to produce a 49 kDa precursor secreted CLU (Shannan *et al*., 2006). This protein is then directed to the lumen of the endoplasmic reticulum by a leader signalling sequence and further undergoes an extensive N-linked glycosylation process, where it becomes a 75-80kDa mature precursor after transportation from the endoplasmic reticulum (ER) to the Golgi apparatus (O'Sullivan *et al*., 2003). Kapron et al (1997) identified six N-linked Glycosylation sites of human CLU, three on the alpha chain (α 64N, α 81N, α 123N) and three on the beta chain (β 64N, β 127N, β 147N). The mature 75-80kDa protein undergoes intracellular cleavage between amino acid residue Arg^{205}- Ser^{206} to form alpha (α) and beta (β) subunits, which are linked together by five disulfide bonds upon extracellular secretion (sCLU) (Figure 1.3.) (Burkey *et al*., 1991). Under reduced conditions, the subunits of CLU can be detected with the approximate size of 35-40kDa (Rodriguez-Pińeiro *et al*., 2006).

O'Sullivan et al (2003) demonstrated that post-translational modifications, such as glycosylation and internal proteolytic cleavage could be blocked when cells are subjected to stress. Failure of protein cleavage leads to the retrograde transport of uncleaved and non-glycosylated (55-60kDa) form of CLU from the Golgi back to the ER. Thus, the secretion of CLU is reduced but not eliminated and intracellular non-glycosylated precursor CLU (pCLU) increased.

Another form of CLU is found in the nucleus and is known to be induced after stress, such as ionizing radiation (IR) (Leskov *et al*., 2003, O'Sullivan *et al*., 2003). Many theories for the synthesis of nuclear CLU (nCLU) have been proposed. One theory postulates that CLU is generated from an alternative splicing event, which results in an N-terminal truncated mRNA lacking exon 2, where the ER reader peptide sequence and the first AUG codon reside (Figure 1.3.A) (Leskov *et al*., 2003). This alternative

transcript is translated into a precursor protein (pnCLU), which is not cleaved into α or β subunits. Upon cell damage, pnCLU undergoes post-translational modification to form a mature ~55-kDa protein, exposing both of its nuclear localization signals (NLSs), and migrates to the nucleus to induce apoptosis (Leskov *et al*., 2003).

Another theory suggests that nCLU could be generated by a second alternative translational starting site (second ATG) and not from a splicing event (Rizzi and Bettuzzi, 2008).

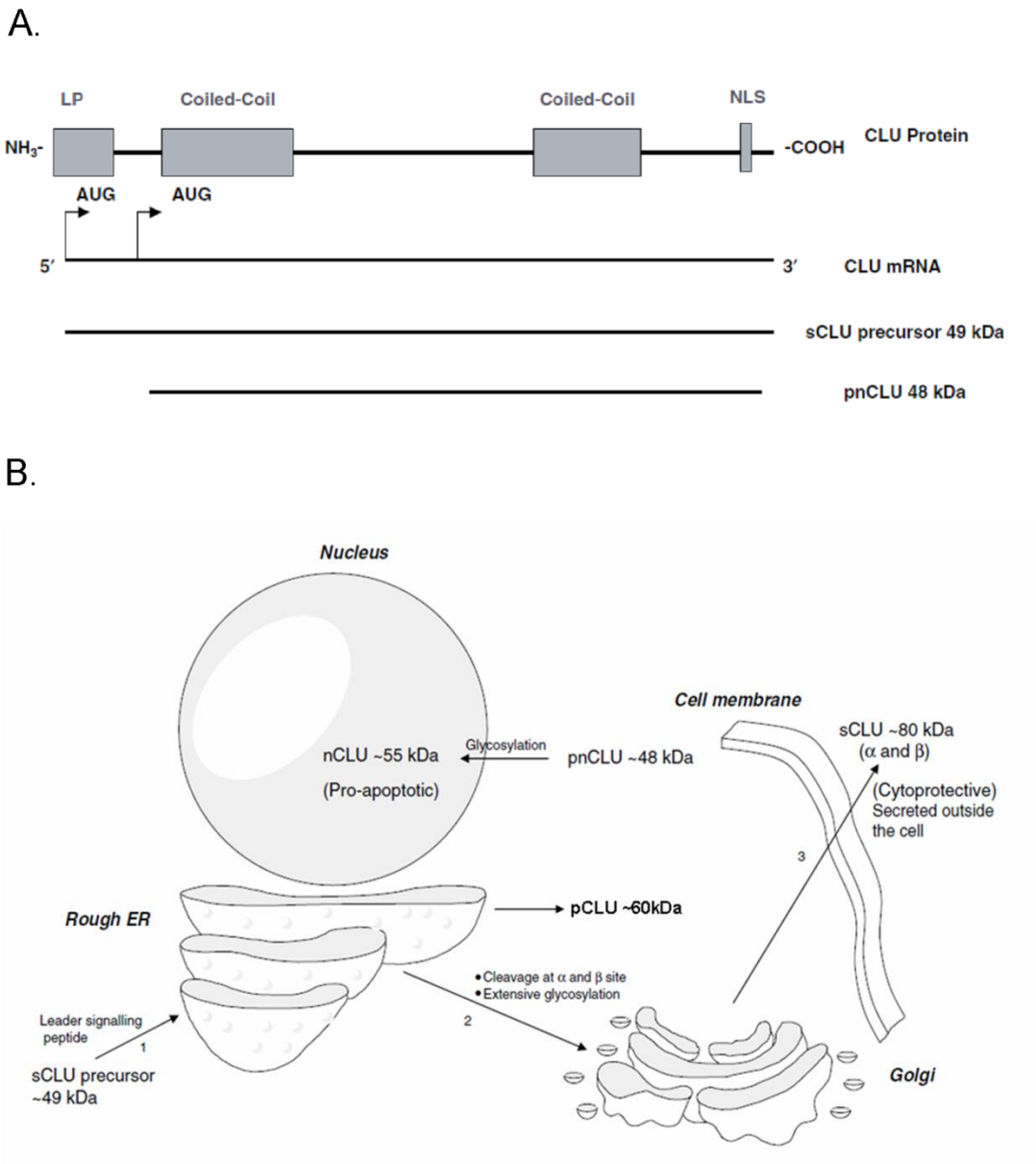

Figure 1.3. Synthesis of different CLU forms (sCLU and nCLU)

A) Transcription of the first AUG codon of the full-length *CLU* mRNA to form the precursor sCLU, while nCLU is believed to be generated from differentially spliced mRNA (LP; leader peptide, NLS; nuclear localization signal).

B) Secreted CLU precursor is transported into the rough ER by leader signalling peptide (1) and then undergoes cleavage upon extensive N-linked Glycosylation upon arrival to the Golgi apparatus (2). The resulting ~80kDa mature CLU with 5 disulfide bonds between the α and β subunit is secreted outside the cells (3). pnCLU remains inside the cytoplasm and upon stress, moves into the nucleus to form a mature ~55kDa nCLU (Adapted from Shannan *et al*., 2006).

1.6.2. Role of CLU in cancer

The exact role of CLU in carcinogenesis remains controversial, with reports of increased or decreased CLU expressions in different cancers and opposing biological effects (Table 1.4.) (Shannan *et al*., 2006, Rizzi and Bettuzzi, 2009). Increased CLU mRNA and/or protein expression have been detected and associated with chemoresistance in prostate cancer (Miyake *et al*., 2003), breast carcinomas (Leskov *et al*., 2003), lung cancer (July *et al*., 2004), colorectal cancer (Rodriguez-Piñeiro *et al*., 2006) and ovarian cancer (Wei *et al*., 2009). In contrast, decreased CLU mRNA and/or protein expressions have been reported in oesophageal squamous carcinoma (Zhang *et al*., 2003), pancreatic cancer (Xie *et al*., 2002), neuroblastoma (Chayka *et al*., 2009) and also in prostate cancers (Bettuzzi *et al*., 2009).

It has been speculated that accumulation of CLU in the nucleus causes apoptosis in prostate and breast cancers (Caccamo *et al*., 2005, O'Sullivan *et al*., 2003). Yang et al (1999) first identified CLU as a stress-inducible protein that is associated with the DNA-dependent protein kinase (DNA-PK), which facilitates double-strand break (DSB) repair by non-homologous end joining. DNA-PK is a nuclear serine/threonine kinase, which contains a catalytic subunit (DNA-PKcs) and a DNA-binding subunit (Ku70 and Ku80). Nuclear CLU, but not sCLU, protein binds to Ku70, forming a trimeric protein complex with Ku80. Overexpression of nCLU reduces the activity of Ku70/Ku80 DNA ends binding, thus, preventing DNA repair and induce apoptosis, in whole-cell extracts of MCF-7 breast cancer cells (Yang *et al*., 1999, Leskov *et al*., 2003).

The group lead by Martin Gleave and others support the hypothesis that *CLU* is an oncogene and is highly expressed in advanced prostate, breast and ovarian cancer (Yang *et al*., 2009, Chi *et al*., 2008, Miyake *et al*., 2003, Shannan *et al*., 2006). In many instances, CLU has been shown to be anti-apoptotic, protecting cells against a variety of death signals. Exogenous CLU protects tumour cells from cytokine- or drug- induced apoptosis and inhibition of CLU results in the increased sensitivity of cancer cells to chemotherapeutic drugs (Gleave and Chi, 2005, Jun *et al*., 2011, Koch-Brandt and Morgans, 1996, Miyake *et al*., 2005, Miyake *et al*., 2003, Sallman *et al*., 2007, Shim *et al*., 2009).

Moreover, intracellular CLU has been shown to inhibit prostate cancer apoptosis by interfering with Bax activation in the mitochondria, which leads to inhibition of cytochrome C release and caspase activation in response to chemotherapeutic drug (Zhang *et al*., 2005). An antisense oligonucleotides (OGX-011), which inhibits CLU expression, has been generated and used in phase I and II-clinical trials in prostate and metastatic breast cancers (Chi *et al*., 2005, Chia *et al*., 2009). The results of the prostate trial suggested that patients do have a benefit when OGX-011 is combined with docetaxel treatment (Chi *et al*., 2010). However, it is difficult to assess whether the clinical effect is truly dependent on the efficiency of CLU suppression in tumour cells or off-target effects due to non-specific interaction between the two drugs. The results from the metastatic breast cancer trial showed a response rate similar to that from single agent treatment, docetaxel alone. Thus, the disappointing findings resulted in no further proceeding of the trial.

In contrast with the findings of Gleave's group, Bettuzzi's group showed that CLU is downregulated and acts as a tumour suppressor of prostate cancer cell proliferation (Caccamo *et al*., 2005, Rizzi and Bettuzzi, 2009). Our group, in collaboration with the Bettuzzi's group, has shown that genetic ablation of *CLU* enhances prostate tumourigenesis in mice due to the finding that either PIN (prostate intraepithelial neoplasia) or differentiated carcinoma was observed in 100% and 87% of mice with homozygous or heterozygous deletion of *CLU*, respectively. Morevoer, the same study also showed that crossing of *CLU* knockout with TRAMP (prostate cancer prone) mice enhanced prostate tumour metastasis. Lastly, *CLU* depletion caused tumourigenesis in female TRAMP mice, which are normally cancer free and that genetic inactivation of *CLU* induced the activation of nuclear factor-kB, a potentially oncogenic transcription factor important for the proliferation and survival of prostate cells, thus supporting the hypothesis that CLU is a suppressor of prostate cancer development (Bettuzzi *et al*., 2009).

Ghimenti et al (1999) reported that most pancreatic tumours displayed loss of heterozygosity on the short arm of chromosome 8 (8p21-22), the same region where the *CLU* gene resides. Xie et al (2002) demonstrated that CLU expression is downregulated in pancreatic cancers and CLU positive patients survived significantly longer than CLU negative patients. Taken together, these results indicate that the role of CLU in cancer is

complex and probably context-dependent. A sensible theory is that CLU may exert both pro- and anti- tumourigenic functions, depending on various factors such as the levels of each CLU isofroms in the cell, the stage, the nature of the tumour and the presence or absence of chemotherapeutic drug treatment.

Tumour	CLU expression	Isoforms
Prostate cancer	↑ mRNA and protein	sCLU
Ovarian cancer	↑ protein	cCLU
Breast carcinoma	↑ mRNA	sCLU
Lung cancer	↑ mRNA	cCLU
Colorectal cancer	↑ mRNA and protein	sCLU
Oesophageal squamous carcinoma	↓ mRNA and Protein	cCLU and sCLU
Neuroblastoma cancers	↓ Protein	cCLU
Pancreatic cancer	↓mRNA	cCLU
Prostate cancer	↓ mRNA	cCLU

Table 1.4. Summary of CLU expression in tumours (↑*: Increase in expression, ↓**: decrease in expression, sCLU is secreted clusterin, cCLU is cytoplasmic clusterin) (Adapted from Shannan *et al*., 2006).

1.6.3. CLU and neuroblastoma

The first evidence linking CLU to neuroblastoma was reported in our laboratory over 10 years ago when we identified CLU as a downstream target gene of the B-MYB transcription factor (Cervellera *et al*., 2000).

More recent work showed that overexpression of CLU reduced, whereas downregulation increased, the growth of neuroblastoma xenograft in immunodeficient mice. Mice in which *CLU* is genetically deleted are more prone to neuroblastoma development (Chayka *et al*., 2009). In agreement with these observations, the expression of CLU is higher in localised and lower in metastatic human neuroblastomas (Chayka *et al*., 2009).

Interestingly, the oncomine database shows an association between *CLU* mRNA to some of the cytogenetic profiles associated with aggressive neuroblastoma. Decreased *CLU* mRNA expression levels are observed in tumours with *MYCN* amplification and loss of heterozygosity in chromosome 1 comparing to non-*MYCN* amplified tumours and tumours with no loss of heterozygosity of chromosome 1 (Figure 1.4.).

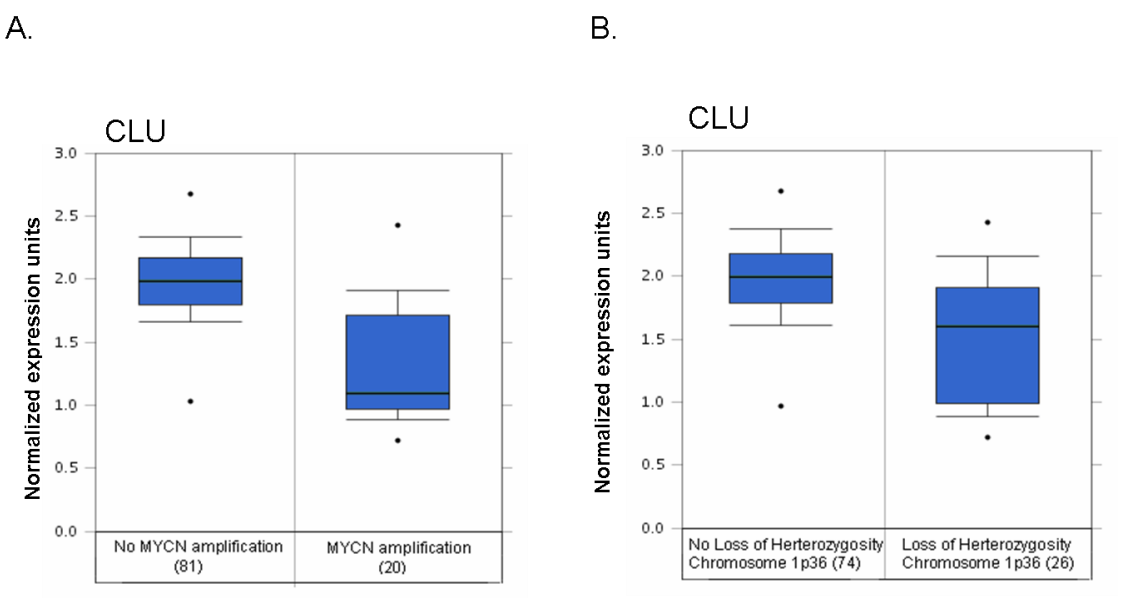

Figure 1.4. An association between *CLU* mRNA to some of the cytogenetic profiles associated with aggressive neuroblastoma

Oncomine database (www.oncomine.org) shows a box plot where *CLU* gene expression is reduced in **A)** 20 *MYCN* amplified neuroblastoma tumours compared with 81 non-*MYCN* amplified neuroblastoma tumours. **B)** 26 neuroblastoma tumours with loss of heterozygosity of chromosome 1p36 compared with 74 neuroblastoma tumours without loss of heterzozygosity of chromosome 1p36.

P-value is $p<0.0001$. The top and bottom edges of each box correspond to the 75th percentile and 25th percentile, respectively. The median value (50th percentile) is shown as a horizontal black line through each box. Whiskers extend from the minimum to the maximum values. The box plot displays the centre portions of the data and the range of the data. Black dots represent outliers.

CLU mRNA and protein are downregulated by *MYCN* in neuroblastoma, in part by inducing the oncogenic 17-92 microRNA cluster (Chayka *et al*., 2009). In recent, still unpublished, experiments we have observed that MycN binds to the CLU promoter, where it recruits co-repressors including histone deacetylases and polycomb proteins that induce a repressed chromatin conformation. Thus, we hypothesise that silencing of CLU by MycN is an important tumourigenic event in neuroblastoma.

Mouse embryonic fibroblasts (MEFs) with a disrupted *CLU* gene show IκB destabilisation, which results in increased NF-κB activity and modulation of NF-κB target genes (Santilli *et al*., 2003). Ectopic expression of CLU resulted in the downregulation of NF-κB, which ultimately inhibited both *in vitro* and *in vivo* invasion of the human neuroblastoma (Chayka *et al*., 2009, Santilli *et al*., 2003). Recently, Liu et al (2011) demonstrated that CLU is a downstream target of *CASZ1* and that *CASZ1*, a tumour suppressor gene, was able to induced CLU expression in association with induced tumour suppression or metastasis suppression (Liu *et al*., 2011).

1.6.4. Mechanism of tumour promotion or suppression used by CLU

The mechanism of tumour promotion or suppression used by CLU is under intense scrutiny. This is because CLU has been shown to act as a signalling molecule that is able to either activate or suppress various signalling pathways including PI3K-AKT, MAP/ERK and NF-κB during tumourigenic progression.

Both PI3K and MAP/ERK pathways are survival pathways, which have been implicated in many types of cancers. Phosphatidylinositol-3 kinase (PI3K) is activated by receptor tyrosine kinases (RTKs) and translocated to the plasma membrane. Activated PI3K converts phosphatidylinositol-3,4,5-triphosphate (PIP3) from the substrate phosphatidylionositol-3,4-diphosphate (PIP2). Accumulation of PIP3 recruits phosphoinositide- dependent kinase 1 (PDK1) and AKT to the plasma membrane. AKT is activated via phosphorylation at two key regulatory sites, Thr^{308} (by PDK1) and Ser^{473} (by mTOR). Activated AKT then promotes survival by mediating nuclear translocation of nuclear factor κB (NF-κB), which further transcriptionally activates multiple genes important for cell survival and proliferation. PTEN is a tumour suppressor that negatively regulates PI3K activity by dephosphorylating PIP3 back to PIP2 and thereby terminating PI3K signalling (Krakstad and Chekenya, 2010). PI3K

pathway crosstalks with Mitogen-Activated Protein Kinase (MAPK, originally called ERK), which can signal cells to survive or grow. MAPK begins with the activation of Ras, triggered also by activated RTKs. Three downstream serine/threonine kinases (called Raf, MEK and ERK) participate in the phosphorylation cascade, which eventually results in changes in gene expressions and protein activities (Figure 1.5.).

Many reports have suggested that sCLU modulates cell survival through the Phosphoinositide-3 Kinase (PI3K) pathway. In epithelial cancer, Jo and coworkers (2008) revealed that during stress (i.e. nutrient deprivation), HeLa cells secrete IGF-1 and CLU constitutively into the tumour microenvironment. Secreted CLU competitively binds to the IGF-1 receptor (IGF-1R) and abolished IGF-1-induced AKT activation, thus, resulting in decreased proliferation. The study concluded that in response to environmental stresses, cellular adaptation by cancer cells such as secretion of cancer cell-derived factors (e.g. CLU) can impose a selective pressure (e.g. anti-proliferation) on neighbouring cells, which gives the cancer cells a selective survival advantage.

However, Ammar and Closset (2008) demonstrated that CLU activates survival through PI3K/AKT pathway in the prostate cancer model via its receptor (megalin). Overexpression of CLU protects prostate cells against TNF-α induced apoptosis by inducing AKT phosphorylation in a dose dependent manner. Increased CLU and phosphorylated AKT also lead to a dose-dependent phosphorylation of Bad, which blocks pore formation and abolishes cytochrome C release from the mitochondria, thus, inhibiting TNF-α induced cell death. The investigators also demonstrated that secreted CLU activates the PI3K survival pathway in a specific manner since complete cell death was observed when a PI3K-specific inhibitor (wortmannin) was used.

It has also been suggested that CLU may act via a PI3K-independent pathway. Chou and coworkers (2009) demonstrated that silencing of CLU induces a mesenchymal-to-epithelial (MET) transition via the ERK/Slug signalling pathway in a lung cancer model. Ablation of CLU resulted in increased E-Cadherin but decreased phosphorylation of ERK, fibronectin and slug expression.

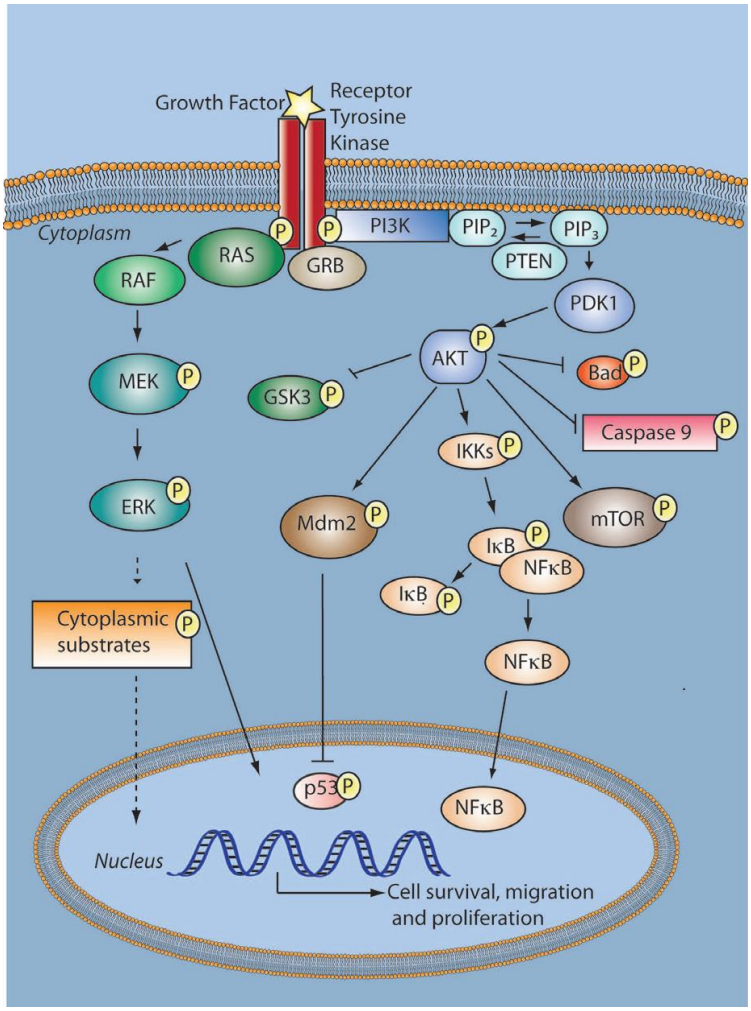

Figure 1.5. Survival signalling pathways

Hyperactive Receptor tyrosine kinases e.g., EGFR, PDGFR signal upon ligand binding or constitutive activation via Ras-MEK-ERK (MAPK) to mediate cell growth and angiogenesis and via PI3K/AKT to mediate survival. AKT phosphorylates multiple substrates that lead to release of survival factors or interference with the execution of apoptosis. Phosphoinositide-dependent kinase 1 (PDK1), phosphatidylinositol-3,4,5 triphosphate (PIP3), phosphoinositide- 4,5 bisphosphate (PIP2), pro-apoptotic BCL-2-associated agonist of cell death (BAD), and Nuclear factor κB (NFκB) (Krakstad and Chekenya, 2010)

Another leading hypothesis is that CLU contributes to tumour restriction by inhibiting the canonical NF-κB pathway (See section 1.7.). NF-κB has been shown to play an important role in the central nervous system by promoting neural survival and protecting neurons from toxic insults (Gutierrez *et al*., 2005). Our group has shown that in the absence of CLU, inhibitors of kappa B (IκBs) alpha and beta get destabilised, leading to aberrant NF-κB activity in *CLU* KO mice (Santilli *et al*., 2003). An increased activity of the p65 NF-κB subunit was observed in neuroblastoma arising in *CLU* KO mice and an NF-κB inhibitor (BAY 11-7082) was shown to reduce *in vitro* invasion activity of neuroblastoma cells deriving from *MYCN* transgenic mice (Chayka *et al*., 2009). CLU has later been confirmed to be an inhibitor of NF-κB, suggesting that the well documented role of CLU as an inflammation and autoimmunity inhibitor could be related to the modulation of this key molecule (Devauchelle *et al*., 2006).

Many tumours show activation of the NF-κB pathway to which they become addicted. Certain types of human leukemias and epithelial cancers like prostate, lung and liver carcinomas are characterized by activation of NF-κB (Naugler and Karin, 2008).

The role of NF-κB in the aggressive behaviour of human neuroblastoma is not yet well established. There is some evidence linking the activation of NF-κB to either survival or death of neuroblastoma cells, depending on tumour histology and the type of death stimuli (Bian *et al*., 2001). In a recent paper, the presence of nuclear or cytoplasmic p65 NF-κB has been linked to upregulated MHC expression in ganglion cells, suggesting that reduced level of p65 NF-κB in neuroblasts could be required for immune escape (Forloni *et al*., 2010). However, in some cases we have also observed strong expression of nuclear p65 NF-κB in neuroblastoma (Sala and Chaiwatanasirikul, in press). Although we do not know the function of p65 NF-κB in these cells, we can hypothesise that activated NF-κB, like in other tumours, could drive the expression of genes involved in metastasis. Little is known regarding the gene expression of NF-κB in neuroblastoma.

Indeed, activated NF-κB in *MYCN* transgenic mice is accompanied by increased expressions of vimentin and fibronectin, suggesting that NF-κB could promote the tumour to gain the ability to migrate (Chayka *et al*., 2009). Moreover, NF-κB has been shown to promote EMT by regulating the expression of transcriptional activators such

as Snail and Slug, which are involved in development and tumourigenesis (Wu and Bonavida, 2009, Zhang *et al*., 2006).

In summary, the ability of CLU to modulate proliferative and survival pathways probably explains the plethora of biological functions attributed to this molecule. It is our goal to verify how CLU-mediated inactivation of NF-κB may play a crucial role in human neuroblastoma.

1.7. NF-kB (Nuclear Factor-kappa B)

Nuclear Factor-kappa B, hereafter referred to as NF-κB, is a transcription factor that plays an important role in converting stress signals from external stimuli such as cytokines, free radicals, ultraviolet irradiation or pathogens to cellular immune response such as cell survival, proliferation, immunity and inflammation (Gilmore, 2006). It was first discovered in 1986 as a protein bound to the kappa immunoglobulin gene enhancer in the nuclei of B cells (Sen and Baltimore, 1986). Moreover, disrupted NF-κB regulation has been linked to inflammatory diseases, autoimmune diseases and cancer (Ghosh and Karin, 2002, Mattson and Camandola, 2001, Karin, 2006).

There are five subunits of the mammalian NF-κB family

1. NF-κB 1 (also known as p50/105)
2. NF-κB 2 (also known as p52/100)
3. Rel A (also known as p65)
4. Rel B
5. c-Rel

All of the NF-κB proteins share a Rel homology domain in their N-terminal domains, which serves as a DNA-binding domain/dimerization domain or a binding domain to inhibitors of NF-κB (IκBs) (Escarcega *et al*., 2007). Members of the NF-κB subfamily (p105 and p100) are distinguished from their Rel subfamily (Rel A, Rel B and c-Rel) by having longer C-terminal domains containing multiple copies of ankyrin repeats, which act to inhibit these proteins. The NF-κB subfamily only becomes shorter, active DNA-binding proteins (p105 to p50 and p100 to p52) either upon limited proteolysis or arrested translation. Therefore, members of the NF-κB subfamily are generally not transcription activators, unless they form dimers with members of the Rel subfamily (Gilmore, 2006).

1.7.1. NF-κB inhibitors

There are many types of NF-κB inhibitors (IκBs) such as IκBα, IκBβ, IkBγ, IκBε, p100, p105 and Bcl-3. All of the IκBs contain ankyrin-like repeats, which facilitate the binding to and inhibition of NF-κB (Bassères and Baldwin, 2006). Each inhibitor has a different affinity for the NF-κB dimers. All the IκB proteins appear to inhibit NF-κB activity by masking a nuclear localization signal (NLS), located at the C-terminal end of the Rel homology region in each of the NF-κB subunits (Jacobs and Harrison, 1998). Activation of NF-κB is initiated by the signal-induced degradation of IκB proteins, by unmasking the NLS, NF-κB is allowed to translocate into the nucleus (Jacobs and Harrison, 1998).

1.7.2. Mechanism of NF-κB activation

The activity of NF-κB is regulated by the interaction with its inhibitors. The two best-described pathways leading to the activation of NF-κB are the canonical (classic) and non-canonical (alternative) pathways (Figure 1.6.). A variety of external stimuli (e.g. ROS, IR, bacterial lipopolysaccharides, LPS and TNFα) can trigger an upstream enzymatic reaction of IκB kinase (IKK).

In the canonical (or classical) NF-κB pathway, NF-κB dimers such as p50/RelA are sequestered in the cytoplasm by interacting with an independent IκB molecule (often IκBα). Binding of a ligand to a cell surface receptor recruits adaptors to the cytoplasmic domain of the receptor, which then recruit an IKK complex (containing the α and β catalytic subunits and two molecules of the regulatory scaffold NEMO) directly onto the cytoplasmic adaptors (Karin and Ben-Neriah, 2000). This clustering of molecules at the receptor activates the IKK complex, which subsequently phosphorylates serine 32 and 36 on human IκBα and is then recognized by the β-TrCP F-box-containing component of a Skp1-Cullin-F-box (SCF)-type E3 ubiquitin-protein ligase complex ($SCF^{\beta TRCP}$), targeting for IκB ubiquitination and proteasomal degradation upon dissociation with NF-κB (Häcker and Karin, 2006) (Figure 1.6.A.).

In response to cell development stimuli, the non-canonical (or alternative) pathway activates p100/RelB complexes during B-and T-cell development. Only certain receptor signals activate this pathway and this pathway occurs through an IKK complex that contains two IKKα subunits (but not NEMO). Receptor binding leads to activation of

the NF-κB-inducing kinase NIK, which phosphorylates and activates an IKKα complex. This complex then phosphorylates two serine residues adjacent to the ankyrin repeat C-terminal IκB domain of p100, leading to its partial proteolysis and liberation of the p52/RelB complex (Gilmore, 2006) (Figure 1.6.B).

The dissociated NF-κB becomes activated upon translocation into the nucleus. Activated NF-κB binds to response element (RE), which is a specific DNA sequence. The interaction between DNA and NF-κB recruits other proteins important for target genes transcription and protein translation. In both pathways, various post-translational modifications (e.g. phosphorylation and acetylation) of the NF-κB subunits can modulate their transcriptional activity (Perkins, 2006). Many NF-κB targets include genes involved in cell proliferation (e.g. cyclin D1, cyclin E and MYCC), survival (e.g. Bcl-2, survivin and XIAP), angiogenesis (e.g. IL-6, VEGF and IL-8), epithelial to mesenchymal transition (e.g. vimentin), metastasis (MMP2/9 and VCAM-1) and inflammation (e.g. TNFα and COX2) (Bassères and Baldwin, 2006). NF-κB also switches on its own inhibitor (IκBα) expression, which re-inhibits NF-κB in a negative feedback loop, thus, keeping the level of NF-κB balanced (Vallabhapurapu and Karin, 2009). In summary, the activation of NF-κB is the result of IKK-mediated, phosphorylation-induced degradation of NF-κB inhibitors (IκBs).

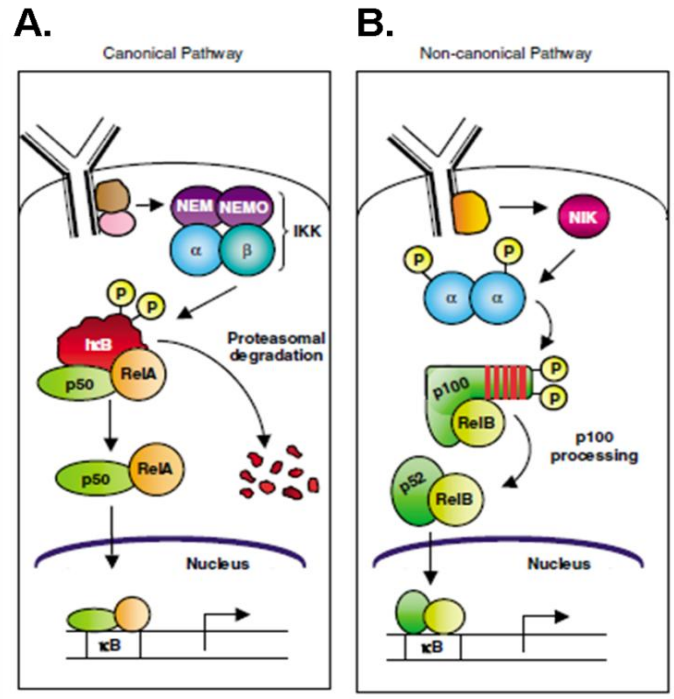

Figure 1.6. NF-κB signal transduction pathways

A) In the canonical (or classical) NF-κB pathway, NF-κB dimers such as p50/RelA are maintained in the cytoplasm by interacting with an independent IκB molecule (often IκBα). The binding of a ligand to a cell surface receptor (e.g. tumour necrosis factor-receptor (TNF-R) or a Toll-like receptor) recruits adaptors (e.g. TRAFs and RIP) to the cytoplasmic domain of the receptor. These adaptors often recruit an IKK complex (containing the α and β catalytic subunits and two molecules of the regulatory scaffold NEMO) directly onto the cytoplasmic adaptors. This clustering of molecules at the receptor activates the IKK complex. IKK then phosphorylates IκB at two serine residues, which leads to its K48 ubiquitination and degradation by the proteasome. NF-κB then enters the nucleus to turn on target genes.

B) The non-canonical (or alternative) pathway activates p100/RelB complexes during B-and T-cell organ development. This pathway differs from the canonical pathway in that only certain receptor signals (e.g., Lymphotoxin B (LTb), B-cell activating factor (BAFF), CD40) activate this pathway and because it occurs via an IKK complex that contains two IKKα subunits (but not NEMO). In this pathway, receptor binding leads to activation of the NF-κB-inducing kinase NIK, which phosphorylates and activates an IKKα complex. This, in turn, phosphorylates two serine residues adjacent to the ankyrin repeat C-terminal IκB domain of p100, leading to its partial proteolysis and liberation of the p52/RelB complex (Adapted from Gilmore, 2006).

1.7.3. NF-κB and Cancer

It is now clear that NF-κB is responsible for the link between inflammation and carcinogenesis because dysregulated NF-κB is often observed in cancers (Karin, 2006). It was shown that inhibition of NF-κB activation could cause a reduction of lipopolysaccharide (LPS) stimulated-inflammation and resulted in the regression of metastatic colon cancer via TRAIL-dependent pathway (Naugler and Karin, 2008).

The exact mechanism of these interconnected processes begins to emerge slowly. NF-κB is known to be a gene regulator and is important in cell proliferation, cell survival and cell invasion (Rayet and Gèlinas, 1999, Chayka *et al*., 2009). Greten et al (2004) has shown that in a mouse model of colitis-associated cancer, genetic deletion of IKKβ in myeloid cells significantly and dramatically decreased tumour proliferation of enterocytes, which are cells that undergo malignant progression in this model, compared to control cells. This study directly indicated that NF-κB signalling is important in early tumour promotion during the initiation stage.

In addition, NF-κB has recently been associated with cancer metastasis via a process called epithelial to mesenchymal transition (EMT) (Huber *et al*., 2004). Chua et al (2007) illustrated that in breast cancer model, NF-κB could regulate E-Cadherin, which is important in cell adhesion and movement. Moreover, inhibition of NF-κB in this model reversed the process of EMT and resulted in decreased cell mobility. Chayka et al (2009) has also shown in *in vitro* and *in vivo* studies that activated NF-κB is associated with metastatic potential of neuroblastoma cells, proving the role NF-κB in tumour invasion.

Activated NF-κB activity has been observed in lung cancer, colon cancer, pancreatic cancer, various types of leukemia, lymphoma and esophageal adenocarcinoma (Yang *et al*., 2007, Scartozzi *et al*., 2007, Weichert *et al*., 2007, Izzo *et al*., 2007, Rae *et al*., 2007, Fabre *et al*., 2007, Zhang *et al*., 2007). This is thought to occur through NF-κB transactivating its target genes by switching on their expressions such as cyclinD1, cyclinE, CDK-2 and MycC or inducing apoptosis-resistance by upregulating genes like the Bcl-2 family members such as Bcl-xL, IAP (inhibitors of apoptosis) and c-FLIP (Pahl, 1999, Karin, 2006).

Other studies have shown NF-κB to play an important role in cancer angiogenesis since NF-κB regulates its target genes that are angiogenic factors such as vascular endothelial growth factor (VEGF) and cytokines such as TNFα, IL-1 and IL-6 which are stimulators of VEGF (Bassères and Baldwin, 2006). NF-κB has been shown to play a pivotal role in neuronal survival and plasticity (Mattson and Camandola, 2001). Santilli et al (2003) illustrated that a putative tumour suppressor protein CLU may play an important role in down regulating NF-κB activity by stabilizing IκBs in neuroblastoma cell line LA-N-5.

1.8. Aim

CLU has been shown to function as a tumour suppressor and oncogene at the same time in different cancers. It is likely that CLU exerts distinct functions in different locations. For example nuclear CLU has been shown to promote apoptosis, and to inhibit prostate cancer cell proliferation (Caccamo *et al*., 2003, Caccamo *et al*., 2005, Yang *et al*., 1999). In neuroblastoma, the expression of nuclear CLU is bearly detectable and we have only observed this variant in terminally necrotic or apoptotic cells, suggesting that its expression is a consequence rather than a cause of cell death in physiological conditions (Chayka *et al*., 2009). Therefore, we believe that nCLU may not play a role in neuroblastoma tumour progression. Instead, CLU is detectable in the cytoplasm, extracellular spaces or the Golgi apparatus and it is not known whether its localisation also affects its biological function (Chayka *et al*., 2009). We hypothesised that the controversial role that CLU plays in cancer could be explained if the expression of intracellular and extracellular CLU has different biological outcomes and that intracellular CLU is a tumour suppressor gene, which negatively regulates NF-κB and metastasis.

Previous work has linked CLU to NF-κB regulation in aggressive neuroblastoma tumours, therefore, the aims of this study are:

1) To understand the function of intracellular and secreted CLU in the regulation of NF-κB activity and other signalling pathways.

2) To identify potential target proteins that may directly interact with CLU and mediate the regulation of NF-κB activity in neuroblastoma.

CHAPTER 2

Materials and Methods

2.1. Reagents

All reagents were purchased from Sigma (UK), unless otherwise stated. Methanol was purchased from Fisher scientific (UK). Ethyl alcohol (ethanol) was purchased from Hayman Limited (UK). Silver nitrate was purchased from BDH limited (Poole). Sodium carbonate and 37% formaldehyde were purchased from Sigma (UK). Propan-2-ol, acetic acid and Tris-base were purchased from AnalaR® (UK).

2.2. Cell Biology

2.2.1. Cell lines

All cell lines were purchased from the American Type Culture Collection, ATCC (Teddington, Middlesex, UK) unless otherwise stated.

2.2.1.1. WI-38

The WI-38 human diploid cell line is fibroblast-liked. The cell line was established by Leonard Hayflick from normal embryonic (3-month gestation) lung tissue of a Caucasian female (Hayflick and Moorhead, 1961). This adherent cell line has a finite lifetime of 50 passages (plus or minus 10) population doublings with a doubling time of 24 hours (Hayflick, 1965).

2.2.1.2. VA-13 (WI-38 subline 2RA)

The VA-13 is a subline of the WI-38 cell line but it is a fibroblast SV40 transformed cell line. The origin of the cells is the same as in section 2.2.1.1.

2.2.1.3. SHSY-5Y

SHSY-5Y cells derived from SK-N-SH neuroblastoma cell line and were established in 1970. The original line was obtained from a bone marrow metastasis of a four year-old female with chromosome 1q abnormality. SHSY-5Y cells are non-*MYCN* amplified cell line (Biedler *et al*., 1978). Morphologically, the cells are epithelial-/ neuronal-like elongated cells (N-type). This is an adherent cell line, which grows in monolayer with the doubling time of around 55 hours.

2.2.1.4. LA-N-1

LA-N-1, is a *MYCN* amplified neuroblastoma cell line. Under the microscope, LA-N-1 cells contain numerous cytoplasmic dense cores, which characterized its tear-drop shape. LA-N-1 cells derived from a bone marrow metastasis, taken from two-year old male with stage IV neuroblastoma. This is an N-type adherent cell line, which tends to grow in clusters with the doubling time of 32 hours (Seeger *et al*., 1977).

2.2.1.5. 293FT

293FT cell line derived from the 293 cell. The original 293 cells were established by Graham and coworkers in 1977, where human embryonic kidney cells were transformed by exposing cells to sheared fragments of adenovirus type 5 DNA. Although, adenoviral vectors allow efficient delivery of the transgene, its expression in the cells remains transient. This is mostly due to the immune response against the transduced cells.

Therefore, the 293FT cells, which stably expressed the SV40 large T antigens under the control of the human cytomegalovirus promoter (pCMVSPORT6Tag.neo), will facilitate the replication of packaging virus with sustained expression, thus, increasing lentiviral production. The 293FT cells grow rapidly and were used for the mass production of secreted proteins or non-replicating viral particles with greater transfer efficiency, integration and sustain expression of the vector in the transduced cells (Naldini *et al*., 1996). The 293FT adherent cell line, which grows in monolayer with the doubling time of approximately 25 hours, was purchased from Invitrogen (UK).

2.2.1.6. HNB

Human neuroblastoma (HNB) cells were isolated from a metastatic relapse tumour, in the neck lymph node of a 3-year old male patient. The tumour was originated in the abdomen, which exhibited *MYCN* amplification as double minutes (DM) rather than as a homogeneously staining region (HSR) as seen in the relapse tumour**.** It is not yet known why this is the case but ongoing work is being carried out to identify more about the tumour's genetics. This is an adherent cell line, which grows in monolayer with the doubling time of approximately 24 hours. The cell line was established by our group in 2010.

2.2.2. Cell culture

WI-38, VA-13, SHSY-5Y, LA-N-1 and 293FT cells were maintained in culture with Dulbecco's Modified Eagle Medium (DMEM) supplemented with 10% heat-inactivated foetal bovine serum (FBS), 2mM l–glutamine, penicillin (100mg/ml), streptomycin (100mg/ml) and 1% (10mM) non-essential amino acid (NEAA).

The human primary neuroblastoma cell line (HNB) was cultured in RPMI-1640 medium supplemented with 20% heat-inactivated foetal bovine serum, 2mM l-glutamine, 10μM 2-mercaptoethanol, 1mM sodium pyruvate, penicillin (100mg/ml), streptomycin (100mg/ml) and 1% (10mM) NEAA. All reagents used for cell culture were purchased from Invitrogen (UK). All tissue culture flasks and dishes were purchased from Nunc^{TM} (Denmark).

2.2.2.1. Harvesting and maintenance of cell lines

The media of cells grown in cultured flasks or dishes were removed and the cells were washed briefly one time in sterile PBS solution. PBS was removed and 1ml Trypsin (0.05% Trypsin-EDTA 1x) was added to detach the cells. The cultured flasks or dishes were incubated in a humidified 37^{o}C incubator at with 5% CO_2 until adherent cells became completely detached. 10ml of complete media was added to the cells and all media containing cells were collected or put at a ratio 1:5 (cells to fresh culture media) in a new flask for the maintenance of the cell line. Cell cultures were regularly checked for mycoplasma contamination using a MycoProbe mycoplasma detection assay (R&D Systems) according to the manufacturer's instructions.

2.2.3. Freezing cultured cells

For long term storage of cell lines, harvested cells were collected in complete media (as described in section 2.2.2.1) and were centrifuged by Rotanta 460 (Hettich Zentrifuge) at 1,200 rpm for 5 minutes at room temperature. The cell pellet was resuspended in freezing solution (containing 90% cultured media and 10% DMSO) at a concentration of 3x10^{6} cells/ml. One ml aliquots were put into cryovials (Nunc^{TM}, Denmark) and transferred to -80^{o}C freezer in a Nalgene freezing container (Nalgene labware) to ensure the optimal cooling rate of -1^{o}C per minute in order to avoid the formation of intracellular ice crystals. After 48 hours, cells were transferred to liquid nitrogen for storage.

2.2.4. Recovery of frozen cells

A cryovial of frozen cells was thawed in a 37 ^{o}C water bath rapidly. The cells were then transferred to a 50ml centrifuge tube containing 20ml of culture medium. The tube was centrifuged at 1,200 rpm for 5 minutes at room temperature to remove the DMSO. Cells were resuspended in complete culture medium, plated in a suitable culture flask or dish and maintained in a humidified 37^{o}C incubator with 5%CO_2 overnight before fresh media was replaced on the next day.

2.2.5. Lentiviral production in 293FT cells

Lentivirus was generated by co-transfection of 293FT cells. Briefly, 293FT cells were seeded at the density of 1x10^{6} cells per 100mm dish 24 hours prior to transient transfection with 5μg of shRNA encoding plasmid, 3.75μg pPAX2 and 1.5μg pMDG2 plasmids in serum-free Opti-MEM® (Invitrogen) using LipofectAMINE 2000 (Invitrogen). Growth media was replaced by DMEM supplemented with 10% heat-inactivated foetal bovine serum (FBS), 2 mM l–glutamine, penicillin (100mg/ml), streptomycin (100mg/ml) and 1% (10mM) non-essential amino acid (NEAA) 16 hours after transfection. Lentivirus containing supernatant was collected 48 hours after transfection.

2.2.6. Lentiviral transduction

The culture medium was filtered through a 0.45μm filter (Minisart®, Sartorius AG, Germany) 48 hours post-transfection to remove cell debris (see section 2.2.5) and the viral supernatant was concentrated 10-fold via ultra microcentrifugation (Sorvall ® Discovery 100, Kendro Laboratory Products) at 17,000rpm, 2 hours at 4^{o}C to increase the virus titre. The concentrated virus was used for transduction of SHSY-5Y or HNB cells in the presence of 8μg/ml polybrene (Sigma-Aldrich). The cells were centrifuged at 1,800 rpm for 45 minutes at 25^{o}C and were allowed to recover in a humidified 37^{o}C incubator with 5% CO_2 for a further 48 hours before selection.

2.2.7. Clonal selection

Transduced cells were selected for 5-10 days with 1μg/ml puromycin (InvivoGen) for all cell lines. Although puromycin selection is normally used for a quick selection of cells, which usually takes a few days until all cells in the mock transduction died, the

saturated level of HSP60 in the cell lines meant it would take longer period of time to start reducing its expression, hence, the selection period was carried out at 10 days to ensure that sufficient amount of endogenous proteins were knockdown.

For the generation of SHSY-5Y cells stably expressing pcDNA3-CLU (full length), pcDNA3-α or pcDNA3-β, cells were selected with 1μg/ml Geneticin®G418 (Invitrogen) for 3 weeks. After the indicated period of selection, a single colony of cell was trypsinized and expanded into a stable clone.

2.2.8. Proliferation assay and live cell count

HNB and SHSY-5Y cells transduced with control shRNAs (shScramble) or shRNAs targeting HSP60 (shHSP60) were seeded at the density of $1x10^5$ cells per 60mm dish. Cells were allowed to grow over the designated period until the scramble shRNAs transduced cells reached confluency. The culture dishes were viewed on an Axiovert200M inverted fluorescence microscope using a *Plan-Apochromat 10x/2.50 objective*. Images were captured at room temperature (20^oC) using an AxioCamHR digital camera and *Axiovision Relative 4.6.3* software (Carl Zeiss, Microimaging GmbH, Germany). Images were then saved as TIFF files.

To score the number of live cells, 10μl of cells suspended in culture media were mixed with 10μl of 0.4% trypan blue solution (T5154, Sigma) and placed in a $0.0025mm^2$ haemocytometer (Marienfeld, Germany). Viable cells exclude the dye, while non-viable cells absorb the dye and appear blue.

2.2.9. Cell treatments

2.2.9.1. Sub-lethal heat shock treatment

In order to induce the endogenous levels CLU protein expression, SHSY-5Y and LA-N-1 cells were seeded at the density of $2x10^6$ cells in four 100mm tissue culture dishes and were grown for 24 hours. To avoid nutrient starvation, the culture medium was changed prior to sub-lethal heat shock treatment. SHSY-5Y and LA-N-1 cells were exposed in the 43^oC water bath for 30 minutes in complete DMEM media, modified by addition of 20 mM HEPES, pH7.5 to maintain constant pH during the shock phase.

Heat shock treatment was done as previously described by Caccamo et al (2006). Briefly, cells were incubated at the indicated temperature in a water bath. After shock, the cells were kept in the humidified incubator at 37^{o}C and 5% CO_2 as indicated (0, 3, 6, 9, 24 and 48 hours) for recovery, and expression of endogenous protein expressions of CLU and HSP60 were analyzed by Western Blot.

2.2.9.2. Doxorubicin treatment

SHSY-5Y stable clones after transduction with control shRNAs (shScramble) or shRNAs targeting HSP60 (shHSP60) were selected for 10 days and seeded at the density of 1x10^{5} cells per 60mm dish 24 hours prior to doxorubicin treatment. Briefly, the culture medium containing 0.5μg/ml doxorubicin was replaced to the cells on the following day and the cell culture was left in the humidified incubator at 37^{o}C and 5% CO_2 for another 24 hours before being subjected to Annexin V staining and flow cytometry analysis (see section 2.2.10.2)

2.2.10. Flow cytometry

2.2.10.1. SubG1 cell cycle analysis

Supernatants for all samples were collected and cells were detached with 300μl Stempro®Accutase® (Invitrogen). All cells were collected by centrifugation at 1,200 rpm for 5 minutes without using brake at room temperature as dead cells become buoyant. The cell pellet was resuspended and fixed in 1ml cold 70% ethanol for at least 30 minutes. After fixation, the cells were centrifuged at 2,000rpm for 5 minutes at room temperature. The pellet was washed twice in 1ml phosphate-citrate buffer (0.2M Na_2HPO_4 and 0.1M Citric acid, pH7.2) at room temperature. During each wash, the cells were pelleted at 2,000rpm for 5 minutes at room temperature. To ensure that only DNA is stained, cells were treated with 50μl ribonuclease A (RNaseA) solution (100μg/ml in PBS). Then 450μl of propidium iodide, PI (50μg/ml in PBS) was added directly to approximately 1x10^{6} cells in RNase A solution. Cells were incubated for 30 minutes on ice. Samples were analyzed in PI/RNase A solution by a BD LSR II flow cytometer (Becton Dickenson, Oxford, UK). All data for flow cytometry were analysed by FlowJo software.

2.2.10.2. Annexin-V staining

Annexin V affinity assay is used for quantification of cells undergoing apoptosis. Apoptotic is a programmed cell death where cells usually expose phosphatidylserine, a negatively charged phospholipid that normally resides on the inner leaflet of cell membrane, once the membrane started to break up upon cell death. Annexin V labelled with fluorescent molecules can bind to the exposed phosphatidylserine and dead cells can be counted by flow cytometry (van Engeland *et al*., 1998). Annexin V conjugate (Annexin V AlexaFluor® 647, Invitrogen) was diluted with Annexin V binding buffer (BD Biosciences, Pharmingen) at the ratio of 1:200. The cell pellets were then resuspended in 300µl of the Annexin V conjugate/ binding buffer mixture. Cells were mixed gently to ensure equal staining and the samples were kept on ice in the dark for 20 minutes. Prior to FACS analysis, 30µl of 50µg/ml propidium iodide (PI) solution was added to each sample. The samples were analyzed by a BD LSR II flow cytometer (Becton Dickenson, Oxford, UK).

2.2.11. Genetically Modified mice

Human *MYCN*-transgenic mice in the CBA genetic background, which are the mouse model of neuroblastoma, were obtained from M.S. Jackson, University of Newcastle, UK and were maintained in the University College London animal facility. The formation of tumours was monitored by inspection every other day until mice were 2-3 months old. The mice were killed by cervical dislocation or CO_2 asphyxiation when a palpable tumour was detected or at the first signs of discomfort or stress, which is indicative of disease. All tumours were obtained from *MYCN*-homozygous mice. Four abdominal tumours originating in the adrenal glands of two females and two males mice and one tumour obtained from the lung of a female mouse were excised and snap-frozen in liquid nitrogen for subsequent protein analysis. All experimental procedures involving transgenic mice were approved by the University College London and were conducted under the Animal (Scientific Procedures) Act, 1986 (United Kingdom) (Chayka *et al*., 2009).

2.2.11.1. Preparation of adrenal glands cell lysate

Adrenal glands were isolated from four males and five females' non-transgenic CBA mice less than 3 months old. All experimental procedures involving mice were

approved by the University College London and were conducted under the Animal (Scientific Procedures) Act, 1986 (United Kingdom). To obtain a single cell suspension, a 70μm cell strainer (BD Biosciences, USA) was used for both tumours and adrenal glands. Lysates were prepared using the same buffers as in section 2.3.1.

2.3. Molecular Biology

2.3.1. Preparation of protein lysates

Cells were harvested by trypsin (0.05% Trypsin-EDTA 1x) and lysed in RIPA buffer (50mM Tris-HCl, pH7.5, 5mM EDTA, 250mM NaCl, 0.1% w/v SDS, 1% Igepal) on ice for 50 minutes with vortexing every 10-minutes interval. Cell lysates were then centrifuged in the Eppendorf centrifuge (5415R) at 13,000rpm for 15 minutes at 4^{o}C and the supernatants were transferred to the new 1.5ml mircrocentrifuge tube (Eppendorf). Each protein sample was measured for protein concentration (see section 2.3.1.1.) before loading onto the gel.

Alternatively, cells were lysed directly on the culture dish by addition of 1xSDS sample buffer (62.5mM Tris-HCl, pH6.8, 50mM DTT, 2% w/v SDS, 10% glycerol, 0.01% w/v bromophenol blue). The adherent cells were detached in 1xSDS sample buffer on ice using a cell scraper. All lysed cells were collected in the 1.5ml microcentrifuge tube and boiled for 5 minutes at 100^{o}C before being loaded onto the gel. 12μl of the prestained molecular weight protein marker (SeeBlue® Plus 2, Invitrogen) was used to assess relative protein sizes.

2.3.1.1 Bradford protein assay

To determine protein concentrations, a protein calibration curve was constructed. Standards containing a range of 0 to 10mg/ml of Bovine Serum Albumin (BSA) were prepared.

Two microlitres of each BSA standards or protein lysates was mixed with 400μl of 1xBIO-RAD protein assay dye reagent (Bio-Rad Laboratories, Germany) and 150μl of the each mixture was added to each well of the 96-well plate. The 96-well plate was kept in the dark at room temperature for 10 minutes before the proteins concentrations

were measured using the microplate reader (model 680, Bio-Rad) at wavelength of 595 nm.

2.3.2. Western Blot analysis

2.3.2.1. Acrylamide gel preparation

One-dimensional SDS-PAGE gels were used to separate protein according to their sizes and for verification of the protein expression. The gels were prepared with the composition of the stacking and resolving gel, shown in table 2.1.

Components (Sources)	10% Resolving gel (ml)	4.5% Stacking gel (ml)
Deionized water	6.25	6.1
4x TrisCl-SDS (pH8.8)	3.75	-
4x TrisCl-SDS (pH6.8)	-	2.5
30% acrylamide / bisacrylamide (37.5:1mix) (National Diagnostics)	5	1.3
10% ammonium persulfate, (Acros Organics)	0.075	0.075
TEMED (Sigma)	0.015	0.015

Table 2.1. Compositions of resolving and stacking gels for SDS-PAGE.

The amount stated is for making 2 small gels (length 10cm, width 8 cm) of the Bio-Rad gel system.

2.3.2.2. Gel electrophoresis and transfer

Proteins at different sizes were allowed to migrate down the resolving gel at 35mA for approximately 90 minutes in 1xTris-glycine SDS running buffer (see Table 2.2.) before being transferred onto the nitrocellulose membrane (Hyperbond-C Extra, Amersham Biosciences) (Figure 2.1) in a transfer buffer (see Table 2.2.) for 1 hour at 100V using the Bio-Rad gel transfer system. All steps were carried out at cool temperature.

The membrane was blocked for an hour at room temperature, with gentle shaking, in the washing buffer containing 5% milk before being probed with a primary antibody (see Table 2.3.) overnight at 4^{o}C. After three 10-minutes washes in the washing buffer, membranes were incubated with an appropriate horseradish peroxidase-conjugated (HRP) secondary antibody (1:10,000) in washing buffer containing 5% milk for another hour at room temperature with gentle shaking (Table 2.3.). The membrane was washed for 3 minutes four times in washing buffer and subjected to chemiluminescence detection (Thermo Scientific, USA) according to the manufacturer's instructions.

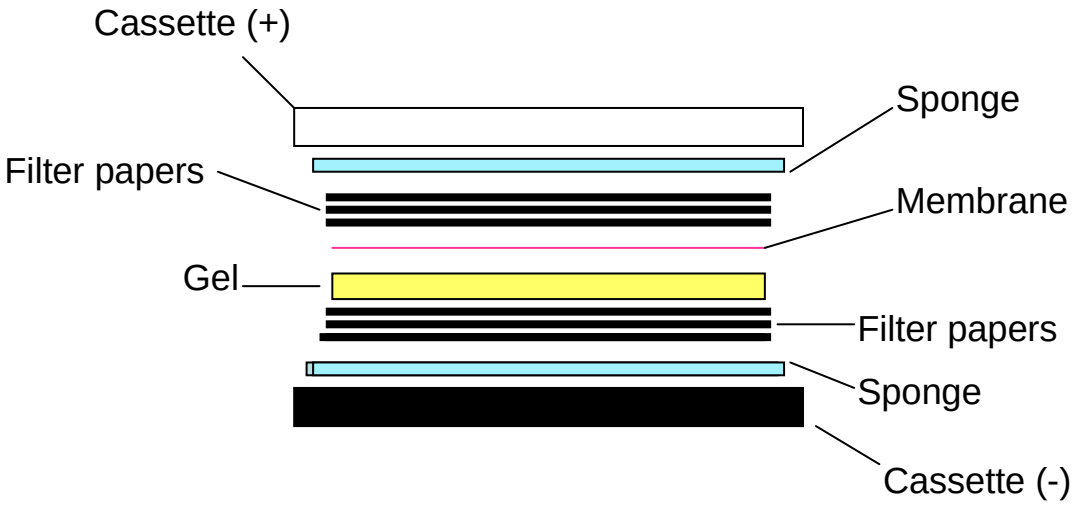

Figure 2.1. A schematic presentation of gel and membrane assembly for protein transfer process in Western Blot analysis

Buffers (1X)	Components for 1 L.
Tris-glycine SDS running buffer (pH>8.3)	3g. Tris (AnalaR ®), 14.4 g. Glycine (Fisher Scientific), 1g. SDS (Sigma) and add deionized water up to 1L.
Transfer buffer	5.82 g. Tris, 2.95 g. Glycine, 100 ml methanol (Fisher Scientific) and add deionized water up to 1L.
Washing buffer (PBS + Igepal, 0.1% v/v)	10 PBS tablets per 1000 ml distilled water and 1 ml Igepal (CA-630, Sigma)

Table 2.2. Compositions of 1xTris-glycine SDS running buffer and 1xTransfer buffer

Antibodies	Company	Origin	Type	Working dilutions
anti-CLU α (clone 41D)	Millipore	mouse	monoclonal	1:500
anti-CLU β (M-18)	Santa Cruz Biotechnology	goat	polyclonal	1:500
anti-HSP60 (H-300)	Santa Cruz Biotechnology	rabbit	polyclonal	1:500
anti-Actin (I-19)	Santa Cruz Biotechnology	goat	polyclonal	1:500
anti-AKT	Cell Signaling technology	rabbit	polyclonal	1:1,000
anti-phosphorylated AKT (Ser473)	Cell Signaling technology	rabbit	polyclonal	1:1,000
anti-ERK	Cell Signaling technology	rabbit	monoclonal	1:1,000
Anti-GAPDH (14C10)	Cell Signaling technology	rabbit	monoclonal	1:1,000
anti-phosphorylated ERK (Thr202/Tyr204)	Cell Signaling technology	mouse	monoclonal	1:2,000
anti-rabbit HRP	Amersham Biosciences	donkey	polyclonal	1:10,000
anti-mouse HRP	Amersham Biosciences	sheep	polyclonal	1:10,000
anti-goat HRP (SC-2033)	Santa Cruz Biotechnology	donkey	polyclonal	1:10,000

Table 2.3. All the primary and secondary antibodies used

2.3.3. GST pull down

2.3.3.1. pGEX4T-1 plasmids generation

To generate GST-fusion protein expression vectors (pGEX4T1-CLU, pGEX4T1-alpha, pGEX4T1-beta), PCR products containing the complete human *CLU*, its alpha chain only and beta chain only cDNA sequences were digested with *SalI* and *NotI* and ligated into pGEX4T1 (GST) empty vectors (GE Healthcare). PCR products were generated using primers designed with *SalI* and *NotI*, with an in-framed start site attached (Table 2.5.) using the template described in section 2.4.2.

cDNA sequences of PCR products were assessed by sequencing services (see section 2.4.11.). Protein expressions were verified by Western Blot analysis with appropriate antibodies.

2.3.3.2. GST-fusion protein expression

pGEX4T1-CLU, pGEX4T1-alpha (α) and pGEX4T1-beta (β) were transformed (see section 2.4.9.) into competent *E.Coli* cells (BL21). The transformed cells were plated onto LB agar plates with 50μg/ml ampicillin, which were incubated in a 37^{o}C incubator overnight until colonies were visible.

A single colony was picked and placed in 10ml LB broth containing 50μg/ml ampicillin (Sigma) in a 37^{o}C incubator, orbital shaking at 250 rpm overnight. The next day, 1ml of the overnight culture was added to 150ml sterile LB broth containing ampicillin in the presence of 1% (v/v) Tween 20. The bacterial culture was grown in a 37^{o}C incubator, shaking at 250 rpm until the exponential growth phase is reached (OD_{595nm} = 0.5). The Optical density (OD) was measured by placing 1ml of the bacterial culture in a 1.5ml cuvette (Plastibrand®, Germany) and the light absorbance was measured at 595nm by a UV/visible spectrophotometer (Ultrospec ® 2100 Pro, Amersham Pharmacia Biotech). GST-fusion protein expression was induced by 0.1mM Isopropyl β-D-1-thiogalactopyranoside (IPTG) (Sigma). The pGEX4T1 empty, pGEX4T1-CLU and pGEX4T1-beta fusion proteins were grown for further 2 hours at 28^{o}C, whereas pGEX4T1-alpha was grown for further 2 hours at 37^{o}C, shaking at 250 rpm.

The bacterial culture was centrifuged at 4^{o}C, 4000rpm for 20 minutes. Supernatant was removed and the pellet was resuspended in 3ml ice-cold buffer (PBS containing protease inhibitors, miniComplete from Roche, 1 tablet per 10ml solution and 1mM DTT). The resuspended bacteria were sonicated (Sonopuls, Bandelin) for 10 seconds at 60% and were left on ice for 60 minutes, during which, the bacterial lysates were vortexed briefly every 10 minutes interval.

GST-fusion protein expression before and after IPTG induction was visualized by coomassie blue staining (1% (w/v) coomassie brilliant blue, 45% (v/v) methanol, 10% (v/v) acetic acid and 45% (v/v) deionized water) of the 10% SDS-polyacrylamide gel for 2 hours (section 2.3.2.1) and de-stain (40% methanol, 10% acetic acid in deionized water) for 24 hours before protein expressions were visualized.

2.3.3.3. Purification of GST-fusion protein

After sonication, the bacterial lysates of different GST-fusion proteins were centrifuged for 5 minutes at 4^{o}C, 4000 rpm before the supernatant was transferred into a new sterile 15ml tube. Then, 500µl of 50% slurry glutathione *S*-transferase (GST) beads (GE Healthcare, UK) were added to the collected supernatant and were mixed on a rotator at room temperature for 10 minutes. After 10 minutes, the mixture was centrifuged at 4^{o}C, 750 rpm for 1 minute before supernatant was removed. The beads were washed in 5ml PBS containing protease inhibitor and DTT (Sigma). The washing step was repeated at least three times. After the last wash, all supernatant was removed and the GST-fusion beads was either run on a 10% polyacrylamide gel and stained with coomassie blue dye to check the purity of the generated GST-fusion protein beads or stored within one month at 4^{o}C for future use.

2.3.3.4. Pull down

Approximately 8x10^{6} LA-N-1 cells were washed with PBS, trypsinized and collected by centrifugation at 1,200rpm for 5 minutes at room temperature. The cell pellet was resuspended on ice in 200µl of bead binding buffer A (50mM KH_2PO_4 pH7.5, 150mM KCl, 1mM $MgCl_2$) containing protease inhibitor and sonicated for 10 seconds. After sonication, 200µl of bead binding buffer B (50mM KH_2PO_4 pH7.5, 150mM KCl, 1mM

$MgCl_2$, 20% glycerol and 2% triton-x100) containing protease inhibitor was added to the cells.

The mixtures were incubated for 60 minutes on ice with vortexing every 10 minutes. The lysed cells were pelleted at 4^oC, 4000rpm for 20 minutes. The supernatant was placed in a new sterile 15ml tube and 50μl of GTS-only beads was added to the supernatant for a pre-clearing step to eliminate non-specific binding. The beads and supernatant mixture was rotated for 30 minutes at 4^oC before being pelleted at 4^oC, 4000rpm for 1 minute. The supernatant was divided equally into 4 separate tubes with 50μl of GST-only (pGEX4T1 no insert), GST-CLU (pGEX4T1-CLU), GST-alpha (pGEX4T1-alpha) or GST-beta (pGEX4T1-beta) beads (section 2.3.3.2.). The GST-fusion protein beads were incubated with the supernatant at 4^oC with rotation for 1 hour. Then the beads were collected by a 10-second centrifugation at 4^oC. All supernatants were removed and the beads were washed with 1ml of bead binding buffer C (50mM KH_2PO_4 pH7.5, 150mM KCl, 1mM $MgCl_2$, 10% glycerol and 1% triton-x100) containing protease inhibitor. The washing step was repeated four times. After the final wash, the pelleted GST-fusion protein beads were boiled in 1xSDS sample buffer and analysed by SDS-PAGE.

2.3.4. Pull down analyses

2.3.4.1. Silver staining

Following gel-electrophoresis, the polyacrylamide gel was placed in a fixing solution for 1 hour and then washed twice in ethanol solution for 30 minutes and three times in deionized water for 10 minutes. After washing, silver nitrate solution was added to the gel for 30 minutes, then the gel was washed briefly with deionized water and a developing solution was added (Table 2.4.). The stained bands were allowed to develop for 15-20 minutes before a stop solution was added. Each step was carried out at room temperature with gentle shaking.

Solutions	Components
Fixing solution	20% (v/v) ethanol and 1%(v/v) acetic acid in deionized water
Ethanol solution	20% (v/v) ethanol in deionized water
Silver nitrate solution	0.1% (w/v) silver nitrate in deionized water
Developing solution	2% (w/v) sodium carbonate and 40 ul of 37% formaldehyde (for every 100ml developing solution, added prior to use)
Stop solution	3% (v/v) acetic acid in deionized water

Table 2.4. Solutions for silver staining

2.3.4.2. Colloidal Coomassie blue staining

Brilliant blue G-colloidal concentrate was purchased from Sigma (UK) for the staining of proteins in the polyacrylamide gels for mass spectrometry. The staining was performed according to the manufacturer's protocol. Briefly after electrophoresis, the gel was fixed for 30-60 minutes, in the fixing solution (7% glacial acetic acid in 40% (v/v) methanol) then the gel was placed into the freshly prepared colloidal coomassie solution (4 parts of the 1xworking solution of brilliant blue concentrate and 1 part methanol) for 1-2 hours. Subsequently, the gel was de-stained in 10% acetic acid in 25% (v/v) methanol for 60 seconds with shaking. The gel was rinsed twice with 25% methanol and scanned at 600nm by Bio-Rad, GS-800 Densitometer (Bio-Rad, UK). Data were analyzed using Bio-Rad Quantity one program.

2.3.4.3. Mass-spectrometry

Bands of interest were excised from the gel and an in-gel trypsin digest was carried out. Each band was destained using 200mM ammonium bicarbonate with 20% acetonitrile, followed by reduction with 10mM DTT (Melford Laboratories Ltd., UK), alkylation with 100mM iodoacetamide (Sigma, UK) and enzymatic digestion with sequencing grade modified porcine trypsin (Promega, UK) using an automated digest robot (Multiprobe II Plus EX, Perkin Elmer, UK).

Liquid Chromatography with tandem mass spectrometry (LC-MS/MS) was carried out upon each sample using a 4000 Q-Trap mass spectrometer (Applied Biosystems, UK). Peptides resulting from in-gel digestion were loaded at high flow rate onto a reverse-phase trapping column (0.3mm i.d.x1mm), containing 5µm C18 300 Å Acclaim PepMap media (Dionex, UK) and eluted through a reverse-phase capillary column (75µm i.d.x150mm) containing Waters Symmetry C18 100 Å media (Waters, UK) that was self-packed using a high pressure packing device (Proxeon Biosystems, Odense, Denmark). The output from the column was sprayed directly into the nanospray ion source of the 4000 Q-Trap mass spectrometer.

Fragment ion spectra generated by LC-MS/MS were searched using the MASCOT search tool against the UniProtKB/Swiss-Prot protein database using appropriate parameters. The criteria for protein identification were based on the manufacturer's definitions (Matrix Science Ltd.). Basically candidate peptides with probability based

Mowse scores exceeding threshold (p<0.05), and thus indicating a significant or extensive homology were referred to as 'hits'. Protein identifications were only considered if they contained 3 or more peptides with scores that exceeded the p<0.05 threshold.

2.3.5. Co-immunoprecipitation

2.3.5.1. *In vivo* study of protein-protein interactions

Briefly, 293FT cells were seeded at the density of $1x10^6$ cells in two 100mm tissue culture dishes and were grown for 24 hours before being transiently transfected with pcDNA3-empty or pcDNA3-CLU (full length) using LipofectAMINE 2000 (Invitrogen). The culture media were replaced on the next day after transfection, supplemented with 20μM proteasome inhibitor, MG132 (C2211, Sigma) and 48 hours after transfection, cells were rinsed in ice-cold PBS twice before 1ml of ice-cold non-denaturing lysis buffer (50mM Tris-Cl, pH 7.5, 150mM NaCl, 1mM EDTA, 1% (v/v) Triton-X100, protease and phosphatase inhibitors (Roche)) was added to the plates. The cell lysate was pre-cleared with Protein G sepharose 4B (GE Healthcare) for 30 minutes on a rotator at 4^oC to minimize non-specific binding. Equal amount of whole-cell protein extracts was incubated with 2μg of anti-CLU (M-18), anti-HSP60 antibody (SC-13966) or normal goat and rabbit IgGs for 1 hour on a rotator at 4^oC. The mixtures were further incubated with Protein G sepharose 4B for 16 hour on a rotator at 4^oC. The immunoprecipitates were washed five times in PBS and were collected by centrifugation. The bound proteins were suspended in 4xSDS sample buffer and analysed by SDS-PAGE. All steps were carried out on ice.

2.3.5.2. *In vivo* study of protein-protein interactions of endogenous proteins

LA-N-1 cells were seeded at the density of $1x10^6$ cells in four 100mm tissue culture dishes and were grown for 24 hours before being subjected to sub-lethal heat shock treatment for 30 minutes at 43^oC in complete DMEM media. After shock, the cells were kept in the humidified incubator at 37^oC and 5% CO_2 for 3 hours to recover. Cells were then lysed and co-immunoprecipitated in the same manner as previously described in section 2.3.5.1.

2.3.6. Generation of conditioned medium

In order to generate conditioned medium containing highly secreted form of CLU, 293FT cells were seeded at the density of $1x10^6$ cells per 100mm dish. Cells were transiently transfected 16 hours after plating with 15µg empty MIG or CLU MIG vectors by the use of lipofectAMINE 2000 as described in the manufacturer's protocol. After 8 hours, fresh medium (supplemented with 0.5% FBS) was added and cells were kept in the humidified incubator at 37^oC and 5% CO_2 for the next 24 hours before conditioned medium was collected and used in the luciferase assay experiments. Protein expression of precursor and secreted forms of CLU were assessed by western blot analysis with anti-CLU antibody (M-18).

Purified human recombinant secreted CLU was purchased from Alexis (UK) to verify that the effect observed was due to sCLU. The working concentration of purified human recombinant secreted CLU was 100ng/ml

2.3.7. Luciferase reporter assay

2.3.7.1. Single luciferase reporter assay

For the investigation of secreted form of CLU in regulating the NF-κB activity, SHSY-5Y and LA-N-1 cells were seeded at the density of $1x10^6$ cells per 60mm dish the day before transient transfection with 5µg NF-κB luciferase reporter vector (NF-κB LUC, Clonetech, CA) per dish using LipofectAMINE 2000 (Invitrogen). After 8 hours, cells were replated at the density of $1x10^4$ cells per well in a 24-well plate with fresh medium (supplemented with 10% FBS) and were left in the humidified incubator at 37^oC and 5% CO_2 overnight. On the next day, fresh or conditioned media with or without CLU (supplemented in 0.5% FBS) were added to the cells in the presence or absence of Tumour necrosis factor (TNF-α, 10mg/ml). Cells were lysed in 1xPassive lysis buffer (Promega) 8 hours later and assayed for luciferase activity using the luciferase assay system (Promega). Relative luciferase activity was calculated by Lumat LB 9507 (Berthold Technologies) and was further normalised to controls.

2.3.7.2. Dual luciferase reporter assay

SHSY-5Y and LA-N-1 cells were seeded at the density of $5x10^4$ cells per well in a 24-well plate 24 hours before being transiently co-transfected with 200ng of the NF-κB LUC reporter plasmid and 5ng of renilla luciferase vector (Promega, UK) in

combination with 400µg of either empty pcDNA3 or pcDNA3-CLU or pcDNA-alpha or pcDNA3-beta per well using LipofectAMINE 2000 (Invitrogen). After 16 hours, the media were replaced with fresh media (supplemented with 10% FBS) in the presence or absence of Tumour necrosis factor (TNF-α, 10mg/ml) (Invitrogen) and were incubated further for 24 hours at 37^{o}C and 5% CO_2. Cells were lysed in 1xPassive lysis buffer (Promega) and luciferase activity was measured as a ratio of luciferase activity/renilla activity by Lumat LB9507 (Berthold Technologies).

The same protocol was also used for the measurement of NF-κB activity in SHSY-5Y or HNB cells, which were transduced with control shRNA (sh-scramble) or shRNA targeting HSP60 (sh-HSP60) for the investigation of the role of HSP60 in the regulation of NF-κB activity.

2.4. Molecular Cloning

2.4.1. Primer design

All primers for the pGEX4T-1 constructs were designed to contain an in-frame start site (ATG). All primers for pcDNA3 (Invitrogen) and pGEX4T1 (GE Healthcare) constructs were designed to contain restriction sited of enzymes to facilitate cloning procedure (see Table 2.5.).

Primer	Sequence (5'-3')	Restriction sites	Vector
1.CLU (FW)	CGG**GGTACC**CAGGACATGTCCAATCAGGGA	*Kpn* I	pcDNA3
2.CLU (RW)	TTT**CGCCGGCG**CTCACTCCTCCCGGTGCTTTTT	*Not* I	pcDNA3
3.ALPHA (RW)	TTT**CGCCGGCG**CTCAGCGGACGATGCGGGACTT	*Not I*	pcDNA3
4.BETA (FW)	CGG**GGTACC**CAGGACATGAGCTGGATGCCCTTC TCTCCGTAC	*Kpn* I	pcDNA3
5.CLU (FW)	ACGC**GTCGAC**ACATGTCCAATCAGGGAAGTAAG	*Sal* I	pGEX-4T1
6.CLU (RW)	TT**CGCCGGCG**TCTCACTCCTCCCGGTGCTTTTT	*Not* I	pGEX-4T1
7.ALPHA (RW)	TT**CGGCGGCG**TCTCAGCGGACGATGCGGGACTT GGG	*Not* I	pGEX-4T1
8.BETA (FW)	ACGC**GTCGAC**ACATGAGCTTGATGCCCTTCTCTC CG	*Sal* I	pGEX-4T1

Table 2.5. Primers used in generating pGEXT-4T1 (GST) and pcDNA3-based protein expression constructs

2.4.2. Polymerase Chain reactions (PCR)

The complete human clusterin (CLU), its alpha chain only and beta chain only cDNAs were amplified using the CLU MIGR1 (hereafter referred to as CLU MIG) retroviral vector as a template (Santilli *et al*., 2003).

CLU full length, CLU alpha chain region only or CLU beta chain region only were generated by polymerase chain reaction (PCR) with oligonucleotide primers specific for the human CLU gene. All reactions were carried out in GeneAmp® PCR system 9700, Applied Biosystems) All reaction conditions are shown in the table below (Table 2.6.).

All PCR products were analyzed on a 2% agarose gel containing ethidium bromide (see section 2.4.7.), cut out of the gel and extracted by Gel extraction kit (Qiagen) according to manufacturer's protocol.

Degree(^{o}C) and time (seconds,s)				
Initial denaturation	94°C , 120s			
3-step cycling (no. of cycles = 40)				
Denaturation	94°C, 15s			
Anneal	65°C, 30s	65°C, 30s	67°C, 30s	69°C, 30s
Extension	68°C, 90s	68°C, 40s	68°C, 40s	68°C, 40s
Final Extension (68°C, 7 minutes)				
Store	4°C			
Name of plasmids	pcDNA3-CLU and pGEX4T1-CLU	pGEX4T1-alpha	pcDNA3-alpha	pcDNA3-beta and pGEX4T1-beta

Table 2.6. PCR conditions to amplify different cDNA sequences used to generate protein expression vectors

2.4.3. Plasmid vectors

2.4.3.1. pcDNA3

The PCR products represented the alpha chain or beta chain only of the complete human CLU cDNA were cloned into *KpnI* and *NotI* digested pcDNA3 vector to obtain pcDNA3-alpha or pcDNA3-beta vectors. To generate pcDNA3-CLU full length plasmid, CLU-containing fragment from TOPO-CLU vector (a gift from Professor Saverio Bettuzzi) was excised with *EcoRI* and ligated into pcDNA3 vector (Invitrogen).

cDNA sequences were assessed by sequencing services (see section 2.4.11.). Protein expressions of the constructs were verified by Western Blot analysis with appropriate antibodies.

2.4.3.2. pGIPZ lentivial vector

Lentiviral short hairpin RNA (shRNA) vectors (pGIPZ) (Figure 2.3.) targeting HSP60 and CLU expression were obtained from Thermo Scientific (UK) and are showed in Table 2.7. The non-silencing shRNAmir construct (scrambled shRNA) served as the negative control.

The Thermo Scientific mir-30 hairpin design has been constructed where the mature microRNA (miRNA) sequence in mir-30 was replaced with gene-specific duplexes (Figure. 2.2.). Addition of the mir-30 loop and the context sequences allow endogenous processing by Drosha, which increases subsequent Dicer recognition and specificity. These lentiviral constructs have been designed to give high specificity and increased knockdown efficiency of the target genes with visual accessibility granted by Turbo-GFP marking cells expressing shRNAmir (Figure. 2.3.) (Silva *et al*., 2005).

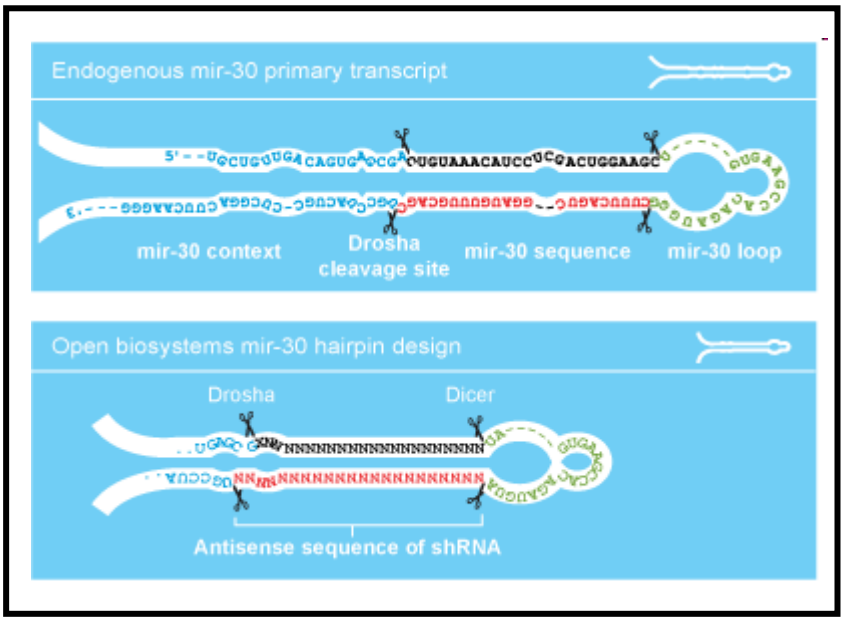

Figure 2.2. Schematic representation of the Thermo Scientific mir-30 hairpin design

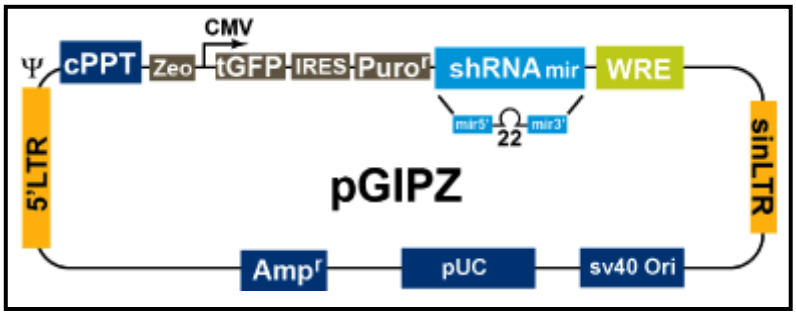

Vector Element	Utility
CMV Promoter	RNA Polymerase II promoter
cPPT	Central Polypurine tract helps translocation into the nucleus of non-dividing cells
WRE	Enhances the stability and translation of transcripts
turbo GFP	Marker to track shRNAmir expression
Puro^r	Mammalian selectable marker
AMP^r	Ampicillin bacterial selectable marker
5'LTR	5' long terminal repeat
pUC ori	High copy replication and maintenance in *e.coli*
SIN-LTR	3' Self inactivating long terminal repeat
RRE	Rev response element
ZEO^r	Bacterial selectable marker

Figure 2.3. Schematic representation of the pGIPZ shRNAmir lentiviral vector

Oligo ID (target)	Type	Homology	Hair-pin Sequence
V3LHS_337304 (CLU)	shRNAmir	Hs	TGCTGTTGACAGTGAGCG ATACGTCAATAAGGAAATTCAA TAGTGAAGCCACAGATGTA TTGAATTTCCTTATTGACGTAC TGCCTACTGCCTCGGA
V3LHS_337305 (CLU)	shRNAmir	Hs	TGCTGTTGACAGTGAGCG CCAGATAAAGACTCTCATAGAA TAGTGAAGCCACAGATGTA TTCTATGAGAGTCTTTATCTGT TGCCTACTGCCTCGGA
V3LHS_337306 (CLU)	shRNAmir	Hs	TGCTGTTGACAGTGAGCG CCAGATAAAGACTCTCATAGAA TAGTGAAGCCACAGATGTA TTCTATGAGAGTCTTTATCTGT TGCCTACTGCCTCGGA
V3LHS_337309 (CLU)	shRNAmir	Hs	TGCTGTTGACAGTGAGCG CGAGGTTGACCAGGAAATACAA TAGTGAAGCCACAGATGTA TTGTATTTCCTGGTCAACCTCT TGCCTACTGCCTCGGA
V2LHS_191368 (HSP60)	shRNAmir	Hs, Rn	TGCTGTTGACAGTGAGCG CCCATTGTACCTGCTCTTGAAA TAGTGAAGCCACAGATGTA TTTCAAGAGCAGGTACAATGGA TGCCTACTGCCTCGGA
V2LHS_233945 (HSP60)	shRNAmir	Hs	TGCTGTTGACAGTGAGCG CGCAATGACCATTGCTAAGAAT TAGTGAAGCCACAGATGTA ATTCTTAGCAATGGTCATTGCT TGCCTACTGCCTCGGA

V2LHS_133208 (HSP60)	shRNAmir	Hs	TGCTGTTGACAGTGAGCG AGCTATATTTCTCCATACTTTA TAGTGAAGCCACAGATGTA TAAAGTATGGAGAAATATAGCC TGCCTACTGCCTCGGA
V2LHS_193423 (HSP60)	shRNAmir	Hs, Mm, Rn	TGCTGTTGACAGTGAGCG CGCTGTAATTGCTGAACTTAAA TAGTGAAGCCACAGATGTA TTTAAGTTCAGCAATTACAGCA TGCCTACTGCCTCGGA

Table 2.7. Information of pGIPZ lentiviral vectors purchased from Thermo Scientific (UK)

Color Codes: mir-30 context sense loop antisense

2.4.4. Restriction digest

Restriction digests were performed according to Promega manufacturer's protocol. Briefly, a reaction mixture containing up to 5µg of plasmid DNA, restriction enzymes and 1xOptimal restriction buffer was incubated in a 37°C water bath for 4 hours. The digested products were mixed with 6xOrange loading dye (40% Glycerol, 0.25% orange G in deionized water) and run on 1% agarose gel in order to extract and purify the digested products.

2.4.5. DNA precipitation

When it was not possible to use the same buffer for two different enzymes, restriction digest were performed in two steps, separated by DNA precipitation.

Briefly, 1/10 volume of 3M sodium acetate and 2 volumes of 100% ethanol were added to the DNA solution and the solution was left for at least 3 hours at -20°C. Then the precipitated mixture was centrifuged at 13,000rpm for 15 minutes at 4°C (Eppendorf centrifuge 5415R). The supernatant was removed and 70% cold ethanol was added to the DNA pellet followed by centrifugation at 13,000rpm for 15 minutes at 4°C to remove salts. After the ethanol was removed, the precipitated DNA was resuspended in 40µl of deionized water and the DNA concentration was measured using the NanoDrop® (Labtech International).

2.4.6. De-phosphorylation of DNA plasmids

In order to prevent self ligation of a plasmid vector after restriction enzyme digest, the ends of the vector was de-phosphorylated with calf intestinal alkaline phosphatase, CIAP (promega) according to the manufacturer's protocol with the following modifications. Briefly, 40µl of ethanol precipitated DNA was added to 1xCIAP reaction buffer and up to 5µl CIAP (0.01u/µl). The mixture was incubated at 37°C for 30 minutes before another 5µl of CIAP (0.01u/µl) was added to the mixture with further incubation at 37°C for 30 minutes. For the blunt ends, the mixture was incubated at 37°C for another 15 minutes and then at 56°C for 15 minutes for optimal condition according to manufacturers protocol. De-phosphorelated vector was then precipitated with ethanol (see section 2.4.5.) and used for ligation.

2.4.7. Agarose gel electrophoresis

DNA plasmids size 4-6kbps were resolved on 1% agarose gels, whereas smaller PCR products (approximately 100-700 bps) were resolved on 2% agarose gels in 1xTAE buffer containing 2M Tris Acetate and 100mM Na_2EDTA (National Diagnostics, UK). Electrophoresis sequencing grade Agarose (Invitrogen) was weighed and then microwaved in 1xTAE buffer. Ethidium bromide was added to the agarose-TAE buffer to a final concentration of 0.5µg/ml, which was poured to set in a gel cast.

Once set, the gel was placed in a Horizon11.14 electrophoresis chamber (Biometra) filled with 1xTAE buffer and DNA samples containing 1xDNA loading dye were loaded into the wells. The first well was usually loaded with a DNA ladder of known size, 1kb Plus DNA ladder (Invitrogen) or GeneRuler 50bp DNA ladder (Fermentas Life Sciences) for restriction enzyme digests or PCR products respectively. Typically, a constant voltage of 100Volts was applied to the gel for 30-60 minutes. After electrophoresis, the DNA bands were visualized under UV light.

2.4.8. Ligation of DNA fragments

A rapid DNA ligation kit was purchased from Roche and the ligation process was performed according to manufacturer's protocol. Briefly, the molar ratios of vector DNA to insert DNA used for a ligation were 1:3 or 1:5. Then 1xConcentrated DNA dilution buffer was mixed thoroughly with a final volume of 10µl. Then 10µl of T4 DNA ligation buffer and 1µl of T4 DNA ligase were added to the mixture. The mixture was then incubated for 5 minutes at 15-25^{o}C. The ligation reaction mixture was used directly for the transformation of competent bacteria or was stored at -15 to -25^{o}C.

2.4.9. Bacterial transformation

2.4.9.1. Competent Bacterial strains

All competent bacterial strains are shown in Table 2.8.

Strains	Genotype	Use	Source
BL21	*E. coli* B F⁻ *dcm ompT hsdS*(r_B^- m_B^-) *gal*	Transformation	Stratagene
TOP10F'	F´{*lac*Iq Tn*10* (TetR)} *mcr*A Δ(*mrr-hsd*RMS-*mcr*BC) Φ80*lac*ZΔM15 Δ*lac*X74 *rec*A1*ara*D139 Δ(*ara-leu*)7697 *gal*U *gal*K *rps*L *end*A1 *nup*G	Re-transformation	Invitrogen

Table 2.8. Genotypes of *E.Coli* bacterial strains for molecular cloning and protein expression

2.4.9.2. Transformation of competent *Escherichia Coli* (*E.Coli*)

Approximately, 200ng of DNA was added to 100µl aliquot of competent cells and was left on ice for 20 minutes. The competent bacteria were heat shocked for 45 seconds at 42^{o}C, followed by an additional incubation of 2 minutes on ice. Then, 500µl of Luria-Bertani (LB) broth (containing no antibiotics) was added to the competent cells, which were incubated for 1 hour in a 37^{o}C incubator shaking at 250rpm. Following the incubation, the transformed bacteria were spread evenly on LB agar plates (containing 50µg/ml ampicillin for selection of a transformed phenotype). The plates were incubated in a 37^{o}C incubator overnight until colonies appeared.

2.4.10. Preparation of plasmid constructs

For a small scale plasmid preparation, a single bacterial colony was inoculated in 5ml of LB broth containing 50µg/ml ampicillin in a 37^{o}C incubator, orbital shaking at 250rpm overnight. Purification of plasmid construct was carried out with a QIAprep Spin Miniprep kit (Qiagen, UK), according to the manufacturer's protocol. For a large scale plasmid preparation, a single bacterial colony is inoculated in 5ml LB broth containing 50µg/ml ampicillin in a 37^{o}C incubator, orbital shaking at 250rpm for 8 hours. After 8 hours, 1ml of the LB broth containing bacteria was inoculated in 100ml LB broth containing 50µg/ml Ampicillin in a 37^{o}C incubator, orbital shaking at 250rpm for another 16 hours before purification of plasmid constructs was carried out using a Plasmid Midi kit (Qiagen, UK) according to manufacturer's protocol.

2.4.11. Sequencing

To check the DNA sequence of PCR products or DNA plasmids, a small amount of purified DNA was sent to The Wolfson Institute for Biomedical Research DNA sequencing facility at UCL to be analysed on an Applied Biosystems 3730xl Genetic Analyser. Sequencing results were provided in the form of .ab1 files which were then examined using FinchTV analysis software (Geospiza). Sequence comparison was performed using the NCBI nucleotide BLAST tools.

2.5. Statistics

Data are expressed as relative means ± Standard Deviation (SD), all experiments were repeated in triplicate (n = 3), unless otherwise stated. Statistical analysis was carried out

using a Student-t-test (unpaired, two-tailed), p-values of equal to or less than 0.05 were considered significant.

CHAPTER 3

Investigating the roles of different CLU isoforms in the control of signalling pathways.

3.1. Introduction

Clusterin (CLU) isoforms are detected both inside and outside the cell. CLU is expressed as a 56-60kDa precursor protein, in the cytoplasm. Precursor CLU (pCLU) undergoes an extensive N-linked glycosylation process where it becomes a 75-80kDa mature precursor upon transportation from the endoplasmic reticulum (ER) to the Golgi apparatus (O'Sullivan *et al*., 2003). The mature 80kDa protein further undergoes intracellular cleavage between amino acid residue Arg^{205}- Ser^{206} to form alpha (α) and beta (β) subunits, which are linked together by five disulfide bonds and ultimately get secreted (sCLU) (Burkey *et al*., 1991). Under reduced condition the subunits of CLU can be detected with the approximate size of around 35-40kDa (Rodriguez-Pińeiro *et al*., 2006).

Previous works have shown that the full-length CLU protein is a repressor of NF-κB activity by stabilizing the inhibitors of NF-κB (IκBs), which blocks NF-κB translocation and activation (Santilli *et al*., 2003, Essabbani *et al*., 2010). Our group demonstrated that overexpression of full-length CLU protein inhibits neuroblastoma cell invasion (Chayka *et al*., 2009). However, the exact role of each CLU isoform in neuroblastoma is still not clear.

This study was set out to investigate whether the cytoplasmic precursor or secreted form of CLU is responsible for the suppression of NF-κB activity and to verify the role of the two CLU isoforms in signalling pathways. Neuroblastoma cell lines (LA-N-1 and SHSY-5Y) were selected because they are both N-type cells, which display morphologic and biologic characteristics of aggressive tumour cell behaviour and that NF-κB has been shown to be activated in these cells when exposed to TNF-α (Seeger *et al*., 1977, Bian *et al*., 2001).

Neuroblastoma cell lines werer transiently transfected with a MIGR1 retroviral vector (hereafter referred to as MIG) containing a full length CLU (CLU MIG) or control

vector (MIG), which was described in Santilli et al (2003) and NF-κB LUC and renilla luciferase reporter constructs.

The MIG vector contains the enhanced GFP gene and allows simultaneous expression of the inserted CLU cDNA through the presence of an IRES sequence (Pear *et al*., 1993). The luciferase activity was measured and normalized against renilla luciferase. Student-t-test was applied to obtain a statistical significance from three independent experiments.

Overexpression of cytoplasmic precursor CLU (pCLU) as a result of transient transfection with CLU MIG plasmid significantly reduced the NF-κB activity in both LA-N-1 and SHSY-5Y in the absence of TNF-α (Figure 3.1. A and B, P=0.001 and P=0.04 respectively). TNF-α, a known regulator of NF-κB, was used to enhance NF-κB activity to see whether cytoplasmic precursor CLU can still maintain the suppression of NF-κB activity. LA-N-1 cells responded to TNF-α treatment and resulted in elevated NF-κB activity. However, the NF-κB activity was significantly reduced in the presence of cytoplasmic precursor CLU (Figure 3.1. A, P=0.02). TNF-α did not elicit NF-κB activation in SHSY-5Y cells. This could possibly be due to the lack of TNF-α receptors in this cell line (data not shown). The results show that cytoplasmic precursor form of CLU has a role in suppressing NF-κB activity in these neuroblastoma cell lines.

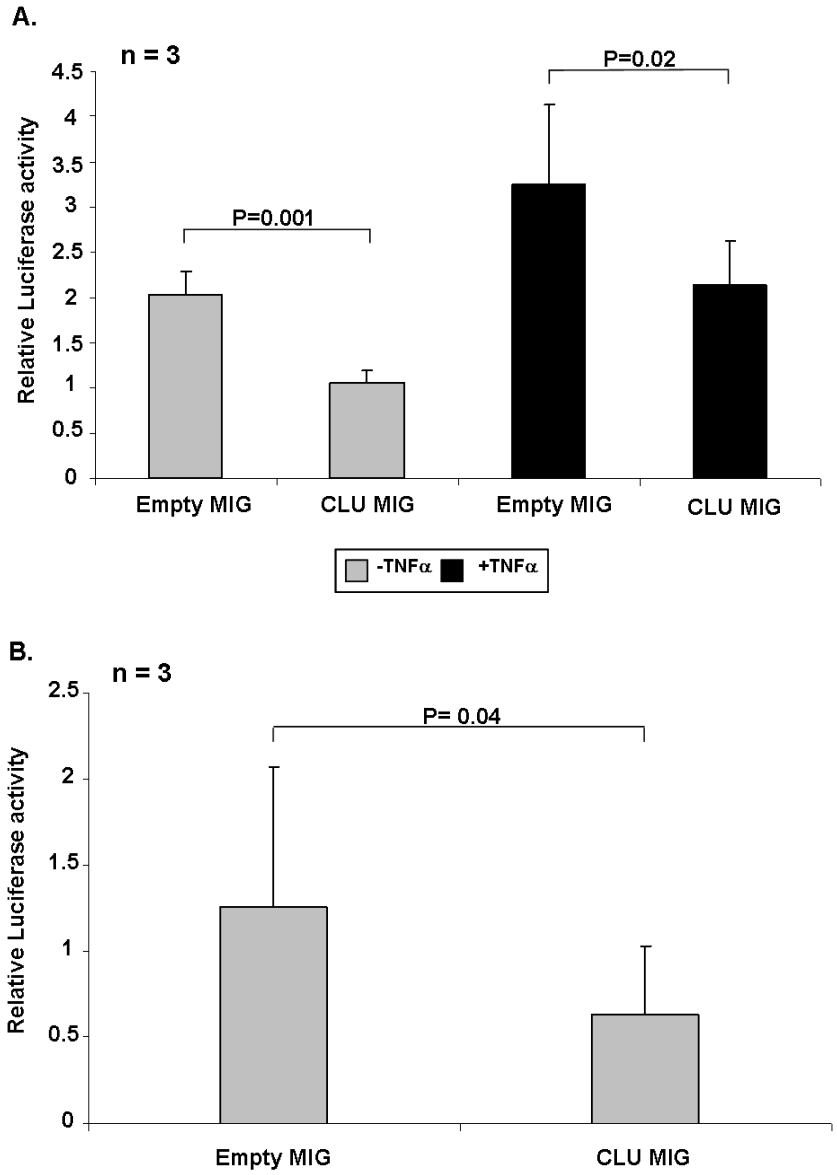

Figure 3.1. Intracellular CLU negatively regulates NF-κB activity in neuroblastoma cell lines

A NF-κB luciferase reporter construct and empty MIG or CLU MIG plasmids were transiently transfected into **A)** LA-N-1 and **B)** SHSY-5Y cells in the presence (*black bar*) or absence (*grey bar*) of TNF-α. The luciferase activity was measured and normalised against renilla luciferase. Data are expressed as relative mean values ±SD of 3 independent experiments, each in triplicate (n=3). Statistical significance was assessed by student-t-test.

3.2. The role of extracellular (secreted) CLU in NF-κB activity

In order to investigate the role of the extracellular form of CLU (sCLU), CLU-conditioned media needed to be generated, since the mature secreted form of CLU can usually be found in the culture supernatants (Humphreys *et al*., 1997). Due to a large amount of secreted CLU required, 293FT cells were used for transfection as the cell line is easily transfectable. Secreted CLU was produced by transient transfection of human 293FT cells with empty MIG or CLU MIG.

Transfection efficiency was checked 24 hours after transfection by fluorescent microscopy (Figure 3.2.A, *middle panel*) and 48 hours later by Western blot (Figure 3.2.B). Western blot analysis showed no expression of endogenous precursor CLU (pCLU) in the 293FT cells transfected with empty MIG (Figure 3.2.B, *top panel* lane 1) and overexpression of the cytoplasmic precursor CLU (pCLU, size ~60kDa) in the 293FT cells transfected with CLU MIG (Figure 3.2.B, *top panel* lane 2).

Cytoplasmic precursor CLU (pCLU) get secreted outside the transfected cells and become secreted CLU (sCLU, size ~35-40kDa detected under reduced condition, Rodriguez-Pińeiro *et al*., 2006) in the medium (Figure 3.2.B, *bottom panel* lane 2). The amount of CLU in the culture supernatants was much higher in the CLU MIG transfected cells in comparison with corresponding control empty MIG. The levels of cytoplasmic precursor and secreted CLU were detected by an anti-CLU (M-18) antibody, which recognized the beta chain of CLU. The media collected from this experiment were used in the investigation of NF-κB regulation by extracellular CLU.

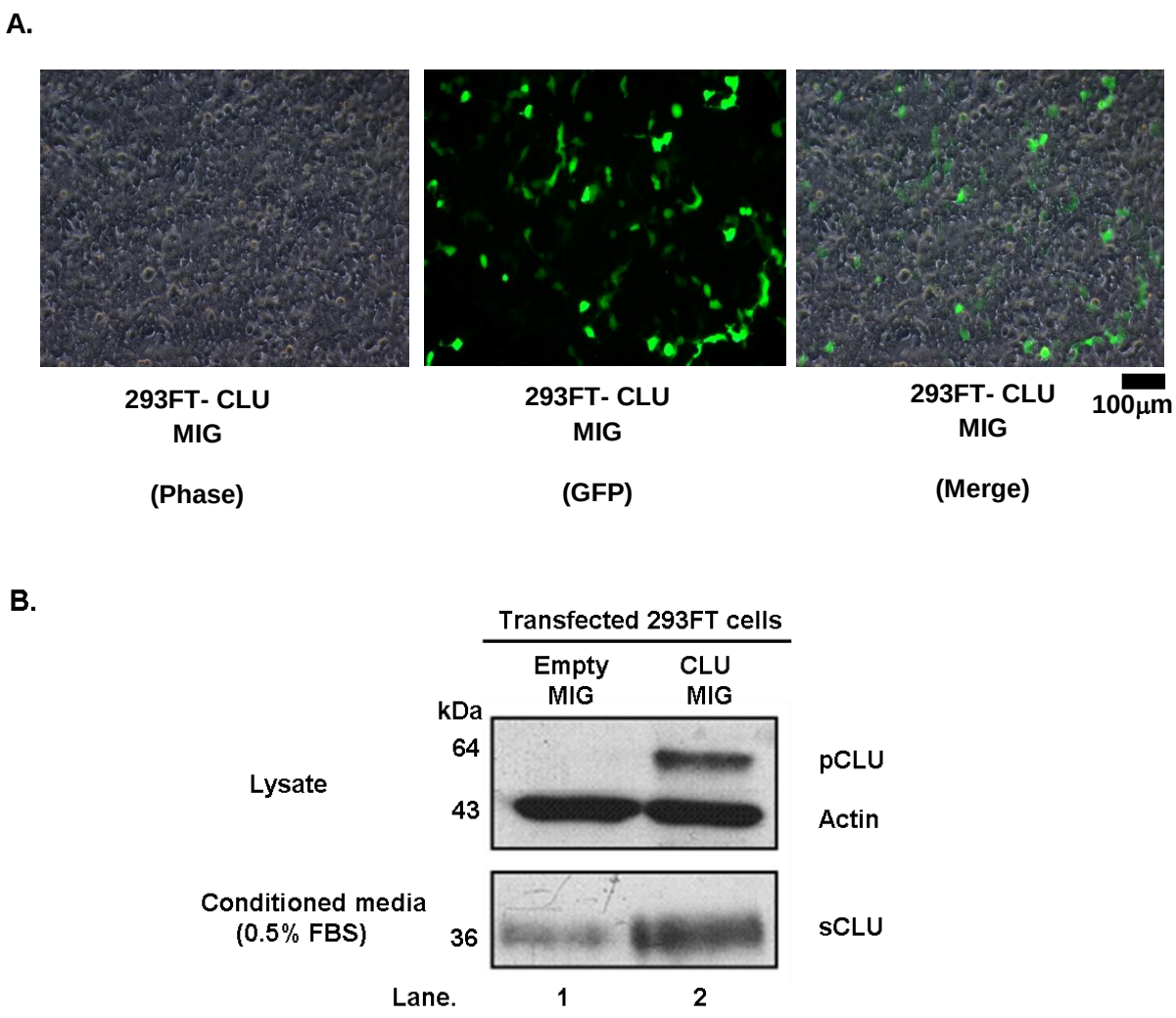

Figure 3.2. Generation of sCLU conditioned media

A) Representative morphology of 293FT cells (*left panel*) at 24 hours after transient transfection with CLU MIG plasmid expressing GFP (*middle panel*) and merge (*right panel*), scale = 100µm. **B)** Western blot analysis of precursor (pCLU) or secreted (sCLU) expression in 293FT cells after transient transfection with empty MIG or CLU MIG plasmids. Cells were lysed in RIPA buffer and subjected to western blot analysis with anti-CLU or Actin (loading control) antibodies, 24 hours after transfection. Positions of the human 60-kDa CLU precursor (pCLU), the mature 35-40 kDa secreted CLU (sCLU) and 43-kDa Actin proteins are shown. Lane 1: cells transfected with empty MIG vector. Lane 2: cells transfected with CLU MIG vector.

Previously, it was shown that intracellular CLU can negatively regulate NF-κB activity. After generating sCLU conditioned media, the role of the secreted form of CLU can be determined to see whether there is an involvement of secreted CLU in the regulation of NF-κB. Neuroblastoma cell lines (LA-N-1 and SHSY-5Y) were transiently transfected with a NF-κB luciferase reporter construct. Conditioned media (supplemented with 0.5% FBS) containing basal level (obtained from 293FT cells transfected with empty MIG) or overexpressed level of sCLU (obtained from 293FT cells transfected with CLU MIG) was added to the cells 24 hours after transfection in the presence or absence of TNF-α and the luciferase activity was assessed 8 hours afterwards.

Secreted CLU failed to inhibit NF-κB activity in both LA-N-1 and SHSY-5Y (Figure 3.3.A and B). The level of NF-κB activity remained unaltered either in the presence or absence of secreted CLU. SHSY-5Y as mentioned previously did not show a good response to TNF-α treatment (Figure 3.3.B).

Purified human recombinant secreted CLU was purchased from Alexis (UK) to corroborate these results. The working concentration of purified human recombinant secreted CLU was 100ng/ml after the titration test (Figure 3.5.). This is due to the strongest stimulation of phosphorylated AKT after serum deprivation, which lasted up to 16 hours (Figure 3.5. *lanes 5* and *6*). Recombinant CLU was unable to alter NF-κB activity (Figure 3.4.), supporting the hypothesis that intracellular CLU, but not secreted CLU, is a negative regulator of NF-κB.

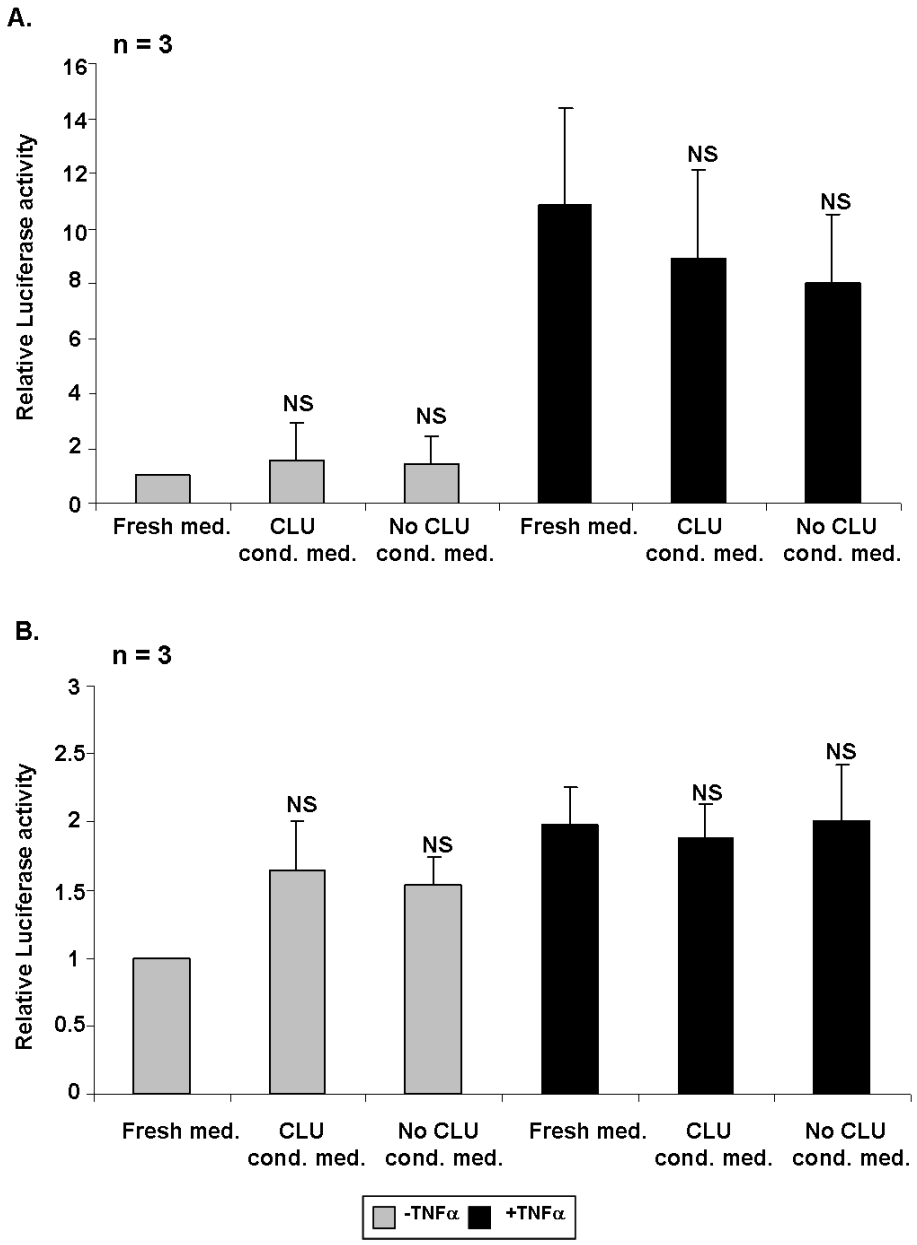

Figure 3.3. Secreted CLU does not regulate NF-κB activity in neuroblastoma cell lines

A NF-κB luciferase reporter construct was transiently transfected into **A)** LA-N-1 and **B)** SHSY-5Y cells in the presence (*black bar*) or absence (*grey bar*) of TNF-α. Conditioned media (containing 0.5% FBS) with or without secreted CLU were added to the cells and incubated for 8 hours before being subjected to luciferase assays. Data are expressed as relative mean values ±SD of 3 independent experiments, each in triplicate (n=3). NS = No significance.

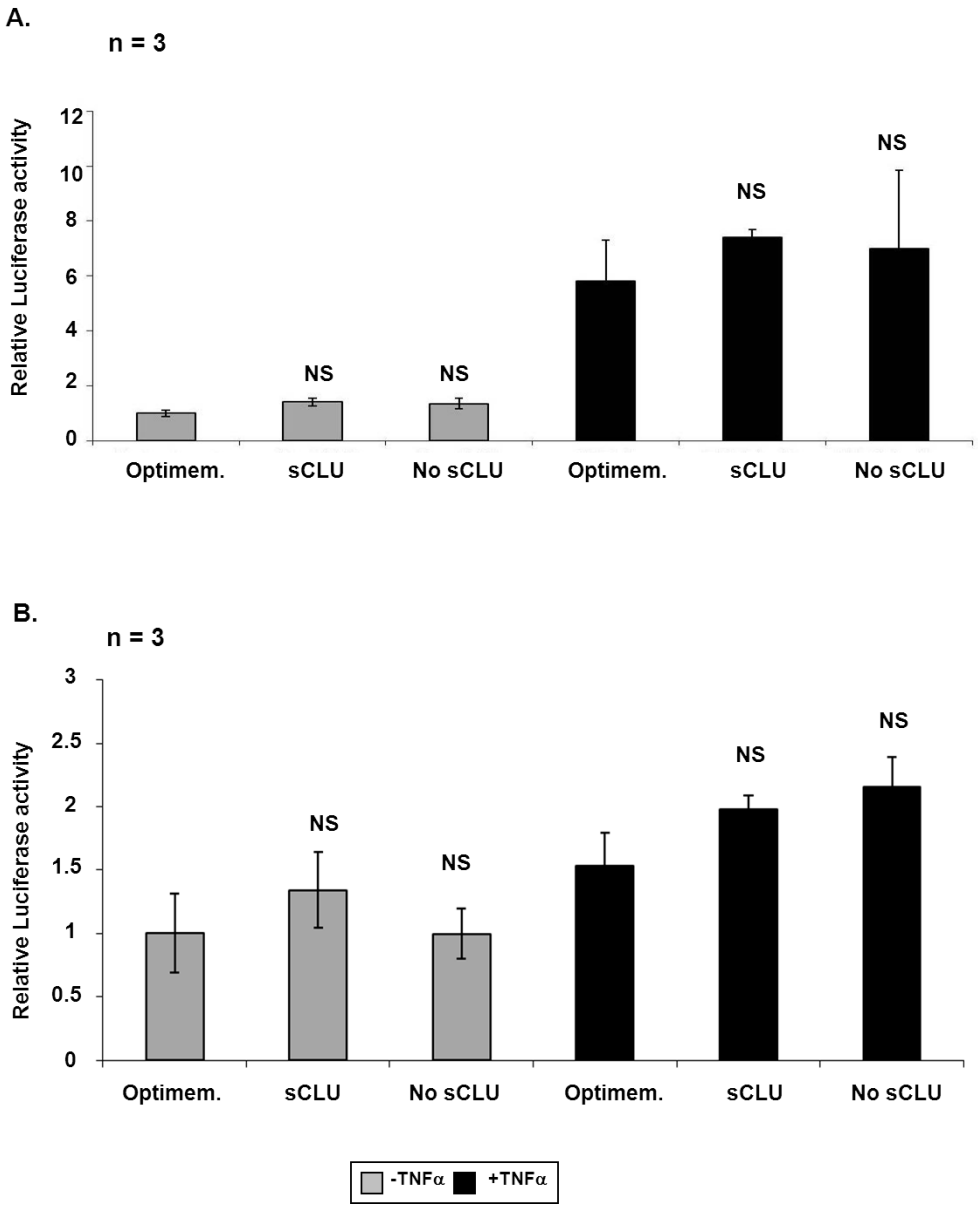

Figure 3.4. Purified secreted CLU does not regulate NF-κB activity in neuroblastoma cell lines

A NF-κB luciferase reporter construct was transiently transfected into **A)** LA-N-1 and **B)** SHSY-5Y cells in the presence (*black bar*) or absence (*grey bar*) of TNF-α. Fresh media (Optimem containing 0% FBS) with or without purified secreted CLU (100ng/ml) were added to the cells and incubated for 8 hours before being subjected to luciferase assays. Data are expressed as relative mean values ±SD of 3 independent experiments, each in triplicate (n=3). NS = No significance.

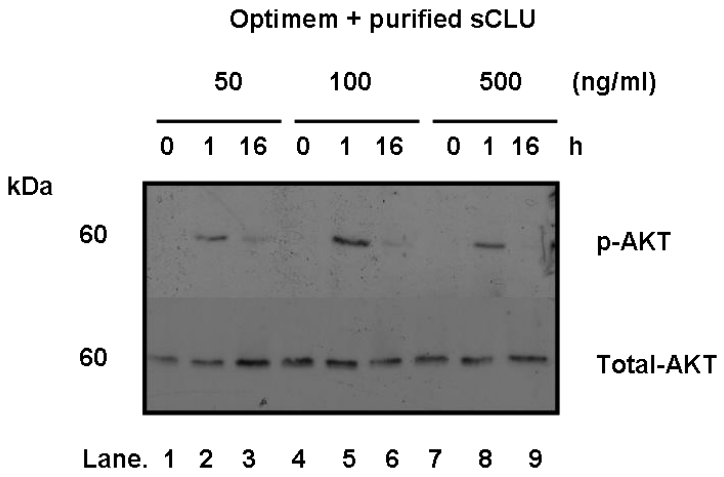

Figure 3.5. Titration test to determine a working concentration of purified sCLU

Western blot analysis of phosphorylated AKT (p-AKT) in LA-N-1 cells treated with fresh media (Optimem) supplemented with 50, 100 or 500ng/ml purified secreted CLU (sCLU). LA-N-1 cells seeded at the density of $1x10^5$ cells per well in a 6-well plate were deprived of serum 16 hours before fresh media was added. Cells were harvested at 0, 1 and 16 hours after sCLU conditioned medium was added. Phosphorylated AKT (~60kDa) were detected by antibodies as indicated. Total AKT was used as the loading controls.

3.3. The role of secreted CLU in other signalling pathways

Previous reports have suggested that sCLU is involved in Phosphoinositide-3 Kinase (PI3K) pathway in epithelial and prostate cancer models (Jo *et al*., 2008, Ammar and Closset, 2008) while Chou and coworkers (2009) suggested that CLU is involved in the Mitogen-Activated Protein Kinase (MAPK, originally called ERK) ERK/Slug signalling pathway in a lung cancer model. The involvement of CLU in different signalling pathways has led to the next experiments where the role of secreted CLU was investigated in our neuroblastoma model.

LA-N-1 and SHSY-5Y cells were deprived of serum for 16 hours, in order to dephosphorylate AKT, thus resulting in the minimal basal level of phosphorylated AKT, before conditioned media containing basal or overexpressed levels of secreted CLU were added to the cells. Cells were collected at different time-points (0, 1, 2, 4, 6 and 16 hours) and western blot analysis was carried out to verify the level of phosphorylated AKT or ERK in both cell lines (Figure.3.6.).

Phosphorylated AKT (~60kDa) remained high throughout the experiment in the presence of sCLU in both LA-N-1 and SHSY-5Y cells (Figure 3.6.A compare *lanes 2-6* to *lanes 8-12*). This illustrated that sCLU can sustain the activation of AKT, which is an essential regulator of cell survival in the PI3K signalling pathway. Similar results were seen when purified human recombinant sCLU was used (Figure 3.7.A).

The level of phosphorylated ERK (~42, 44 kDa) remained unchanged in LA-N-1 and SHSY-5Y cells in the presence or absence of sCLU (Figure 3.6.B). When purified human recombinant sCLU was used, the level of phosphorylated ERK (~42, 44 kDa) remained unchanged in SHSY-5Y in the presence or absence of sCLU and there was no activation of ERK in LA-N-1 cells (Figure 3.7.B). Therefore, it is likely that MAPK/ERK activity is not stimulated by sCLU.

In summary, secreted CLU does not have a role in NF-κB and MAPK/ERK signalling pathways, but it might be a stimulator of the PI3K/AKT pathway.

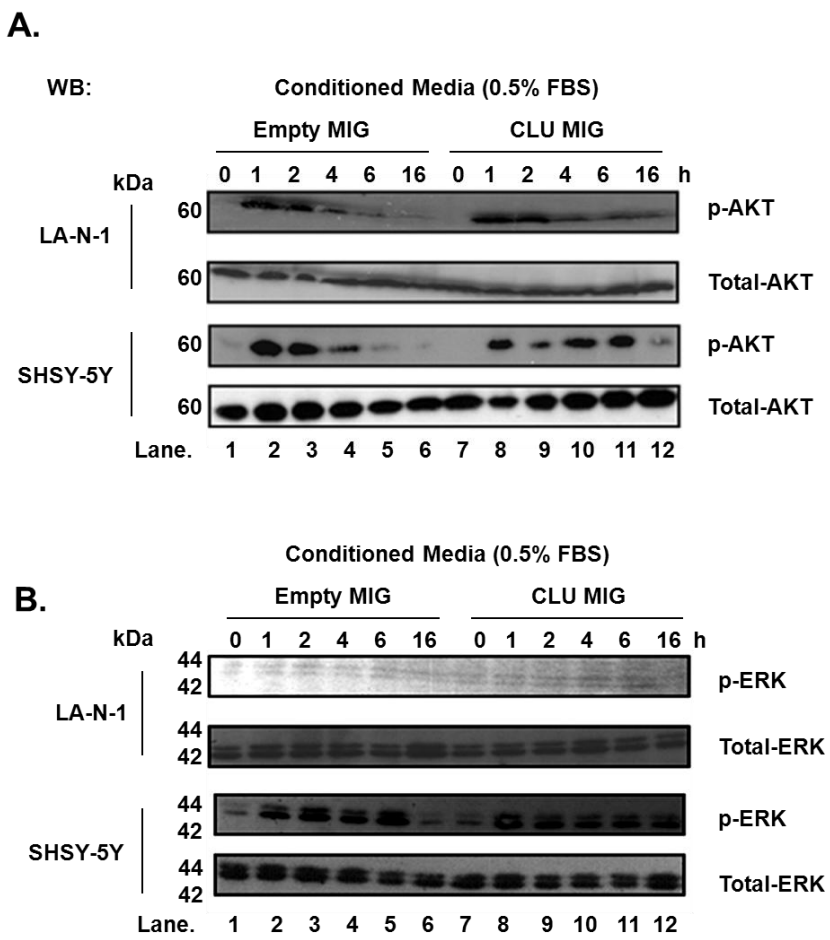

Figure 3.6. Secreted CLU activates the PI3K pathway

Western blot analysis of **A)** phosphorylated AKT (p-AKT) and **B)** phosphorylated ERK (p-ERK) in LA-N-1 and SHSY-5Y cells treated with conditioned media containing secreted CLU. Cells were harvested at 0, 1, 2, 4, 6, 16 hours after CLU conditioned medium was added. Phosphorylated AKT (~60kDa) and ERK (~42, 44 kDa) were detected by antibodies as indicated. Total AKT and ERK were used as the loading controls.

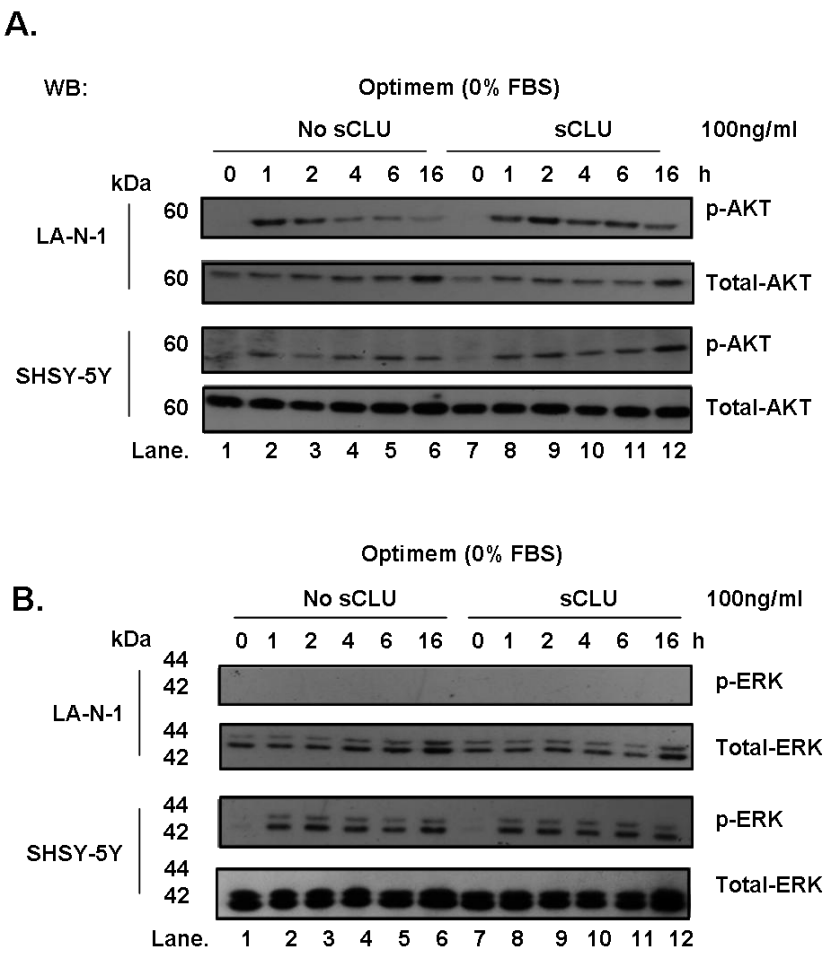

Figure 3.7. Purified secreted CLU activates the PI3K pathway

Western blot analysis of **A)** phosphorylated AKT (p-AKT) and **B)** phosphorylated ERK (p-ERK) in LA-N-1 and SHSY-5Y cells treated with fresh media (optimum, 0% FBS) supplemented with or without 100 ng/ml purified secreted CLU. Cells were harvested at 0, 1, 2, 4, 6, 16 hours after CLU conditioned medium was added. Phosphorylated AKT (~60kDa) and ERK (~42, 44 kDa) were detected by antibodies as indicated. Total AKT and ERK were used as the loading controls.

3.4. Alteration of pCLU and sCLU expressions during cell transformation

Since intracellular CLU inhibits NF-κB, which is involved in the promotion of metastasis (Julien *et al*., 2007, Radisky and Bissell, 2007), it may act as a tumour suppressor protein. On the other hand, sCLU appeared to promote cell survival by activating the PI3K signalling pathway.

The opposing roles of these two CLU isoforms prompted us to investigate whether these different forms of CLU may become imbalanced during cell transformation. Western Blot analysis was carried out in 2 non-cancer cell lines, one is a mortal human fibroblast cell line (WI-38) and another is its SV40-transformed version (VA-13). Figure 3.8.A shows that once the cells have undergone transformation, the level of CLU (pCLU) reduced approximately 3-fold, compared to the normal cell state. No change in the sCLU expression was observed during cell transformation.

After this observation, it was interesting to verify whether this phenomenon may also occur during neuroblastoma cell transformation. To test this hypothesis, cell lysates of whole adrenal glands (both adrenal cortex and medulla) taken from non-transgenic CBA mice and neuroblastoma tumour lysates taken from *MYCN* transgenic mice of the same genetic background (Weiss *et al*., 1997) were probed for pCLU and sCLU expressions. The exposure time of both membranes was 45 minutes. Figure 3.8.B (*left panel*) showed six out of eight (75%) adrenal glands contained detectable expressions of tumour suppressor pCLU. One adrenal sample had low protein concentration, which resulted in no bands detected (Figure.3.8B *left panel*, *lane 3*). However, pCLU were not detected in any of the tumour cell lysates (Figure 3.8.B, *right panel*).

This suggests that CLU expression or sub-localization is strictly related to cell fate. We hypothesise that a shift towards the loss of tumour suppressor cytoplasmic precursor CLU (pCLU) may favour cell transformation.

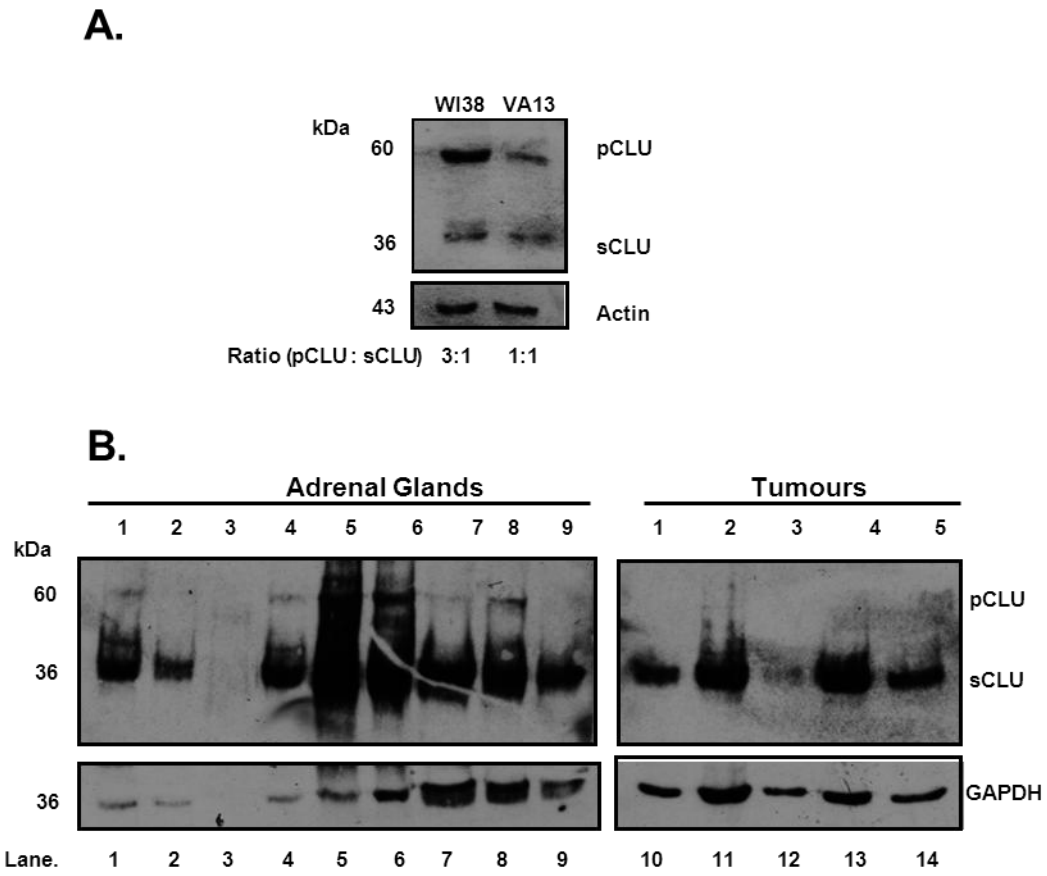

Figure 3.8. Modulation of pCLU and sCLU during cell transformation

Western Blot analysis of endogenous precursor CLU (pCLU) and secreted CLU (sCLU) in **A)** WI-38 and VA-13 cell lines and **B)** in 9 adrenal glands (*lanes 1-9*) of CBA mice and 5 neuroblastoma tumours (four with abdominal origin *lanes 10-11, 13-14*, and one from the lung, *lane 12*) isolated from human *MYCN*-transgenic CBA mice. The exposure time for both membranes was 45 minutes.

3.5. Discussion

Previously, CLU was hypothesised to be a tumour promoter acting downstream of an oncogene, *B-MYB*, in neuroblastoma. However, interestingly in that study, secreted CLU was shown to exert an anti-apoptotic function in neuroblastoma cells (Cervellera *et al*., 2000). Zhang and coworkers (2005) showed that cytoplasmic precursor CLU (pCLU) acts as an anti-apoptotic factor, interfering with Bax activation in the mitochondria, causing inhibition of cytochrome C release and caspase activation in the human prostate cancer cell line PC3M. In contrast, several studies linked nuclear CLU (nCLU) to apoptosis, since its expression is restricted within the area of apoptotic or necrotic cells in prostate, breast and neuroblastoma tumours (Caccamo *et al*., 2005, O'Sullivan *et al*., 2003, Chayka *et al*., 2009).

Other studies showed that CLU mediates tumour suppressing activities in prostate cancer and Von Hippel–Lindau disease (VHL), which causes hemangioblastomas (Nakamura *et al*., 2006, Zhou *et al*., 2007, Bettuzzi *et al*., 2009). In 2009, our research group demonstrated that *CLU* is a tumour suppressor gene negatively regulated by the proto-oncogene *MYCN*, which is associated with aggressive neuroblastoma. Overexpression of CLU caused decreased metastasis of neuroblastoma tumours, whereas, suppression of CLU in neuroblastoma cells elicited NF-κB activation and increased expressions of vimentin and fibronectin, markers for epithelial-to-mesenchymal transition (EMT) and metastatic behaviour (Chayka *et al*., 2009). Therefore, the evaluation of the biological role of CLU has been complicated by the existence of various forms of CLU.

In this chapter, the role of CLU isoforms has been studied in neuroblastoma. Firstly, overexpression of intracellular CLU caused significant inhibition of NF-κB activity in both LA-N-1 and SHSY-5Y cell lines (Figure 3.1.). This observation, in agreement with previous work, confirmed that intracellular CLU is a negative regulator of NF-κB signalling and possibly a tumour suppressor protein (Santilli *et al*., 2003, Essabbani *et al*., 2010).

On the other hand, luciferase assays demonstrated that sCLU is not involved in the regulation of NF-κB, as it failed to inhibit NF-κB activity in both LA-N-1 and SHSY-

5Y (Figure 3.3.). This suggests that sCLU is not involved in NF-κB signalling. Previous studies suggested that sCLU is a key regulator of both PI3K and ERK/MAPK signalling pathways. For example, sCLU was confirmed to be pro-survival and associated with AKT regulation in prostate and epithelial cancer cells (Ammar and Closset, 2008, Jo *et al*., 2008). Secreted CLU was proposed to be released by cancer cells and competitively inhibits IGF-1 binding to its receptor, inhibiting the AKT/PI3K pathway and pushing epithelial cancer cells to proliferate more than normal neighbouring cells (Jo *et al*., 2008). Opel and coworkers (2007) showed that activated AKT may be used as a marker for poor outcome in neuroblastoma. These observations, together with our results, prompted us to investigate the role of sCLU in the cell signalling process of neuroblastoma.

Our results show that sCLU can activate AKT in neuroblastoma (Figures 3.6.A and 3.7.A). AKT activation could allow neuroblastoma cells to be more resistant to cell death or gain proliferative advantage over normal cells. This result is supported by previous work in our laboratory where we observed an anti-apoptotic function of secreted CLU in neuroblastoma (Cervellera *et al*., 2000). Although sCLU can be detected in adrenal and tumour lysates (Figure 3.8.B), Cervellera et al (2000) demonstrated that sCLU is important for neuroblastoma survival and resistance to cytotoxic drug where blockage of sCLU by a monoclonal antibody resulted in increased apoptosis of neuroblastoma cells exposed to doxorubicin. Thus, sCLU may not play a major role in neuroblastoma development; it has been shown to be important in neuroblastoma cell survival and resistance to chemotherapeutic drugs.

The results presented in this chapter could explain the controversial role of CLU in cancer. Shifting the balance between the secreted and intracellular forms of CLU could affect different signalling pathways, ultimately resulting in the increased or decreased tumourigenesis. This work also confirmed a link between CLU and the NF-κB transcription factor, which plays a pivotal role in the cellular immune response and carcinogenesis, due to its constitutive expressions in many types of cancers (Karin, 2006).

CHAPTER 4

Identification of CLU-interacting proteins

4.1. Introduction

The previous experiments confirmed that intracellular CLU regulates NF-κB activity. In order to find out which region of CLU is responsible for the regulation of NF-κB activity. It would be interesting to see whether the alpha chain region of CLU or the beta chain region of CLU is more potent in the suppression of NF-κB activity by dual luciferase assay. As a first step, three constructs containing full length, α or β chains of CLU (pcDNA3-CLU, pcDNA3-α and pcDNA3-β respectively) were generated (see Appendix I).

4.2. Regulation of NF-κB activity by full length precursor CLU (pCLU) and its truncated forms

Figure 4.1. A and B show western blot analyses of protein lysates prepared 24 hours after transient transfection of 293FT cells with pcDNA3-CLU full length, pcDNA3-α and pcDNA3-β. No CLU protein expression was observed in non-transfected (NT) or empty pcDNA3 vector transfected cells (Figure 4.1.A and B, *lanes 1* and *2*).

Transfection of the pcDNA3-CLU full length construct resulted in significant overexpression of CLU with the approximate size of 60kDa (Figure 4.1.A, *lane 3*). The transgene also produced a fully glycosylated protein of 35-40 kDa under reduced condition. The CLU-α chain mutant was expressed (Figure 4.1.B *lane 3*) and showed an approximate size of 36kDa. The CLU-β chain mutant was expressed with a size of ~29kDa. CLU-β chain dimers were also detected at approximately 58kDa (Figure 4.1.A *lane 4*).

Next we assessed the involvement of different regions of CLU in the regulation of NF-κB activity. SHSY-5Y cells were transiently co-transfected with a NF-κB luciferase reporter construct and pcDNA3-only, pcDNA3-CLU, pcDNA3-α or pcDNA3-β vectors. In the presence or absence of TNF-α, the α chain caused almost a 50% suppression in

NF-κB activity (P=0.01) in comparison to the other constructs (Figure 4.1.C). The β chain did not have any significant effect on NF-κB activity.

In summary, the alpha region near the N-terminal of CLU may be involved in regulating NF-κB. There were some limitations to the experiments, which should be noted. Eventhough SHSY-5Y cells were not as responsive to TNF-α as LA-N-1 cells, we have decided to use this cell line due to the ability of these cells to form stable clones with expressions of CLU full length, CLU alpha chain region only or CLU beta chain region only. Moreover, we wanted to make sure that the unresponsiveness to TNF-α is not due to transfection problem so we decided to carry out the luciferase assay in both the presence and absence of TNF-α. Figure 4.1.C has shown that indeed, there was no problem with transfection and that there may be lower levels of TNF-α receptors on SHSY-5Y cells.

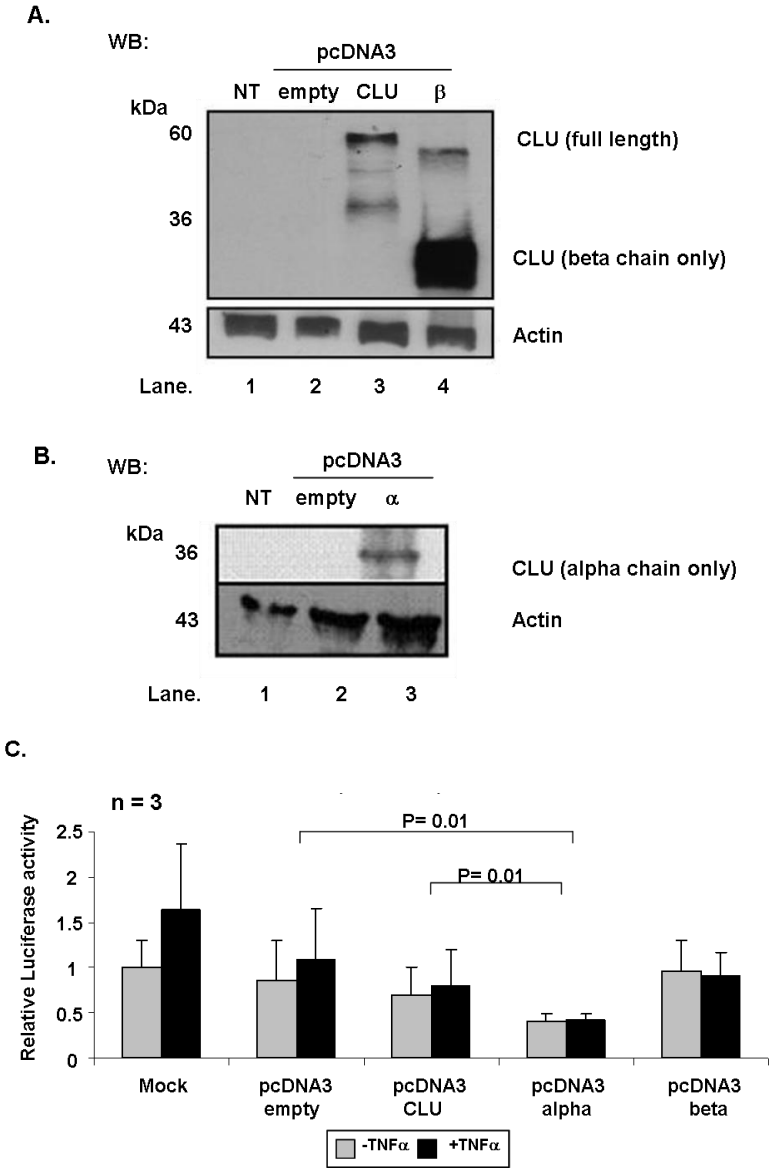

Figure 4.1. The alpha chain of CLU (CLU-α) negatively regulates NF-κB activity

A) Western blot analysis of exogenous CLU expression in 293FT cells after transient transfection with pcDNA3-CLU and pcDNA3-β plasmids (*lanes 3-4*) and **B)** pcDNA3-α (*lane 3*). Blots were incubated with Actin antibody for loading controls. NT = non-transfected lysate sample (*lane 1*). Empty = empty pcDNA3 vector (*lane 2*). **C)** Empty pcDNA3, pcDNA3-CLU, pcDNA3-α or pcDNA3-β plasmids were transfected into SHSY-5Y and cells were selected with Geneticin (1μg/ml) for 3 weeks to generate stable clones of cells overexpressing CLU (full length), CLU-α only and CLU-β only proteins. The established cell clones were used for co-transfection with NF-κB luciferase reporter construct and renilla luciferase in the presence (*black bar*) or absence (*grey bar*) of TNF-α. The luciferase activity was measured and normalised against renilla luciferase. Statistical significance was assessed by student-t-test. Data are expressed as relative mean values ±SD of 3 independent experiments, each in triplicate (n=3). The p-value is indicated for statistical significance.

4.3. Generation of GST-fusion protein constructs for GST-pull down assays

To identify CLU-interacting proteins that may be involved in the regulation of NF-κB activity, we generated GST-fusion proteins containing various segments of CLU. Full length CLU or the α or β chain were subcloned into pGEX4T1. The resulting pGEX4T1-CLU (GST-CLU), pGEX4T1-α (GST-α) and pGEX4T1-β (GST-β) were generated (See Appendix I).

The GST-fusion protein constructs were sequenced and used to transform *E. coli* strain BL21, which is widely used for protein expression.

4.4. Identification of CLU-interacting proteins

GST-fusion proteins were induced and purified as described in sections 2.3.3.2. and 2.3.3.3. The purified GST-fusion CLU full length and its α and β chain are shown in figure 4.2.A (*lanes 9-11*). Interacting proteins from LA-N-1 cell lysates were pulled down by using the GST-fusion proteins as bait. A silver stained polyacrylamide gel with potential CLU-binding proteins (marked by asterisks) is shown in figure 4.2.B. Non-specific proteins binding to the GST beads are in lane 2. Some proteins showed preferential binding to the CLU full length or the α or β chains.

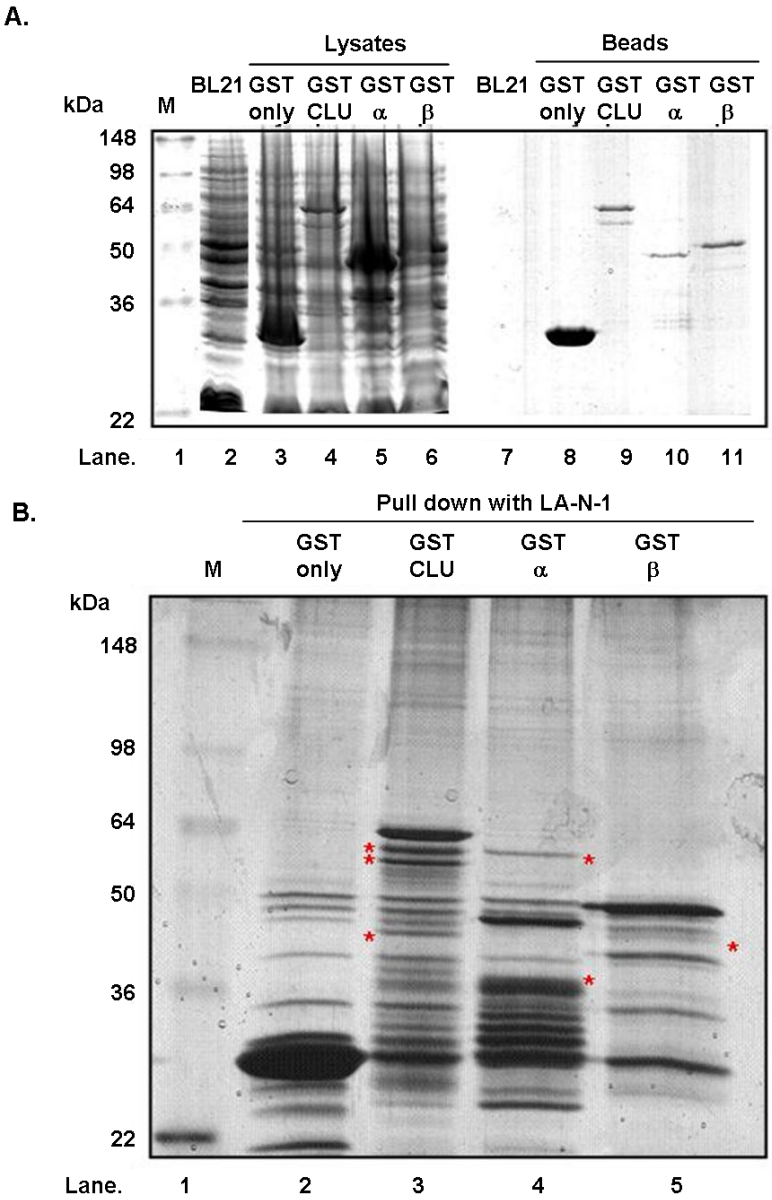

Figure 4.2. Identification of CLU-interacting proteins by GST-pull down

A) Expression of the fusion proteins was assessed by SDS polyacrylamide gel stained with coomassie blue. **B**) A small scale pull down assay performed in LA-N-1 cells using equivalent amounts of control GST protein and GST-CLU, GST-α or GST-β fusion peptides (*lanes 2-5*). The samples were run on a 10% SDS polyacrylamide gel, which was stained with silver nitrate and potential targets are shown in red asterisk (*). M = prestained protein molecular weight marker. The sizes of GST-empty, GST-CLU, GST-alpha, α and GST-beta, β were ~26, ~64, ~ 45 and ~50 kDa respectively.

4.5. Identification of CLU-interacting proteins using a large-scale GST-pull down assay

Although potential binding proteins have been observed in the small scale pull down assay, the amount of proteins were not enough to be identified by mass-spectrometry as the technique requires relatively high level of protein for analysis. In addition, silver staining technique can sometimes interfere with the mass-spectrometry analysis. Therefore, a large-scale pull down assay was performed, followed by colloidal coomassie blue staining, which is more appropriate for mass-spectrometry analysis.

The GST-fusion protein induction and purification were repeated as previously described. Approximately $4x10^7$ LA-N-1 cells were used per GST-fusion protein for the large-scale pull down.

Figure 4.3.A and B show a 10% SDS polyacrylamide gel stained with the silver nitrate and colloidal coomassie blue dye respectively. The GST empty beads and fusion proteins (pGEX4T1-empty, pGEX4T1-CLU, pGEX4T1-α and pGEX4T1-β) are shown clearly on the 10% SDS polyacrylamide gel, at the sizes of ~26, ~64,~45 and ~50kDa respectively (Figure 4.3.B). Potential binding proteins were selected according to the previously described band pattern (section 4.4.) The selected bands of ~60kDa were excised and sent for mass-spectrometry analysis. The band of ~60kDa was selected because this protein is bigger in size than the alpha chain protein, which would eliminate any alpha chain-digested products being analysed by mass-spectrometry. In addition, we were able to obtain the interaction between the ~60kDa protein with CLU full length and CLU-alpha chain region in three different pull down assays, thus, this protein may serves as a potential CLU binding protein. Although the ~60kDa band in figure 4.3B (*lane* 4) appeared to be quite faint on the gel, this is likely to be due to the different types of staining technique. Colloidal coomassie blue stains protein in a light blue colour, whereas, silver nitrate stains protein in a brown/black colour. Hence, the band on figure 4.3B (*lane* 4) appeared much weaker in comparison to figure 4.3A (*lane* 3).

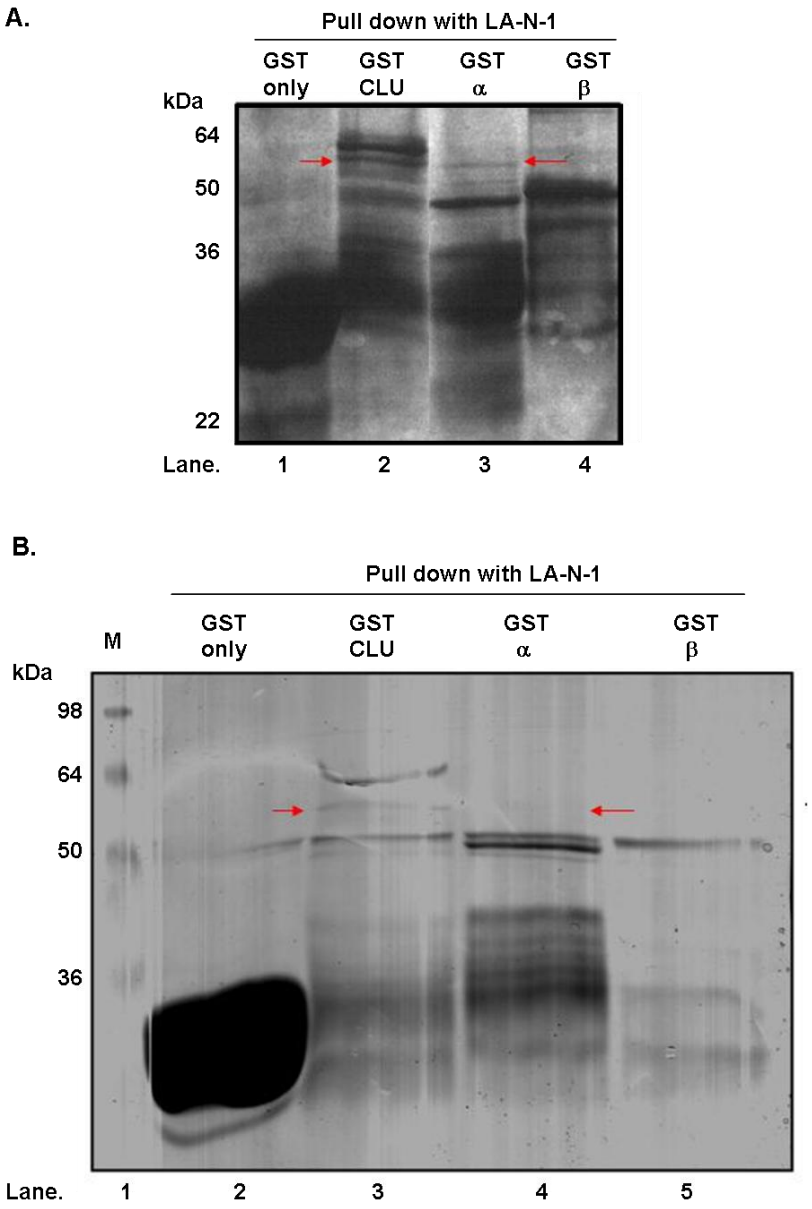

Figure 4.3. Potential CLU-interacting protein of approximately 60 kDa identified by large-scale pull down assays

The pull down assay was performed in LA-N-1 cells using equivalent amounts of control GST protein and GST-CLU, GST-α GST-β fusion peptides. The samples were run on a 10% SDS polyacrylamide gel, which was stained by **A)** Silver nitrate solution **B)** Colloidal coomassie blue dye and potential target proteins (~60 kDa), indicated with red arrows (→) were sent for mass-spectrometry analysis. M = protein molecular weight marker.

4.6. Mass-spectrometry analysis

The proteins from the excised bands were trypsin-digested and the peptide solution was separated by mass within the mass-spectrometer. Fragmented amino acid sequences were aligned against the human amino acid sequence database called Basic Alignment Search Tool (BLAST). The list of potential proteins bound to CLU full length identified from the mass-spectrometry is shown (Figure 4.4.A).

Keratin is a well known contaminant in mass-spectrometry analysis and is, therefore, not accounted as a genuine binding protein. Keratin appeared relatively higher on the list in both figure 4.4.A and B, which indicated the relative amount of protein presented. Low-density lipoprotein receptor-related protein 2 or LRP2 (also known as megalin, approximately 522 kDa) is a known membrane receptor for CLU (Bartl *et al*., 2001), which in this case have been pulled down with the wild type CLU protein but not the α mutant chain and therefore can be accounted as a positive control to show that the pull down assay worked efficiently.

Another interesting protein identified from the mass-spectrometry shown in both figure 4.4. A and B was heat shock protein 60, HSP60 (the protein is encoded by the gene, *HSPD1*). HSP60 is the mitochondrial chaperonin that promotes the folding of the imported protein to native conformation (Chun *et al*., 2010). The role of HSP60 is discussed in more detail in chapter 5.

Since, HSP60 bound to full length and the N-terminal region of CLU protein (i.e. the α chain sequence) and the size of HSP60 corresponded to the size of the band excised, therefore HSP60 was considered as a genuine target in this experiment. Thus, HSP60 appeared to be a potential CLU-interacting protein that is bound to the α region near the N-terminus of the protein.

A.

Protein Hits – CLU full length *Homo sapiens* (Humans)	
CLUS_HUMAN	Clusterin
K2C1_HUMAN	Keratin, Type II skeletal 1
K22E_HUMAN	Keratin, Type II skeletal 2
K1C10_HUMAN	Keratin, Type I skeletal 10
LRP2_HUMAN	Low-density Lipoprotein receptor-related protein 2
K1C9_HUMAN	Keratin, Type I skeletal 9
CH60_HUMAN	60 kDa heat shock protein, mitochondrial
41_HUMAN	Protein 4.1
PRAM7_HUMAN	PRAME family member 7
A16L1_HUMAN	Autophagy-related protein 16-1
FA48A_HUMAN	Protein FAM 48A
NCKPL_HUMAN	Nck-associated protein 1-like
YI028_HUMAN	Putative UPF0609 protein C4orf27-like
UBR3_HUMAN	E3-ubiquitin protein ligase UBR3

B.

Protein Hits – CLU α chain only *Homo sapiens* (Humans)	
K2C1_HUMAN	Keratin, Type II skeletal 1
K1C10_HUMAN	Keratin, Type I skeletal 10
CLUS_HUMAN	Clusterin
K22E_HUMAN	Keratin, Type II skeletal 2
CH60_HUMAN	60 kDa heat shock protein, mitochondrial
LMNB1_HUMAN	Lamin-B1
SYYC_HUMAN	Tyrosyl –tRNA synthetase, cytoplasmic
K1C9_HUMAN	Keratin, Type I skeletal 9
PUF60_HUMAN	Poly (U) binding splicing factor PUF60
EF1G_HUMAN	Elongation factor 1-gamma
HDAC1_HUMAN	Histone-deacetylase 1
RCC2_HUMAN	Protein RCC2
TBA1A_HUMAN	Tubulin alpha-1A chain

Figure 4.4. HSP60 was identified as an interacting partner of CLU within its α chain

Results of mass spectrometry analysis of GST-CLU and GST-α protein bands showed a list of peptide fragments binding to **A)** GST-CLU (full length) and **B)** GST-α chain only. The sequences were aligned against the human amino acid sequence database. CLU membrane receptor (LRP2) and heat shock protein 60 (HSP60) are highlighted in a box.

4.7. The results of mass-spectrometry analysis of HSP60 in GST-pull down assay

To confirm that HSP60 is a genuine CLU-interacting protein, western blot analysis of HSP60 in GST-pull down was performed to locate the domain of CLU responsible for the interaction with HSP60.

LA-N-1 cells were lysed by RIPA buffer, pulled down with the GST-fusion proteins; lysates were run on a 10% polyacrylamide and probed with anti-HSP60 antibody to check the endogenous level of HSP60. LA-N-1 expressed a high level of HSP60 endogenously with the size of ~ 60kDa (Figure 4.5. *lane 5*).

GST alone shows no interaction with HSP60 (Figure 4.5. *lane 1*). We observed that CLU full length and alpha chain were more efficient than the beta chain in binding to HSP60 (Figure 4.5. compare *lanes 2* and *3* to *lane 4*), confirming that the alpha chain of CLU is the major interacting domain.

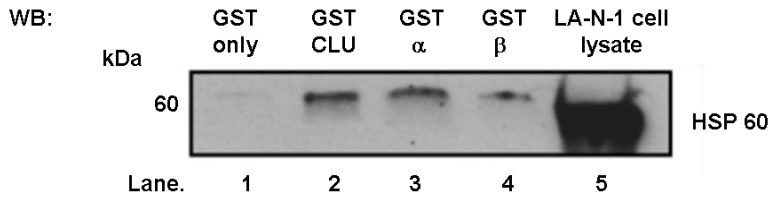

Figure 4.5. HSP60 expressions in the pull down lysates of CLU

Western blot analysis of endogenous Heat Shock Protein 60 (HSP60) expression in LA-N-1 cells (*lane 5*) and GST pull down with LA-N-1 cell lysate (GST-CLU, GST-α and GST-β, *lanes 2-4* respectively). Position of the human 60-kDa heat shock protein (HSP60) is shown.

4.8. Co-immunoprecipitation of CLU and HSP60 *in vivo*

Previous findings of a possible interaction between CLU and HSP60 have led to a further investigation to identify whether this interaction occurs *in vivo*. To check this, pcDNA3 empty or pcDNA3-CLU was transiently transfected into 293FT cells. Cell lysates were collected and immunoprecipitated with anti-HSP60 or anti-CLU antibodies. Western blot analysis was carried out and the membrane was probed against anti-HSP60 antibody.

CLU and HSP60 showed interaction *in vivo* (Figure 4.6. *lane 8*). No binding between CLU and HSP60 was detected in the pcDNA3 empty transfected cells (Figure 4.6. *lane 3*). Goat (Figure 4.6. *lanes 2* and *7*) and Rabbit (Figure 4.6. *lanes 4* and *9*) IgGs were used as negative controls. Minimal bindings between HSP60 and the rabbit IgG control antibody were also observed (Figure 4.6. *lanes 4* and *9*). However, the interaction between CLU and HSP60 showed a much stronger signal, therefore, we believed that the interaction between CLU and HSP60 also occurs *in vivo*.

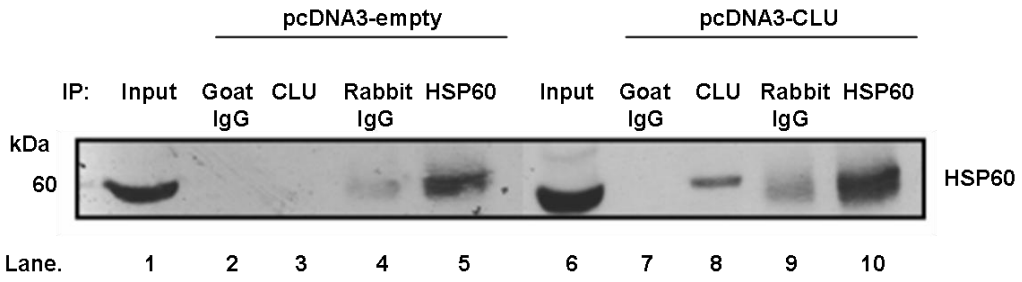

Figure 4.6. CLU interacts with HSP60 *in vivo*

The 293FT cells were transiently transfected with empty pcDNA3 or pcDNA3-CLU for 24 hours before cell lysates were immunoprecipitated with anti-CLU (*lanes 3* and *8*), anti-HSP60 (*lanes 5* and *10*) antibodies or goat (*lanes 2* and *7*) and rabbit (*lanes 4* and *9*) IgG controls. Lanes 1 and 6 indicate input proteins where no co-immunoprecipitation was carried out. The immunoprecipitated samples were run on a 10% SDS polyacrylamide gel and were subjected to western blot analysis with anti-HSP60 antibody. Position of the human 60-kDa heat shock protein (HSP60) is shown.

4.9. A complex containing endogenous CLU and HSP60 is detected in neuroblastoma cells

We wanted to verify that endogenous CLU and HSP60 interacted in neuroblastoma cells *in vivo*. In neuroblastoma cells, CLU level is low making it difficult to carry out immunoprecipitation experiments with endogenous proteins.

Caccamo et al (2006) demonstrated that sub-lethal heat shock could inhibit the secretion of CLU (sCLU) and lead to increased cytoplasmic accumulation of CLU (pCLU) in a prostate cancer cell line PNT1A. Therefore, a sub-lethal heat shock treatment was carried out in LA-N-1 and SHSY-5Y cells as described in section 2.2.9.1. To evaluate the pCLU level in these cells, cells were incubated at the indicated temperature in a water bath (Figure 4.7.A and B). After shock, the cells were kept in the humidified incubator at 37^{o}C and 5% CO_2 as indicated (0, 3, 6, 9, 24 and 48 hours) for recovery and expression of endogenous expression of CLU and HSP60 was analyzed by western blot.

Representative western blot analyses of LA-N-1 and SHSY-5Y cells that had undergone sub-lethal heatshock are shown (Figure 4.7.A and B). For both cell lines, the endogenous level of CLU was relatively low at 37^{o}C (*lane 1*), as expected. However, when cells underwent a sub-lethal heat shock at 43^{o}C, CLU (pCLU) was dramatically increased and peaked within 3 hours (*lane 3*) and remained high up to 9 hours (*lane 5*) after the heat shock treatment in both cell lines, before gradually decreasing after 24 hours (*lane 6*). HSP60 expression was high in both cell lines and the heatshock treatment did not seem to induce its expression. To obtain optimal levels of both precursor CLU and HSP60, LA-N-1 cells were selected and co-immunoprecipiation was carried out after a sub-lethal heat shock at 43^{o}C for 30 minutes followed by a 3 hours recovery period at 37^{o}C. A representative western blot analysis of the interaction between precursor CLU and HSP60 in LA-N-1 cells is shown in figure 4.8, where A and B show the same blot. Lane 1 shows the input protein and the interaction between precursor (pCLU) and HSP60 is visible in lanes 3 and 5. Goat (Figure 4.8. *lane 2*) and Rabbit (Figure 4.8. *lane 4*) IgGs were used as negative controls. Minimal bindings between CLU and the goat IgG control antibody were also observed (Figure 4.8.B *lane 2*).

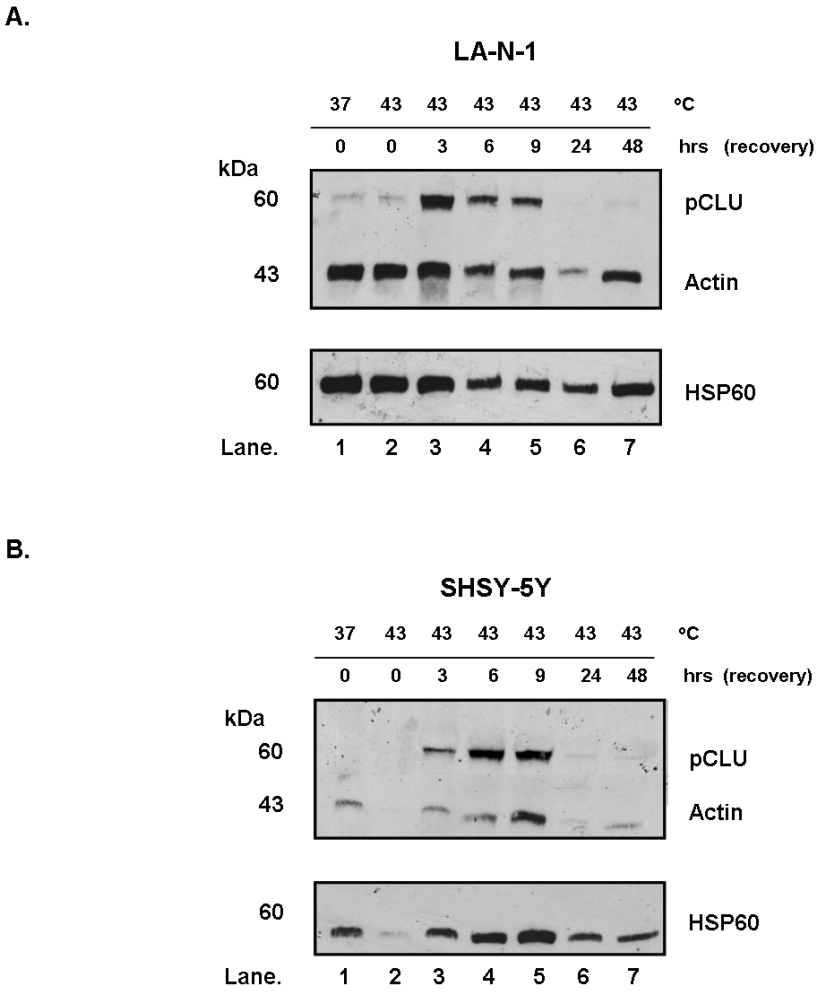

Figure 4.7. Sub-lethal heat shock can induce endogenous CLU expression

A) LA-N-1 and **B)** SHSY-5Y cells were treated with indicated temperature (^{o}C) for 30 minutes and were left to recover (recovery) in the 37^{o}C incubator as indicated.

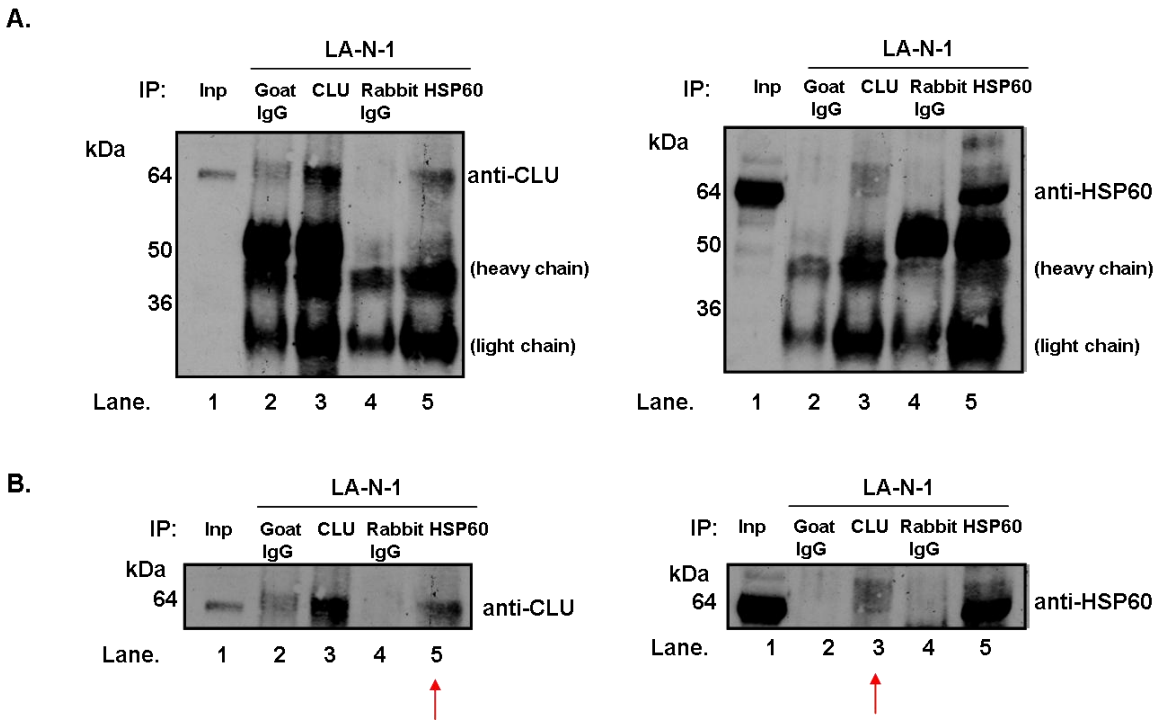

Figure 4.8. Endogenous CLU and HSP60 interact directly *in vivo* in LA-N-1 cells

Co-immunoprecipitation of intracellular CLU and HSP60 **A)** The whole membrane is shown to illustrate that only the intracellular form of CLU is interacting with HSP60. Heavy and light immunoglobulin chains (non-specific bindings) are shown in brackets. **B)** A focused section of the same membrane showing co-immunoprecipitation of heat-shocked LA-N-1 cells with CLU, HSP60 and control antibodies. The native CLU/HSP60 complex is indicated by the arrows. Inp = input.

4.10. Discussion

CLU is a sulphated glycoprotein, which is known to interact with various other proteins important in biological functions. For example, its direct interaction with SCLIP (SCG10-liked protein) promotes neurite outgrowth of PC12 cells and its direct interaction with Bax promotes cell survival (Kang *et al*., 2005, Zhang *et al*., 2005). Essabbani et al (2010) reported that the CLU interacts directly with phosphorylated-IκBα and decreases the translocation of p50/p65 to the nucleus. Moreover, Santilli et al (2003) showed that CLU is involved in the regulation of NF-κB activity in neuroblastoma cells. In this study, CLU was proposed to enhance the stability of the NF-κB inhibitors (IκBs) by inhibiting IκBs proteasomal degradation. Moreover, the same study also demonstrated that activated NF-κB resulted in increased invasion of human neuroblastoma cell lines. Given the hypothesis that CLU could behave as a tumour suppressor gene in neuroblastoma by suppressing NF-κB, the experiments in this chapter were aimed at identifying the protein region that pCLU utilises in the control of NF-κB activity and identification of novel CLU-interacting proteins that may play a role in NF-κB activation.

Luciferase assays showed that the region near the N-terminus of precursor CLU (i.e. the α chain only vector) caused a significant decrease in the NF-κB activity (Figure 4.1.C) while the beta chain region of CLU did not alter the NF-κB activity. The full length CLU caused less reduction in the NF-κB activity than the α chain only may possibly be due to the conformational change of the α chain in the full length CLU.

By mass-spectrometry analysis (Figure 4.4.), we identified a CLU-interacting protein of approximately 60 kDa in size, Heat shock protein 60 (HSP60). Human heat shock protein 60 (CPN60, GROEL, HSP60, HSP65, HuCHA60 or SPG13) is encoded by a gene *HSPD1*, which is localized on chromosome 2q33.1 (Hansen *et al*., 2003). Although HSP60 is a mitochondrial chaperone, in recent years, it has become clear that HSP60 also occurs in the cytosol (Chandra *et al*., 2007), the cell surface of normal and cancer cells (Soltys and Gupta, 1997, Piselli *et al*., 2000), the extracellular space (Gupta and Knowlton, 2007) and in the peripheral blood (Shamaei-Tousi *et al*., 2007).

Eventhough we set out to evaluate potential intracellular CLU-binding proteins in neuroblastoma and that the interaction between intracellular CLU and HSP60 has been identified, it cannot be concluded whether this interaction occurs inside or outside the mitochondria and further investigation is warranted.

HSP60 plays a role in correcting protein folding (Hartl, 1996) and in carcinogenesis, specifically tumour cell survival and proliferation (Ghosh *et al*., 2008, Di Felice *et al*., 2005, Tsai *et al*., 2008). It is also known that HSP60 can interfere with Bax-dependent apoptosis (Ghosh *et al*., 2008). Elevated levels of this protein in tumour cells have been linked to cell survival, loss of replicative senescence, uncontrolled proliferation and neoplastic transformation (Ghosh *et al*., 2008, Di Felice *et al*., 2005, Tsai *et al*., 2008)

Therefore, it is not surprising that HSP60 is overexpressed in neuroblastoma, since other groups have reported increased expression of HSP60 in other types of human cancers, such as ovarian cancer, pancreatic cancer, large bowel carcinoma (Schneider *et al*., 1999, Piselli *et al*., 2000, Cappello *et al*., 2005).

CHAPTER 5

The roles of HSP60 and CLU in neuroblastoma

5.1. Introduction

Heat shock proteins (HSPs) are ubiquitous and evolutionary conserved proteins (Czarnecka *et al*., 2006). Their fundamental role in cellular homeostasis and cell viability was discovered in 1962 when F. Ritossa exposed *Drosophila* to 37°C for 30 minutes and proteins of 70 and 26 kDa were highly expressed, suggesting they are indispensable to overcome heat-induced stress (Ritossa 1962, Ritossa, 1996). HSPs are functionally related stress proteins, which are classified into families according to molecular weight. In most organisms, stress proteins are represented by families of HSP100, HSP90, HSP70, HSP60 and small HSPs (e.g. HSP27, HSP10), with several members in each class. Proteins are affiliated to these diverse groups of molecular chaperones by their capacity to recognize and bind substrate proteins that are in an unstable or inactive state (Bukau and Horwich, 1998).

Heat shock proteins (HSPs) have a role in carcinogenesis. Molecular chaperones may promote cell survival, but how this process is regulated, particularly in cancer, is not well understood. Increased expression of HSP60 is observed in many types of human cancers including cervical, ovarian, breast, pancreatic, colon, lung, prostate and brain (Hwang *et al*., 2009, Ghosh *et al*., 2008, Ghosh *et al*., 2010, Schneider *et al*., 1999, Piselli *et al*., 2000 and Cappello *et al*., 2005).

Tsai et al (2008) demonstrated that MycC directly activated HSP60 transcription through an E-box (CACGTG) site located in the proximal promoter of the HSP60 gene (*HSPD1*) and that MycC induced overexpression of HSP60 resulted in transformation. Therefore, MycC could induce transformation by expression of HSP60.

Many groups have also shown that HSP60 is involved in tumour cell apoptosis. Ghosh et al (2008) demonstrated that acute ablation of HSP60 by siRNA destabilized the mitochondrial pool of survivin (an apoptosis inhibitor) in the breast adenocarcinoma cell line MCF7 and colon adenocarcinoma cell line HCT116. This response appeared to involve the disruption of an HSP60-p53 complex, which resulted in p53 stabilization, increased expression of pro-apoptotic Bax, and Bax-dependent apoptosis. HSP60 is

abundantly expressed in primary human tumours (breast, colon and lung), whereas it is marginally expressed by normal tissues, and siRNA ablation of HSP60 in normal cells is well tolerated without causing apoptosis. Elevated HSP60 is thought to be selected by cancer cells to achieve survival advantage over normal cells (Ghosh *et al*., 2008).

Ghosh et al (2010) also demonstrated that HSP60 formed a multi-chaperone complex with cyclophillin D (CypD), a component of the mitochondrial permeability transition pore, HSP90 and tumour necrosis-factor receptor-associated protein-1 (TRAP-1), which selectively assembled in tumour but not in normal mitochondria. Targeting HSP60 by siRNA triggered CypD-dependent mitochondrial permeability transition, caspase-dependent apoptosis and suppression of intracranial glioblastoma growth *in vivo*.

In this chapter, the role of HSP60 in neuroblastoma is verified and discussed. Experiments were designed to see whether HSP60 is involved in determining neuroblastoma cell survival and whether clusterin (CLU) is involved in the mechanism.

5.2. Reduced expression of endogenous HSP60 decreased SHSY-5Y cell proliferation and increased cell death

To investigate the functional role of HSP60 in neuroblastoma, SHSY-5Y cells were transduced with lentivirus containing a control shRNA (sh-Scramble) or shRNA targeting endogenous HSP60 (sh-HSP60) and western blot analysis was carried out to determine the knockdown efficiency of each clone. We were unable to obtain stable clones of sh-Scramble or sh-HSP60 in LA-N-1 cells because these cells often had low transduction efficiency. Therefore, the experiments were carried out in easily transduced SHSY-5Y and HNB cells.

Six SHSY-5Y stable clones (clones 1-6) were generated from a single transduction with either control shRNA (sh-Scramble) or shRNA targeting endogenous HSP60 (sh-HSP60) and each scramble clone was randomly paired to the sh-HSP60 clone (Figure 5.1.). Both shRNA-scramble and shRNA-HSP60 expressed GFP, therefore, cell proliferation was monitored using fluorescent microscopy to exclude non-transduced cells. Clone 1 and 2 showed the best knockdown of endogenous HSP60 (50% and 40% respectively), whereas clone 4, 5, 6 and 3 showed less efficient suppression of HSP60. Thus, clone 1-3 were chosen for further experiments.

Three independent clones of SHSY-5Y transduced with control shRNA (non-targeting shRNA, sh-Scramble), grew and filled the entire surface of the 60mm tissue culture dishes (Figure 5.2. A). In comparison, three independent SHSY-5Y clones transduced with shRNA targeting HSP60 (Clones 1, 2 and 3) showed a significantly decreased cell proliferation after 6 days in culture (Figure 5.2.B.). The total cell number was quantified (Figure 5.2.C) and results showed that all three independent clones showed approximately three-fold decrease in cell number after HSP60 knockdown when compared to controls (P=0.03, P=0.02 and P=0.05 respectively).

To verify whether the decreased number of cells is due to increased cell death (apoptosis), we carried out Annexin-V staining for quantification of cell death (see section 2.2.10.2).

Our preliminary data of the flow cytometry analysis of 3 independent clones of SHSY5Y cells expressing normal (sh-Scramble) or knockdown HSP60 (sh-HSP60) showed increased percentage of late apoptotic cells (highlighted on the top right quadrant of each graph, *bottom panel*) (23.6% 22.6% and 15.6% for clones 1, 2 and 3 with targeted HSP60 respectively). Clones with scramble shRNA appeared to have less cell death (highlighted on the top right quadrant of each graph, *top panel*) (17.5%, 16.8% and 8.1% for clones 1, 2 and 3 respectively) (Figure 5.3.A and C). However, there were some limitations to the experiments, which should be mentioned. The control cells (scramble) had very high level of basal cell death (only 30-60% viable cells in PI negative, Annexin-V negative quadrant). This could affect the interpretation of the data and a conclusion cannot be drawn on this preliminary findings.

Doxorubicin (tradename Adriamycin, also known as hydroxydaunorubicin) is one of the chemotherapeutic drugs used in treatments of neuroblastoma. It is an intercalating agent that unwinds and changes DNA structure to prevent the DNA from repairing itself. Doxorubicin prevents progression of topoisomerase II enzyme, which relaxes DNA supercoil for transcription, and subsequently inhibits DNA replication (Fornari *et al*., 1994). In order to test the hypothesis that knockdown of HSP60 may cause neuroblastoma cells to become more sensitive to the chemotherapeutic drug, SHSY-5Y clones (sh-Scramble or sh-HSP60) were treated with doxorubicin (0.5μg/ml) for 24

hours before being subjected to Annexin-V staining for quantification of cell death (see section 2.2.10.2). Cervellera et al (2000) demonstrated that 0.5μg/ml doxorubicin was able to kill neuroblastoma cells, therefore, we have selected this concentration to induce neuroblastoma cell death in our experiment.

The preliminary results of flow cytometry also showed that neuroblastoma cells are sensitive to doxorubicin killing. Clones 1, 2 and 3 expressing normal level of HSP60 showed percentage of cells in late apoptosis (highlighted on the top right quadrant of each graph, *top panel*) (20.5%, 25.5% and 23.5% respectively). After doxorubicin treatment, the corresponding clones with knockdown HSP60 expression appeared to have higher percentages of late apoptotic/necrotic (highlighted on the top right quadrant of each graph, *bottom panel*) (44.6%, 40.4% and 27.7% respectively) (Figure 5.3.B and C).

However, we could not conclude at this point that loss of HSP60 expression increased neuroblastoma cell death using Annexin-V staining or that the sensitivity of doxorubicin-induced neuroblastoma cell death is achieved through loss of HSP60 because the experiment has only been carried out once and the knockdown efficiency in shHSP60 was low. Moreover, Annexin-V staining is known to give false positive results, hence the low numbers of live cells (bottom left quadrant) in each clone at the start of the assay. Therefore, further experiment is warranted to give a more conclusive result.

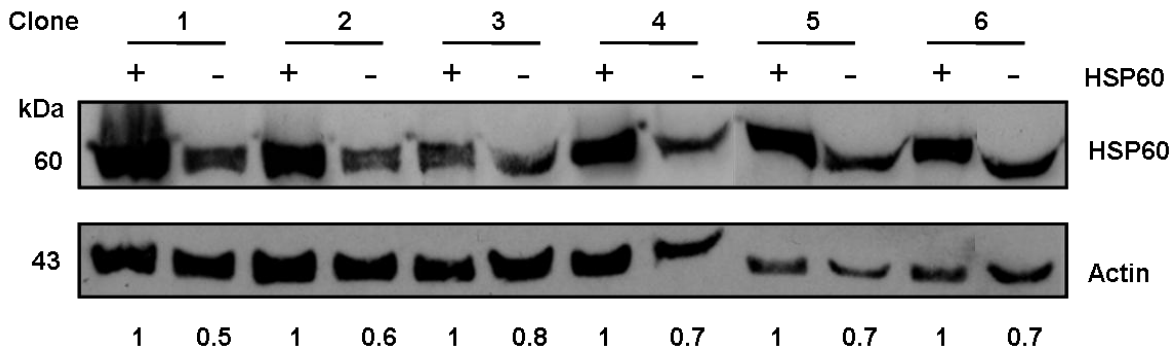

Figure 5.1. Endogenous expression of HSP60 in response to shRNAs knockdown

Western Blot analysis of endogenous HSP60 expression in SHSY-5Y cells where cells were transduced with sh-scramble and sh-HSP60 (+ and – HSP60 respectively) and undergo clonal selection and expansion with 1μg/ml puromycin for 10 days. Overall, twelve independent clones, which derived from a single transduction were selected (six clones contained the sh-scramble and six clones contained the sh-HSP60). Protein bands of six clones were quantified with Quantity One software and the expression ratios are indicated below.

Figure 5.2. Reduced expression of endogenous HSP60 decreased SHSY-5Y cell proliferation

Analysis of SHSY-5Y cells proliferation after transduction with **A)** sh-Scramble and **B)** sh-HSP60 expressing GFP (*Top* and *Bottom panel* respectively). After clonal selection with 1μg/ml puromycin for 10 days, each clone was seeded at $1x10^5$ cells per 60 mm dish (day 0). Cells were allowed to grow until confluency is reached (day 6) and viewed under fluorescent microscope to exclude non-transduced cells. **C)** Quantification of live cell analysis performed in triplicates by trypan blue cell exclusion assay. Data are expressed as relative mean values ±SD of 3 independent experiments. Statistical significance was assessed by student-t-test. The p-value is indicated for statistical significance.

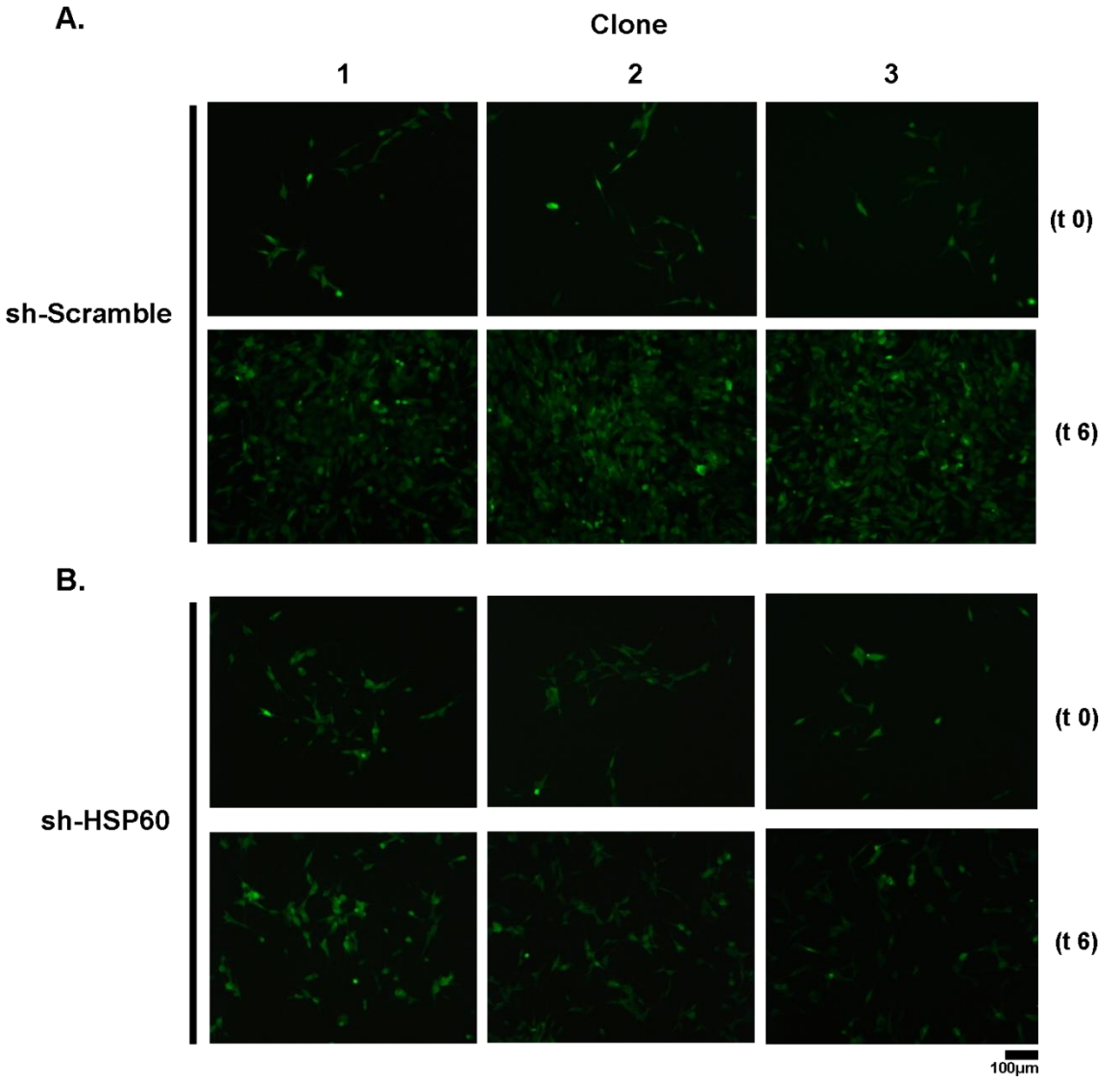
A.
Clone
1
2
3
sh-Scramble
(t 0)
(t 6)
B.
sh-HSP60
(t 0)
(t 6)
100µm

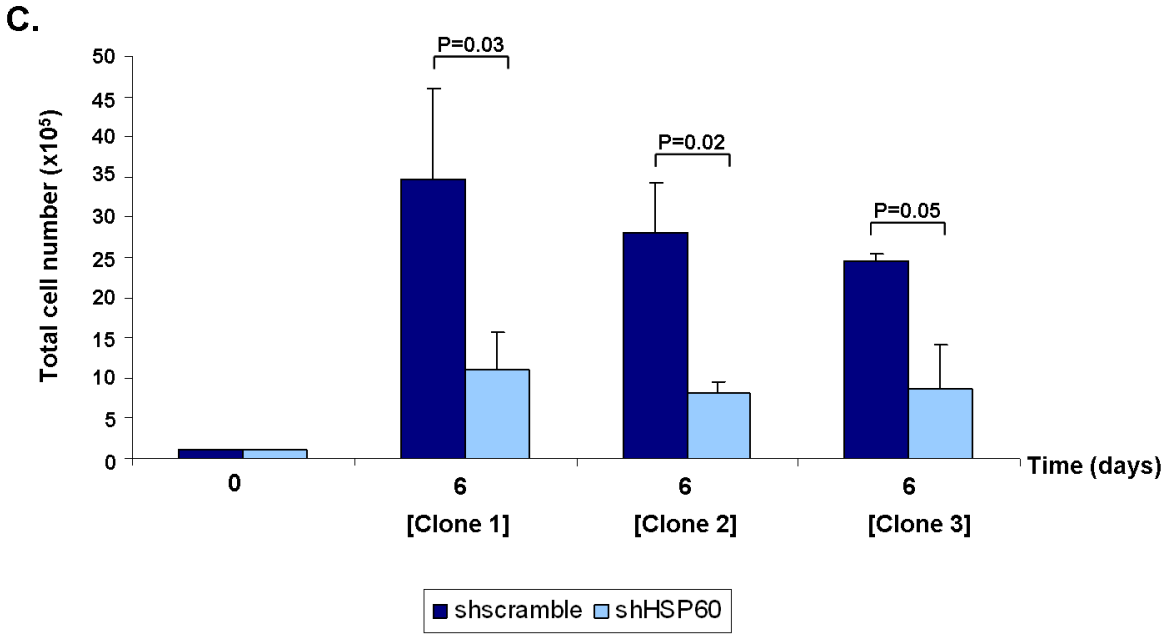
C.
Total cell number (x10⁵)
50
45
40
35
30
25
20
15
10
5
0
P=0.03
P=0.02
P=0.05
0
6
6
6
[Clone 1]
[Clone 2]
[Clone 3]
Time (days)
shscramble
shHSP60

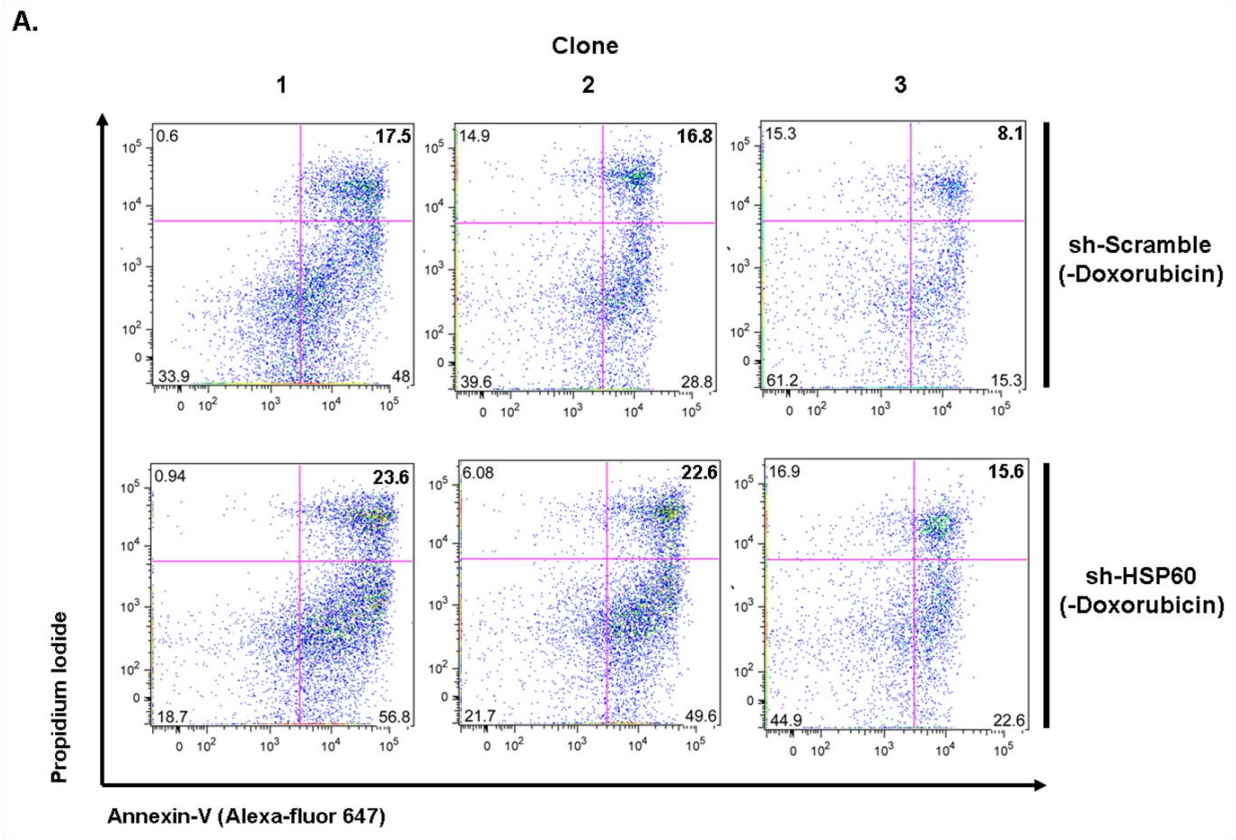
A.
Clone
1
2
3
0.6
17.5
33.9
48
14.9
16.8
39.6
28.8
15.3
8.1
61.2
15.3
sh-Scramble
(-Doxorubicin)
0.94
23.6
18.7
56.8
6.08
22.6
21.7
49.6
16.9
15.6
44.9
22.6
sh-HSP60
(-Doxorubicin)
Propidium Iodide
Annexin-V (Alexa-fluor 647)

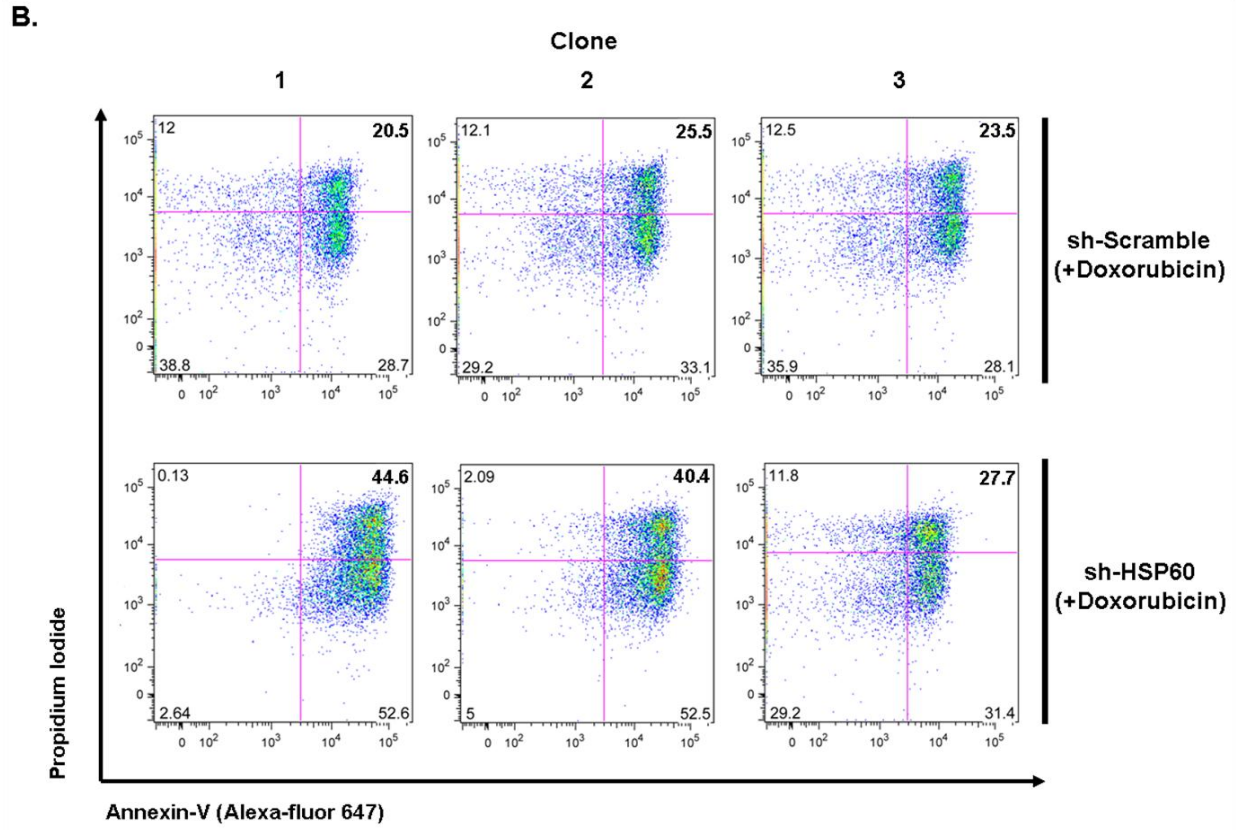
B.
Clone
1
2
3
12
20.5
38.8
28.7
12.1
25.5
29.2
33.1
12.5
23.5
35.9
28.1
sh-Scramble
(+Doxorubicin)
0.13
44.6
2.64
52.6
2.09
40.4
5
52.5
11.8
27.7
29.2
31.4
sh-HSP60
(+Doxorubicin)
Propidium Iodide
Annexin-V (Alexa-fluor 647)

C.

	Percentage (%) of apoptotic cells		
Clone	**Sh-scramble**	**Sh-HSP60**	**Doxrorubicin treatment**
1	17.5	23.6	No
2	16.8	22.6	No
3	8.1	15.6	No
1	20.5	44.6	Yes
2	25.5	40.4	Yes
3	23.5	27.7	Yes

Figure 5.3. Reduced expression of endogenous HSP60 increased cell death and sensitivity to doxorubicin-induced death

SHSY-5Y clones, which were transduced with sh-Scramble and sh-HSP60 and selected with 1μg/ml puromycin for 10 days. SHSY-5Y clones were either cultured **A)** without or **B)** with doxorubicin (0.5μg/ml) for 24 hours before stained with Annexin-V conjugate (Alexa-fluor 647). Early apoptotic cells were detected in the Propidium Iodide positive (PI+) and Annexin-V positive (Annexin-V+) quadrant (*Top right*). **C)** A summary table to show the percentage of apoptotic cells in the presence or absence of doxorubicin treatment. The experiment was carried out once.

5.3. Reduced expression of endogenous HSP60 decreased human neuroblastoma (HNB) cell proliferation

A human neuroblastoma cell line (hereafter referred as HNB), was established by our group in 2010. This cell line was derived from a tumour metastasized in the neck of a 3-year old male patient. The tumour originated in the adrenal gland and has *MYCN* amplification. The aim of the next experiment was to verify the role of HSP60 in a primary neuroblastoma tumour.

Representative morphology of the HNB tumour is shown in figure 5.4.A with heterogenousity observed throughout early passages (passages 7-15). Western Blot analysis of HNB cell lysate (taken from passage 10) revealed levels of HSP60 and CLU similar to the neuroblastoma cell lines SHSY-5Y and LA-N-1, with high endogenous level of HSP60 and trace level of CLU expressions (Figure 5.4.B).

Proliferation assay was conducted to determine the effect of HSP60 knockdown on HNB cell proliferation. Non-targeting shRNA (sh-Scramble) did not inhibit cell proliferation as the cells grew to confluency by day 14. However, the targeting of HSP60 in HNB cells significantly reduced cell proliferation and total cell numbers by approximately 3-folds (P=0.005) (Figure 5.5.A and B). A representative western blot analysis shows 60% HSP60 knockdown in HNB cells (Figure 5.5.C). The reasons for reduced growth rate is due to decreased proliferation and increased cell death since the percentage of cells in subG1 increased from 17.4 to 28.9 after HSP60 is knockdown (Figure 5.5.D).

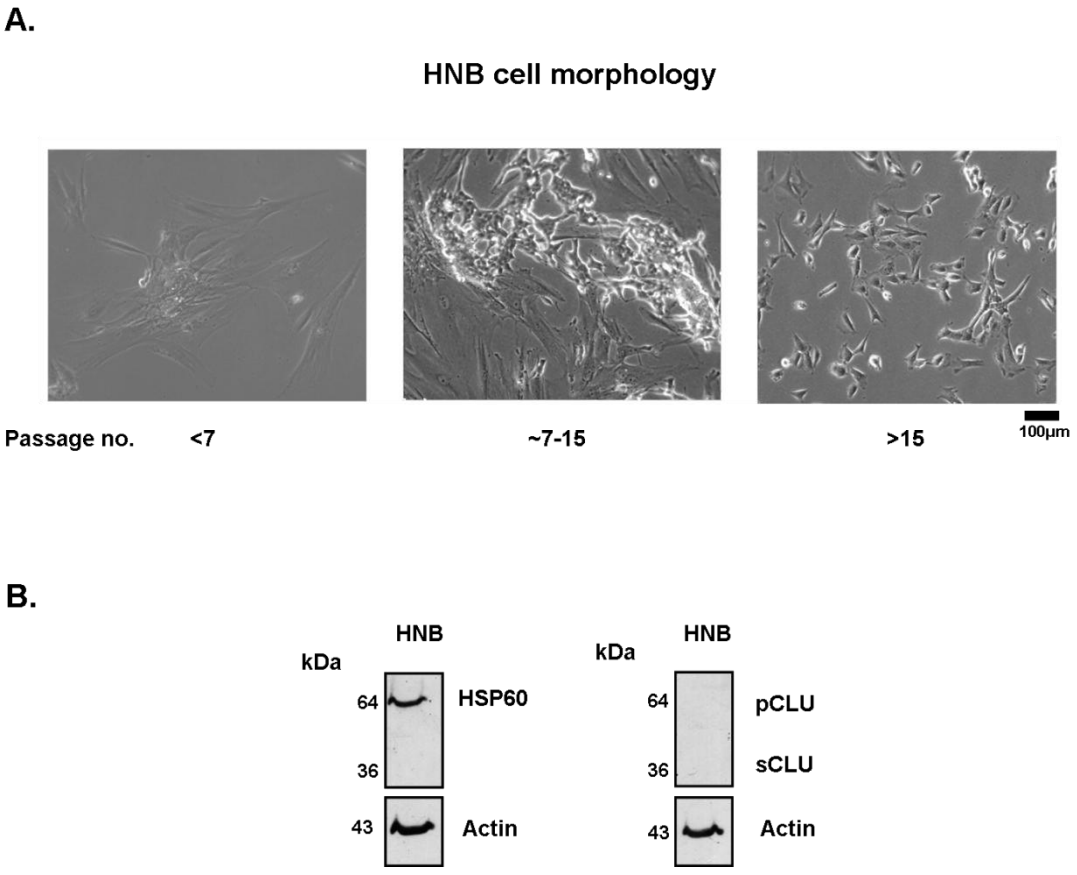

Figure 5.4. Primary human neuroblastoma cells (HNB) showed high level of endogenous HSP60 and low CLU expressions

A) Representative cell morphology of primary human neuroblastoma cells (HNB) throughout cell culture. Scale = 100µm. **B)** Western Blot analysis of endogenous Clusterin expressions (pCLU) and HSP60 in HNB cells (passage 10). Cells were lysed in RIPA and probed with anti-CLU, anti-HSP60 and for control loading (anti-Actin).

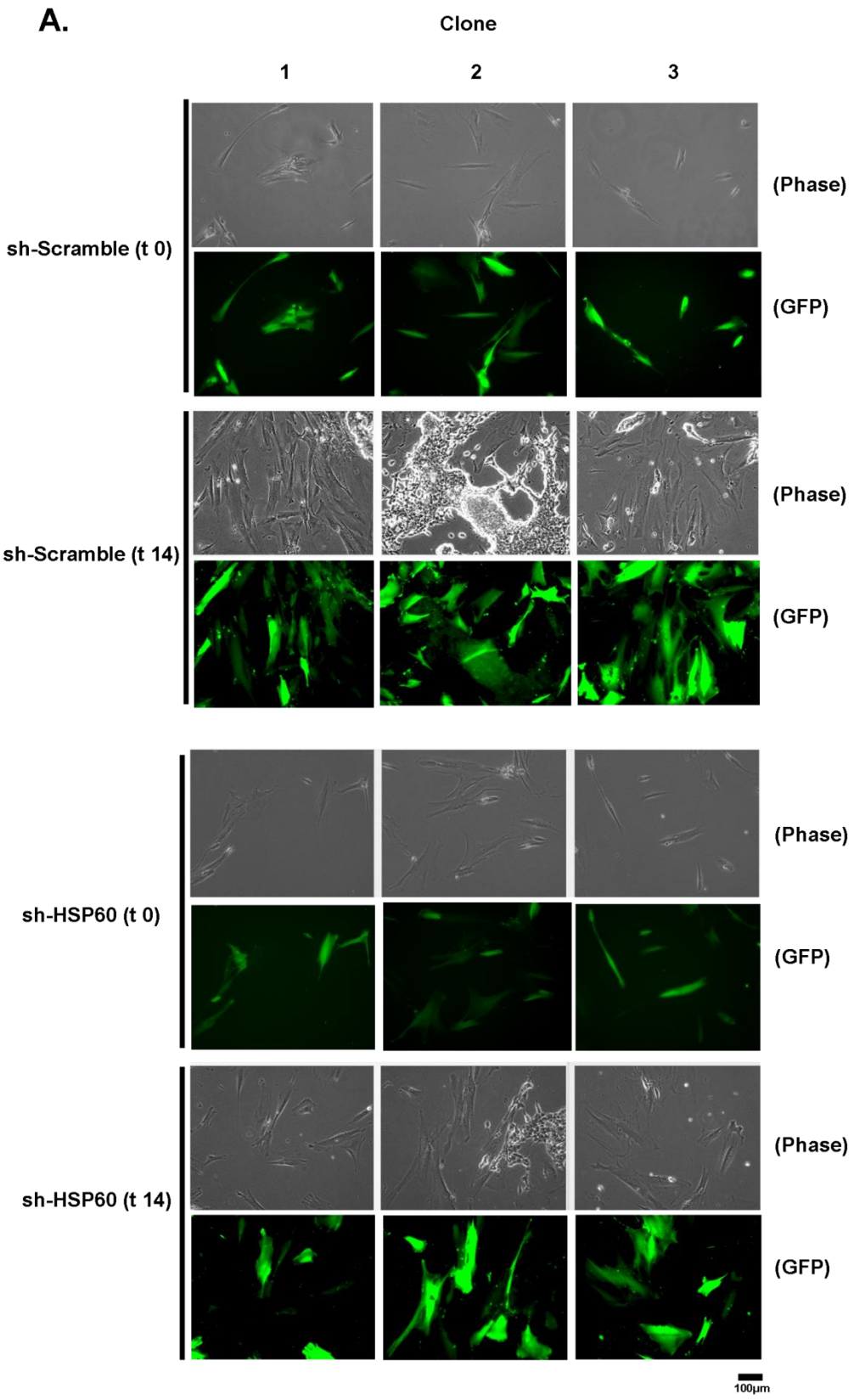
A.
Clone
1
2
3
sh-Scramble (t 0)
(Phase)
(GFP)
sh-Scramble (t 14)
(Phase)
(GFP)
sh-HSP60 (t 0)
(Phase)
(GFP)
sh-HSP60 (t 14)
(Phase)
(GFP)
100μm

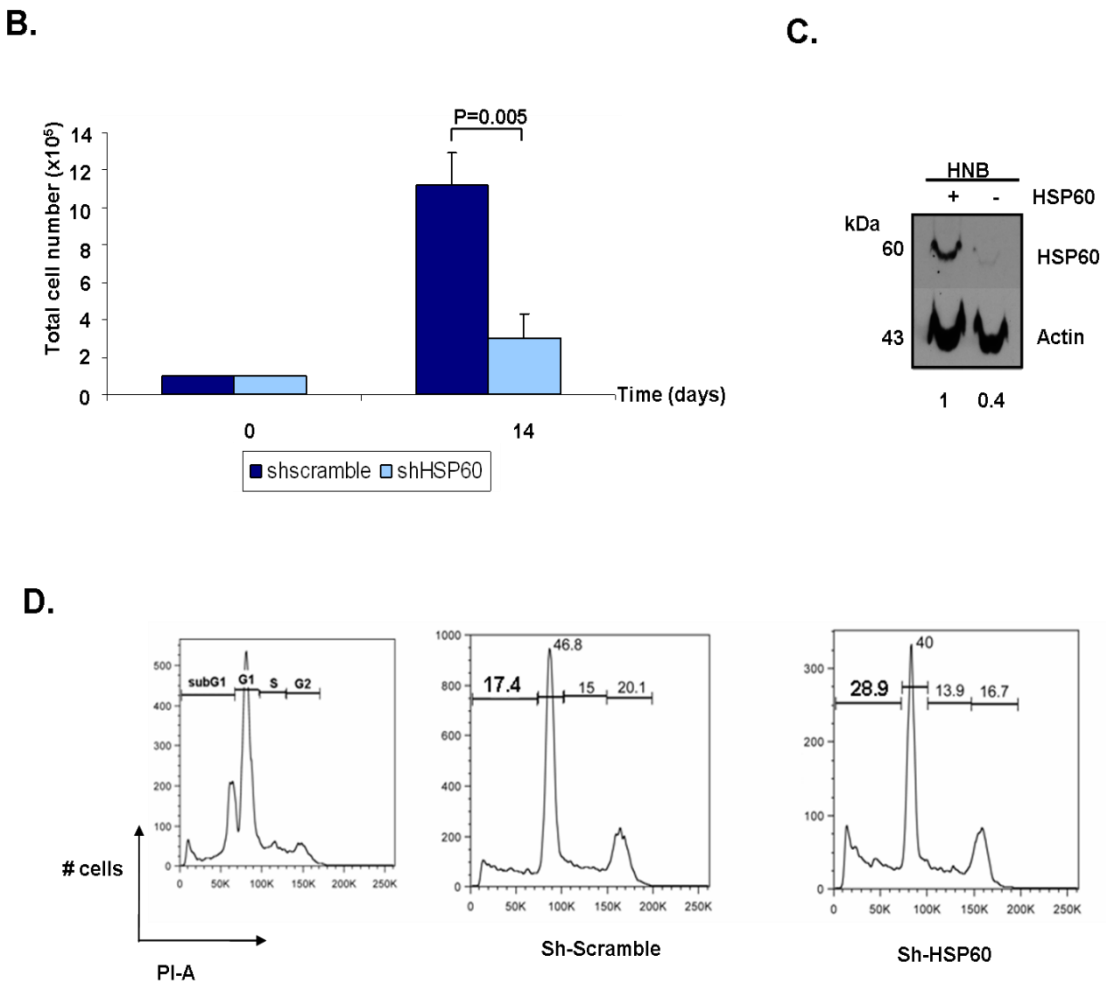

Figure 5.5. Reduced expression of endogenous HSP60 decreased HNB cell proliferation and increased neuroblastoma cell death

A) Analysis of HNB cell proliferation after transduction with sh-Scramble and sh-HSP60 expressing GFP. After clonal selection with 1μg/ml puromycin for 10 days, each clone was seeded at $1x10^5$ cells per 60 mm dish (day 0). Cells were allowed to grow until confluency is reached (day 14) and viewed under fluorescent microscope to exclude non-transduced cells. **B)** Quantification of live cell analysis performed in triplicates by trypan blue cell exclusion assay. The p-value is indicated for statistical significance. **C)** Western Blot analysis of endogenous HSP60 in HNB cells after the knockdown. Cells were lysed in RIPA and probed with anti-HSP60 and for control loading (anti-Actin). **D)** Percentage cell death (SubG1) of HNB after knockdown of HSP60. Cell cycle analysis was carried out by flow cytometry analysis.

5.4. HSP60 acts upstream of CLU

Since expression of CLU is inversely correlated with that of MycN and it marks patients with better probability of survival (Chayka *et al*., 2009), we hypothesised that the physical interaction between CLU and HPS60 could be antagonistic.

To directly address this point, we generated neuroblastoma cell lines with downregulation of HSP60 ($HSP60^{-}CLU^{+}$), CLU ($HSP60^{+}CLU^{-}$) or both HSP60 and CLU ($HSP60^{-}CLU^{-}$) in two independent experiments (Figure 5.7.A-C). The two independent sets of clones (1-3) originally transduced with sh-Scramble (HSP60+, *left panels*) or sh-HSP60 (HSP60-, *right panels*) in figure 5.2.A-C were further transduced with sh-Scramble or sh-CLU. Clones 1, 2 and 3 showed approximately 30%, 50% and 60% HSP60 knockdown expressions respectively (Figure 5.6.A).

If CLU is a downstream target of HSP60, its knockdown should rescue the apoptotic phenotype that follows HSP60 ablation. Percentage of cells in subG1 (DNA fragmentation indicating apoptosis) was measured by propidium iodide staining (Figure 5.7. A and B) and summarized in a bar chart (Figure 5.7.C).

Suppression of CLU ($HSP60^{+}CLU^{-}$) may decrease apoptosis (Figures 5.7.A and B, compare *second column from left* to *first column from left*). In experiment 1, knockdown of CLU ($HSP60^{+}CLU^{-}$) appeared to reduce percentage of apoptotic cells from 20.8%, 24.5% and 28.6% to 8.46%, 20.8% and 12.1% for clone 1, 2 and 3 respectively. In contrast, suppression of HSP60 alone ($HSP60^{-}CLU^{+}$) appeared to increase apoptotic cells (Figure 5.7.A and B, *third column*). In experiment 1, loss of HSP60 ($HSP60^{-}CLU^{+}$) appeared to increase the percentage of late apoptotic cells to 62.9%, 40.4% and 34.4% for clone 1, 2 and 3 respectively. Thus, HSP60 and CLU may cause an antagonistic effect on neuroblastoma cell survival. We observed that DNA fragmentation caused by reduced levels of HSP60 was generally rescued by ablation of CLU (Figure 5.7. A-C, *arrows*).

In experiment 1, ablation of CLU after targeting HSP60 ($HSP60^{-}CLU^{-}$) appeared to reduce the percentage of cells in late apoptosis to 52.8%, 25.1% and 18.7% for clone 1, 2 and 3 respectively (Figures 5.7.A-B, compare the two columns on the *right panels*). We postulated that HSP60 may work upstream of CLU by inhibiting the effect of CLU.

A model for HSP60 mechanism of action is proposed, HSP60 may inhibit the tumour suppressor CLU to promote neuroblastoma survival (Figure 5.8.A). Ablation of CLU alone ($HSP60^{+}CLU^{-}$) may enhance neuroblastoma cell survival (Figure 5.8.B). Loss of HSP60, in the presence of tumour suppressor CLU ($HSP60^{-}CLU^{+}$) may likely to promote neuroblastoma cell death (apoptosis) (Figure 5.8.C). Lastly, loss of tumour suppressor (CLU) may rescue the apoptotic phenotype that follows HSP60 ablation to alleviate neuroblastoma cell death (Figure 5.8.D). In a separate experiment, the same rescue pattern is also observed (Figure 5.7.B and C).

In summary, our preliminary data suggested that DNA fragmentation caused by reduced levels of HSP60 may be rescued by ablation of CLU in SHSY-5Y clones in two independent experiments. We hypothesised that CLU may be a critical downstream target of HSP60 anti-apoptotic activity. However, there were some limitations in replicating our results even though the experiment was carried out twice in three independent clones, it should be noted that the knockdown efficiencies of HSP60 and CLU varied in each clone. Hence, in clone 2 of experiment 2, there was no increased in cell death when HSP60 is ablated and there were very high basal levels of cell death, which could be due to an extended period of selection with puromycin. Morevoer, very low protein knockdown was achieved, particularly in shCLU in experiment 1. Thus, the data in this chapter can not be concluded until further experiments have been carried out with a more consistant knockdown efficiency and startistical significance calculated.

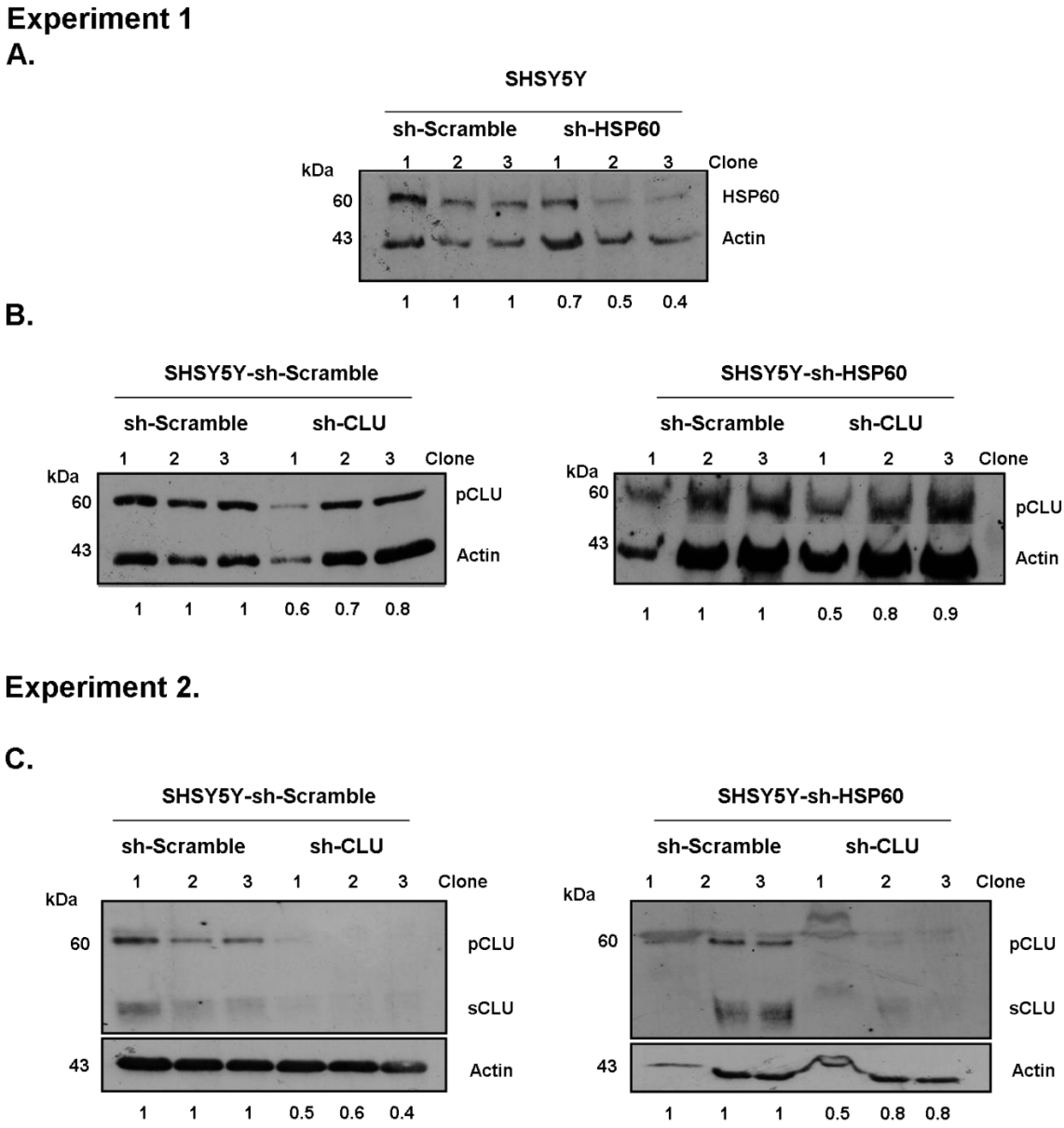

Figure 5.6. Endogenous HSP60 and CLU expressions can be reduced by shRNAs knockdown

A) Western Blot analysis of SHSY-5Y clones with or without HSP60 knockdown. **B)** Second transduction of SHSY-5Y (Scramble or HSP60 knockdown clones) with shRNA-Scramble and -CLU. **C)** Repeat of second transduction of SHSY-5Y (HSP60 knockdown clones) with shRNA-Scramble and -CLU. Cells were lysed in RIPA and protein expressions are quantified against loading control (Actin) as indicated by Quantity One software.

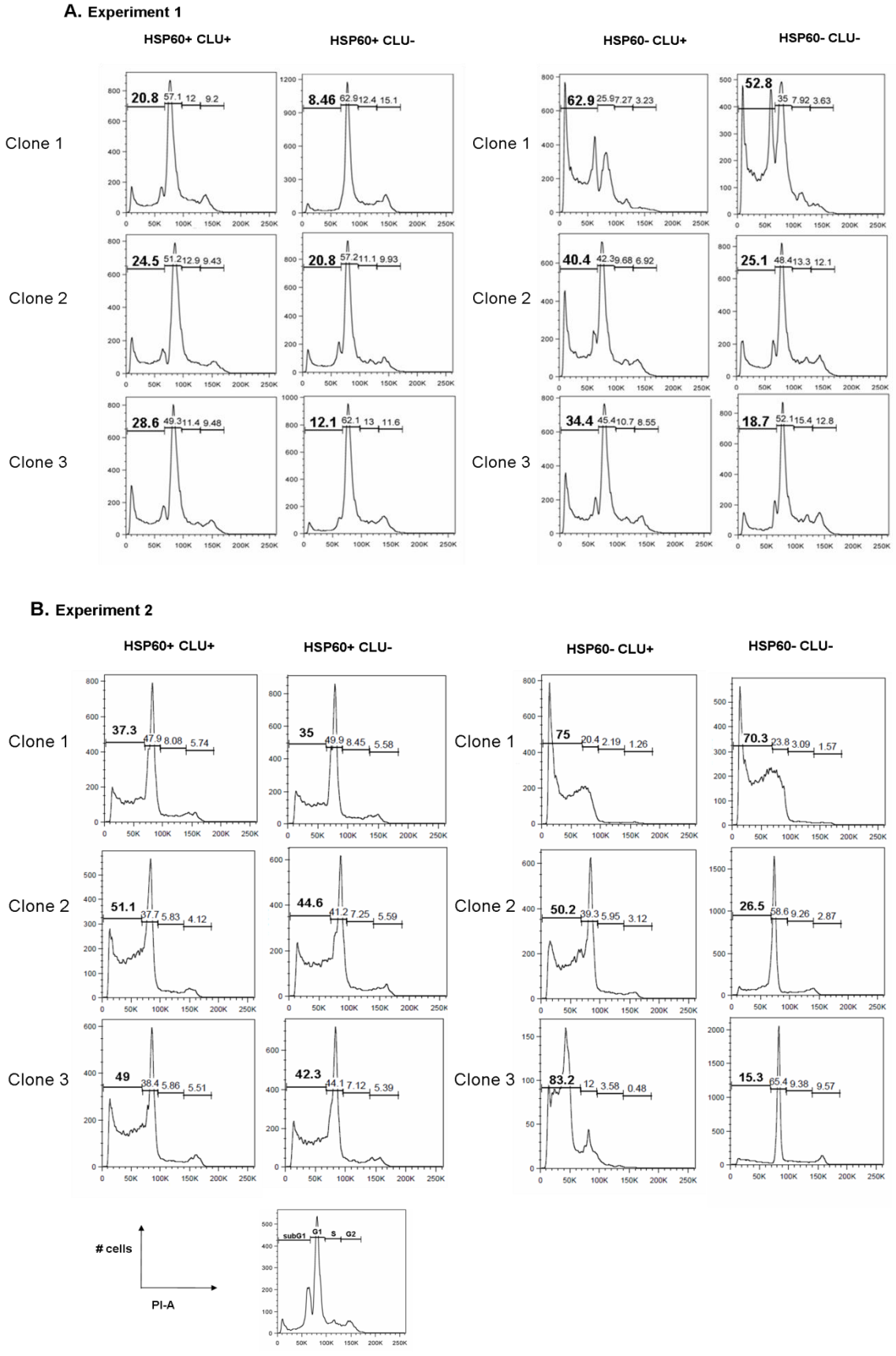
A. Experiment 1
HSP60+ CLU+
HSP60+ CLU-
HSP60- CLU+
HSP60- CLU-
Clone 1
Clone 2
Clone 3
20.8 57.1 12 9.2
8.46 62.9 12.4 15.1
62.9 25.9 7.27 3.23
52.8 35 7.92 3.63
24.5 51.2 12.9 9.43
20.8 57.2 11.1 9.93
40.4 42.3 9.68 6.92
25.1 48.4 13.3 12.1
28.6 49.3 11.4 9.48
12.1 62.1 13 11.6
34.4 45.4 10.7 8.55
18.7 52.1 15.4 12.8
B. Experiment 2
HSP60+ CLU+
HSP60+ CLU-
HSP60- CLU+
HSP60- CLU-
Clone 1
Clone 2
Clone 3
37.3 47.9 8.08 5.74
35 49.9 8.45 5.58
75 20.4 2.19 1.26
70.3 23.8 3.09 1.57
51.1 37.7 5.83 4.12
44.6 41.2 7.25 5.59
50.2 39.3 5.95 3.12
26.5 58.6 9.26 2.87
49 38.4 5.86 5.51
42.3 44.1 7.12 5.39
83.2 12 3.58 0.48
15.3 65.4 9.38 9.57
cells
PI-A
subG1 G1 S G2

C.

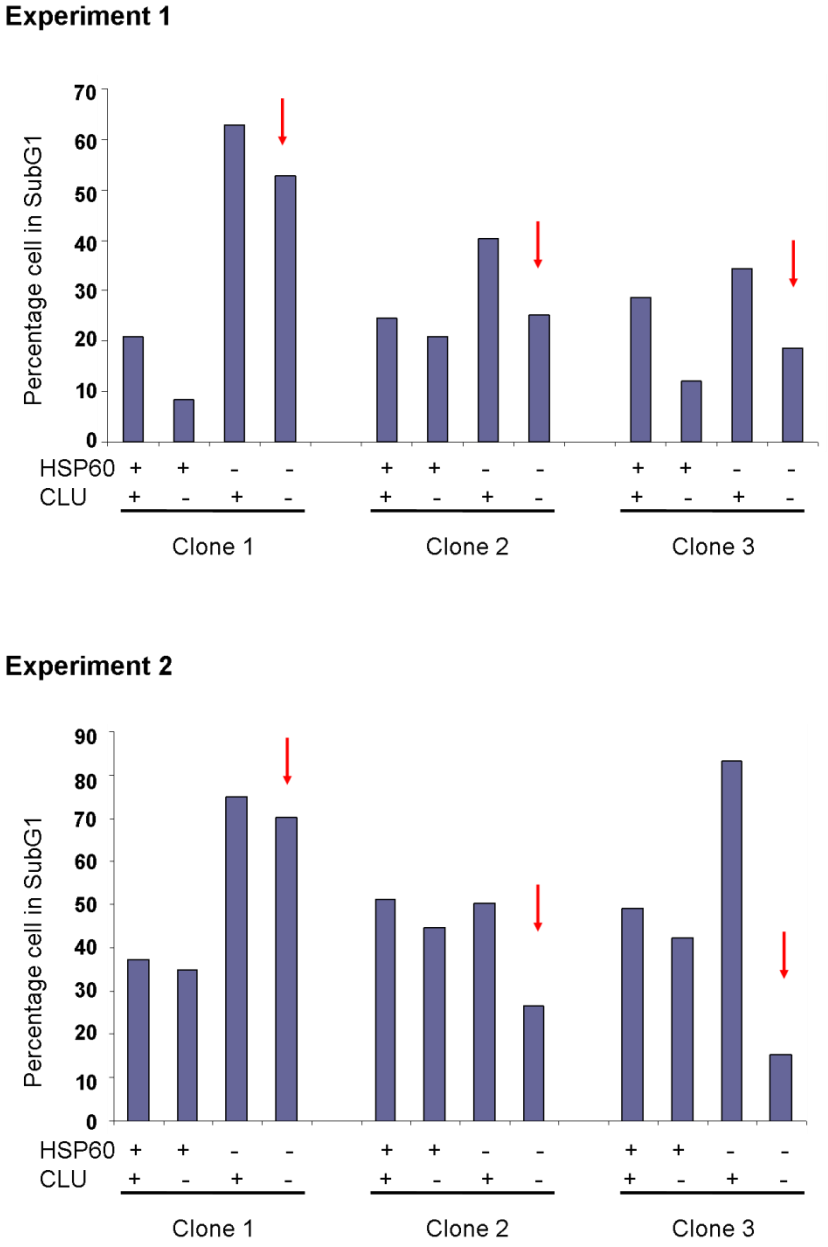

Figure 5.7. HSP60 acts upstream of CLU by promoting neuroblastoma cell survival and reduced expression of CLU can restore cells back to normal cell cycle

Percentage cell death (SubG1) of SHSY-5Y clones after knockdown of HSP60 (-) and/or CLU (-) was carried out by FACS analysis in **A)** Experiment 1 and **B)** Experiment 2. **C)** The percentage of cell in SubG1 was quantified and showed in a bar chart. Rescue of apoptotic phenotype is indicated by arrows. The data were obtained from two independent experiments.

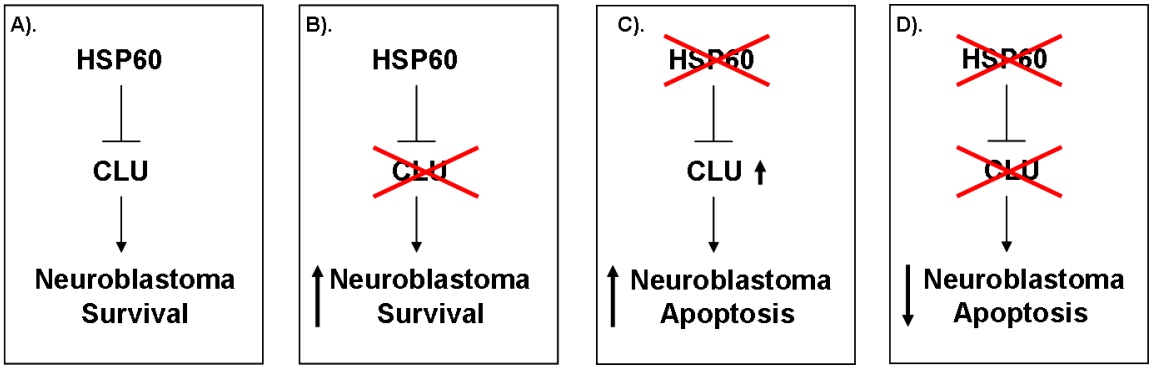

Figure 5.8. HSP60 is upstream of CLU. Proposed model for the mechanism of action of HSP60 in neuroblastoma cell survival

A) High HSP60 expression in neuroblastoma may cause suppression of tumour suppressor CLU, which could favour neuroblastoma cell survival. **B)** Knockdown of CLU may cause HSP60 to exert more effect on neuroblastoma cell survival, resulting in less cell death. **C)** Knockdown of HSP60 may cause unchecked CLU activity, which could increase neuroblastoma cell death. **D)** Knockdown of both HSP60 and CLU is likely to result in rescue of neuroblastoma cell survival.

5.5. Discussion

In this chapter, we attempted to demonstrate that HSP60 is essential for the regulation of neuroblastoma cell survival. Knockdown of HSP60 by shRNAs decreased neuroblastoma cell proliferation and increased cell death both in SHSY-5Y and HNB. This observation was similar to Wadhwa et al (2005) who also reported that suppression of HSP60 expression by shRNA caused the growth arrest of osteosarcoma (U2OS) cells.

Our preliminary data suggested that knockdown of HSP60 by shRNAs appeared to increase the sensitivity of neuroblastoma cells to doxorubicin-induced death (Figure 5.3.). Therefore, HSP60 could act as a tumour promoter, due to its high expression commonly observed in aggressive human tumours compared to normal tissues.

The pathway that HSP60 uses to promote neuroblastoma cell survival has been postulated. HSP60 could inhibit the downstream tumour suppressor protein CLU, as shown in figure 5.8. Knockdown of both HSP60 and CLU may rescue the apoptotic phenotype caused by HSP60 ablation, resulting in decreased neuroblastoma cell death (apoptosis).

Annexin V was not an ideal tool for cell death analysis in adherent cells due to the damage of plasma membrane in an attempt to disaggregate cells to obtain single cell suspension. Therefore, to prevent positive reading, cell death analyses were performed by propidium iodide-staining to provide evidence for loss of plasma membrane integrity subG1 cell count.

Moreover, the use of shRNAs with GFP (pGIPZ) for lentiviral transduction did not give consistent knock down efficiencies of both endogenous HSP60 and CLU expressions (Figure 5.6.). This is because shRNAs targeting HSP60 and CLU were both carrying the same fluorescent marker (GFP) and resistance (puromycin). This has limited the ability to select transduced cells with the maximum knock down efficiency during double transduction experiments. Therefore in future experiments, two different lentiviral vectors carrying different fluorescent markers should be used. PGIPZ-transduced cells should be sorted by FACS analysis with the brightest GFP signal as this represents the amount of shRNA in the cells in order to achieve the maximum knock down clones.

Then in the second transduction, pTRIPZ lentiviral shRNAs can be used to control the knock down efficiency. They are designed for a tightly regulatable RNAi, with a Tet-On ® inducibility and a powerful delivery of shRNAmir to any cell types. The pTRIPZ shRNAmir contained a turbo RFP (red fluorescent protein), which makes it distinguishable from the pGIPZ shRNAs and would allow selection of clones with the maximum HSP60 and CLU knock down expressions. Moreover, the knock down of pTRIPZ-transduced cells can be achieved in a controlled manner after doxycycline addition (see www.openbiosystem.com). It is important to achieve the maximum knock down efficiency as our current data reamained inconclusive due to the various effects seen by inconsistent knockdown expressions of HSP60 and CLU as well as the limitation in replicacting the experiments.

CHAPTER 6

HSP60 is required for NF-κB activity and its high expression predicts poor survival in neuroblastoma patients

6.1. Introduction

Young et al (1987) first demonstrated the link between HSPs and the immune system where microbial HSPs were identified as a common dominant antigen recognized by the immune system of subjects infected with different micro-organisms. Soon after, self-HSPs were found to be targeted by the immune system in response to inflammation (van Eden *et al*., 1988, Anderton *et al*., 1993). Various studies have proposed HSP60 to be a marker for inflammation, autoimmune diseases (Xu *et al*., 2000, Gülden *et al*., 2009, Foteinos *et al*., 2005) and to play an important role in the innate immune system due to its ability to influence the activity of human Tregs (regulatory T cells, $CD4^+CD25^+Foxp3^+$) via TLR-2 signalling (Zanin-Zhorov *et al*., 2006). Moreover, the presence of antibodies to HSP60 in NOD mice identifies those that would later develop autoimmune diabetes (Quintana *et al*., 2004).

HSP60 could play a role in the regulation of NF-κB, a transcription factor involved in the inflammatory immune response (Zanin-Zhorov *et al*., 2005, Chun *et al*., 2010). Some studies suggested that HSP60, which is up-regulated by stress and inflammation, can modulate T-cell mediated inflammation (Zanin-Zhorov *et al*., 2005, Zanin-Zhorov *et al*., 2006). HSP60-treated Tregs suppressed target T cells both via cell-to-cell contact and by secretion of TGFβ and IL-10, which subsequently lead to the inhibition of NF-κB (Zanin-Zhorov *et al*., 2006).

Other studies have shown that HSP60 could be a promoter of tumour cell invasion (metastasis) via the regulation of β-catenin and NF-κB signalling (Piselli *et al*., 2000, Cappello *et al*., 2005).

Tsai et al (2009) demonstrated that overexpression of HSP60 could induce a metastatic phenotype in head and neck cancer model. The same study also showed a direct interaction between HSP60 and β-catenin, where enhanced transcriptional activity of β-catenin and its protein expression is regulated by HSP60. The role of β-catenin includes the regulation of the Wnt signalling pathway and structural components of cell-cell

adherens junctions (Morin, 1999). β-catenin is important for epithelial-to-mesenchymal transition, a process utilized by cancer cells for invasion (Medici *et al*., 2008). Chun and coworkers (2010) demonstrated that cytosolic HSP60 is involved in survival of cancer cells via inhibitor of κB kinase (IKK) regulation, thus, allowing nuclear translocation and activation of NF-κB. NF-κB orchestrates the cell survival response as well as inflammatory immune response and is upregulated in many types of cancers.

HSP60 interacted directly with IKKα/β in the cytosol (Chun *et al*., 2010). The same study showed *in vivo* evidence that cytosolic expression of HSP60 protected hepatic cells against chemical-induced damages via enhancing IKK activation, thus, confirming HSP60's survival function. Moreover, selective loss or blockade of cytosolic HSP60 by antisense oligodeoxynucleotide (AS-ODN) or neutralizing antibody of surface-bound HSP60 resulted in decreased NF-κB transcriptional activities in 293T and A549 cell lines and diminished expression of NF-κB target genes such as MnSOD and Bfl-1/A1 (Chun *et al*., 2010).

In this chapter, we investigated the role of HSP60 in NF-κB regulation in neuroblastoma.

6.2. HSP60 is required for NF-κB activity and its high expression predicts poor survival in neuroblastoma patients

In order to investigate the role of HSP60 in the regulation of NF-κB activity, SHSY-5Y and HNB cells were transduced with non-targeting shRNA (sh-Scramble) and shRNA targeting HSP60 (sh-HSP60). Cells were selected with 1μg/ml puromycin for 10 days before undergoing a transient co-transfection with NF-κB LUC and renilla luciferase reporter constructs, followed by luciferase assays.

Approximately 70% and 50% of HSP60 knockdown was achieved in SHSY-5Y and HNB cell lines respectively. NF-κB activity was also significantly reduced after HSP60 targeting (Figure 6.1.A and B). This suggests that HSP60 promotes NF-κB activity in neuroblastoma cells. Since CLU is a negative regulator of NF-κB, we investigated whether HSP60 could affect expression of CLU, thus indirectly affecting NF-κB activity.

CLU isoforms (pCLU and sCLU) increased by 40% in the presence of reduced level of HSP60 (Figure 6.1.C). This result is consistent with our model of how loss of CLU rescues HSP60 knockdown (Figure 5.8).

To confirm that HSP60 regulation of NF-κB could be important in neuroblastoma, we performed *in silico* analysis of different sets of primary neuroblastoma tumours (available at the oncomine database, www.oncomine.org). Oncomine is a cancer microarray database and web-based data-mining platform where differential expression analyses comparing most types of cancer with respect to the normal tissues or a variety of cancer subtypes could allow clinical-based and pathology-based analyses to become available for exploration. Data can be queried, visualized and calculated for statistical significance from a pool of published literature for a selected gene across all analyses or for multiple genes in a selected analysis. Since genes are usually considered as potential targets or markers if they are highly overexpressed in a particular cancer, the use of oncomine database may provide a platform to explore the expression of all known therapeutic targets in cancer where the user can apply the therapeutic target filter to identify the targets most overexpressed in a particular differential expression analysis (Rhodes *et al*., 2004). The cancer outlier profile analysis (COPA) score identifies gene that displays the most profound expression in a subset of tumours (Rhodes *et al*., 2007).

Upon filtering the database specifically for neuroblastoma tumours using Argharzadeh et al (2006) and Wang et al (2006) studies, high HSP60 expression was observed in neuroblastoma tumours as well as being positively correlated with increased expression of NF-κB target genes such as CCR7, IL-6, IL-8, RELB, NF-κB1A and NF-κB2, IRF4 and IER3 (Pahl, 1999) (Figure 6.2.).

In addition, according to the Oncomine database, the HSP60 gene (*HSPD1*) is highly expressed in *MYCN* amplified neuroblastoma tumours (Figure 6.3.A). Two independent studies (Oberthuer and Seeger) from the Oncogenomics database (http://home.ccr.cancer.gov/oncology/oncogenomics/) also showed that high expression of HSP60 is correlated with poor survival (Figure 6.3.B and C). Therefore, HSP60 is likely to function as a tumour promoter in neuroblastoma by antagonising the effect of tumour suppressor (CLU) and activating NF-κB activity (Figure 6.4.).

Figure 6.1. Knockdown of HSP60 decreases NF-κB activity and induces accumulation of CLU

NF-κB luciferase reporter construct and the renilla luciferase plasmids were transiently transfected into **A)** SHSY-5Y and **B)** Primary human neuroblastoma cells (HNB) cells, which express normal level of HSP60 (+) (sh-Scramble) and cells with HSP60 knockdown (-) (sh-HSP60). Statistical significance was assessed by student-t-test. Data are expressed as relative mean values ±SD of 3 independent experiments, each in triplicates (n =3). The p-value is indicated to show statistical significance. **C)** Western Blot analysis showing increased CLU expression in the primary neuroblastoma cells (HNB) after sh-RNA induced downregulation of HSP60.

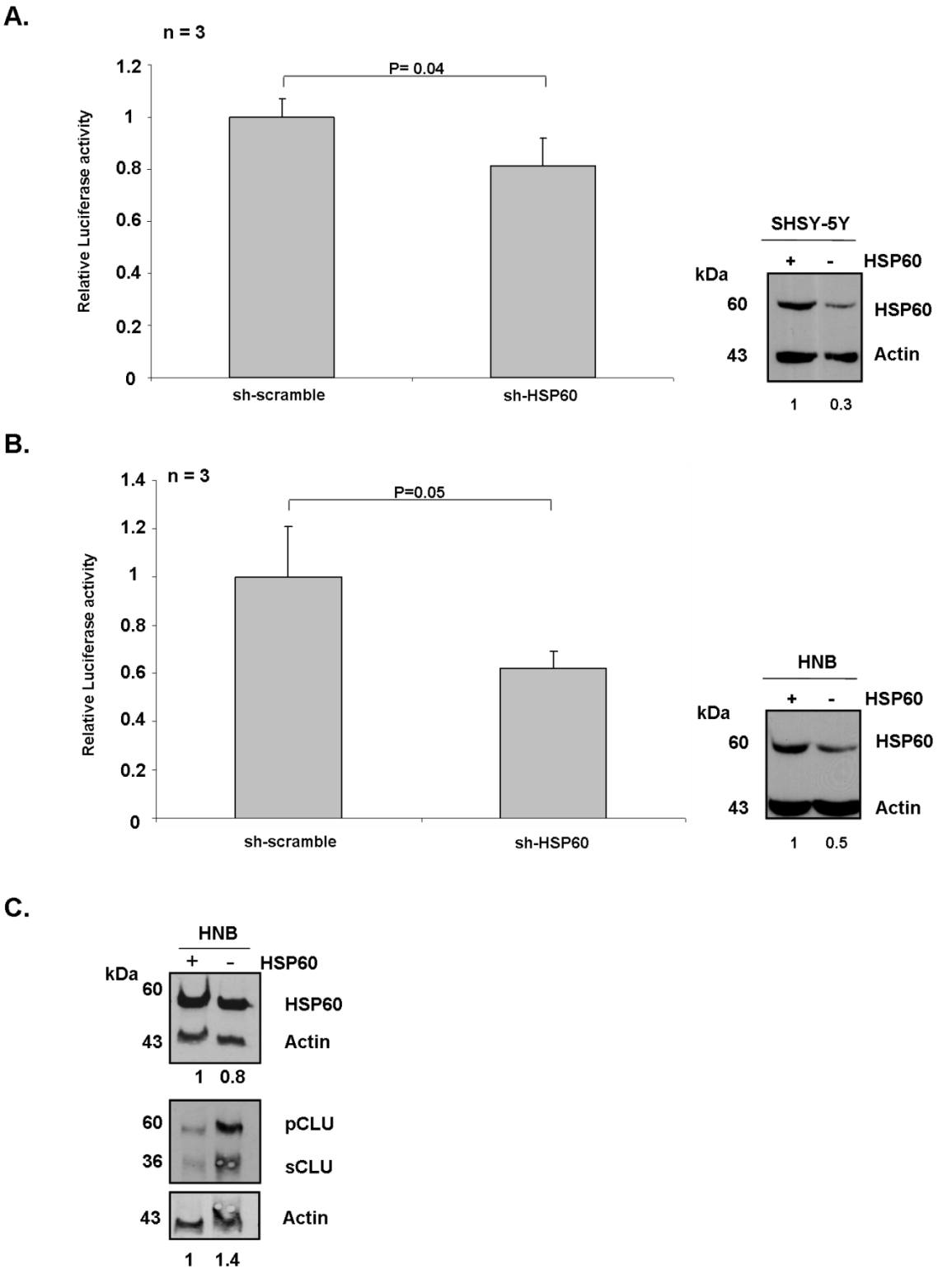
A.
n = 3
P= 0.04
Relative Luciferase activity
1.2
1
0.8
0.6
0.4
0.2
0
sh-scramble
sh-HSP60
SHSY-5Y
+
-
HSP60
kDa
60
HSP60
43
Actin
1
0.3
B.
n = 3
P=0.05
Relative Luciferase activity
1.4
1.2
1
0.8
0.6
0.4
0.2
0
sh-scramble
sh-HSP60
HNB
+
-
HSP60
kDa
60
HSP60
43
Actin
1
0.5
C.
HNB
+
-
HSP60
kDa
60
HSP60
43
Actin
1
0.8
60
pCLU
36
sCLU
43
Actin
1
1.4

A.

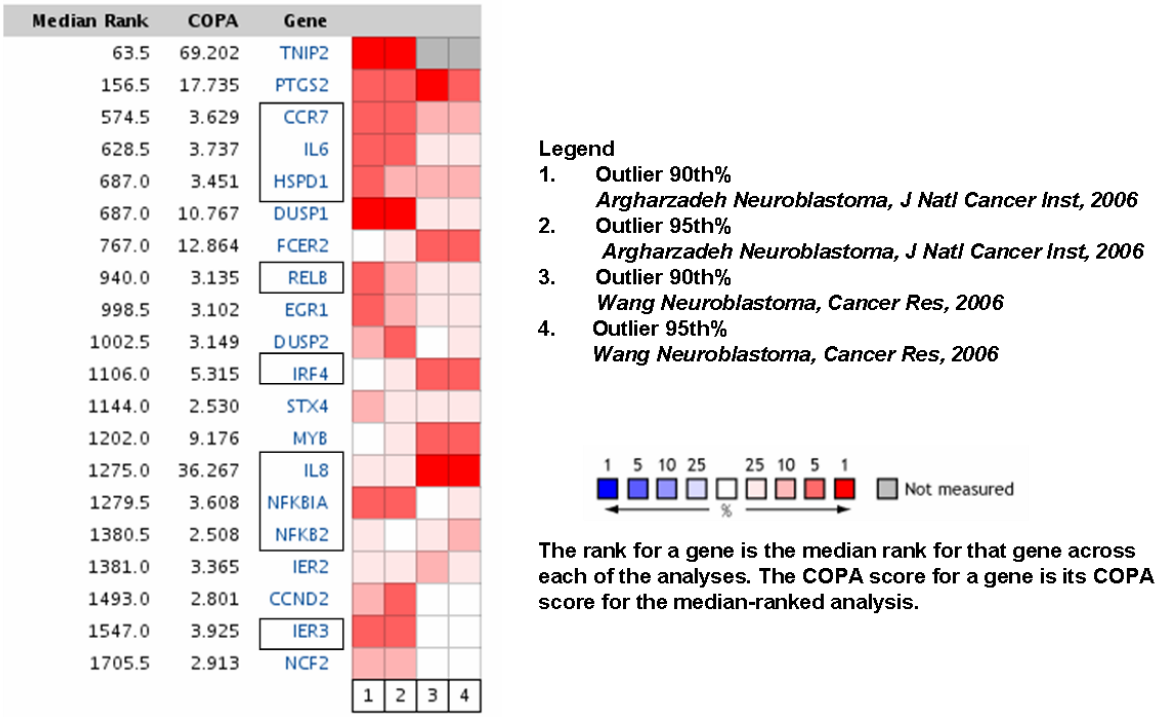

Figure 6.2. Expression of HSP60 in neuroblastoma is correlated with that of NF-κB target genes

Upon filtering the oncomine database (https://www.oncomine.org) specifically for neuroblastoma tumours using Argharzadeh and Wang studies, high HSP60 expression was observed in neuroblastoma tumours from both studies. In addition high expression of HSP60 is positively correlated with increased expression of direct NF-κB target genes, highlighted in a box. P-value is $p<0.0001$. The numbers of patients in the Argharzadeh and Wang studies were 117 and 102 respectively (Argharzadeh *et al*., 2006, Wang *et al*., 2006).

Figure 6.3. Expression of HSP60 in neuroblastoma is correlated with *MYCN* amplification and poor survival

A) Oncomine analysis (www.oncomine.org) showing a box plot where HSP60 gene (*HSPD1*) is highly expressed in 20 *MYCN* amplified neuroblastoma tumours compared with 81 non-*MYCN* amplified neuroblastoma tumours. P-value is $p<0.0001$. The top and bottom edges of each box correspond to the 75th percentile and 25th percentile, respectively. The median value (50th percentile) is shown as a horizontal black line through each box. Whiskers extend from the minimum to the maximum values. The box plot displays the centre portions of the data and the range of the data. Black dots represent outliers **B)** Kaplan Meier analysis showing high level of HSP60 gene (*HSPD1*) is correlated to poor survival in neuroblastoma patients. P-value is $p<0.0001$. The numbers of patients in HSP60 high- or low- expression groups are 126 and 125 respectively. The data was extracted from Oberthuer affymetrix dataset with the cutoff value of 0. **C)** The numbers of patients in HSP60 high- or low- expression groups are 11 and 91 respectively. The data was extracted from Seeger affymetrix dataset with a cutoff of 0.39. (http://home.ccr.cancer.gov/oncology/oncogenomics/)

Oncomine database compared gene expression levels in tumours and normal tissue and calculated the p values using student-t-test. Data for the Kaplan Meier analyses were log-transformed to intensify signal and to normalize arrays using the median normalization over the entire array method. Pearson's correlation coefficient was also used to assess the correlation between gene expression levels. The prognostic value of genes was studied by dividing the tumours into two groups, high-expressors and low-expressors, using the median value of the gene analyzed (*HSPD1*) as a cutoff. In other words, any value higher than the cutoff value is considered as high expression and below the cut off value is considered as low expression.

A.

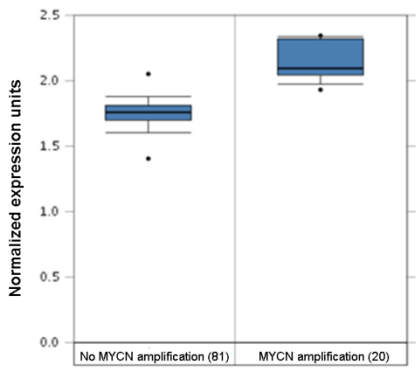
HSPD1
Normalized expression units
2.5
2.0
1.5
1.0
0.5
0.0
No MYCN amplification (81)
MYCN amplification (20)

B.

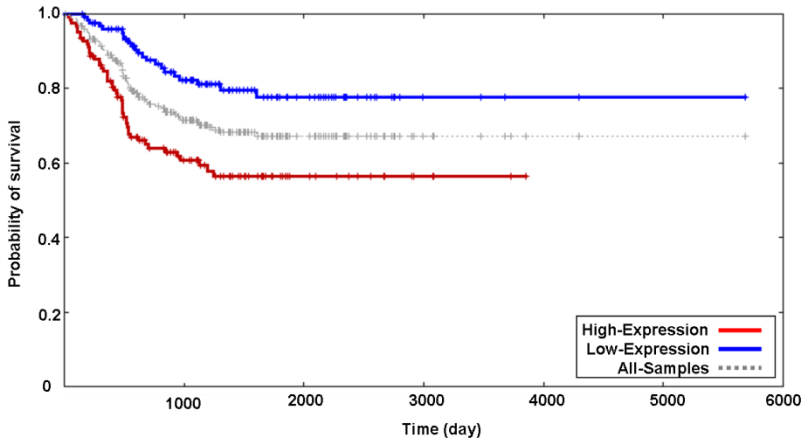
Probability of survival
1.0
0.8
0.6
0.4
0.2
0
1000
2000
3000
4000
5000
6000
Time (day)
High-Expression
Low-Expression
All-Samples

C.

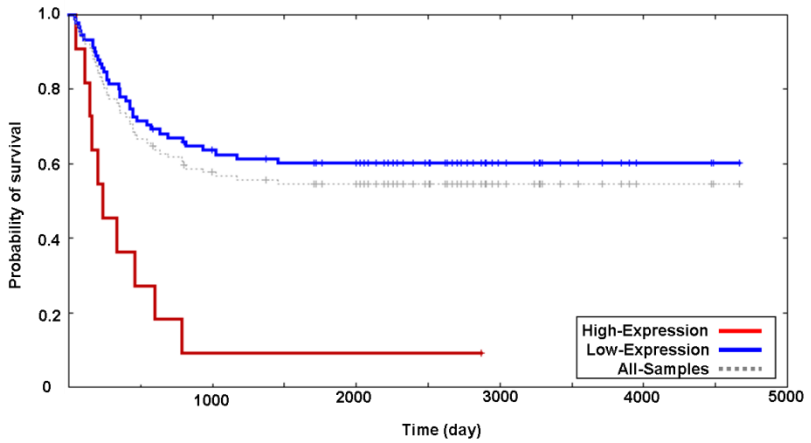
Probability of survival
1.0
0.8
0.6
0.4
0.2
0
1000
2000
3000
4000
5000
Time (day)
High-Expression
Low-Expression
All-Samples

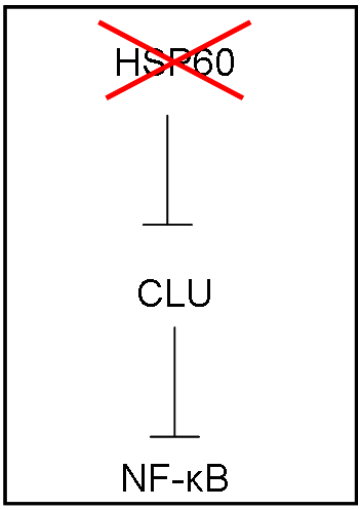

Figure 6.4. Proposed model for the mechanism of action of HSP60 in the control of NF-κB signalling pathway

In neuroblastoma, HSP60 acts upstream of CLU by inhibiting CLU function and indirectly promote NF-κB activity. By targeting HSP60 expression by shRNA, NF-κB activity was reduced, possibly due to the accumulation of CLU. Thus, HSP60 is likely to function as a tumour promoter in neuroblastoma by antagonising the effect of tumour suppressor (CLU) and activating NF-κB activity

6.3. Discussion

HSP60 has been known for a long time to be the major component of the chaperonins complex, which plays a vital role in folding newly synthesized proteins to reach their native forms (Nielsen and Cowan, 1998). Recently, HSP60 has been shown to be involved in the cellular inflammatory immune response and tumour metastasis (Tsai *et al*., 2008, Tsai *et al*., 2009). In addition, HSP60 has been shown to be required for MycC transformation (Tsai *et al*., 2008).

Chemokine productions during inflammation have multiple effects on tumour cell growth, invasion and metastasis. Lin et al (2010) demonstrated that persistence infection of *Helicobacter pylori* triggered chronic inflammation and that *H. pylori* heat shock protein 60 (HpHSP60) enhanced gastric cancer cell migration. Therefore, the link between HSP60, a well-known chaperone protein, in the induction of inflammation and cancer development is becoming more apparent.

In this chapter, reduction of endogenous HSP60 expression via RNA interference resulted in significant decreased of NF-κB activity (Figure 6.1.A and B). Therefore, HSP60 is likely to be a regulator of NF-κB in neuroblastoma. Reduced expression of HSP60 also caused accumulation of pCLU (dominant tumour suppressive role) and sCLU (Figure 6.1.C), which has been shown to regulate neuroblastoma cell death and may antagonise the prosurvival of HSP60 in the previous chapter. This suggested that HSP60 may have an additional function in the regulation of NF-κB by antagonising the effect of CLU. The proposed mechanism shown in figure 6.4 may help explain that in normal state of neuroblastoma, HSP60 is likely to act upstream of CLU by inhibiting CLU function and indirectly promote NF-κB activity, resulting in neuroblastoma cell survival. However, by targeting HSP60 expression using shRNA, NF-κB activity was reduced, possibly due to the accumulation of CLU. Thus, HSP60 is likely to function as a tumour promoter in neuroblastoma by antagonising the effect of tumour suppressor (CLU) and activating NF-κB activity.

In future experiments, it will be interesting to show that the effect of HSP60 on NF-κB signalling is specifc by reconstituting NF-κB back into the HSP60 knock down clones

to see whether the apoptotic phenotype can be restored. This will confirm that HSP60 is acting specifically via the NF-κB-dependent pathway in neuroblastoma.

In addition, microarray database also showed that elevated HSP60 mRNA expressions (*HSPD1*) is correlated with *MYCN* amplification, which is associated with aggressive neuroblastoma (Figure 6.3A.). High expression of HSP60 is also correlated with increased expression of NF-κB target genes and poorer survival rate of neuroblastoma patients (Figure 6.2. and 6.3.). Thus, HSP60 is likely to function as a tumour promoter in neuroblastoma, possibly by inhibiting the tumour suppressor protein (CLU), which has been shown to facilitate inhibitors of NF-κB (IκBs) stabilization (Santilli *et al*., 2003, Chun *et al*., 2010). The inhibition of CLU by HSP60 may allow NF-κB to be released from its inhibitor, translocated into the nucleus and become activated to promote tumour cell invasion and survival.

CHAPTER 7

Conclusions

Neuroblastoma is the most common extracranial solid tumour in children, which accounts for up to 10% of all childhood malignancies (Brodeur, 2003). There is probably not a unique but many genetic aberrations, which might cause the disease. Curable tumours, often treat by surgery, are classified as low-risk disease and are most common in infants (Brodeur, 2003). However, some subsets of patients present an aggressive disease with poor clinical outcome (Brodeur, 2003).

There is a need to identify prognostic markers in neuroblastoma. We showed an association between CLU expressions and cytogenetic profiles associated with aggressive neuroblastoma (Figure 1.4.). Tumours with *MYCN* amplification, show decreased levels of CLU mRNA and protein compared with non-*MYCN* amplified tumours (Chayka *et al*., 2009).

Conflicting observations regarding the physiological role of CLU has complicated the understanding of its function in tumourigenesis. Up or down regulation of CLU has been reported in different types of cancers (Shannan *et al*., 2006). While some of the discrepancies could be due to different experimental settings and reagents, we speculated that CLU exerts its effects in cancer in a context dependent manner (Sala *et al*., 2009). In addition, a further level of complexity results from the intricate regulation of CLU isoforms, which can be found in multiple cellular compartments (i.e. nucleus, cytoplasm, mitochondria, Golgi apparatus and ER) or in the extracellular spaces and body fluids.

Some research groups have shown that CLU is a tumour promoter, due to its anti-apoptotic function in neuroblastoma and prostate cancers (Cervellera *et al*., 2000, Zhang *et al*., 2005). A second generation antisense oligonucleotide (OGX-011), which inhibits CLU expression, has been generated by Martin Gleave and coworkers and it has been tested in phase I and II-clinical trials in prostate and metastatic breast cancers respectively (Chi *et al*., 2005, Chia *et al*., 2009).

Other groups have shown that CLU has tumour inhibiting activity in prostate cancer and Von Hippel-Lindau disease (VHL), which causes hemangioblastomas (Nakamura *et al*., 2006, Zhou *et al*., 2007, Bettuzzi *et al*., 2009). CLU was proposed to be a putative tumour suppressor protein because overexpression of CLU inhibits both *in vitro* and *in vivo* invasion of the human neuroblastoma cells and prostate tumours (Chayka *et al*., 2009, Santilli *et al*., 2003, Bettuzzi *et al*., 2009).

In the light of previous works done by our group, it is important to investigate further how CLU is involved in the regulation of neuroblastoma. We verified the role of different forms of CLU (secreted or intracellular) in NF-κB regulation and neuroblastoma development.

Firstly, we tried to dissect the physiological role of intracellular and extracellular CLU. The hypothesis that the biological function of secreted CLU could be different from that of intracellular CLU is based on several points of evidence. For example, in prostate and bladder cancer, secreted CLU is associated with tumour progression and used as a biomarker of the disease (Gleave and Chi, 2005, Hazzaa *et al*., 2010). Secreted CLU could be involved in survival signalling by modulating the PI3K pathways or by behaving like an extracellular chaperone, as described in previous studies (Jones and Jomary, 2002, Wyatt *et al*., 2009, Ammar and Closset, 2008).

However, genetic ablation of the *CLU* gene, which results in the loss of both intracellular and secreted forms of CLU, causes increased tumourigenesis in mice, indicating that the intracellular form could play a dominant, tumour suppressive role (Bettuzzi *et al*., 2009, Chayka *et al*., 2009). In neuroblastoma, secreted and intracellular CLUs are likely to play a different role. We have previously observed that in the presence of a CLU blocking antibody, neuroblastoma cells are sensitised to doxorubicin killing, suggesting that secreted CLU is a survival factor and potential oncogene (Cervellera *et al*., 2000). In spite of this, disruption of the CLU gene causes increased tumourigenesis in neuroblastoma prone mice (Chayka *et al*., 2009). The logical conclusions of these observations is that intracellular and extracellular CLU must play an opposing role in tumourigenesis and cell signalling, and the purpose of this study was to validate this hypothesis in a coherent system.

We started our investigation by verifying that transient transfection of CLU plasmid caused significant inhibition of NF-κB activity in both LA-N-1 and SHSY-5Y cell lines (Figure 3.1.). This observation, in agreement with previous works, confirmed that intracellular CLU is a negative regulator of NF-κB and a putative tumour suppressor protein (Santilli *et al*., 2003, Essabbani *et al*., 2010).

Secreted CLU (sCLU), on the other hand, is not involved in the regulation of NF-κB activity, as it failed to inhibit NF-κB activity in both LA-N-1 and SHSY-5Y (Figure 3.3.). In addition, western blot analysis showed that the conditioned media containing overexpressed sCLU was able to sustain levels of phosphorylated AKT, an anti-apoptotic molecule (Figure 3.6.). Purified human recombinant sCLU was used to confirm that the effect is due to sCLU (Figure3.7.). These results supported previous work in our laboratory, where we observed that the anti-apoptotic functions of CLU in neuroblastoma cells is due to the secreted form of CLU (Cervellera *et al*., 2000).

Other groups have also shown that sCLU is a positive regulator of the PI3K signalling pathway, where sCLU exerted pro-survival effects by activating AKT in prostate cancer cells (Ammar and Closset, 2008). Therefore, one may hypothesise that activation of AKT by sCLU could allow neuroblastoma cells to be more resistant to cell death or gaining proliferative advantage over normal cells.

Chou and coworkers (2009) have proposed sCLU to be a key regulator of ERK/MAPK signalling pathway in a lung cancer model. This finding has prompted us to investigate whether other signalling pathways are also regulated by sCLU in neuroblastoma. In contrast to Chou and coworkers, our western blot analyses did not suggest a role for sCLU in the ERK/MAPK signalling pathway, as the level of phosphorylated ERK remained unaltered in the presence or absence of sCLU (Figure 3.6 and 3.7.).

Thus, we conclude that the various effects of CLU reported previously are likely to be caused by the different forms of CLU in different location of the cell. The shifting balance between tumour promoter sCLU and tumour suppressor pCLU may affect the outcome of neuroblastoma cell fate. Therefore, we set out to isolate CLU-interacting proteins, which may take part in the control of NF-κB activity by pCLU.

Mass spectrometry and co-immunoprecipitation assays showed a direct interaction between Heat Shock Protein 60 (HSP60) with the alpha chain region of pCLU. One could argue that heatshock treatment may result in a stress-related interaction of HSP60 and CLU. However, numerous experiments in this study (GST-pull down, mass-spectrometry and co-immunoprecipitation) have shown that the interaction also occurred in the absence of stress. In addition, there is growing evidence that the heat shock protein family (especially HSP90, 70, 27 and more recently HSP60) plays a major role in carcinogenesis and is often upregulated in tumour metastases (Wadhwa *et al*., 2005, Hwang *et al*., 2009, Glaessgen *et al*., 2008, Tsai *et al*., 2008, Tsai *et al*., 2009).

The role of HSP60 in neuroblastoma was addressed further by proliferation assays and survival analyses (e.g. Annexin V and Propidium iodide staining). Lentiviral short hairpin RNA (shRNA) transduction targeting endogenous HSP60 decreased neuroblastoma cell proliferation and may increase death (Figure 5.3. and 5.5.). This observation was similar to Wadhwa et al (2005) who also reported that suppression of HSP60 expression by shRNA caused the growth arrest of osteosarcoma (U2OS) cells. Moreover, targeted HSP60 by shRNAs may increase the sensitivity of neuroblastoma cells to doxorubicin-induced death (Figure 5.3.).

Our preliminary Annexin V and propidium iodide staining data suggested that loss of HSP60 expression may cause apoptosis of neuroblastoma. This is not surprising, since intracellular HSP60 directly interacts with various components of the tightly regulated programmed cell death machinery, upstream and downstream of mitochondrial events. For instance, the direct interaction between HSP60, cyclophyllin D (CypD), HSP90 and TRAP-1 is important for glioblastoma growth *in vivo*. Genetic targeting of HSP60 by siRNA triggered CypD-dependent mitochondrial permeability transition, increased cytochrome C release, caspase-dependent apoptosis and suppression of intracranial glioblastoma growth *in vivo* (Ghosh *et al*., 2010).

Ghosh et al (2008) also demonstrated that HSP60 directly interacted with an apoptosis inhibitor (survivin), which caused the disruption of HSP60-p53 interaction, resulting in p53 stabilization, increased expression of pro-apoptotic Bax and Bax-dependent apoptosis in breast and colon adenocarcinoma models. In contrast, siRNA-silencing of HSP60 in normal cells did not elicit apoptosis. Thus, it would appear that knocking

down or disabling HSP60 would promote apoptosis in cancer cells only, which would make this treatment specific to malignant cells.

It was our goal to clarify whether CLU is involved in the regulation of neuroblastoma cell survival by HSP60. Downregulation of CLU expression appeared to result in less neuroblastoma cell death and rescue of neuroblastoma apoptosis that follows the loss of HSP60 expression (Figure 5.7.). However, the knock down efficiencies in each clone varied, thus, further experimental replication is warranted.

Reduction of endogenous HSP60 expression resulted in significant decrease of NF-κB activity (Figure 6.1.A and B). Therefore, HSP60 is likely to be a regulator of NF-κB in neuroblastoma cells. Loss of HSP60 expression also caused an accumulation of CLU (Figure 6.1.C), which is a negative regulator of NF-κB activity.

Moreover, elevated expression of HSP60 gene (*HSPD1*) in different sets of primary neuroblastoma tumours (Figure 6.2.) is correlated with increased NF-κB target genes such as CCR7, IL-6, IL-8, RELB, NF-κB1A and NF-κB2, IRF4 and IER3 (Pahl, 1999). Oncomine database also showed that HSP60 gene (*HSPD1*) is highly expressed in *MYCN* amplified neuroblastoma tumours (Figure 6.3.A). Two independent affymetrix datasets showed that high expression of HSP60 is correlated with poor survival (Figure 6.3.B and C), suggesting that HSP60 could function as a tumour promoter by inhibiting the effect of CLU, subsequently activating NF-κB (Figure 6.4.).

It will be interesting to see whether HSP60 is required for neuroblastoma tumour growth *in vivo*. Ghosh et al (2010) demonstrated that stable silencing of HSP60 using shRNA in U87-expressing luciferase (U87-LUC) glioblastoma cells could suppress the growth of intracranial glioblastoma *in vivo* and significantly prolonged survival of all animals in this group.

In future experiments, it is important to improve the knock down efficiencies of both HSP60 and CLU and to repeat more experiments where necessary. Reconstitution of NF-κB back into HSP60 knockdown clones would help confirm the effect of HSP60 on NF-κB signalling. We could also assess tumour growth in *MYCN* transgenic mice

injected with a commercially available HSP60 inhibitor called epolactaene tertiary butyl ester (ETB).

The *in vivo* data will be important to assess the significance of HSP60 in neuroblastoma and could be key for the development of novel therapeutic interventions. Currently, there are many HSP inhibitors, which have been approved for cancer treatments (Allegra *et al*., 2011). Some are natural compounds, which could be an attractive choice for the treatment of younger patients (Bohonowych *et al*., 2010). Kakeya et al (1997) demonstrated that ETB could promote neurite outgrowth and arresting the cell cycle at G_0/G_1 phase in a human neuroblastoma cell line (SHSY-5Y).

In summary, the observations in the literature and those presented in this work support the hypothesis that secreted and intracellular CLU have different biological functions; the former activates survival pathway, whereas the latter interferes with the activity of protooncogenes such as NF-κB and HSP60. By mass-spectrometry and co-immunoprecipitation experiments, we have identified HSP60 as a new CLU-interacting partner and a potential neuroblastoma oncogene. We showed that ablation of HSP60 by RNA interference appeared to cause increased apoptosis upstream of CLU, demonstrating that in neuroblastoma there is a HSP60-CLU axis involved with the regulation of NF-κB. This axis is likely to have clinical importance, as shown by the significant association of elevated HSP60 and NF-κB target genes with disease outcome.

Another interesting observation presented in this study is that CLU isoforms are modulated during tumourigenesis. After transformation, human and mouse cells showed decreased expression of intracellular pCLU, corroborating the hypothesis that intracellular CLU is tumour suppressive, whereas secreted CLU is oncogenic.

Finally, this study showed that in aggressive neuroblastoma cells, the expression of HSP60 is upregulated. Thus, HSP60 plays an important role in neuroblastoma cell survival and may be used as a new prognostic marker. Anticancer therapeutic approaches targeting HSP60 should cause cancer cell death and benefit patients with aggressive disease. We believe that the observations presented in this study are a further

step towards a better understanding of the role of CLU in cancer, and helped explain some of the controversies surrounding this intriguing molecule.

REFERENCES

Allegra,A., E.Sant'antonio, G.Penna, A.Alonci, A.D'Angelo, S.Russo, A.Cannavo, D.Gerace, and C.Musolino. 2011. Novel therapeutic strategies in multiple myeloma: role of the heat shock protein inhibitors. *Eur.J.Haematol.* 86:93-110.

Ammar,H. and J.L.Closset. 2008. Clusterin activates survival through the phosphatidylinositol 3-kinase/Akt pathway. *J.Biol.Chem.* 283:12851-12861.

Anderton,S.M., R.van der Zee, J.A.Goodacre. 1993. Inflammation activates self hsp60-specific T cells. *Eur J Immunol.* 23:33–38

Asgharzadeh,S., R.Pique-Regi, R.Sposto, H.Wang, Y.Yang, H.Shimada, K.Matthay, J.Buckley, A.Ortega, R.C.Seeger. 2006. Prognostic significance of gene expression profiles of metastatic neuroblastomas lacking MYCN gene amplification. *J Natl Cancer Inst.*98(17):1193-203.

Bader,S.A., C.Fasching, G.M.Brodeur, and E.J.Stanbridge. 1991. Dissociation of suppression of tumorigenicity and differentiation in vitro effected by transfer of single human chromosomes into human neuroblastoma cells. *Cell Growth Differ.* 2:245-255.

Barak,Y., T.Juven, R.Haffner, and M.Oren. 1993. Mdm2 expression is induced by wild type p53 activity. *EMBO J.* 12:461-468.

Barbacid,M. 1995. Neurotrophic factors and their receptors. *Curr.Opin.Cell Biol.* 7:148-155.

Barbieri,E., P.Mehta, Z.Chen, L.Zhang, A.Slack, S.Berg, and J.M.Shohet. 2006. MDM2 inhibition sensitizes neuroblastoma to chemotherapy-induced apoptotic cell death. *Mol.Cancer Ther.* 5:2358-2365.

Bartl,M.M., T.Luckenbach, O.Bergner, O.Ullrich, and C.Koch-Brandt. 2001. Multiple receptors mediate apoJ-dependent clearance of cellular debris into nonprofessional phagocytes. *Exp.Cell Res.* 271:130-141.

Basseres,D.S. and A.S.Baldwin. 2006. Nuclear factor-kappaB and inhibitor of kappaB kinase pathways in oncogenic initiation and progression. *Oncogene* 25:6817-6830.

Bell,E., R.Premkumar, J.Carr, X.Lu, P.E.Lovat, U.R.Kees, J.Lunec, and D.A.Tweddle. 2006. The role of MYCN in the failure of MYCN amplified neuroblastoma cell lines to G1 arrest after DNA damage. *Cell Cycle* 5:2639-2647.

Bell,E., J.Lunec, and D.A.Tweddle. 2007. Cell cycle regulation targets of MYCN identified by gene expression microarrays. *Cell Cycle* 6:1249-1256.

Bell,E., L.Chen, T.Liu, G.M.Marshall, J.Lunec, and D.A.Tweddle. 2010. MYCN oncoprotein targets and their therapeutic potential. *Cancer Lett.* 293:144-157.

Bettuzzi,S., P.Davalli, S.Davoli, O.Chayka, F.Rizzi, L.Belloni, D.Pellacani, G.Fregni, S.Astancolle, M.Fassan, A.Corti, R.Baffa, and A.Sala. 2009. Genetic inactivation of ApoJ/clusterin: effects on prostate tumourigenesis and metastatic spread. *Oncogene* 28:4344-4352.

Bian,X., L.M.McAllister-Lucas, F.Shao, K.R.Schumacher, Z.Feng, A.G.Porter, V.P.Castle, and A.W.Opipari, Jr. 2001. NF-kappa B activation mediates doxorubicin-induced cell death in N-type neuroblastoma cells. *J.Biol.Chem.* 276:48921-48929.

Biedler,J.L., S.Roffler-Tarlov, M.Schachner, and L.S.Freedman. 1978. Multiple neurotransmitter synthesis by human neuroblastoma cell lines and clones. *Cancer Res.* 38:3751-3757.

Birren,S.J., L.Lo, and D.J.Anderson. 1993. Sympathetic neuroblasts undergo a developmental switch in trophic dependence. *Development* 119:597-610.

Bohonowych,J.E., U.Gopal, and J.S.Isaacs. 2010. Hsp90 as a gatekeeper of tumor angiogenesis: clinical promise and potential pitfalls. *J.Oncol.* 2010:412985.

Bondurand,N., M.Girard, V.Pingault, N.Lemort, O.Dubourg, and M.Goossens. 2001. Human Connexin 32, a gap junction protein altered in the X-linked form of Charcot-Marie-Tooth disease, is directly regulated by the transcription factor SOX10. *Hum.Mol.Genet.* 10:2783-2795.

Breit,S. and M.Schwab. 1989. Suppression of MYC by high expression of NMYC in human neuroblastoma cells. *J.Neurosci.Res.* 24:21-28.

Breit,S., K.Ashman, J.Wilting, J.Rossler, E.Hatzi, T.Fotsis, and L.Schweigerer. 2000. The N-myc oncogene in human neuroblastoma cells: down-regulation of an angiogenesis inhibitor identified as activin A. *Cancer Res.* 60:4596-4601.

Brodeur,G.M., G.Sekhon, and M.N.Goldstein. 1977. Chromosomal aberrations in human neuroblastomas. *Cancer* 40:2256-2263.

Brodeur,G.M., R.C.Seeger, M.Schwab, H.E.Varmus, and J.M.Bishop. 1984. Amplification of N-myc in untreated human neuroblastomas correlates with advanced disease stage. *Science* 224:1121-1124.

Brodeur,G.M., J.Pritchard, F.Berthold, N.L.Carlsen, V.Castel, R.P.Castelberry, B.B.De, A.E.Evans, M.Favrot, F.Hedborg, and . 1993. Revisions of the international criteria for neuroblastoma diagnosis, staging, and response to treatment. *J.Clin.Oncol.* 11:1466-1477.

Brodeur,G.M. 2003. Neuroblastoma: biological insights into a clinical enigma. *Nat.Rev.Cancer* 3:203-216.

Bukau,B. and A.L.Horwich. 1998. The Hsp70 and Hsp60 chaperone machines. *Cell* 92:351-366.

Burkey,B.F., H.V.deSilva, and J.A.Harmony. 1991. Intracellular processing of apolipoprotein J precursor to the mature heterodimer. *J.Lipid Res.* 32:1039-1048.

Burkey,B.F., W.D.Stuart, and J.A.Harmony. 1992. Hepatic apolipoprotein J is secreted as a lipoprotein. *J.Lipid Res.* 33:1517-1526.

Caccamo,A.E., M.Scaltriti, A.Caporali, D.D'Arca, F.Scorcioni, G.Candiano, M.Mangiola, and S.Bettuzzi. 2003. Nuclear translocation of a clusterin isoform is associated with induction of anoikis in SV40-immortalized human prostate epithelial cells. *Ann.N.Y.Acad.Sci.* 1010:514-519.

Caccamo,A.E., M.Scaltriti, A.Caporali, D.D'Arca, A.Corti, D.Corvetta, A.Sala, and S.Bettuzzi. 2005. Ca2+ depletion induces nuclear clusterin, a novel effector of apoptosis in immortalized human prostate cells. *Cell Death.Differ.* 12:101-104.

Caccamo,A.E., S.Desenzani, L.Belloni, A.F.Borghetti, and S.Bettuzzi. 2006. Nuclear clusterin accumulation during heat shock response: implications for cell survival and thermo-tolerance induction in immortalized and prostate cancer cells. *J.Cell Physiol* 207:208-219.

Calero,M., A.Rostagno, E.Matsubara, B.Zlokovic, B.Frangione, and J.Ghiso. 2000. Apolipoprotein J (clusterin) and Alzheimer's disease. *Microsc.Res.Tech.* 50:305-315.

Cano,A., M.A.Perez-Moreno, I.Rodrigo, A.Locascio, M.J.Blanco, M.G.del Barrio, F.Portillo, and M.A.Nieto. 2000. The transcription factor snail controls epithelial-mesenchymal transitions by repressing E-cadherin expression. *Nat.Cell Biol.* 2:76-83.

Cappello,F., S.David, F.Rappa, F.Bucchieri, L.Marasa, T.E.Bartolotta, F.Farina, and G.Zummo. 2005. The expression of HSP60 and HSP10 in large bowel carcinomas with lymph node metastase. *BMC.Cancer* 5:139.

Caron,H., S.P.Van, H.M.van, K.J.de, J.Bras, R.Slater, M.Mannens, P.A.Voute, A.Westerveld, and R.Versteeg. 1993. Allelic loss of chromosome 1p36 in neuroblastoma is of preferential maternal origin and correlates with N-myc amplification. *Nat.Genet.* 4:187-190.

Caron,H., N.Spieker, M.Godfried, M.Veenstra, S.P.Van, K.J.de, P.Voute, and R.Versteeg. 2001. Chromosome bands 1p35-36 contain two distinct neuroblastoma tumor suppressor loci, one of which is imprinted. *Genes Chromosomes.Cancer* 30:168-174.

Carpenter E HE, Chow A, Christensen J, Maris J, Mosse Y. Mechanisms of resistance to small molecule inhibition of anaplastic lymphoma kinase in human neuroblastoma [abstract]. In: Proceedings of the 102nd Annual Meeting of the American Association for Cancer Research; 2011 Apr 2–6; Orlando, Florida. Philadelphia (PA): AACR; 2011 [Abstract nr 742].

Carr-Wilkinson,J., K.O'Toole, K.M.Wood, C.C.Challen, A.G.Baker, J.R.Board, L.Evans, M.Cole, N.K.Cheung, J.Boos, G.Kohler, I.Leuschner, A.D.Pearson, J.Lunec, and D.A.Tweddle. 2010. High Frequency of p53/MDM2/p14ARF Pathway Abnormalities in Relapsed Neuroblastoma. *Clin.Cancer Res.* 16:1108-1118.

Carr,J., E.Bell, A.D.Pearson, U.R.Kees, H.Beris, J.Lunec, and D.A.Tweddle. 2006. Increased frequency of aberrations in the p53/MDM2/p14(ARF) pathway in neuroblastoma cell lines established at relapse. *Cancer Res.* 66:2138-2145.

Cervellera,M., G.Raschella, G.Santilli, B.Tanno, A.Ventura, C.Mancini, C.Sevignani, B.Calabretta, and A.Sala. 2000. Direct transactivation of the anti-apoptotic gene apolipoprotein J (clusterin) by B-MYB. *J.Biol.Chem.* 275:21055-21060.

Chambery,D., S.Mohseni-Zadeh, G.B.de, and S.Babajko. 1999. N-myc regulation of type I insulin-like growth factor receptor in a human neuroblastoma cell line. *Cancer Res.* 59:2898-2902.

Chandra,D., G.Choy, and D.G.Tang. 2007. Cytosolic accumulation of HSP60 during apoptosis with or without apparent mitochondrial release: evidence that its pro-apoptotic or pro-survival functions involve differential interactions with caspase-3. *J.Biol.Chem.* 282:31289-31301.

Chayka,O., D.Corvetta, M.Dews, A.E.Caccamo, I.Piotrowska, G.Santilli, S.Gibson, N.J.Sebire, N.Himoudi, M.D.Hogarty, J.Anderson, S.Bettuzzi, A.Thomas-Tikhonenko, and A.Sala. 2009. Clusterin, a haploinsufficient tumor suppressor gene in neuroblastomas. *J.Natl.Cancer Inst.* 101:663-677.

Chen,L., N.Iraci, S.Gherardi, L.D.Gamble, K.M.Wood, G.Perini, J.Lunec, and D.A.Tweddle. 2010. p53 is a direct transcriptional target of MYCN in neuroblastoma. *Cancer Res.* 70:1377-1388.

Chen,Y., J.Takita, Y.L.Choi, M.Kato, M.Ohira, M.Sanada, L.Wang, M.Soda, A.Kikuchi, T.Igarashi, A.Nakagawara, Y.Hayashi, H.Mano, and S.Ogawa. 2008. Oncogenic mutations of ALK kinase in neuroblastoma. *Nature* 455:971-974.

Cheung,N.K., B.H.Kushner, I.Y.Cheung, K.Kramer, A.Canete, W.Gerald, M.A.Bonilla, R.Finn, S.J.Yeh, and S.M.Larson. 1998. Anti-G(D2) antibody treatment of minimal residual stage 4 neuroblastoma diagnosed at more than 1 year of age. *J.Clin.Oncol.* 16:3053-3060.

Cheung,M., M.C.Chaboissier, A.Mynett, E.Hirst, A.Schedl, and J.Briscoe. 2005. The transcriptional control of trunk neural crest induction, survival, and delamination. *Dev.Cell* 8:179-192.

Chi,K.N., E.Eisenhauer, L.Fazli, E.C.Jones, S.L.Goldenberg, J.Powers, D.Tu, and M.E.Gleave. 2005. A phase I pharmacokinetic and pharmacodynamic study of OGX-011, a 2'-methoxyethyl antisense oligonucleotide to clusterin, in patients with localized prostate cancer. *J.Natl.Cancer Inst.* 97:1287-1296.

Chi,K.N., A.Zoubeidi, and M.E.Gleave. 2008. Custirsen (OGX-011): a second-generation antisense inhibitor of clusterin for the treatment of cancer. *Expert.Opin.Investig.Drugs* 17:1955-1962.

Chi,K.N., S.J.Hotte, E.Y.Yu, D.Tu, B.J.Eigl, I.Tannock, F.Saad, S.North, J.Powers, M.E.Gleave, and E.A.Eisenhauer. 2010. Randomized phase II study of docetaxel and prednisone with or without OGX-011 in patients with metastatic castration-resistant prostate cancer. *J.Clin.Oncol.* 28:4247-4254.

Chia,S., S.Dent, S.Ellard, P.M.Ellis, T.Vandenberg, K.Gelmon, J.Powers, W.Walsh, L.Seymour, and E.A.Eisenhauer. 2009. Phase II trial of OGX-011 in combination with docetaxel in metastatic breast cancer. *Clin.Cancer Res.* 15:708-713.

Chou,T.Y., W.C.Chen, A.C.Lee, S.M.Hung, N.Y.Shih, and M.Y.Chen. 2009. Clusterin silencing in human lung adenocarcinoma cells induces a mesenchymal-to-epithelial transition through modulating the ERK/Slug pathway. *Cell Signal.* 21:704-711.

Chua,H.L., P.Bhat-Nakshatri, S.E.Clare, A.Morimiya, S.Badve, and H.Nakshatri. 2007. NF-kappaB represses E-cadherin expression and enhances epithelial to mesenchymal transition of mammary epithelial cells: potential involvement of ZEB-1 and ZEB-2. *Oncogene* 26:711-724.

Chun,J.N., B.Choi, K.W.Lee, D.J.Lee, D.H.Kang, J.Y.Lee, I.S.Song, H.I.Kim, S.H.Lee, H.S.Kim, N.K.Lee, S.Y.Lee, K.J.Lee, J.Kim, and S.W.Kang. 2010. Cytosolic Hsp60 is involved in the NF-kappaB-dependent survival of cancer cells via IKK regulation. *PLoS.One.* 5:e9422.

Cohn,S.L., A.D.Pearson, W.B.London, T.Monclair, P.F.Ambros, G.M.Brodeur, A.Faldum, B.Hero, T.Iehara, D.Machin, V.Mosseri, T.Simon, A.Garaventa, V.Castel, and K.K.Matthay. 2009. The International Neuroblastoma Risk Group (INRG) classification system: an INRG Task Force report. *J.Clin.Oncol.* 27:289-297.

Czarnecka,A.M., C.Campanella, G.Zummo, and F.Cappello. 2006. Mitochondrial chaperones in cancer: from molecular biology to clinical diagnostics. *Cancer Biol.Ther.* 5:714-720.

D'Angio,G.J., A.E.Evans, and C.E.Koop. 1971. Special pattern of widespread neuroblastoma with a favourable prognosis. *Lancet* 1:1046-1049.

Deloukas,P., G.D.Schuler, G.Gyapay, E.M.Beasley, C.Soderlund, P.Rodriguez-Tome, L.Hui, T.C.Matise, K.B.McKusick, J.S.Beckmann, S.Bentolila, M.Bihoreau, B.B.Birren, J.Browne, A.Butler, A.B.Castle, N.Chiannilkulchai, C.Clee, P.J.Day, A.Dehejia, T.Dibling, N.Drouot, S.Duprat, C.Fizames, S.Fox, S.Gelling, L.Green, P.Harrison, R.Hocking, E.Holloway, S.Hunt, S.Keil, P.Lijnzaad, C.Louis-Dit-Sully, J.Ma, A.Mendis, J.Miller, J.Morissette, D.Muselet, H.C.Nusbaum, A.Peck, S.Rozen, D.Simon, D.K.Slonim, R.Staples, L.D.Stein, E.A.Stewart, M.A.Suchard, T.Thangarajah, N.Vega-Czarny, C.Webber, X.Wu, J.Hudson, C.Auffray, N.Nomura, J.M.Sikela, M.H.Polymeropoulos, M.R.James, E.S.Lander, T.J.Hudson, R.M.Myers, D.R.Cox, J.Weissenbach, M.S.Boguski, and D.R.Bentley. 1998. A physical map of 30,000 human genes. *Science* 282:744-746.

Devauchelle,V., A.Essabbani, P.G.De, S.Germain, L.Tourneur, S.Mistou, F.Margottin-Goguet, P.Anract, H.Migaud, N.D.Le, T.Lequerre, A.Saraux, M.Dougados, M.Breban, C.Fournier, and G.Chiocchia. 2006. Characterization and functional consequences of underexpression of clusterin in rheumatoid arthritis. *J.Immunol.* 177:6471-6479.

DiFelice,V., N.Ardizzone, V.Marciano, T.Bartolotta, F.Cappello, F.Farina, and G.Zummo. 2005. Senescence-associated HSP60 expression in normal human skin fibroblasts. *Anat.Rec.A Discov.Mol.Cell Evol.Biol.* 284:446-453.

DuBois,S.G., Y.Kalika, J.N.Lukens, G.M.Brodeur, R.C.Seeger, J.B.Atkinson, G.M.Haase, C.T.Black, C.Perez, H.Shimada, R.Gerbing, D.O.Stram, and K.K.Matthay.

1999. Metastatic sites in stage IV and IVS neuroblastoma correlate with age, tumor biology, and survival. *J.Pediatr.Hematol.Oncol.* 21:181-189.

Dutton,J.R., A.Antonellis, T.J.Carney, F.S.Rodrigues, W.J.Pavan, A.Ward, and R.N.Kelsh. 2008. An evolutionarily conserved intronic region controls the spatiotemporal expression of the transcription factor Sox10. *BMC.Dev.Biol.* 8:105.

Eischen,C.M., J.D.Weber, M.F.Roussel, C.J.Sherr, and J.L.Cleveland. 1999. Disruption of the ARF-Mdm2-p53 tumor suppressor pathway in Myc-induced lymphomagenesis. *Genes Dev.* 13:2658-2669.

Endo,Y., N.Osumi, and Y.Wakamatsu. 2002. Bimodal functions of Notch-mediated signaling are involved in neural crest formation during avian ectoderm development. *Development* 129:863-873.

Ernsberger,U. and H.Rohrer. 1996. The development of the noradrenergic transmitter phenotype in postganglionic sympathetic neurons. *Neurochem.Res.* 21:823-829.

Escarcega,R.O., S.Fuentes-Alexandro, M.Garcia-Carrasco, A.Gatica, and A.Zamora. 2007. The transcription factor nuclear factor-kappa B and cancer. *Clin.Oncol.(R.Coll.Radiol.)* 19:154-161.

Essabbani,A., F.Margottin-Goguet, and G.Chiocchia. 2010. Identification of clusterin domain involved in NF-kappaB pathway regulation. *J.Biol.Chem.* 285:4273-4277.

Evans,A.E., K.D.Kisselbach, D.J.Yamashiro, N.Ikegaki, A.M.Camoratto, C.A.Dionne, and G.M.Brodeur. 1999. Antitumor activity of CEP-751 (KT-6587) on human neuroblastoma and medulloblastoma xenografts. *Clin.Cancer Res.* 5:3594-3602.

Fabre,C., G.Carvalho, E.Tasdemir, T.Braun, L.Ades, J.Grosjean, S.Boehrer, D.Metivier, S.Souquere, G.Pierron, P.Fenaux, and G.Kroemer. 2007. NF-kappaB inhibition sensitizes to starvation-induced cell death in high-risk myelodysplastic syndrome and acute myeloid leukemia. *Oncogene* 26:4071-4083.

Forloni,M., S.Albini, M.Z.Limongi, L.Cifaldi, R.Boldrini, M.R.Nicotra, G.Giannini, P.G.Natali, P.Giacomini, and D.Fruci. 2010. NF-kappaB, and not MYCN, regulates

MHC class I and endoplasmic reticulum aminopeptidases in human neuroblastoma cells. *Cancer Res.* 70:916-924.

Fornari,F.A., J.K.Randolph, J.C.Yalowich, M.K.Ritke, and D.A.Gewirtz. 1994. Interference by doxorubicin with DNA unwinding in MCF-7 breast tumor cells. *Mol.Pharmacol.* 45:649-656.

Foteinos,G., A.R.Afzal, K.Mandal, M.Jahangiri, and Q.Xu. 2005. Anti-heat shock protein 60 autoantibodies induce atherosclerosis in apolipoprotein E-deficient mice via endothelial damage. *Circulation* 112:1206-1213.

Friedman,G.K. and R.P.Castleberry. 2007. Changing trends of research and treatment in infant neuroblastoma. *Pediatr.Blood Cancer* 49:1060-1065.

Fritz,I.B., K.Burdzy, B.Setchell, and O.Blaschuk. 1983. Ram rete testis fluid contains a protein (clusterin) which influences cell-cell interactions in vitro. *Biol.Reprod.* 28:1173-1188.

Fujita,T., J.Igarashi, E.R.Okawa, T.Gotoh, J.Manne, V.Kolla, J.Kim, H.Zhao, B.R.Pawel, W.B.London, J.M.Maris, P.S.White, and G.M.Brodeur. 2008. CHD5, a tumor suppressor gene deleted from 1p36.31 in neuroblastomas. *J.Natl.Cancer Inst.* 100:940-949.

Fulda,S., H.Sieverts, C.Friesen, I.Herr, and K.M.Debatin. 1997. The CD95 (APO-1/Fas) system mediates drug-induced apoptosis in neuroblastoma cells. *Cancer Res.* 57:3823-3829.

Galderisi,U., B.G.Di, M.Cipollaro, G.Peluso, A.Cascino, R.Cotrufo, and M.A.Melone. 1999. Differentiation and apoptosis of neuroblastoma cells: role of N-myc gene product. *J.Cell Biochem.* 73:97-105.

Gamble,L.D., U.R.Kees, D.A.Tweddle, and J.Lunec. 2011. MYCN sensitizes neuroblastoma to the MDM2-p53 antagonists Nutlin-3 and MI-63. *Oncogene*.

Gammill,L.S. and M.Bronner-Fraser. 2002. Genomic analysis of neural crest induction. *Development* 129:5731-5741.

Gammill,L.S. and M.Bronner-Fraser. 2003. Neural crest specification: migrating into genomics. *Nat.Rev.Neurosci.* 4:795-805.

Garcia,I., G.Mayol, E.Rodriguez, M.Sunol, T.R.Gershon, J.Rios, N.K.Cheung, M.W.Kieran, R.E.George, A.R.Perez-Atayde, C.Casala, P.Galvan, T.C.de, J.Mora, and C.Lavarino. 2010. Expression of the neuron-specific protein CHD5 is an independent marker of outcome in neuroblastoma. *Mol.Cancer* 9:277.

George,R.E., T.Sanda, M.Hanna, S.Frohling, W.Luther, J.Zhang, Y.Ahn, W.Zhou, W.B.London, P.McGrady, L.Xue, S.Zozulya, V.E.Gregor, T.R.Webb, N.S.Gray, D.G.Gilliland, L.Diller, H.Greulich, S.W.Morris, M.Meyerson, and A.T.Look. 2008. Activating mutations in ALK provide a therapeutic target in neuroblastoma. *Nature* 455:975-978.

Ghimenti,C., A.Lonobile, D.Campani, G.Bevilacqua, and M.A.Caligo. 1999. Microsatellite instability and allelic losses in neuroendocrine tumors of the gastro-entero-pancreatic system. *Int.J.Oncol.* 15:361-366.

Ghosh,J.C., T.Dohi, B.H.Kang, and D.C.Altieri. 2008. Hsp60 regulation of tumor cell apoptosis. *J.Biol.Chem.* 283:5188-5194.

Ghosh,J.C., M.D.Siegelin, T.Dohi, and D.C.Altieri. 2010. Heat shock protein 60 regulation of the mitochondrial permeability transition pore in tumor cells. *Cancer Res.* 70:8988-8993.

Ghosh,S. and M.Karin. 2002. Missing pieces in the NF-kappaB puzzle. *Cell* 109 Suppl:S81-S96.

Giannini,G., F.Cerignoli, M.Mellone, I.Massimi, C.Ambrosi, C.Rinaldi, C.Dominici, L.Frati, I.Screpanti, and A.Gulino. 2005. High mobility group A1 is a molecular target for MYCN in human neuroblastoma. *Cancer Res.* 65:8308-8316.

Gilbert,F., M.Feder, G.Balaban, D.Brangman, D.K.Lurie, R.Podolsky, V.Rinaldt, N.Vinikoor, and J.Weisband. 1984. Human neuroblastomas and abnormalities of chromosomes 1 and 17. *Cancer Res.* 44:5444-5449.

Gilmore,T.D. 2006. Introduction to NF-kappaB: players, pathways, perspectives. *Oncogene* 25:6680-6684.

Glaessgen,A., S.Jonmarker, A.Lindberg, B.Nilsson, R.Lewensohn, P.Ekman, A.Valdman, and L.Egevad. 2008. Heat shock proteins 27, 60 and 70 as prognostic markers of prostate cancer. *APMIS* 116:888-895.

Gleave,M. and H.Miyake. 2005. Use of antisense oligonucleotides targeting the cytoprotective gene, clusterin, to enhance androgen- and chemo-sensitivity in prostate cancer. *World J.Urol.* 23:38-46.

Gleave,M. and K.N.Chi. 2005. Knock-down of the cytoprotective gene, clusterin, to enhance hormone and chemosensitivity in prostate and other cancers. *Ann.N.Y.Acad.Sci.* 1058:1-15.

Goldman,S.C., C.Y.Chen, T.J.Lansing, T.M.Gilmer, and M.B.Kastan. 1996. The p53 signal transduction pathway is intact in human neuroblastoma despite cytoplasmic localization. *Am.J.Pathol.* 148:1381-1385.

Goridis,C. and H.Rohrer. 2002. Specification of catecholaminergic and serotonergic neurons. *Nat.Rev.Neurosci.* 3:531-541.

Graham,A., J.Begbie, and I.McGonnell. 2004. Significance of the cranial neural crest. *Dev.Dyn.* 229:5-13.

Graham,F.L., J.Smiley, W.C.Russell, and R.Nairn. 1977. Characteristics of a human cell line transformed by DNA from human adenovirus type 5. *J.Gen.Virol.* 36:59-74.

Greten,F.R., L.Eckmann, T.F.Greten, J.M.Park, Z.W.Li, L.J.Egan, M.F.Kagnoff, and M.Karin. 2004. IKKbeta links inflammation and tumorigenesis in a mouse model of colitis-associated cancer. *Cell* 118:285-296.

Guccione,E., F.Martinato, G.Finocchiaro, L.Luzi, L.Tizzoni, O.Dall', V, G.Zardo, C.Nervi, L.Bernard, and B.Amati. 2006. Myc-binding-site recognition in the human genome is determined by chromatin context. *Nat.Cell Biol.* 8:764-770.

Gulden,E., T.Marker, J.Kriebel, V.Kolb-Bachofen, V.Burkart, and C.Habich. 2009. Heat shock protein 60: evidence for receptor-mediated induction of proinflammatory mediators during adipocyte differentiation. *FEBS Lett.* 583:2877-2881.

Gupta,A., B.R.Williams, S.M.Hanash, and J.Rawwas. 2006. Cellular retinoic acid-binding protein II is a direct transcriptional target of MycN in neuroblastoma. *Cancer Res.* 66:8100-8108.

Gupta,S. and A.A.Knowlton. 2007. HSP60 trafficking in adult cardiac myocytes: role of the exosomal pathway. *Am.J.Physiol Heart Circ.Physiol* 292:H3052-H3056.

Gurney,J.G., J.A.Ross, D.A.Wall, W.A.Bleyer, R.K.Severson, and L.L.Robison. 1997. Infant cancer in the U.S.: histology-specific incidence and trends, 1973 to 1992. *J.Pediatr.Hematol.Oncol.* 19:428-432.

Gutierrez,H., V.A.Hale, X.Dolcet, and A.Davies. 2005. NF-kappaB signalling regulates the growth of neural processes in the developing PNS and CNS. *Development* 132:1713-1726.

Haber,M., S.B.Bordow, J.Gilbert, J.Madafiglio, M.Kavallaris, G.M.Marshall, E.B.Mechetner, J.P.Fruehauf, L.Tee, S.L.Cohn, H.Salwen, M.L.Schmidt, and M.D.Norris. 1999. Altered expression of the MYCN oncogene modulates MRP gene expression and response to cytotoxic drugs in neuroblastoma cells. *Oncogene* 18:2777-2782.

Hacker,H. and M.Karin. 2006. Regulation and function of IKK and IKK-related kinases. *Sci.STKE.* 2006:re13.

Han,B.H., R.B.DeMattos, L.L.Dugan, J.S.Kim-Han, R.P.Brendza, J.D.Fryer, M.Kierson, J.Cirrito, K.Quick, J.A.Harmony, B.J.Aronow, and D.M.Holtzman. 2001. Clusterin contributes to caspase-3-independent brain injury following neonatal hypoxia-ischemia. *Nat.Med.* 7:338-343.

Hansen,J.J., P.Bross, M.Westergaard, M.N.Nielsen, H.Eiberg, A.D.Borglum, J.Mogensen, K.Kristiansen, L.Bolund, and N.Gregersen. 2003. Genomic structure of the human mitochondrial chaperonin genes: HSP60 and HSP10 are localised head to head on chromosome 2 separated by a bidirectional promoter. *Hum.Genet.* 112:71-77.

Harris,R.G., E.White, E.S.Phillips, and K.A.Lillycrop. 2002. The expression of the developmentally regulated proto-oncogene Pax-3 is modulated by N-Myc. *J.Biol.Chem.* 277:34815-34825.

Hartl,F.U. 1996. Molecular chaperones in cellular protein folding. *Nature* 381:571-579.

Hatzi,E., S.Breit, A.Zoephel, K.Ashman, U.Tontsch, H.Ahorn, C.Murphy, L.Schweigerer, and T.Fotsis. 2000. MYCN oncogene and angiogenesis: down-regulation of endothelial growth inhibitors in human neuroblastoma cells. Purification, structural, and functional characterization. *Adv.Exp.Med.Biol.* 476:239-248.

Hatzi,E., C.Murphy, A.Zoephel, H.Rasmussen, L.Morbidelli, H.Ahorn, K.Kunisada, U.Tontsch, M.Klenk, K.Yamauchi-Takihara, M.Ziche, E.K.Rofstad, L.Schweigerer, and T.Fotsis. 2002 (i). N-myc oncogene overexpression down-regulates IL-6; evidence that IL-6 inhibits angiogenesis and suppresses neuroblastoma tumor growth. *Oncogene* 21:3552-3561.

Hatzi,E., C.Murphy, A.Zoephel, H.Ahorn, U.Tontsch, A.M.Bamberger, K.Yamauchi-Takihara, L.Schweigerer, and T.Fotsis. 2002 (ii). N-myc oncogene overexpression down-regulates leukemia inhibitory factor in neuroblastoma. *Eur.J.Biochem.* 269:3732-3741.

Hayflick,L. and P.S.Moorhead. 1961. The serial cultivation of human diploid cell strains. *Exp.Cell Res.* 25:585-621.

Hayflick,L. 1965. The limited *in vitro* lifetime of human diploid cell strains. *Exp.Cell Res.* 37:614-636.

Hazzaa,S.M., O.M.Elashry, and I.K.Afifi. 2010. Clusterin as a diagnostic and prognostic marker for transitional cell carcinoma of the bladder. *Pathol.Oncol.Res.* 16:101-109.

Hermeking,H. and D.Eick. 1994. Mediation of c-Myc-induced apoptosis by p53. *Science* 265:2091-2093.

Hirai,M., S.Yoshida, H.Kashiwagi, T.Kawamura, T.Ishikawa, M.Kaneko, H.Ohkawa, A.Nakagawara, M.Miwa, and K.Uchida. 1999. 1q23 gain is associated with progressive

neuroblastoma resistant to aggressive treatment. *Genes Chromosomes.Cancer* 25:261-269.

Hiyama,E., K.Hiyama, T.Yokoyama, Y.Matsuura, M.A.Piatyszek, and J.W.Shay. 1995. Correlating telomerase activity levels with human neuroblastoma outcomes. *Nat.Med.* 1:249-255.

Hiyama,E., K.Hiyama, K.Ohtsu, H.Yamaoka, I.Fukuba, Y.Matsuura, and T.Yokoyama. 2001. Biological characteristics of neuroblastoma with partial deletion in the short arm of chromosome 1. *Med.Pediatr.Oncol.* 36:67-74.

Hosoi,G., J.Hara, T.Okamura, Y.Osugi, S.Ishihara, M.Fukuzawa, A.Okada, S.Okada, and A.Tawa. 1994. Low frequency of the p53 gene mutations in neuroblastoma. *Cancer* 73:3087-3093.

Hossain,M.S., T.Ozaki, H.Wang, A.Nakagawa, H.Takenobu, M.Ohira, T.Kamijo, and A.Nakagawara. 2008. N-MYC promotes cell proliferation through a direct transactivation of neuronal leucine-rich repeat protein-1 (NLRR1) gene in neuroblastoma. *Oncogene* 27:6075-6082.

Howard,M.J. 2005. Mechanisms and perspectives on differentiation of autonomic neurons. *Dev.Biol.* 277:271-286.

Huber,M.A., N.Azoitei, B.Baumann, S.Grunert, A.Sommer, H.Pehamberger, N.Kraut, H.Beug, and T.Wirth. 2004. NF-kappaB is essential for epithelial-mesenchymal transition and metastasis in a model of breast cancer progression. *J.Clin.Invest* 114:569-581.

Humphreys,D., T.T.Hochgrebe, S.B.Easterbrook-Smith, M.P.Tenniswood, and M.R.Wilson. 1997. Effects of clusterin overexpression on TNFalpha- and TGFbeta-mediated death of L929 cells. *Biochemistry* 36:15233-15243.

Hwang,Y.J., S.P.Lee, S.Y.Kim, Y.H.Choi, M.J.Kim, C.H.Lee, J.Y.Lee, and D.Y.Kim. 2009. Expression of heat shock protein 60 kDa is upregulated in cervical cancer. *Yonsei Med.J.* 50:399-406.

Islam,A., H.Kageyama, N.Takada, T.Kawamoto, H.Takayasu, E.Isogai, M.Ohira, K.Hashizume, H.Kobayashi, Y.Kaneko, and A.Nakagawara. 2000. High expression of Survivin, mapped to 17q25, is significantly associated with poor prognostic factors and promotes cell survival in human neuroblastoma. *Oncogene* 19:617-623.

Iwahara,T., J.Fujimoto, D.Wen, R.Cupples, N.Bucay, T.Arakawa, S.Mori, B.Ratzkin, and T.Yamamoto. 1997. Molecular characterization of ALK, a receptor tyrosine kinase expressed specifically in the nervous system. *Oncogene* 14:439-449.

Izzo,J.G., U.Malhotra, T.T.Wu, R.Luthra, A.M.Correa, S.G.Swisher, W.Hofstetter, K.S.Chao, M.C.Hung, and J.A.Ajani. 2007. Clinical biology of esophageal adenocarcinoma after surgery is influenced by nuclear factor-kappaB expression. *Cancer Epidemiol.Biomarkers Prev.* 16:1200-1205.

Jacobs,M.D. and S.C.Harrison. 1998. Structure of an IkappaBalpha/NF-kappaB complex. *Cell* 95:749-758.

Janoueix-Lerosey,I., D.Lequin, L.Brugieres, A.Ribeiro, P.L.de, V.Combaret, V.Raynal, A.Puisieux, G.Schleiermacher, G.Pierron, D.Valteau-Couanet, T.Frebourg, J.Michon, S.Lyonnet, J.Amiel, and O.Delattre. 2008. Somatic and germline activating mutations of the ALK kinase receptor in neuroblastoma. *Nature* 455:967-970.

Janoueix-Lerosey,I., G.Schleiermacher, E.Michels, V.Mosseri, A.Ribeiro, D.Lequin, J.Vermeulen, J.Couturier, M.Peuchmaur, A.Valent, D.Plantaz, H.Rubie, D.Valteau-Couanet, C.Thomas, V.Combaret, R.Rousseau, A.Eggert, J.Michon, F.Speleman, and O.Delattre. 2009. Overall genomic pattern is a predictor of outcome in neuroblastoma. *J.Clin.Oncol.* 27:1026-1033.

Janoueix-Lerosey,I., G.Schleiermacher, and O.Delattre. 2010. Molecular pathogenesis of peripheral neuroblastic tumors. *Oncogene* 29:1566-1579.

Jazii,F.R., Z.Najafi, R.Malekzadeh, T.P.Conrads, A.A.Ziaee, C.Abnet, M.Yazdznbod, A.A.Karkhane, and G.H.Salekdeh. 2006. Identification of squamous cell carcinoma associated proteins by proteomics and loss of beta tropomyosin expression in esophageal cancer. *World J.Gastroenterol.* 12:7104-7112.

Jenne,D.E. and J.Tschopp. 1989. Molecular structure and functional characterization of a human complement cytolysis inhibitor found in blood and seminal plasma: identity to sulfated glycoprotein 2, a constituent of rat testis fluid. *Proc.Natl.Acad.Sci.U.S.A* 86:7123-7127.

Jo,H., Y.Jia, K.K.Subramanian, H.Hattori, and H.R.Luo. 2008. Cancer cell-derived clusterin modulates the phosphatidylinositol 3'-kinase-Akt pathway through attenuation of insulin-like growth factor 1 during serum deprivation. *Mol.Cell Biol.* 28:4285-4299.

Jones,S.E. and C.Jomary. 2002. Clusterin. *Int.J.Biochem.Cell Biol.* 34:427-431.

Juin,P., A.O.Hueber, T.Littlewood, and G.Evan. 1999. c-Myc-induced sensitization to apoptosis is mediated through cytochrome c release. *Genes Dev.* 13:1367-1381.

Julien,S., I.Puig, E.Caretti, J.Bonaventure, L.Nelles, R.F.van, C.Dargemont, A.G.de Herreros, A.Bellacosa, and L.Larue. 2007. Activation of NF-kappaB by Akt upregulates Snail expression and induces epithelium mesenchyme transition. *Oncogene* 26:7445-7456.

July,L.V., E.Beraldi, A.So, L.Fazli, K.Evans, J.C.English, and M.E.Gleave. 2004. Nucleotide-based therapies targeting clusterin chemosensitize human lung adenocarcinoma cells both in vitro and in vivo. *Mol.Cancer Ther.* 3:223-232.

Jun,H.O., D.H.Kim, S.W.Lee, H.S.Lee, J.H.Seo, J.H.Kim, J.H.Kim, Y.S.Yu, B.H.Min, and K.W.Kim. 2011. Clusterin protects H9c2 cardiomyocytes from oxidative stress-induced apoptosis via Akt/GSK-3beta signaling pathway. *Exp.Mol.Med.* 43:53-61.

Kaelin,W.G., Jr. 2005. The concept of synthetic lethality in the context of anticancer therapy. *Nat.Rev.Cancer* 5:689-698.

Kakeya,H., C.Onozawa, M.Sato, K.Arai, and H.Osada. 1997. Neuritogenic effect of epolactaene derivatives on human neuroblastoma cells which lack high-affinity nerve growth factor receptors. *J.Med.Chem.* 40:391-394.

Kang,J.H., P.G.Rychahou, T.A.Ishola, J.Qiao, B.M.Evers, and D.H.Chung. 2006. MYCN silencing induces differentiation and apoptosis in human neuroblastoma cells. *Biochem.Biophys.Res.Commun.* 351:192-197.

Kang,S.W., Y.J.Shin, Y.J.Shim, S.Y.Jeong, I.S.Park, and B.H.Min. 2005. Clusterin interacts with SCLIP (SCG10-like protein) and promotes neurite outgrowth of PC12 cells. *Exp.Cell Res.* 309:305-315.

Kapron,J.T., G.M.Hilliard, J.N.Lakins, M.P.Tenniswood, K.A.West, S.A.Carr, and J.W.Crabb. 1997. Identification and characterization of glycosylation sites in human serum clusterin. *Protein Sci.* 6:2120-2133.

Karin,M. and Y.Ben-Neriah. 2000. Phosphorylation meets ubiquitination: the control of NF-[kappa]B activity. *Annu.Rev.Immunol.* 18:621-663.

Karin,M. 2006. Nuclear factor-kappaB in cancer development and progression. *Nature* 441:431-436.

Kelsh,R.N. 2006. Sorting out Sox10 functions in neural crest development. *Bioessays* 28:788-798.

Kim,J., L.Lo, E.Dormand, and D.J.Anderson. 2003. SOX10 maintains multipotency and inhibits neuronal differentiation of neural crest stem cells. *Neuron* 38:17-31.

Knoepfler,P.S., P.F.Cheng, and R.N.Eisenman. 2002. N-myc is essential during neurogenesis for the rapid expansion of progenitor cell populations and the inhibition of neuronal differentiation. *Genes Dev.* 16:2699-2712.

Knudson,A.G., Jr. and L.C.Strong. 1972. Mutation and cancer: neuroblastoma and pheochromocytoma. *Am.J.Hum.Genet.* 24:514-532.

Koch-Brandt,C. and C.Morgans. 1996. Clusterin: a role in cell survival in the face of apoptosis? *Prog.Mol.Subcell.Biol.* 16:130-149.

Kohl,N.E., N.Kanda, R.R.Schreck, G.Bruns, S.A.Latt, F.Gilbert, and F.W.Alt. 1983. Transposition and amplification of oncogene-related sequences in human neuroblastomas. *Cell* 35:359-367.

Krakstad,C. and M.Chekenya. 2010. Survival signalling and apoptosis resistance in glioblastomas: opportunities for targeted therapeutics. *Mol.Cancer* 9:135.

Kroll,E.S., K.M.Hyland, P.Hieter, and J.J.Li. 1996. Establishing genetic interactions by a synthetic dosage lethality phenotype. *Genetics* 143:95-102.

Kulesa,P.M., F.Lefcort, and J.C.Kasemeier-Kulesa. 2009. The migration of autonomic precursor cells in the embryo. *Auton.Neurosci.* 151:3-9.

Lambert,J.C., S.Heath, G.Even, D.Campion, K.Sleegers, M.Hiltunen, O.Combarros, D.Zelenika, M.J.Bullido, B.Tavernier, L.Letenneur, K.Bettens, C.Berr, F.Pasquier, N.Fievet, P.Barberger-Gateau, S.Engelborghs, D.P.De, I.Mateo, A.Franck, S.Helisalmi, E.Porcellini, O.Hanon, M.M.de Pancorbo, C.Lendon, C.Dufouil, C.Jaillard, T.Leveillard, V.Alvarez, P.Bosco, M.Mancuso, F.Panza, B.Nacmias, P.Bossu, P.Piccardi, G.Annoni, D.Seripa, D.Galimberti, D.Hannequin, F.Licastro, H.Soininen, K.Ritchie, H.Blanche, J.F.Dartigues, C.Tzourio, I.Gut, B.C.Van, A.Alperovitch, M.Lathrop, and P.Amouyel. 2009. Genome-wide association study identifies variants at CLU and CR1 associated with Alzheimer's disease. *Nat.Genet.* 41:1094-1099.

Lasorella,A., R.Boldrini, C.Dominici, A.Donfrancesco, Y.Yokota, A.Inserra, and A.Iavarone. 2002. Id2 is critical for cellular proliferation and is the oncogenic effector of N-myc in human neuroblastoma. *Cancer Res.* 62:301-306.

Lavenius,E., C.Gestblom, I.Johansson, E.Nanberg and S.Pahlman.1995. Transfection of TRK-A into human neuroblastoma cells restores their ability to differentiate in response to nerve growth factor. *Cell Growth Differ* 6:727-736.

LeDouarin,N. and C.Kalcheim. The Neural Crest (eds. Bard,J., Barlow,P. and Kirk,D.) *Cambridge Univ. Press*, 1999.

Lasorella,A., R.Boldrini, C.Dominici, A.Donfrancesco, Y.Yokota, A.Inserra, and A.Iavarone. 2002. Id2 is critical for cellular proliferation and is the oncogenic effector of N-myc in human neuroblastoma. *Cancer Res.* 62:301-306.

Lee,W.H., A.L.Murphree, and W.F.Benedict. 1984. Expression and amplification of the N-myc gene in primary retinoblastoma. *Nature* 309:458-460.

Leskov,K.S., D.Y.Klokov, J.Li, T.J.Kinsella, and D.A.Boothman. 2003. Synthesis and functional analyses of nuclear clusterin, a cell death protein. *J.Biol.Chem.* 278:11590-11600.

Lewis,J.L., J.Bonner, M.Modrell, J.W.Ragland, R.T.Moon, R.I.Dorsky, and D.W.Raible. 2004. Reiterated Wnt signaling during zebrafish neural crest development. *Development* 131:1299-1308.

Li,J. and L.Kretzner. 2003. The growth-inhibitory Ndrg1 gene is a Myc negative target in human neuroblastomas and other cell types with overexpressed N- or c-myc. *Mol.Cell Biochem.* 250:91-105.

Lin,C.S., P.J.He, N.M.Tsai, C.H.Li, S.C.Yang, W.T.Hsu, M.S.Wu, C.J.Wu, T.L.Cheng, and K.W.Liao. 2010. A potential role for Helicobacter pylori heat shock protein 60 in gastric tumorigenesis. *Biochem.Biophys.Res.Commun.* 392:183-189.

Liu,T., A.E.Tee, A.Porro, S.A.Smith, T.Dwarte, P.Y.Liu, N.Iraci, E.Sekyere, M.Haber, M.D.Norris, D.Diolaiti, V.G.Della, G.Perini, and G.M.Marshall. 2007. Activation of tissue transglutaminase transcription by histone deacetylase inhibition as a therapeutic approach for Myc oncogenesis. *Proc.Natl.Acad.Sci.U.S.A* 104:18682-18687.

Liu,Z., X.Yang, F.Tan, K.Cullion, and C.J.Thiele. 2006. Molecular cloning and characterization of human Castor, a novel human gene upregulated during cell differentiation. *Biochem.Biophys.Res.Commun.* 344:834-844.

Liu,Z., A.Naranjo, and C.J.Thiele. 2011. CASZ1b, the short isoform of CASZ1 gene, coexpresses with CASZ1a during neurogenesis and suppresses neuroblastoma cell growth. *PLoS.One.* 6:e18557.

Liu,Z., X.Yang, Z.Li, C.McMahon, C.Sizer, L.Barenboim-Stapleton, V.Bliskovsky, B.Mock, T.Ried, W.B.London, J.Maris, J.Khan, and C.J.Thiele. 2011. CASZ1, a candidate tumor-suppressor gene, suppresses neuroblastoma tumor growth through reprogramming gene expression. *Cell Death.Differ.* 18:1174-1183.

Look,A.T., F.A.Hayes, R.Nitschke, N.B.McWilliams, and A.A.Green. 1984. Cellular DNA content as a predictor of response to chemotherapy in infants with unresectable neuroblastoma. *N.Engl.J.Med.* 311:231-235.

Look,A.T., F.A.Hayes, J.J.Shuster, E.C.Douglass, R.P.Castleberry, L.C.Bowman, E.I.Smith, and G.M.Brodeur. 1991. Clinical relevance of tumor cell ploidy and N-myc

gene amplification in childhood neuroblastoma: a Pediatric Oncology Group study. *J.Clin.Oncol.* 9:581-591.

Lovat,P.E., M.Ranalli, F.Bernassola, M.Tilby, A.J.Malcolm, A.D.Pearson, M.Piacentini, G.Melino, and C.P.Redfern. 2000. Synergistic induction of apoptosis of neuroblastoma by fenretinide or CD437 in combination with chemotherapeutic drugs. *Int.J.Cancer* 88:977-985.

Lu,X., A.Pearson, and J.Lunec. 2003. The MYCN oncoprotein as a drug development target. *Cancer Lett.* 197:125-130.

Luo,T., M.Matsuo-Takasaki, J.H.Lim, and T.D.Sargent. 2001. Differential regulation of Dlx gene expression by a BMP morphogenetic gradient. *Int.J.Dev.Biol.* 45:681-684.

Luscher,B. 2001. Function and regulation of the transcription factors of the Myc/Max/Mad network. *Gene* 277:1-14.

Lutz,W., M.Stohr, J.Schurmann, A.Wenzel, A.Lohr, and M.Schwab. 1996. Conditional expression of N-myc in human neuroblastoma cells increases expression of alpha-prothymosin and ornithine decarboxylase and accelerates progression into S-phase early after mitogenic stimulation of quiescent cells. *Oncogene* 13:803-812.

Mac,S.M., C.A.D'Cunha, and P.J.Farnham. 2000. Direct recruitment of N-myc to target gene promoters. *Mol.Carcinog.* 29:76-86.

Manohar,C.F., J.A.Bray, H.R.Salwen, J.Madafiglio, A.Cheng, C.Flemming, G.M.Marshall, M.D.Norris, M.Haber, and S.L.Cohn. 2004. MYCN-mediated regulation of the MRP1 promoter in human neuroblastoma. *Oncogene* 23:753-762.

Maris,J.M. and K.K.Matthay. 1999. Molecular biology of neuroblastoma. *J.Clin.Oncol.* 17:2264-2279.

Maris,J.M., M.D.Hogarty, R.Bagatell, and S.L.Cohn. 2007. Neuroblastoma. *Lancet* 369:2106-2120.

Matthay,K.K., J.G.Villablanca, R.C.Seeger, D.O.Stram, R.E.Harris, N.K.Ramsay, P.Swift, H.Shimada, C.T.Black, G.M.Brodeur, R.B.Gerbing, and C.P.Reynolds. 1999. Treatment of high-risk neuroblastoma with intensive chemotherapy, radiotherapy,

autologous bone marrow transplantation, and 13-cis-retinoic acid. Children's Cancer Group. *N.Engl.J.Med.* 341:1165-1173.

Mattson,M.P. and S.Camandola. 2001. NF-kappaB in neuronal plasticity and neurodegenerative disorders. *J.Clin.Invest* 107:247-254.

Mazur,K.A. 2010. Neuroblastoma: What the nurse practitioner should know. *J.Am.Acad.Nurse Pract.* 22:236-245.

McLaughlin,L., G.Zhu, M.Mistry, C.Ley-Ebert, W.D.Stuart, C.J.Florio, P.A.Groen, S.A.Witt, T.R.Kimball, D.P.Witte, J.A.Harmony, and B.J.Aronow. 2000. Apolipoprotein J/clusterin limits the severity of murine autoimmune myocarditis. *J.Clin.Invest* 106:1105-1113.

Measday,V. and P.Hieter. 2002. Synthetic dosage lethality. *Methods Enzymol.* 350:316-326.

Medici,D., E.D.Hay, and B.R.Olsen. 2008. Snail and Slug promote epithelial-mesenchymal transition through beta-catenin-T-cell factor-4-dependent expression of transforming growth factor-beta3. *Mol.Biol.Cell* 19:4875-4887.

Meltzer,S.J., S.P.O'Doherty, C.N.Frantz, K.Smolinski, J.Yin, A.B.Cantor, J.Liu, M.Valentine, G.M.Brodeur, and P.E.Berg. 1996. Allelic imbalance on chromosome 5q predicts long-term survival in neuroblastoma. *Br.J.Cancer* 74:1855-1861.

Mertens,F., B.Johansson, M.Hoglund, and F.Mitelman. 1997. Chromosomal imbalance maps of malignant solid tumors: a cytogenetic survey of 3185 neoplasms. *Cancer Res.* 57:2765-2780.

Michalak,E., A.Villunger, M.Erlacher, and A.Strasser. 2005. Death squads enlisted by the tumour suppressor p53. *Biochem.Biophys.Res.Commun.* 331:786-798.

Minturn,J.E., A.E.Evans, J.G.Villablanca, G.A.Yanik, J.R.Park, S.Shusterman, S.Groshen, E.T.Hellriegel, D.Bensen-Kennedy, K.K.Matthay, G.M.Brodeur, and J.M.Maris. 2011. Phase I trial of lestaurtinib for children with refractory neuroblastoma: a new approaches to neuroblastoma therapy consortium study. *Cancer Chemother.Pharmacol.*

Miyake,I., Y.Hakomori, A.Shinohara, T.Gamou, M.Saito, A.Iwamatsu, and R.Sakai. 2002. Activation of anaplastic lymphoma kinase is responsible for hyperphosphorylation of ShcC in neuroblastoma cell lines. *Oncogene* 21:5823-5834.

Miyake,H., I.Hara, S.Kamidono, M.E.Gleave, and H.Eto. 2003. Resistance to cytotoxic chemotherapy-induced apoptosis in human prostate cancer cells is associated with intracellular clusterin expression. *Oncol.Rep.* 10:469-473.

Miyake,H., I.Hara, and M.E.Gleave. 2005. Antisense oligodeoxynucleotide therapy targeting clusterin gene for prostate cancer: Vancouver experience from discovery to clinic. *Int.J.Urol.* 12:785-794.

Molenaar,J.J., M.E.Ebus, D.Geerts, J.Koster, F.Lamers, L.J.Valentijn, E.M.Westerhout, R.Versteeg, and H.N.Caron. 2009. Inactivation of CDK2 is synthetically lethal to MYCN over-expressing cancer cells. *Proc.Natl.Acad.Sci.U.S.A* 106:12968-12973.

Moll,U.M., A.G.Ostermeyer, R.Haladay, B.Winkfield, M.Frazier, and G.Zambetti. 1996. Cytoplasmic sequestration of wild-type p53 protein impairs the G1 checkpoint after DNA damage. *Mol.Cell Biol.* 16:1126-1137.

Monclair,T., G.M.Brodeur, P.F.Ambros, H.J.Brisse, G.Cecchetto, K.Holmes, M.Kaneko, W.B.London, K.K.Matthay, J.G.Nuchtern, S.D.von, T.Simon, S.L.Cohn, and A.D.Pearson. 2009. The International Neuroblastoma Risk Group (INRG) staging system: an INRG Task Force report. *J.Clin.Oncol.* 27:298-303.

Monsoro-Burq,A.H., R.B.Fletcher, and R.M.Harland. 2003. Neural crest induction by paraxial mesoderm in Xenopus embryos requires FGF signals. *Development* 130:3111-3124.

Mora,J., N.K.Cheung, B.H.Kushner, M.P.LaQuaglia, K.Kramer, M.Fazzari, G.Heller, L.Chen, and W.L.Gerald. 2000. Clinical categories of neuroblastoma are associated with different patterns of loss of heterozygosity on chromosome arm 1p. *J.Mol.Diagn.* 2:37-46.

Morin,P.J. 1999. beta-catenin signaling and cancer. *Bioessays* 21:1021-1030.

Morris,S.W., M.N.Kirstein, M.B.Valentine, K.G.Dittmer, D.N.Shapiro, D.L.Saltman, and A.T.Look. 1994. Fusion of a kinase gene, ALK, to a nucleolar protein gene, NPM, in non-Hodgkin's lymphoma. *Science* 263:1281-1284.

Mosse,Y.P., M.Laudenslager, D.Khazi, A.J.Carlisle, C.L.Winter, E.Rappaport, and J.M.Maris. 2004. Germline PHOX2B mutation in hereditary neuroblastoma. *Am.J.Hum.Genet.* 75:727-730.

Mosse,Y.P., M.Laudenslager, L.Longo, K.A.Cole, A.Wood, E.F.Attiyeh, M.J.Laquaglia, R.Sennett, J.E.Lynch, P.Perri, G.Laureys, F.Speleman, C.Kim, C.Hou, H.Hakonarson, A.Torkamani, N.J.Schork, G.M.Brodeur, G.P.Tonini, E.Rappaport, M.Devoto, and J.M.Maris. 2008. Identification of ALK as a major familial neuroblastoma predisposition gene. *Nature* 455:930-935.

Mosse,Y.P., A.Wood, and J.M.Maris. 2009. Inhibition of ALK signaling for cancer therapy. *Clin.Cancer Res.* 15:5609-5614.

Nakamura,E., Abreu-e-Lima, Y.Awakura, T.Inoue, T.Kamoto, O.Ogawa, H.Kotani, T.Manabe, G.J.Zhang, K.Kondo, V.Nose, and W.G.Kaelin, Jr. 2006. Clusterin is a secreted marker for a hypoxia-inducible factor-independent function of the von Hippel-Lindau tumor suppressor protein. *Am.J.Pathol.* 168:574-584.

Naldini,L., U.Blomer, F.H.Gage, D.Trono, and I.M.Verma. 1996. Efficient transfer, integration, and sustained long-term expression of the transgene in adult rat brains injected with a lentiviral vector. *Proc.Natl.Acad.Sci.U.S.A* 93:11382-11388.

Nara,K., T.Kusafuka, A.Yoneda, T.Oue, S.Sangkhathat, and M.Fukuzawa. 2007. Silencing of MYCN by RNA interference induces growth inhibition, apoptotic activity and cell differentiation in a neuroblastoma cell line with MYCN amplification. *Int.J.Oncol.* 30:1189-1196.

Naugler,W.E. and M.Karin. 2008. NF-kappaB and cancer-identifying targets and mechanisms. *Curr.Opin.Genet.Dev.* 18:19-26.

Nielsen,K.L. and N.J.Cowan. 1998. A single ring is sufficient for productive chaperonin-mediated folding in vivo. *Mol.Cell* 2:93-99.

Norris,M.D., S.B.Bordow, G.M.Marshall, P.S.Haber, S.L.Cohn, and M.Haber. 1996. Expression of the gene for multidrug-resistance-associated protein and outcome in patients with neuroblastoma. *N.Engl.J.Med.* 334:231-238.

Norris,M.D., S.B.Bordow, P.S.Haber, G.M.Marshall, M.Kavallaris, J.Madafiglio, S.L.Cohn, H.Salwen, M.L.Schmidt, D.R.Hipfner, S.P.Cole, R.G.Deeley, and M.Haber. 1997. Evidence that the MYCN oncogene regulates MRP gene expression in neuroblastoma. *Eur.J.Cancer* 33:1911-1916.

O'Sullivan,J., L.Whyte, J.Drake, and M.Tenniswood. 2003. Alterations in the post-translational modification and intracellular trafficking of clusterin in MCF-7 cells during apoptosis. *Cell Death.Differ.* 10:914-927.

Oncogenomics database (http://home.ccr.cancer.gov/oncology/oncogenomics/)

Oncomine database (www.oncomine.org)

Opel,D., C.Poremba, T.Simon, K.M.Debatin, and S.Fulda. 2007. Activation of Akt predicts poor outcome in neuroblastoma. *Cancer Res.* 67:735-745.

Osajima-Hakomori,Y., I.Miyake, M.Ohira, A.Nakagawara, A.Nakagawa, and R.Sakai. 2005. Biological role of anaplastic lymphoma kinase in neuroblastoma. *Am.J.Pathol.* 167:213-222.

Otto,T., S.Horn, M.Brockmann, U.Eilers, L.Schuttrumpf, N.Popov, A.M.Kenney, J.H.Schulte, R.Beijersbergen, H.Christiansen, B.Berwanger, and M.Eilers. 2009. Stabilization of N-Myc is a critical function of Aurora A in human neuroblastoma. *Cancer Cell* 15:67-78.

Pahl,H.L. 1999. Activators and target genes of Rel/NF-kappaB transcription factors. *Oncogene* 18:6853-6866.

Paratore,C., D.E.Goerich, U.Suter, M.Wegner, and L.Sommer. 2001. Survival and glial fate acquisition of neural crest cells are regulated by an interplay between the transcription factor Sox10 and extrinsic combinatorial signaling. *Development* 128:3949-3961.

Pear,W.S., G.P.Nolan, M.L.Scott, and D.Baltimore. 1993. Production of high-titer helper-free retroviruses by transient transfection. *Proc.Natl.Acad.Sci.U.S.A* 90:8392-8396.

Peirano,R.I., D.E.Goerich, D.Riethmacher, and M.Wegner. 2000. Protein zero gene expression is regulated by the glial transcription factor Sox10. *Mol.Cell Biol.* 20:3198-3209.

Perkins,N.D. 2006. Post-translational modifications regulating the activity and function of the nuclear factor kappa B pathway. *Oncogene* 25:6717-6730.

Piselli,P., S.Vendetti, D.Vismara, R.Cicconi, F.Poccia, V.Colizzi, and A.Delpino. 2000. Different expression of CD44, ICAM-1, and HSP60 on primary tumor and metastases of a human pancreatic carcinoma growing in scid mice. *Anticancer Res.* 20:825-831.

Ponzoni,M., P.Bocca, V.Chiesa, A.Decensi, V.Pistoia, L.Raffaghello, C.Rozzo, and P.G.Montaldo. 1995. Differential effects of N-(4-hydroxyphenyl)retinamide and retinoic acid on neuroblastoma cells: apoptosis versus differentiation. *Cancer Res.* 55:853-861.

Powers,C., A.Aigner, G.E.Stoica, K.McDonnell, and A.Wellstein. 2002. Pleiotrophin signaling through anaplastic lymphoma kinase is rate-limiting for glioblastoma growth. *J.Biol.Chem.* 277:14153-14158.

Pucci,S., E.Bonanno, F.Pichiorri, C.Angeloni, and L.G.Spagnoli. 2004. Modulation of different clusterin isoforms in human colon tumorigenesis. *Oncogene* 23:2298-2304.

Quintana,F.J., P.H.Hagedorn, G.Elizur, Y.Merbl, E.Domany, I.R.Cohen. 2004. Functional immunomics: microarray analysis of IgG autoantibody repertoires predicts the future response of mice to induced diabetes. *Proc Natl Acad Sci USA.* 101 Suppl 2:14615–14621

Radisky,D.C. and M.J.Bissell. 2007. NF-kappaB links oestrogen receptor signalling and EMT. *Nat.Cell Biol.* 9:361-363.

Rae,C., S.Langa, S.J.Tucker, and D.J.MacEwan. 2007. Elevated NF-kappaB responses and FLIP levels in leukemic but not normal lymphocytes: reduction by salicylate allows TNF-induced apoptosis. *Proc.Natl.Acad.Sci.U.S.A* 104:12790-12795.

Rayet,B. and C.Gelinas. 1999. Aberrant rel/nfkb genes and activity in human cancer. *Oncogene* 18:6938-6947.

Reynolds,C.P. 2000. Differentiating agents in pediatric malignancies: retinoids in neuroblastoma. *Curr.Oncol.Rep.* 2:511-518.

Rhodes,D.R., J.Yu, K.Shanker, N.Deshpande, R.Varambally, D.Ghosh, T.Barrette, A.Pandey, and A.M.Chinnaiyan. 2004. ONCOMINE: a cancer microarray database and integrated data-mining platform. *Neoplasia.* 6:1-6.

Rhodes,D.R., S.Kalyana-Sundaram, V.Mahavisno, R.Varambally, J.Yu, B.B.Briggs, T.R.Barrette, M.J.Anstet, C.Kincead-Beal, P.Kulkarni, S.Varambally, D.Ghosh, and A.M.Chinnaiyan. 2007. Oncomine 3.0: genes, pathways, and networks in a collection of 18,000 cancer gene expression profiles. *Neoplasia.* 9:166-180.

Rikova,K., A.Guo, Q.Zeng, A.Possemato, J.Yu, H.Haack, J.Nardone, K.Lee, C.Reeves, Y.Li, Y.Hu, Z.Tan, M.Stokes, L.Sullivan, J.Mitchell, R.Wetzel, J.Macneill, J.M.Ren, J.Yuan, C.E.Bakalarski, J.Villen, J.M.Kornhauser, B.Smith, D.Li, X.Zhou, S.P.Gygi, T.L.Gu, R.D.Polakiewicz, J.Rush, and M.J.Comb. 2007. Global survey of phosphotyrosine signaling identifies oncogenic kinases in lung cancer. *Cell* 131:1190-1203.

Ritossa, F.1962. A new puffing pattern induced by temperature shock and DNP in *Droshophila*. *Experientia.* 18:571-573.

Ritossa,F. 1996. Discovery of the heat shock response. *Cell Stress.Chaperones.* 1:97-98.

Rizzi,F. and S.Bettuzzi. 2008. Targeting Clusterin in prostate cancer. *J.Physiol Pharmacol.* 59 Suppl 9:265-274.

Rizzi,F. and S.Bettuzzi. 2009. Clusterin (CLU) and prostate cancer. *Adv.Cancer Res.* 105:1-19.

Rodriguez-Pineiro,A.M., M.P.de la Cadena, A.Lopez-Saco, and F.J.Rodriguez-Berrocal. 2006. Differential expression of serum clusterin isoforms in colorectal cancer. *Mol.Cell Proteomics.* 5:1647-1657.

Sala,A., S.Bettuzzi, S.Pucci, O.Chayka, M.Dews, and A.Thomas-Tikhonenko. 2009. Regulation of CLU gene expression by oncogenes and epigenetic factors implications for tumorigenesis. *Adv.Cancer Res.* 105:115-132.

Sala,A. and K.Chaiwatanasirikul. Neuroblastoma, Volume 1. *Springer* (In press).

Sallman,D.A., X.Chen, B.Zhong, D.L.Gilvary, J.Zhou, S.Wei, and J.Y.Djeu. 2007. Clusterin mediates TRAIL resistance in prostate tumor cells. *Mol.Cancer Ther.* 6:2938-2947.

Santilli,G., B.J.Aronow, and A.Sala. 2003. Essential requirement of apolipoprotein J (clusterin) signaling for IkappaB expression and regulation of NF-kappaB activity. *J.Biol.Chem.* 278:38214-38219.

Sasaki,H., Y.Sato, S.Kondo, I.Fukai, M.Kiriyama, Y.Yamakawa, and Y.Fujii. 2001. Expression of the prothymosin alpha mRNA correlated with that of N-myc in neuroblastoma. *Cancer Lett.* 168:191-195.

Sauka-Spengler,T. and M.Bronner-Fraser. 2008. Evolution of the neural crest viewed from a gene regulatory perspective. *Genesis.* 46:673-682.

Sawai,S., A.Shimono, K.Hanaoka, and H.Kondoh. 1991. Embryonic lethality resulting from disruption of both N-myc alleles in mouse zygotes. *New Biol.* 3:861-869.

Scartozzi,M., I.Bearzi, C.Pierantoni, A.Mandolesi, F.Loupakis, A.Zaniboni, V.Catalano, A.Quadri, F.Zorzi, R.Berardi, T.Biscotti, R.Labianca, A.Falcone, and S.Cascinu. 2007. Nuclear factor-kB tumor expression predicts response and survival in irinotecan-refractory metastatic colorectal cancer treated with cetuximab-irinotecan therapy. *J.Clin.Oncol.* 25:3930-3935.

Schneider,J., E.Jimenez, K.Marenbach, H.Romero, D.Marx, and H.Meden. 1999. Immunohistochemical detection of HSP60-expression in human ovarian cancer. Correlation with survival in a series of 247 patients. *Anticancer Res.* 19:2141-2146.

Schwab,M., K.Alitalo, K.H.Klempnauer, H.E.Varmus, J.M.Bishop, F.Gilbert, G.Brodeur, M.Goldstein, and J.Trent. 1983. Amplified DNA with limited homology to myc cellular oncogene is shared by human neuroblastoma cell lines and a neuroblastoma tumour. *Nature* 305:245-248.

Schwab,M., F.Westermann, B.Hero, and F.Berthold. 2003. Neuroblastoma: biology and molecular and chromosomal pathology. *Lancet Oncol.* 4:472-480.

Seeger,R.C., S.A.Rayner, A.Banerjee, H.Chung, W.E.Laug, H.B.Neustein, and W.F.Benedict. 1977. Morphology, growth, chromosomal pattern and fibrinolytic activity of two new human neuroblastoma cell lines. *Cancer Res.* 37:1364-1371.

Sen,R. and D.Baltimore. 1986. Multiple nuclear factors interact with the immunoglobulin enhancer sequences. *Cell* 46:705-716.

Shamaei-Tousi,A., A.Steptoe, K.O'Donnell, J.Palmen, J.W.Stephens, S.J.Hurel, M.Marmot, K.Homer, F.D'Aiuto, A.R.Coates, S.E.Humphries, and B.Henderson. 2007. Plasma heat shock protein 60 and cardiovascular disease risk: the role of psychosocial, genetic, and biological factors. *Cell Stress.Chaperones.* 12:384-392.

Shannan,B., M.Seifert, K.Leskov, J.Willis, D.Boothman, W.Tilgen, and J.Reichrath. 2006. Challenge and promise: roles for clusterin in pathogenesis, progression and therapy of cancer. *Cell Death.Differ.* 13:12-19.

Sherwood L., 2008. Human Physiology: From Cells to Systems (7 ed.). *Cengage Learning.* pg. 240

Shim,Y.J., Y.J.Shin, S.Y.Jeong, S.W.Kang, B.M.Kim, I.S.Park, and B.H.Min. 2009. Epidermal growth factor receptor is involved in clusterin-induced astrocyte proliferation. *Neuroreport* 20:435-439.

Shohet,J.M., M.J.Hicks, S.E.Plon, S.M.Burlingame, S.Stuart, S.Y.Chen, M.K.Brenner, and J.G.Nuchtern. 2002. Minichromosome maintenance protein MCM7 is a direct target of the MYCN transcription factor in neuroblastoma. *Cancer Res.* 62:1123-1128.

Shojaei-Brosseau,T., A.Chompret, A.Abel, V.F.de, M.A.Raquin, L.Brugieres, J.Feunteun, O.Hartmann, and C.Bonaiti-Pellie. 2004. Genetic epidemiology of

neuroblastoma: a study of 426 cases at the Institut Gustave-Roussy in France. *Pediatr.Blood Cancer* 42:99-105.

Silva,J.M., M.Z.Li, K.Chang, W.Ge, M.C.Golding, R.J.Rickles, D.Siolas, G.Hu, P.J.Paddison, M.R.Schlabach, N.Sheth, J.Bradshaw, J.Burchard, A.Kulkarni, G.Cavet, R.Sachidanandam, W.R.McCombie, M.A.Cleary, S.J.Elledge, and G.J.Hannon. 2005. Second-generation shRNA libraries covering the mouse and human genomes. *Nat.Genet.* 37:1281-1288.

Slack,A., Z.Chen, R.Tonelli, M.Pule, L.Hunt, A.Pession, and J.M.Shohet. 2005. The p53 regulatory gene MDM2 is a direct transcriptional target of MYCN in neuroblastoma. *Proc.Natl.Acad.Sci.U.S.A* 102:731-736.

Soda,M., Y.L.Choi, M.Enomoto, S.Takada, Y.Yamashita, S.Ishikawa, S.Fujiwara, H.Watanabe, K.Kurashina, H.Hatanaka, M.Bando, S.Ohno, Y.Ishikawa, H.Aburatani, T.Niki, Y.Sohara, Y.Sugiyama, and H.Mano. 2007. Identification of the transforming EML4-ALK fusion gene in non-small-cell lung cancer. *Nature* 448:561-566.

Soengas,M.S., R.M.Alarcon, H.Yoshida, A.J.Giaccia, R.Hakem, T.W.Mak, and S.W.Lowe. 1999. Apaf-1 and caspase-9 in p53-dependent apoptosis and tumor inhibition. *Science* 284:156-159.

Soltys,B.J. and R.S.Gupta. 1997. Cell surface localization of the 60 kDa heat shock chaperonin protein (hsp60) in mammalian cells. *Cell Biol.Int.* 21:315-320.

Souttou,B., N.B.Carvalho, D.Raulais, and M.Vigny. 2001. Activation of anaplastic lymphoma kinase receptor tyrosine kinase induces neuronal differentiation through the mitogen-activated protein kinase pathway. *J.Biol.Chem.* 276:9526-9531.

Stoica,G.E., A.Kuo, A.Aigner, I.Sunitha, B.Souttou, C.Malerczyk, D.J.Caughey, D.Wen, A.Karavanov, A.T.Riegel, and A.Wellstein. 2001. Identification of anaplastic lymphoma kinase as a receptor for the growth factor pleiotrophin. *J.Biol.Chem.* 276:16772-16779.

Stoica,G.E., A.Kuo, C.Powers, E.T.Bowden, E.B.Sale, A.T.Riegel, and A.Wellstein. 2002. Midkine binds to anaplastic lymphoma kinase (ALK) and acts as a growth factor for different cell types. *J.Biol.Chem.* 277:35990-35998.

Stottmann,R.W. and J.Klingensmith. 2011. Bone morphogenetic protein signaling is required in the dorsal neural folds before neurulation for the induction of spinal neural crest cells and dorsal neurons. *Dev.Dyn.* 240:755-765.

Suzuki,T., J.Yokota, H.Mugishima, I.Okabe, M.Ookuni, T.Sugimura, and M.Terada. 1989. Frequent loss of heterozygosity on chromosome 14q in neuroblastoma. *Cancer Res.* 49:1095-1098.

Sylvester,S.R., M.K.Skinner, and M.D.Griswold. 1984. A sulfated glycoprotein synthesized by Sertoli cells and by epididymal cells is a component of the sperm membrane. *Biol.Reprod.* 31:1087-1101.

Takita,J., Y.Hayashi, K.Takei, N.Yamaguchi, R.Hanada, K.Yamamoto, and J.Yokota. 2000. Allelic imbalance on chromosome 18 in neuroblastoma. *Eur.J.Cancer* 36:508-513.

Tang,X.X., H.Zhao, B.Kung, D.Y.Kim, S.L.Hicks, S.L.Cohn, N.K.Cheung, R.C.Seeger, A.E.Evans, and N.Ikegaki. 2006. The MYCN enigma: significance of MYCN expression in neuroblastoma. *Cancer Res.* 66:2826-2833.

The Universal Mutation Database (www.umd.be:2072)

Thompson,P.M., B.A.Seifried, S.K.Kyemba, S.J.Jensen, C.Guo, J.M.Maris, G.M.Brodeur, D.O.Stram, R.C.Seeger, R.Gerbing, K.K.Matthay, T.C.Matise, and P.S.White. 2001. Loss of heterozygosity for chromosome 14q in neuroblastoma. *Med.Pediatr.Oncol.* 36:28-31.

Thompson,P.M., T.Gotoh, M.Kok, P.S.White, and G.M.Brodeur. 2003. CHD5, a new member of the chromodomain gene family, is preferentially expressed in the nervous system. *Oncogene* 22:1002-1011.

Trochet,D., F.Bourdeaut, I.Janoueix-Lerosey, A.Deville, P.L.de, G.Schleiermacher, C.Coze, N.Philip, T.Frebourg, A.Munnich, S.Lyonnet, O.Delattre, and J.Amiel. 2004. Germline mutations of the paired-like homeobox 2B (PHOX2B) gene in neuroblastoma. *Am.J.Hum.Genet.* 74:761-764.

Trougakos,I.P. and E.S.Gonos. 2002. Clusterin/apolipoprotein J in human aging and cancer. *Int.J.Biochem.Cell Biol.* 34:1430-1448.

Trougakos,I.P., A.So, B.Jansen, M.E.Gleave, and E.S.Gonos. 2004. Silencing expression of the clusterin/apolipoprotein j gene in human cancer cells using small interfering RNA induces spontaneous apoptosis, reduced growth ability, and cell sensitization to genotoxic and oxidative stress. *Cancer Res.* 64:1834-1842.

Tsai,Y.P., S.C.Teng, and K.J.Wu. 2008. Direct regulation of HSP60 expression by c-MYC induces transformation. *FEBS Lett.* 582:4083-4088.

Tsai,Y.P., M.H.Yang, C.H.Huang, S.Y.Chang, P.M.Chen, C.J.Liu, S.C.Teng, and K.J.Wu. 2009. Interaction between HSP60 and beta-catenin promotes metastasis. *Carcinogenesis* 30:1049-1057.

Tsarovina,K., J.Schellenberger, C.Schneider, and H.Rohrer. 2008. Progenitor cell maintenance and neurogenesis in sympathetic ganglia involves Notch signaling. *Mol.Cell Neurosci.* 37:20-31.

Tweddle,D.A., A.D.Pearson, M.Haber, M.D.Norris, C.Xue, C.Flemming, and J.Lunec. 2003. The p53 pathway and its inactivation in neuroblastoma. *Cancer Lett.* 197:93-98.

Vallabhapurapu,S. and M.Karin. 2009. Regulation and function of NF-kappaB transcription factors in the immune system. *Annu.Rev.Immunol.* 27:693-733.

Van Engeland,M., L.J.Nieland, F.C.Ramaekers, B.Schutte, and C.P.Reutelingsperger. 1998. Annexin V-affinity assay: a review on an apoptosis detection system based on phosphatidylserine exposure. *Cytometry.* 31:1-9.

Van Eden, W., J.E.R.Thole, R.van der Zee, A.Noordzij, J.D.A.van Embden, A.J.Hensen, I.R.Cohen. 1988. Cloning of the mycobacterial epitope recognized by T lymphocytes in adjuvant arthritis. *Nature.* 331: 171–173.

Van Maerken,T., F.Speleman, J.Vermeulen, I.Lambertz, C.S.De, S.E.De, N.Yigit, V.Coppens, J.Philippe, P.A.De, J.C.Marine, and J.Vandesompele. 2006. Small-molecule MDM2 antagonists as a new therapy concept for neuroblastoma. *Cancer Res.* 66:9646-9655.

Van Maerken,T., L.Ferdinande, J.Taildeman, I.Lambertz, N.Yigit, L.Vercruysse, A.Rihani, M.Michaelis, J.Cinatl, Jr., C.A.Cuvelier, J.C.Marine, P.A.De, M.Bracke,

F.Speleman, and J.Vandesompele. 2009. Antitumor activity of the selective MDM2 antagonist nutlin-3 against chemoresistant neuroblastoma with wild-type p53. *J.Natl.Cancer Inst.* 101:1562-1574.

Wadhwa,R., S.Takano, K.Kaur, S.Aida, T.Yaguchi, Z.Kaul, T.Hirano, K.Taira, and S.C.Kaul. 2005. Identification and characterization of molecular interactions between mortalin/mtHsp70 and HSP60. *Biochem.J.* 391:185-190.

Wang,Q., S.Diskin, E.Rappaport, E.Attiyeh, Y.Mosse, D.Shue, E.Seiser, J. Jagannathan, S.Shusterman, M.Bansal, D.Khazi, C.Winter, E.Okawa, G.Grant, A.Cnaan, H.Zhao, N.Cheung, W.Gerald, W.London, K. K. Matthay, G.M. Brodeur, J.M. Maris. 2006. Integrative Genomics Identifies Distinct Molecular Classes of Neuroblastoma and Shows That Multiple Genes Are Targeted by Regional Alterations in DNA Copy Number. *Cancer Res.* 66:(12):6050-6062.

Wartiovaara,K., F.Barnabe-Heider, F.D.Miller, and D.R.Kaplan. 2002. N-myc promotes survival and induces S-phase entry of postmitotic sympathetic neurons. *J.Neurosci.* 22:815-824.

Webb,T.R., J.Slavish, R.E.George, A.T.Look, L.Xue, Q.Jiang, X.Cui, W.B.Rentrop, and S.W.Morris. 2009. Anaplastic lymphoma kinase: role in cancer pathogenesis and small-molecule inhibitor development for therapy. *Expert.Rev.Anticancer Ther.* 9:331-356.

Wei,L., T.Xue, J.Wang, B.Chen, Y.Lei, Y.Huang, H.Wang, and X.Xin. 2009. Roles of clusterin in progression, chemoresistance and metastasis of human ovarian cancer. *Int.J.Cancer* 125:791-806.

Weichert,W., M.Boehm, V.Gekeler, M.Bahra, J.Langrehr, P.Neuhaus, C.Denkert, G.Imre, C.Weller, H.P.Hofmann, S.Niesporek, J.Jacob, M.Dietel, C.Scheidereit, and G.Kristiansen. 2007. High expression of RelA/p65 is associated with activation of nuclear factor-kappaB-dependent signaling in pancreatic cancer and marks a patient population with poor prognosis. *Br.J.Cancer* 97:523-530.

Weiss,W.A., K.Aldape, G.Mohapatra, B.G.Feuerstein, and J.M.Bishop. 1997. Targeted expression of MYCN causes neuroblastoma in transgenic mice. *EMBO J.* 16:2985-2995.

White,P.S., J.M.Maris, C.Beltinger, E.Sulman, H.N.Marshall, M.Fujimori, B.A.Kaufman, J.A.Biegel, C.Allen, C.Hilliard, and . 1995. A region of consistent deletion in neuroblastoma maps within human chromosome 1p36.2-36.3. *Proc.Natl.Acad.Sci.U.S.A* 92:5520-5524.

Wilson,M.R. and S.B.Easterbrook-Smith. 2000. Clusterin is a secreted mammalian chaperone. *Trends Biochem.Sci.* 25:95-98.

Woo,C.W., F.Tan, H.Cassano, J.Lee, K.C.Lee, and C.J.Thiele. 2008. Use of RNA interference to elucidate the effect of MYCN on cell cycle in neuroblastoma. *Pediatr.Blood Cancer* 50:208-212.

Wood AC LM, Haglund EA, Attiyeh EF, Pawel B, Courtright J, Plegaria J, et al. Inhibition of ALK mutated neuroblastomas by the selective inhibitor PF-02341066.

J Clin Oncol 2009;27:15s (suppl; abstr 10008b) 2009

Woodage,T., M.A.Basrai, A.D.Baxevanis, P.Hieter, and F.S.Collins. 1997. Characterization of the CHD family of proteins. *Proc.Natl.Acad.Sci.U.S.A* 94:11472-11477.

Wu,K. and B.Bonavida. 2009. The activated NF-kappaB-Snail-RKIP circuitry in cancer regulates both the metastatic cascade and resistance to apoptosis by cytotoxic drugs. *Crit Rev.Immunol.* 29:241-254.

Wyatt,A., J.Yerbury, S.Poon, R.Dabbs, and M.Wilson. 2009. Chapter 6: The chaperone action of Clusterin and its putative role in quality control of extracellular protein folding. *Adv.Cancer Res.* 104:89-114.

Xie,M.J., Y.Motoo, S.B.Su, H.Mouri, K.Ohtsubo, F.Matsubara, and N.Sawabu. 2002. Expression of clusterin in human pancreatic cancer. *Pancreas* 25:234-238.

Xu,Q., G.Schett, H.Perschinka, M.Mayr, G.Egger, F.Oberhollenzer, J.Willeit, S.Kiechl, and G.Wick. 2000. Serum soluble heat shock protein 60 is elevated in subjects with atherosclerosis in a general population. *Circulation* 102:14-20.

Yang,C.R., S.Yeh, K.Leskov, E.Odegaard, H.L.Hsu, C.Chang, T.J.Kinsella, D.J.Chen, and D.A.Boothman. 1999. Isolation of Ku70-binding proteins (KUBs). *Nucleic Acids Res.* 27:2165-2174.

Yang,G.F., X.M.Li, and D.Xie. 2009. Overexpression of clusterin in ovarian cancer is correlated with impaired survival. *Int.J.Gynecol.Cancer* 19:1342-1346.

Yang,S.R., J.Wright, M.Bauter, K.Seweryniak, A.Kode, and I.Rahman. 2007. Sirtuin regulates cigarette smoke-induced proinflammatory mediator release via RelA/p65 NF-kappaB in macrophages in vitro and in rat lungs in vivo: implications for chronic inflammation and aging. *Am.J.Physiol Lung Cell Mol.Physiol* 292:L567-L576.

Young, D.B., J.Ivanyi, J.H.Cox, J.R.Lamb. 1987. The 65 kDa antigen of mycobacteria-a common bacterial protein? *Immunol Today.* 8:215–219

Yu,A.L., M.M.Uttenreuther-Fischer, C.S.Huang, C.C.Tsui, S.D.Gillies, R.A.Reisfeld, and F.H.Kung. 1998. Phase I trial of a human-mouse chimeric anti-disialoganglioside monoclonal antibody ch14.18 in patients with refractory neuroblastoma and osteosarcoma. *J.Clin.Oncol.* 16:2169-2180.

Zanin-Zhorov,A., R.Bruck, G.Tal, S.Oren, H.Aeed, R.Hershkoviz, I.R.Cohen, and O.Lider. 2005. Heat shock protein 60 inhibits Th1-mediated hepatitis model via innate regulation of Th1/Th2 transcription factors and cytokines. *J.Immunol.* 174:3227-3236.

Zanin-Zhorov,A., L.Cahalon, G.Tal, R.Margalit, O.Lider, and I.R.Cohen. 2006. Heat shock protein 60 enhances CD4+ CD25+ regulatory T cell function via innate TLR2 signaling. *J.Clin.Invest* 116:2022-2032.

Zhang,B., Z.Wang, T.Li, E.N.Tsitsikov, and H.F.Ding. 2007. NF-kappaB2 mutation targets TRAF1 to induce lymphomagenesis. *Blood* 110:743-751.

Zhang,C., T.F.Carl, E.D.Trudeau, T.Simmet, and M.W.Klymkowsky. 2006. An NF-kappaB and slug regulatory loop active in early vertebrate mesoderm. *PLoS.One.* 1:e106.

Zhang,H., J.K.Kim, C.A.Edwards, Z.Xu, R.Taichman, and C.Y.Wang. 2005. Clusterin inhibits apoptosis by interacting with activated Bax. *Nat.Cell Biol.* 7:909-915.

Zhang,L.Y., W.T.Ying, Y.S.Mao, H.Z.He, Y.Liu, H.X.Wang, F.Liu, K.Wang, D.C.Zhang, Y.Wang, M.Wu, X.H.Qian, and X.H.Zhao. 2003. Loss of clusterin both in serum and tissue correlates with the tumorigenesis of esophageal squamous cell carcinoma via proteomics approaches. *World J.Gastroenterol.* 9:650-654.

Zhou,M., D.Shen, J.E.Head, E.Y.Chew, P.Chevez-Barrios, W.R.Green, and C.C.Chan. 2007. Ocular clusterin expression in von Hippel-Lindau disease. *Mol.Vis.* 13:2129-2136.

Zhu,Q. and M.S.Center. 1994. Cloning and sequence analysis of the promoter region of the MRP gene of HL60 cells isolated for resistance to adriamycin. *Cancer Res.* 54:4488-4492.

Zimmerman,K.A., G.D.Yancopoulos, R.G.Collum, R.K.Smith, N.E.Kohl, K.A.Denis, M.M.Nau, O.N.Witte, D.Toran-Allerand, C.E.Gee, and . 1986. Differential expression of myc family genes during murine development. *Nature* 319:780-783.

Zindy,F., C.M.Eischen, D.H.Randle, T.Kamijo, J.L.Cleveland, C.J.Sherr, and M.F.Roussel. 1998. Myc signaling via the ARF tumor suppressor regulates p53-dependent apoptosis and immortalization. *Genes Dev.* 12:2424-2433.

APPENDIX I

Description : human CLU full length was cloned from a blunt-end cutting of TOPO-CLU plasmid construct, which was a gift from Professor Saverio Bettuzzi.. The insert was cloned into the blunt *EcoRI* site to generate pcDNA3-CLU (full length).

Vector : pcDNA3 (Invitrogen)

Insert : Clusterin full length

Resistance : Ampicilllin/Neomycin

Name : pcDNA-CLU

Constructed by : Korn-Anong Chaiwatanasirikul

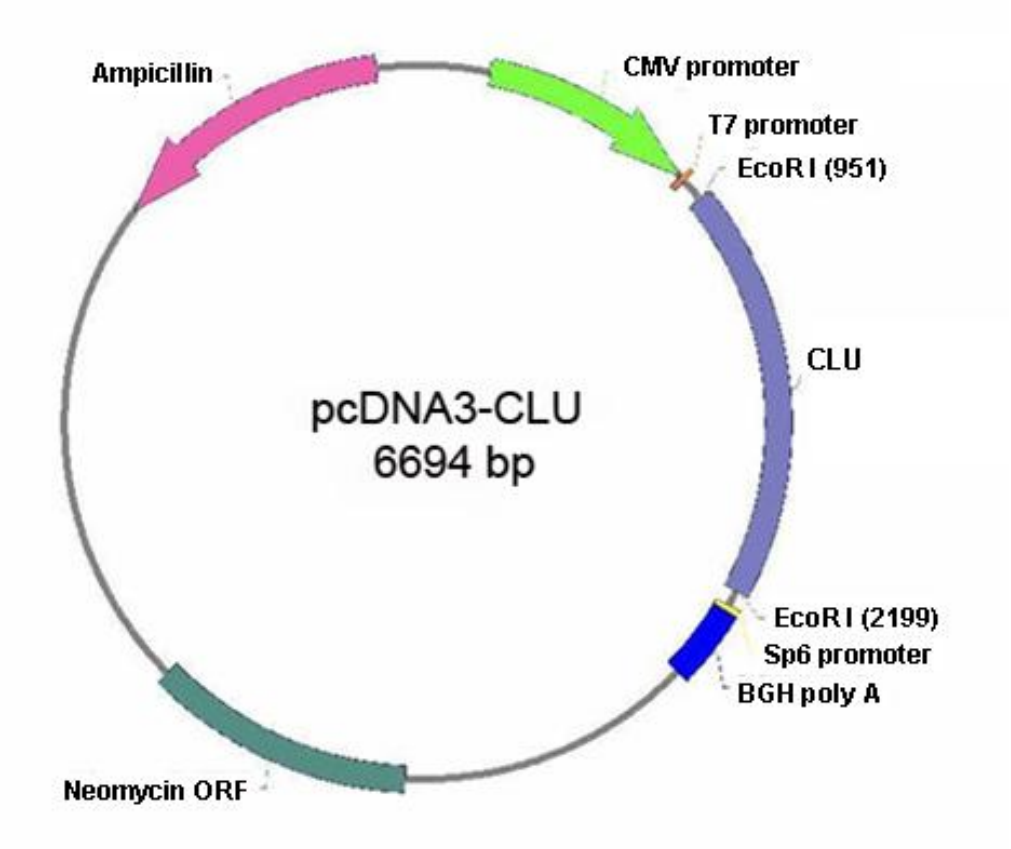

Description : Alpha chain only of the complete human CLU cDNA sequence was subcloned into pcDNA3 empty vector. The cDNA sequence of the CLU alpha chain region was amplified by PCR and cloned into *KpnI* and *NotI* digested pcDNA3 vector.

Insert : Clusterin (alpha chain only)

Resistance : Ampicilllin/Neomycin

Name : pcDNA-alpha (pcDNA-α)

Constructed by : Korn-Anong Chaiwatanasirikul

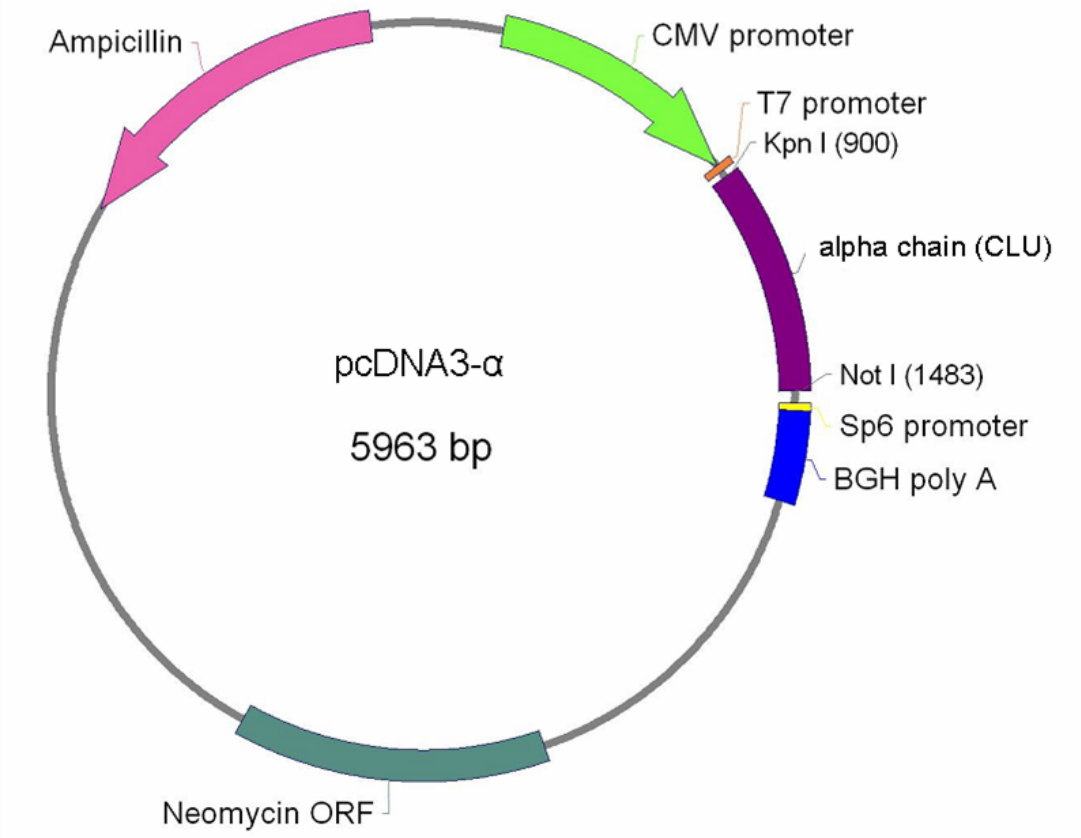

Description : Beta chain only of the complete human CLU cDNA sequence was subcloned into pcDNA3 empty vector. The cDNA sequence of the CLU beta chain region was amplified by PCR and cloned into *KpnI* and *NotI* digested pcDNA3 vector.

Insert : Clusterin (beta chain only)

Resistance : Ampicilllin/Neomycin

Name : pcDNA-beta (pcDNA-β)

Constructed by : Korn-Anong Chaiwatanasirikul

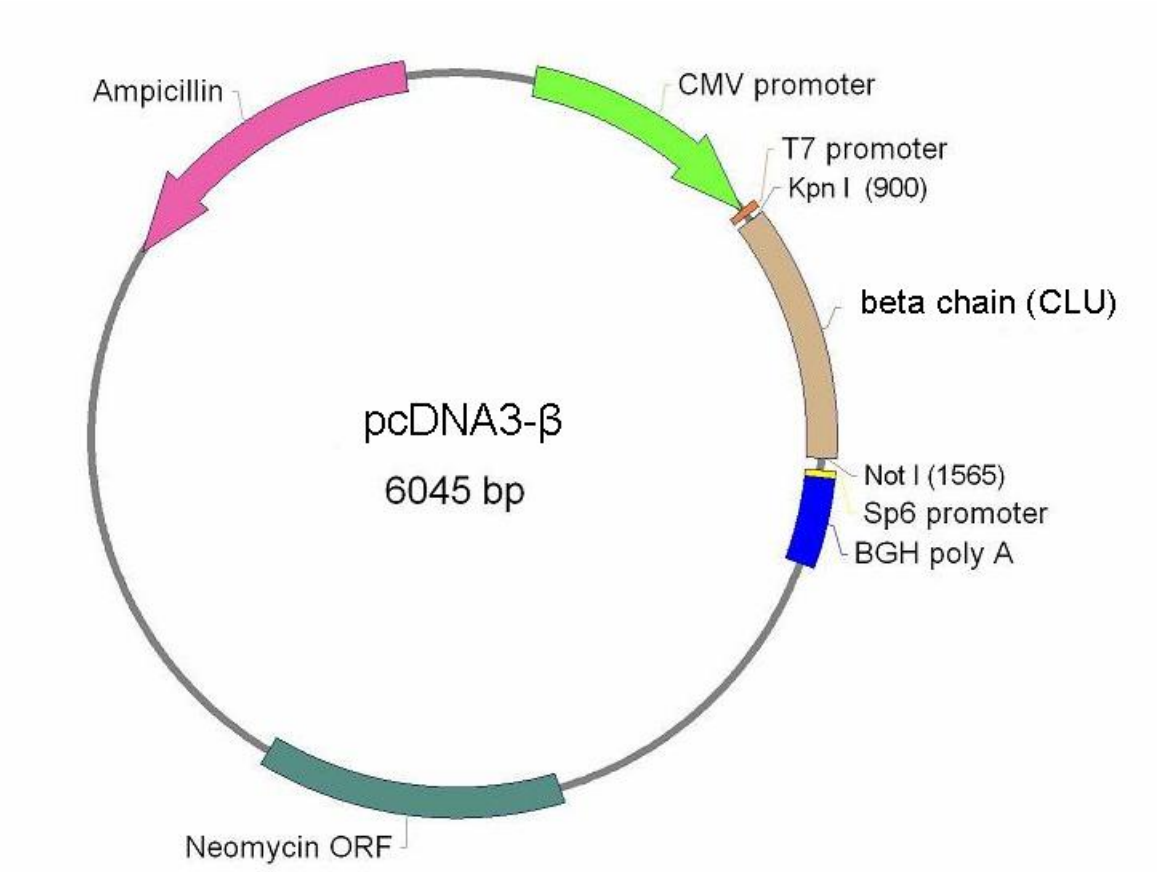

Description : The complete human CLU cDNA sequence was subcloned into pGEX-4T1 (GST) empty vectors to create GST-fusion protein expression vectors. Primers were designed with appropriate restriction site recognizing nucleotides with an in-framed start site (ATG) attached (Table 2.5.). In addition, the PCR products were also cloned into *SalI* and *NotI*-digested pGEX4T1 vector to obtain pGEX4T1-CLU.

Vector : pGEX4T-1 (GE Healthcare)

Insert : Clusterin full length

Resistance : Ampicilllin

Name : pGEX4T1-CLU

Constructed by : Korn-Anong Chaiwatanasirikul

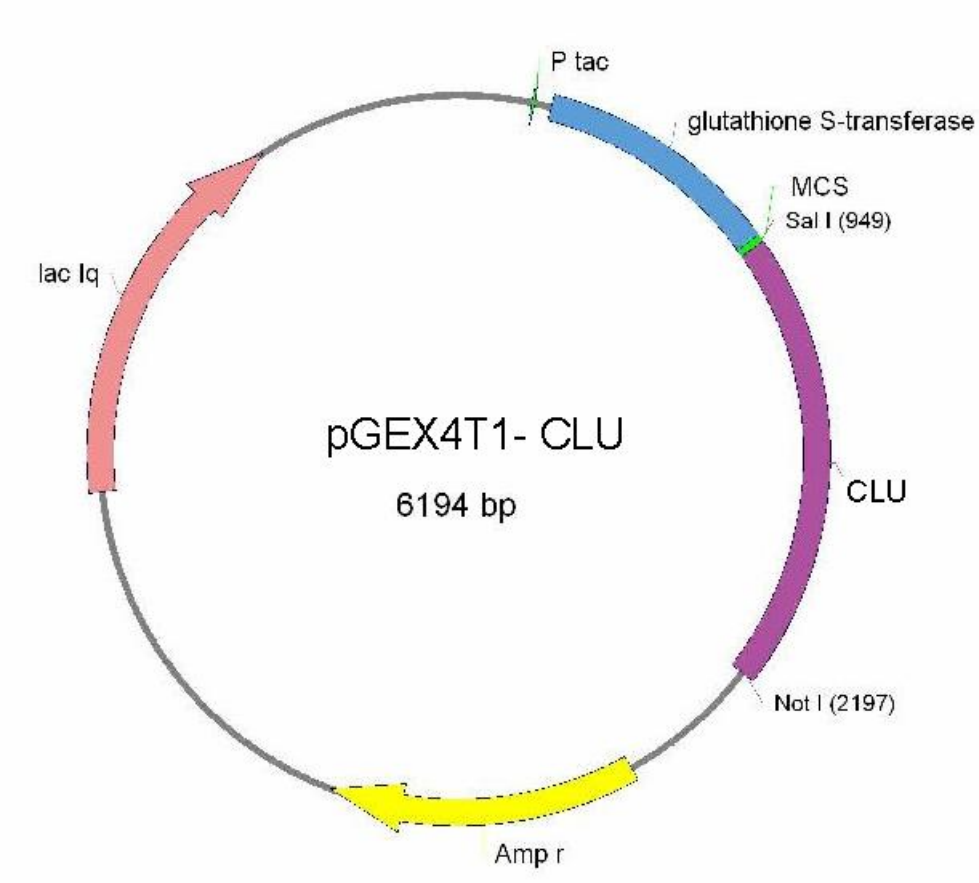

Description : The complete human CLU alpha chain only cDNA sequence was subcloned into pGEX-4T1 (GST) empty vectors to create GST-fusion protein expression vectors. Primers were designed with appropriate restriction site recognizing nucleotides with an in-framed start site (ATG) attached (Table 2.5.). In addition, the PCR products were also cloned into *SalI* and *NotI*-digested pGEX4T1 vector.

Vector : pGEX4T-1 (GE Healthcare)

Insert : Clusterin (alpha chain only)

Resistance : Ampicilllin

Name : pGEX4T1-alpha (pGEX4T1-α)

Constructed by : Korn-Anong Chaiwatanasirikul

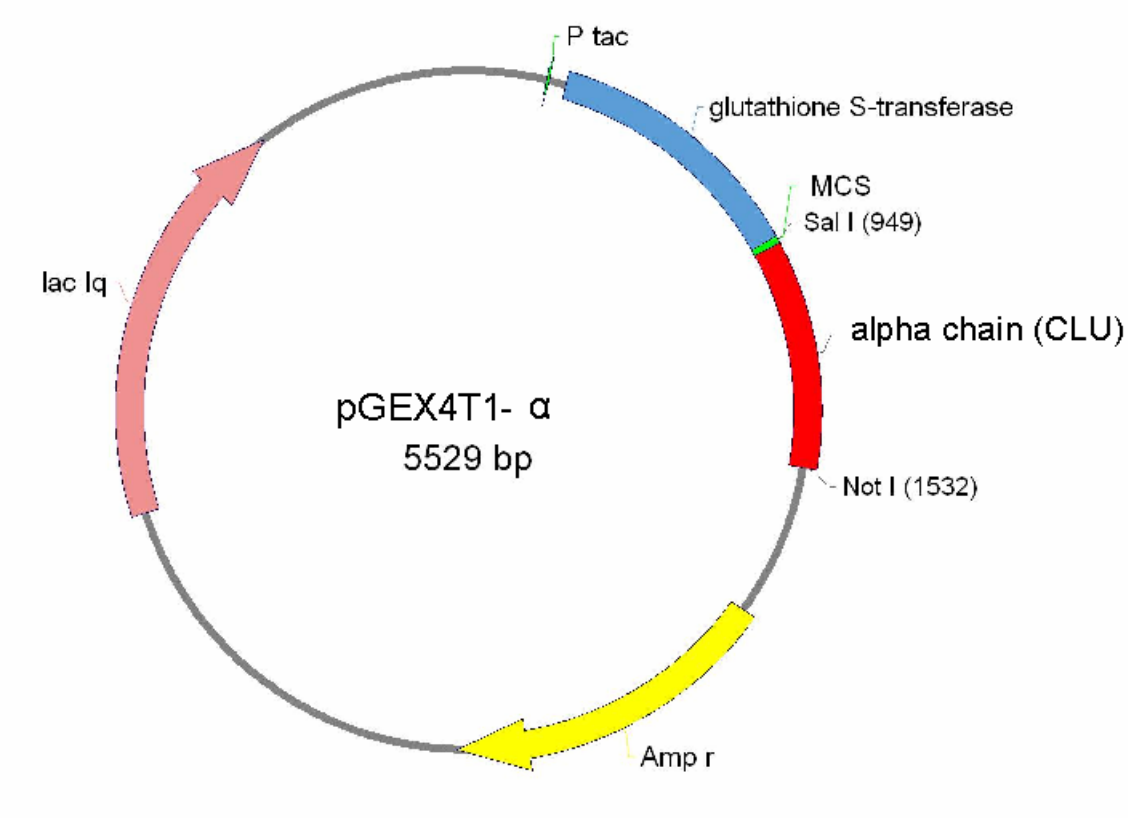

Description : The complete human CLU beta chain only cDNA sequence was subcloned into pGEX-4T1 (GST) empty vectors to create GST-fusion protein expression vectors. Primers were designed with appropriate restriction site recognizing nucleotides with an in-framed start site (ATG) attached (Table 2.5.). In addition, the PCR products were also cloned into *SalI* and *NotI*-digested pGEX4T1 vector.

Vector : pGEX4T-1 (GE Healthcare)

Insert : Clusterin (beta chain only)

Resistance : Ampicilllin

Name : pGEX4T1-beta (pGEX4T1-β)

Constructed by : Korn-Anong Chaiwatanasirikul

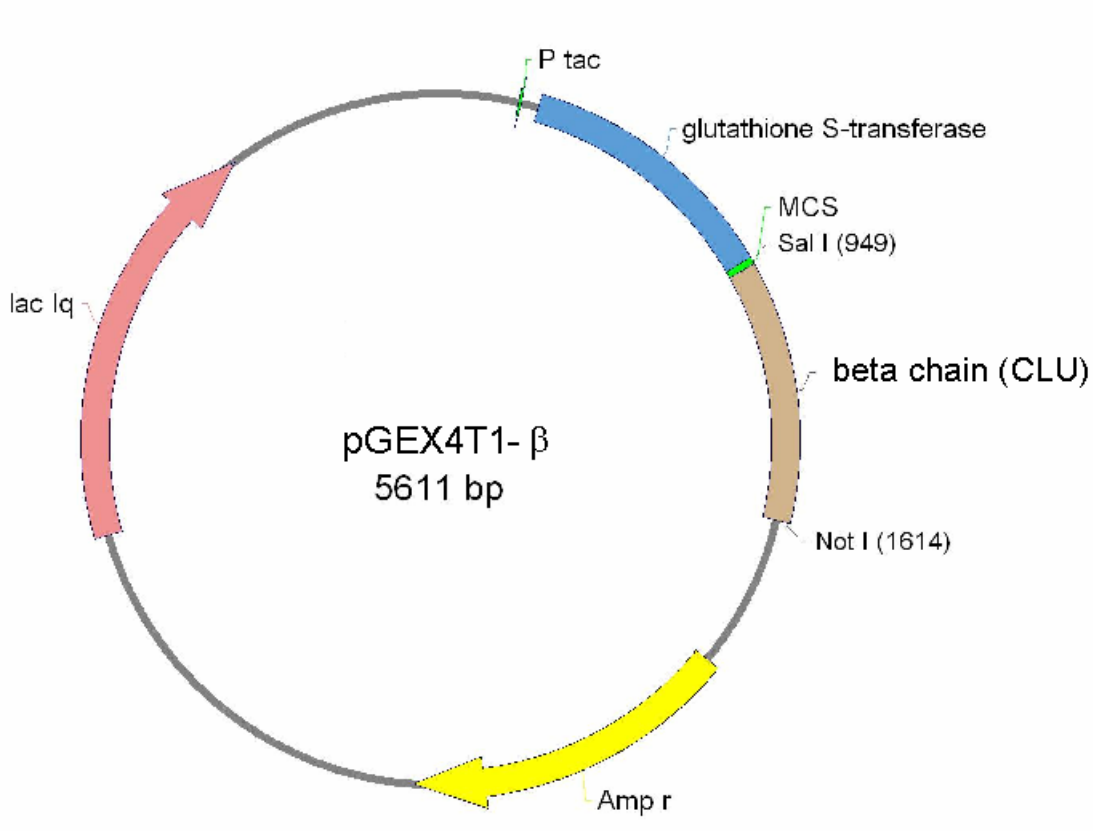

APPENDIX II

The following article has been accepted for publication in Cell Death and Disease journal. The article will be available online later this year.

The complexity of the tumour suppressive function of CLU is explained by its localisation and interaction with HSP60.

Korn-Anong Chaiwatanasirikul and Arturo Sala

Molecular Haematology and Cancer Biology Unit, UCL Institute of Child Health, 30 Guilford st. WC1N 1EH, London UK

Correspondence: Dr. Arturo Sala, a.sala@ich.ucl.ac.uk

Abstract

The product of the CLU gene promotes or inhibits tumourigenesis in a context dependent manner. It has been hypothesised that different CLU isoforms have different, even opposing biological functions but this theory has not been experimentally validated. Here we show that molecules involved in survival pathways are differentially modulated by the intracellular or secreted forms of CLU. Secreted CLU, which is selectively increased after transformation, activates the survival factor AKT, whereas intracellular CLU inhibits the activity of the oncogenic transcription factor NF-κB. Furthermore, intracellular CLU suppresses the pro-proliferative and pro-survival activity of the chaperone protein HSP60 in neuroblastoma cells by forming a physical complex. Thus, localisation is key for CLU physiology, explaining the wide range of effects in cell survival and transformation.

Key words: *Apolipoprotein J, clusterin, HSP60, apoptosis, neuroblastoma, AKT, NF-κB*